Keith Nicholson

Geothermal Fluids

Chemistry and Exploration Techniques

With 30 Figures

Springer-Verlag
Berlin Heidelberg New York
London Paris Tokyo
Hong Kong Barcelona
Budapest

Dr. Keith Nicholson
School of Applied Sciences
The Robert Gordon University
Aberdeen AB1 1HG, Scotland
United Kingdom

ISBN-13 : 978-3-642-77846-9 e-ISBN-13 : 978-3-642-77844-5
DOI: 10.1007 / 978-3-642-77844-5

Library of Congress Cataloging-in-Publication Data. Nicholson, Keith, 1955- , Geothermal fluids: chemistry and exploration techniques/Keith Nicholson. p. cm. . Includes bibliographical references and index
ISBN-13 : 978-3-642-77846-9 1. Geothermal resources. 2. Geochemistry. 3. Water chemistry. I. Title.
GB1199.5.N53 1993 551.2'3--dc20 93-29590

Typesetting: Camera-ready by author
32/3145-5 4 3 2 1 0 – Printed on acid-free paper

Preface

This book introduces aqueous geochemistry applied to geothermal systems. It is specifically designed for readers first entering into the world of geothermal energy from a variety of scientific and engineering backgrounds, and consequently is not intended to be the last word on geothermal chemistry. Instead it is intended to provide readers with sufficient background knowledge to permit them to subsequently understand more complex texts and scientific papers on geothermal energy. The book is structured into two parts. The first explains how geothermal fluids and their associated chemistry evolve, and shows how the chemistry of these fluids can be used to deduce information about the resource. The second part concentrates on survey techniques explaining how these should be performed and the procedures which need to be adopted to ensure reliable sampling and analytical data are obtained.

A geothermal system requires a heat source and a fluid which transfers the heat towards the surface. The fluid could be molten rock (magma) or water. This book concentrates on the chemistry of the water, or hydrothermal, systems. Consequently, magma-energy systems are not considered. Hot-dry rock (HDR) systems are similarly outside the scope of this text, principally because they contain no indigenous fluid for study. Both magma-energy and HDR systems have potential as energy sources but await technological developments before they can be exploited commercially. Geothermal systems based on water, however, are proven energy resources which have been successfully developed throughout the world. The energy within such systems has been directly employed for space heating and other direct-use applications, and for the generation of electricity.

The chemistry of the terrestrial geothermal systems considered in this work are (or should be) also of interest to economic geologists, since they represent the modern equivalents of certain epithermal-gold and porphyry-copper deposits. Terrestrial systems, being more accessible, also provide insights into the processes active in submarine geothermal systems which are themselves modern analogues of ancient stratiform iron, manganese and massive sulphide mineralisation.

Being able to touch waters which have circulated through the Earth's crust, waters which may have deposited gold just a few hundred metres below and which can provide clues to geochemical processes active in the Earth, is one of the most exciting aspects of geothermal chemistry. All this and energy too.

Aberdeen, Scotland.
August 1993

KEITH NICHOLSON

DEDICATION

For

Angela

Acknowledgements

When a work such as this is produced over a long period of time, it is difficult to limit acknowledgements as many people have contributed in different, often subtle ways. However, I should first like to thank Dick Glover, John Hulston and Mike Stewart of DSIR, New Zealand, for finding time in busy schedules to provide helpful, detailed reviews of earlier chapters. I am also grateful to the many graduate students, from over 25 countries, who I taught during my time in New Zealand. Discussions about geothermal developments in their countries, made me appreciate the difficulties scientists and engineers from different technical backgrounds have in interpreting geothermal fluid chemistry. These discussions convinced me of the need for an introductory text on geothermal chemistry, and formed the basis for the contents of this work. I should also like to thank Pat Browne (Auckland University) who provided moral support and valuable discussions over the contents of the book, particularly in the early months of writing. In the later months, John Harper (RGU) generously provided me with the time and facilities to complete this work. Throughout all this time however, my greatest supporter and source of encouragement has been Angela, my wife, who not only drew all the figures in this volume, but also patiently got on with the more serious business of building a home, while I got deeper into hot water.

August 1993

Contents

Part II
Exploration Techniques & Surveys

5 EXPLORATION TECHNIQUES

6 WATER SURVEYS

8 SOIL AND SOIL-GAS SURVEYS

APPENDICES

Part I

Geothermal Fluid Chemistry

CHAPTER 1

GEOTHERMAL SYSTEMS

Geothermal fields are found throughout the world in a range of geological settings, and are increasingly being developed as an energy source. Each of the different types of geothermal system has distinct characteristics which are reflected in the chemistry of the geothermal fluids and their potential applications. However, they all have in common a heat source at a few kilometres depth, and it is this which sets water, present in the upper sections of the Earth's crust, into convection. Most geothermal resources can be used for space heating applications (eg. urban district heating schemes, fish farming, greenhouse heating), but it is only the hotter systems (>~180°C) which are used to generate electricity through the production of steam (see Rowley, 1982, for a review of systems worldwide). Since aqueous geochemistry is involved in all stages of the exploration, evaluation, and production of a geothermal field, an understanding of the chemistry of the fluids is essential for the development of a resource. The chemistry of the geothermal waters and gases contains important information about the hydrology of the field and conditions in the reservoir. These aspects of geothermal fluid chemistry are discussed in the following chapters. However, before looking at specific aspects of geothermal chemistry, it will be useful to first place the fluids in context by briefly describing the different types of geothermal system.

1.1 SYSTEM TYPES AND CHARACTERISTICS

Geothermal fields are commonly classified or divided by a series of descriptive terms. They are referred to as liquid or vapour dominated, low or high temperature, sedimentary or volcanic hosted etc. This section outlines the meaning of these and other descriptive classification terms found in the literature.

Reservoir equilibrium state: This is the fundamental division between geothermal systems and is based on the circulation of the reservoir fluid and the mechanism of heat transfer. Systems in *dynamic equilibrium* are continually recharged by water entering the reservoir. The water is heated and then discharged out of the reservoir,

either to the surface or to underground permeable horizons. Heat is transferred through the system by *convection* and *circulation* of the fluid. Systems in *static equilibrium* (also known as stagnant or storage systems) have only minor or no recharge to the reservoir and heat is transferred only by *conduction*.

Fluid type: The reservoir fluid can be composed mainly of liquid water (*liquid-dominated*) or steam (*vapour-dominated*). In most reservoirs, both steam and liquid water exist in varying proportions as two-phase zones. Liquid-dominated systems are most common, and may contain a steam cap which can expand or develop on exploitation as happened at Wairakei, New Zealand. Systems which discharge only steam are rare - the best known are Larderello, Italy and The Geysers, USA. Note that liquid-dominated systems are sometimes called water-dominated; this is not a good term since all hydrothermal fields are composed of water in either the liquid or vapour phase. Vapour-dominated systems are also referred to as steam fields. The source of the water in a geothermal system is discussed below.

Reservoir temperature: The temperature (or enthalpy) of geothermal reservoirs is an important discriminator in terms of fluid chemistry and potential resource usage. Systems are commonly described as *low-temperature* (<~150°C) or *high-temperature* (>~150°C). The discriminatory temperatures are not rigid, and some workers also use the term "intermediate" to indicate reservoir temperatures in the 120-180°C range. Low-temperature systems can only be used for "direct-use" applications (eg. heating), while high-temperature systems can be used for electricity generation as well as direct-use applications.

Host rock: The rocks which contain the geothermal reservoir (the "host rocks") react with the geothermal fluid. As rock-fluid reactions determine the final composition of the geothermal waters and gases, a knowledge of the host rocks is important for confident application of geothermometers and predictions on potential scaling problems if the field is developed. Only broad distinctions such as *volcanic* or *sedimentary* (clastic/carbonate) are necessary. Metamorphosed equivalents of these lithologies can be indicated by adding the prefix "meta-" to the above terms. Volcanic, clastic-sedimentary and carbonate-sedimentary rocks (and the metamorphic equivalents of these lithologies) all yield geothermal fluids with contrasting and distinct chemistries. If the geology is poorly known, it may be possible to predict the sub-surface lithologies from the water chemistry.

Heat source: The heat source for the system is a function of the geological or tectonic setting. If the driving heat flux is provided by a magma, then such systems are termed *volcanogenic*. They are invariably high-temperature systems. Heat does not, however, have to be supplied by a magma, and a geothermal system can be generated in areas of tectonic activity. For example, heat may be supplied by the tectonic uplift of hot basement rocks, or water can be heated by unusually deep circulation created by folding of a permeable horizon or faulting. These are termed *non-volcanogenic* systems and include examples of both high and low-temperature reservoirs.

Classification

A simple classification based on reservoir equilibrium state, fluid type and temperature is used in this text (see box). Geothermal systems are primarily divided into dynamic (convective) systems, and static (conductive) systems. These are subdivided on the basis of reservoir temperature. The topography can also influence the structure of the system, and this creates a further subdivision for high-temperature, liquid-dominated reservoirs, as discussed in Section 1.3.

A classification of geothermal systems

Dynamic systems (convective)
High temperature
- liquid-dominated
  - low-relief
  - high-relief
- vapour-dominated

Low-temperature

Static systems (conductive)
Low-temperature
Geopressurised

More detailed categories can be devised, but this is adequate for general discussion.

Dynamic (convective) systems

High - temperature systems: These are found in geological settings where the geothermal gradient is several times above the crustal average of ~30°C/km, and where rock temperatures of several hundred degrees Celcius exist at depths of only a few kilometres. The locations of geothermal fields is invariably tectonically controlled, and they are often found in areas of block faulting, grabens or rifting and in collapsed caldera structures, with reservoir depths of around 1-3km. Typical settings are around active plate margins such as subduction zones (eg. Pacific Rim), spreading ridges (eg. Mid-Atlantic) and rift zones (eg. East Africa) and within orogenic belts (eg. Mediterranean, Himalayas).

High-temperature systems are often volcanogenic, with the heat provided by intrusive masses commonly of rhyolitic-andesitic composition. Examples include El Tatio, Chile; fields in the Taupo Volcanic Zone, New Zealand; Cerro Prieto, Mexico; Imperial Valley, The Geysers, Roosevelt Hot Springs, USA. Hot or boiling springs typically discharge chloride waters (with the exception of The Geysers which is a vapour-dominated system and discharges steam) with a total dissolved solids (TDS) concentration of ~3000-5000 mg/kg. Silica sinter is often deposited around boiling or near-boiling springs. Saline, or brine fields form where seawater is involved in the system or where the chloride fluids pass through evaporite sequences (eg. Cerro Prieto TDS = ~40,000 mg/kg; Salton Sea TDS = ~300,000 mg/kg).

Geothermal systems also develop on the flanks of young volcanoes (eg. Ahuachapan, El Salvador; Kawah Kamojang, Indonesia; Puna, Hawaii). In coastal locations these may incorporate seawater into the circulating waters (eg. Reykjanes, Iceland). The deep chloride fluids are often not discharged at the surface because of the high relief. If they do emerge it is usually as dilute warm springs many kilometres along the flanks of the volcano at lower elevations. Fumaroles are more common and any springs near the upflow zone discharge acidic sulphate and/or bicarbonate waters. Sub-surface mixing and hydrology can be complex in these fields.

High-temperature systems with a non-volcanogenic or tectonic heat source are less common. They occur in areas which are tectonically active, but which are not areas of active vulcanism. The most well known examples are Larderello, Italy and Kizildere, Turkey. Larderello discharges steam, whereas Kizildere springs used to discharge a bicarbonate water prior to production. Recently, Minissale (1991) has

demonstrated that Larderello shows many characteristics more typical of a static (conductive) system in steady state.

Low - temperature systems: Low-temperature (also called low-enthalpy) systems can occur in a variety of geological settings of both elevated and normal heat flow. Deep fluid circulation through faults or folded permeable strata, tectonic uplift of hotter rocks from depth and the residual heat from intruded plutons can all yield low-temperature fields. These are found throughout Europe and Asia, and along some areas of Tertiary vulcanism in the Pacific. The structure of low-temperature systems is not illustrated as no idealised model can be developed given the varied origins of these types of system. They usually discharge dilute waters, with total dissolved solids concentrations of around 1000mg/kg or less, through warm springs at ~30-65°C. Many such springs deposit minerals of retrograde solubility (calcite, gypsum) with only minor or no silica deposition. The composition of the waters will depend on the relative contributions of formation waters and meteoric waters to the discharge features. Waters held in limestone and other carbonate-rich reservoir lithologies will be bicarbonate-rich, possibly with low chloride concentration. Waters from reservoirs composed of marine clastic sediments, especially shales, often have high concentrations of chloride, boron and carbon dioxide.

Static (conductive) systems

Static systems are characteristically found in strata deposited in deep sedimentary basins. The fluids are derived from the formation waters trapped within the thick sedimentary sequences. These waters attain reservoir temperatures of around 70-150°C at depths of 2-4km, and are therefore *low-temperature* systems. The fluids are typically very saline chloride waters or brines, which remain trapped, as the vertical permeability is low within the formations until released tectonically or by drilling. Examples of such fields have been reported from Eastern Europe, USSR and Australia.

Within this category can be included the *geopressurised* system (eg. Gulf of Mexico, USA). Such systems are found at depths of ~3-7km and consist of permeable sedimentary rocks, contained within impermeable, low-conductivity strata (eg. shale). Under these conditions the heat and fluids within the permeable strata cannot be expelled on compaction, as would normally occur, and are therefore trapped within the system. The pore fluids actually bear a proportion of the pressure of the overlying lithologies, and the fluid pressure therefore approaches lithostatic

pressure, greatly exceeding that of the water column (hydrostatic pressure). Such systems can also contain substantial amounts of methane.

1.2 GENESIS OF GEOTHERMAL FLUIDS

Origin of water and solutes

The water constituting the geothermal fluid can be derived from a number of sources. It may represent surface (*meteoric*) water which has gained depths of several kilometres through fractures and permeable horizons, or it can be water which was buried along with the host sediments (*formation* or *connate* waters). Other sources of water in geothermal systems have been suggested; these include waters evolved in metamorphism (*metamorphic* waters) and from magmas (*juvenile* waters), but the importance of these sources of water is uncertain.

Magmas were initially thought to be the source of the heat, water and solutes of geothermal systems. However, this neat model was radically changed in the early 1960's when it was demonstrated that the fluids were of dominantly meteoric origin, and solutes could be derived from rock-water reactions. Work on the isotopic signature of the fluids by Craig (1963) showed that they had the same deuterium signature as that of local meteoric water and could not be magmatic. In a series of now classic studies in aqueous geochemistry, Ellis and Mahon (1964, 1967) and Mahon (1967) demonstrated that all the solutes in geothermal fluids could be derived from reactions between the meteoric groundwater and the host lithologies. Later experiments with seawater and basalt (eg. Bischoff et al., 1981) produced solutions of similar chemistry to seawater-influenced geothermal systems such as those in Iceland. Rock-water reaction is therefore thought to be the major source for many of the solutes, although they may also be contributed by mixing with formation waters, seawater or magmatic brine.

While there is no doubt that the geothermal fluids are of a predominantly meteoric origin, there is sufficient latitude in the isotope data to permit 5-10% of the fluid to be from an alternative source, possibly a magmatic brine. Mixing with even a small amount of magmatic brine would significantly affect the chemistry of the final geothermal fluid, and isotope determinations cannot discount a magmatic contribution subsequently diluted by meteoric waters. However, mass balance considerations using typical values for:

- water-rock ratios
- the chloride content of host rocks
- the concentration of chloride in waters from high-temperature systems
- the aerial extent of geothermal systems
- the duration of geothermal activity

indicate that unrealistically large volumes of rock would have to be leached over the lifetime of a geothermal system. A small but significant magmatic contribution to the geothermal fluid is therefore thought to be likely. Density differences would, however, preclude any intimate mixing between meteoric waters and a magmatic brine. If small pulses of magmatic brine did enter the geothermal convection cell then, while not detectable isotopically, they would make a major contribution to the solute composition. Such brines would be at temperatures in excess of 400°C and be rich in solutes such as Cl, SO_2 and CO_2. Although the extent to which mixing may occur is uncertain, recent analytical advances now make it possible to distinguish between the isotopes of chlorine and boron. Information from these may isotopes may enable a model of magmatic brine-meteoric water mixing to be derived.

Evolution of geothermal fluids

Bearing in mind the possible additional sources of both the fluid and solutes discussed above, the evolution of geothermal fluids in dynamic, liquid-dominated systems can be summarised as follows. Meteoric waters penetrate the crust through permeable zones and circulate to depths of up to around 5-7km. As they descend, they are heated, react with the host rocks and rise by convection. These deep waters are the primary geothermal chloride fluid and all other types of geothermal water are derived directly or indirectly from these chloride waters. At depth, the fluids typically contain 1000 - 10,000 mg/kg Cl at temperatures of about 350°C. The "soluble-group" elements are the first to be leached from the host rocks by the waters, followed by other elements which are controlled by temperature-dependent reactions (see Chapter 2). These reactions change the primary mineralogy of the host rocks to a distinctive alteration assemblage characteristic of the fluid and its temperature. The fluids are retained within a permeable horizon forming a reservoir in which mineral-fluid equilibria, and a suite of secondary alteration minerals, are established. As the chloride fluids leave the reservoir and ascend to the surface they may boil to create a two-phase (steam + liquid) boiling zone. The residual chloride water can discharge at the surface in hot springs or travel laterally to finally emerge many kilometres from the upflow zone. The vapours from this boiling zone may migrate to the surface

independently of the liquid phase and discharge as fumaroles. Alternatively, the vapours may dissolve in groundwaters or condense in the cooler ground to form steam-heated, acid sulphate and/or bicarbonate waters. The conceptual structure of geothermal systems, and the inter-relationship of the fluid types, is discussed in Section 1.3 and illustrated in Figures 1.4-1.6.

Evolution of steam: boiling point-depth relations

As a geothermal fluid ascends towards the surface, the pressure imposed upon it by the overlying column of water (hydrostatic pressure) will decrease. Eventually, the pressure will drop to a level which permits the dissolved gases and steam to separate from the liquid phase. This phase separation is commonly referred to as "boiling". It is one of the most important processes controlling the chemistry of liquid and vapour (ie. water and steam) discharges.

Enthalpy-temperature and enthalpy-temperature-pressure-density relationships are shown in Figs 1.1 and 1.2, which summarise the data presented in steam tables (Appendix 1). The relationship between boiling point and depth has been described by Haas (1971) and is illustrated in Fig. 1.3. The curve indicates the maximum temperature a fluid can attain at any given depth (or pressure), and therefore shows the depth at which a reservoir fluid at a given temperature will commence boiling. From this depth the boiling, or two-phase zone, can extend upwards towards the surface. The curve assumes that only hydrostatic pressure acts upon the fluid. In practice however, it has been found that hydrodynamic pressures exist at depth in a geothermal system at about 10% above hydrostatic. This excess pressure is necessary to maintain flow through the system. It is created by the buoyancy of hot water relative to cold water recharge and by a hydrostatic head in recharge waters from areas of greater relief (Grant et al., 1982; Henley, 1985). This means that higher temperatures can exist at shallower depths than indicated by the curve, and therefore that boiling will occur at shallower depths.

The relationship shown in Fig. 1.3 is for pure water. An increase in the salinity of water lowers the vapour pressure of water, raises the curve and prevents boiling until shallower depths are attained (Sutton and McNabb, 1977). However, for most geothermal systems, the fluids are dilute and small changes in salinity will not significantly alter the boiling point-depth profile of the system. More significant however, is the gas content of the fluid. The presence of several wt% gas in the fluid will depress the isotherms in a system below the usual boiling point-depth curve.

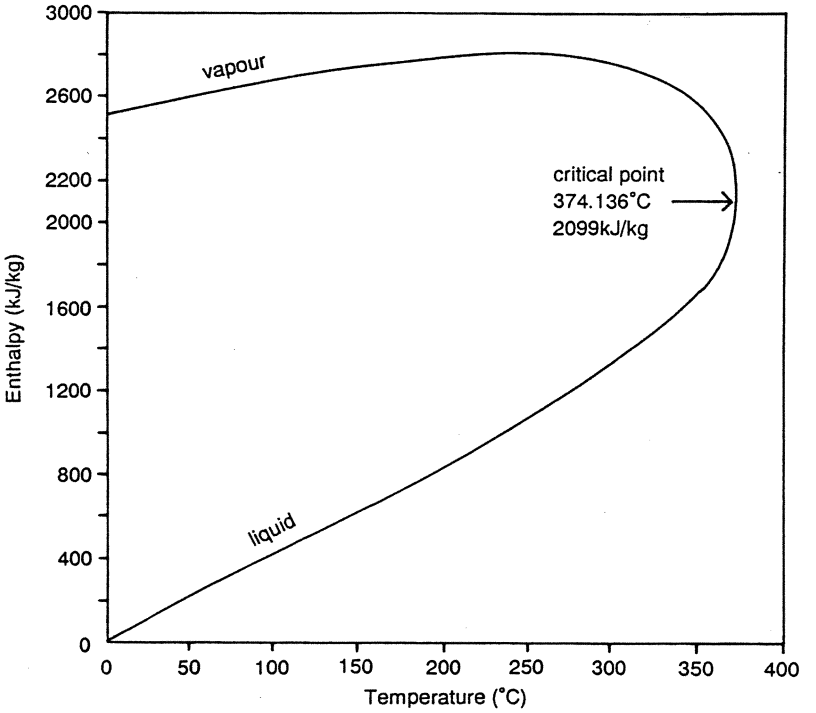

Figure 1.1. Enthalpy-temperature relationship for saturated water vapour and liquid water to the critical point (374.136°C). Note the narrow range of enthalpy change with increasing temperature for water vapour ("steam") compared with that of liquid water, and the maximum plateau of 2804 kJ/kg at 227-242°C (Appendix 1).

This means that boiling zones in high-gas systems will appear at far greater depths than for gas-poor systems, which follow the relationship for pure water. This is demonstrated in Fig. 1.3 for a fluid containing 4.4wt% CO_2 (such as that found at Ohaki-Broadlands, New Zealand). This depression of the boiling point is caused by an increase in the vapour pressure of the fluid, and this is created by the additional pressure of the dissolved gases. (A higher gas content requires greater confining pressure to prevent the gases from exsolving from solution.) Production from a gas-rich field can rapidly depressurise the system as the gases are removed from the fluid,

and this drop in pressure may permit the entry of cold groundwaters into the field. Boiling leads to a drop in the temperature of the residual liquid as steam separation involves both mass and enthalpy loss. Dilution with ground water and conduction are the other two main processes which lower fluid temperature. Fluids which are diluted may never attain boiling point before discharge at the surface. As none of the original gas has been lost, these waters can be recognised from their chemistry.

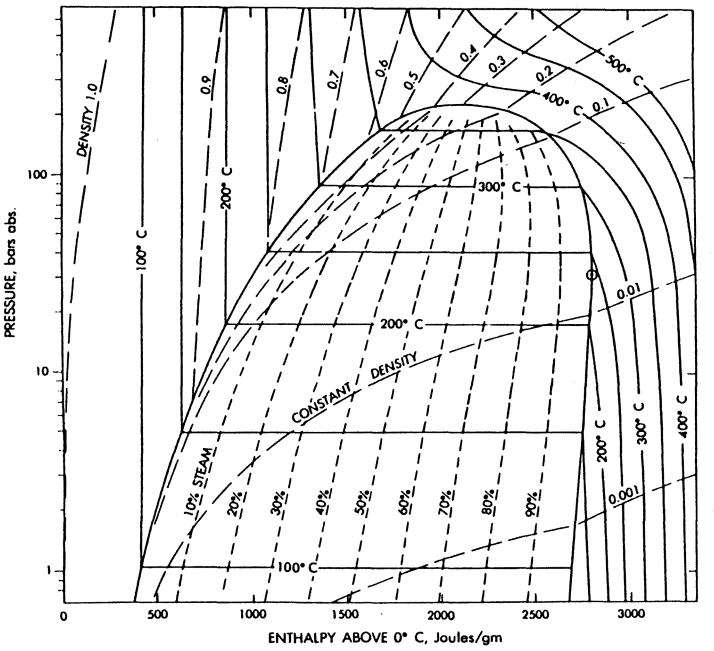

Figure 1.2. Enthalpy-temperature-pressure-density relationships for water to 500°C and 600 bars (from Henley et al., 1984).

When production from a liquid-dominated (hot-water) field exceeds recharge, the water level in the reservoir will fall. The void created by this fall can be filled with steam formed by evaporation of the remaining fluid, creating a steam cap over the liquid reservoir (eg. Wairakei-Tauhara, New Zealand; Henley and Stewart, 1983). In vapour-dominated reservoirs evaporation of pore waters, together with conditions of restricted permeability and only minor recharge, create a zone where steam in the dominant phase (eg. Lardarello, Italy; The Geysers, USA) and no liquid water is

discharged. Steam reservoir temperatures are consistently around 236°C, the maximum enthalpy of dry steam, pressures are almost constant throughout the reservoir (White, 1970; White et al., 1971) and gas contents within the vapour are around 0.5-2.0%. This compares with ~0.01-0.5% in liquid-dominated systems where the vapour represents 10-30% of the fluid.

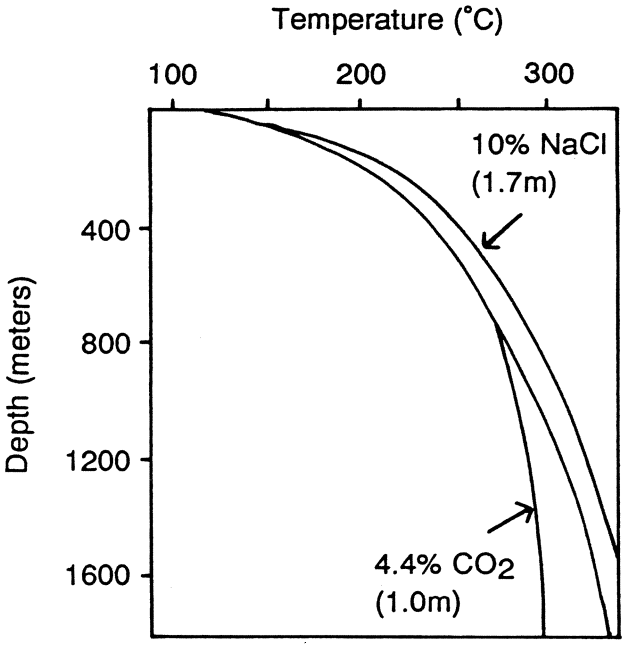

Figure 1.3. Boiling-point - depth relationship under hydrostatic conditions. Note that increases in salinity and gas content have opposite effects on the boiling-point - depth profile. For a fluid at a given temperature, increasing the salinity prevents the fluid boiling until shallower depths are attained; by contrast, increasing the gas content permits the fluid to boil at greater depths (see Fig. 3.5 also). Note too that increasing the salinity has only a slight effect on the boiling profile, while relatively small increases in the gas content of the fluid significantly alters the boiling-depth relationship.

Age of geothermal fluids and geothermal systems

The time the meteoric water spends in the geothermal system being heated, reacting with the host rocks, stored in the reservoir and finally discharged at the surface (the "residence time") is difficult to determine. Contamination with carbon from several sources makes ^{14}C-dating ineffective and tritium has too short a half-life to be useful except for very brief residence times. Circulation models for geothermal fluids estimate residence times can be around 10,000 years, although 100-1000 years may be more typical (Rybach, 1981). The residence time of the brine in the Salton Sea geothermal system has been estimated to be 100-1000 years from uranium-thorium decay isotopes, with the age of the system itself placed at 20,000-40,000 years (Zukin et al., 1987).

The lifetime of a geothermal system is difficult to determine and will vary between systems. Often limits on the age of a system are determined indirectly through geological relationships. For example, Browne (1979) determined from the presence of alteration minerals in a clast within a hydrothermal eruption breccia of known age that geothermal activity at Kawerau, New Zealand commenced over 200,000 years ago. A literature review by P.R.L. Browne (unpublished) shows that active geothermal systems around the world are estimated to be between ~2,000 years (Nesjavellir, Iceland; Kristmannsdottir and Tomasson 1974; Stefansson et al., 1983) and ~ 3 million years old (Larderello, Italy; Del Moro et al., 1982; Steamboat Springs, Nevada, USA; White, 1979). Although each geothermal system will follow an individual evolution path, typical lifetimes may be around 500,000 years. Note that over this period of time the system need not be continuously discharging fluids, and it is most likely that activity will be episodic following fluctuations in heat flux, sealing of fluid pathways and tectonic fracturing creating new permeable zones. During such cycles of flow, sealing and fracture the centre of activity may move as the underground plumbing, and therefore hydrology, of the system changes.

1.3 THERMAL, HYDROLOGICAL AND CHEMICAL STRUCTURE

The emphasis of this text is on dynamic, high-temperature, liquid-dominated systems. Such systems commonly have a magmatic heat source at depths of ~8km or more. The magma itself must be convecting to keep the upper sections molten, and thereby provide a continuous source of heat to drive the geothermal convection system. The dynamic nature of the system is shown by the cycle: meteoric water

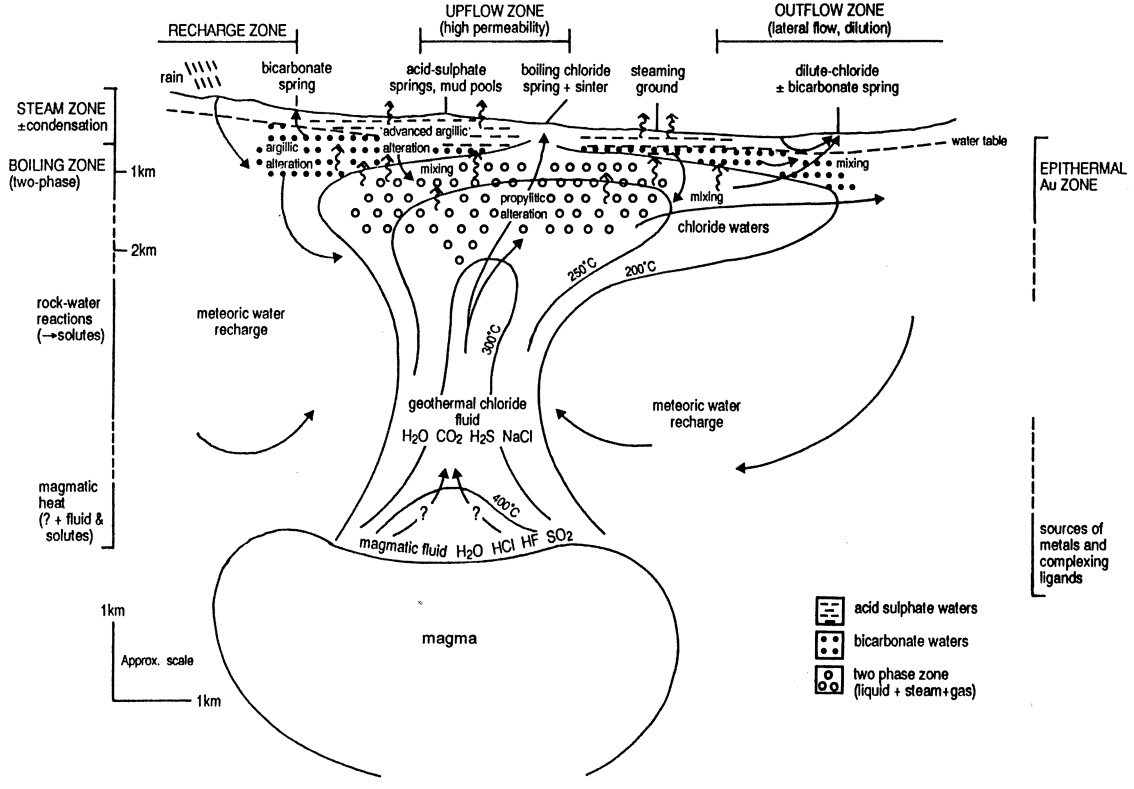

Figure 1.4. Conceptual structure of liquid-dominated geothermal systems in a low-relief setting. Note that the deep chloride fluid attains the surface and that, despite the low relief, lateral flow is possible.

descent, geothermal fluid formation, (replenished by meteoric waters descending from the recharge zone) and surface discharge of geothermal waters and vapours through springs and fumaroles.

However, fluid flow from depth is unlikely to follow the idealised vertical path shown in Figures 1.4 and 1.5, and some degree of lateral flow is probable. Once the geothermal fluid is a few hundred metres from the surface, local topographic and structural influences will exert an important control on the direction of flow and area of discharge.

The thermal, hydrological and chemical structure of high-temperature dynamic systems are illustrated in the conceptual models of Figures 1.4-1.6. The hydrology and distribution of discharge features is controlled by topography and permeable structures, eg. faults and the conduits produced by hydrothermal eruptions. Vapour-fed discharge features occupy higher ground than the chloride-water springs, and include fumaroles, hot springs discharging steam-heated waters and steaming ground. These can form above boiling zones where carbon dioxide and hydrogen sulphide dissolve into groundwaters or steam condensates. Bicarbonate waters (CO_2-rich steam heated waters) are also common on the margins of many fields. Condensation of volcanic gases at elevated levels in andesitic terrain create acidic chloride-sulphate waters. These can filter back down into the system as is seen in many fields in the Philippines.

Liquid-dominated systems

Many systems display lateral flow structures created by strong hydraulic gradients. These is turn are formed due to high relief, often with a near-surface low-permeability horizon. Cooling by conduction and groundwater mixing are reflected in the chemistry of the discharges. Even in low-relief (<~250m) settings, including those typical of silicic volcanic terrain (eg. Taupo Volcanic Zone, New Zealand), near-surface lateral flows can extend for several kilometres. This is greatly extended in terrain of high relief (>~1000m), typical of andesitic volcanoes, where flows are 10-50km in length.

Low-relief (Fig. 1.4)

Such systems are characterised by springs and pools of chloride water. The deep geothermal fluid can attain the surface, often close to the upflow area, because of the gentle topography. Lateral flow is possible but is not as extensive as in areas of

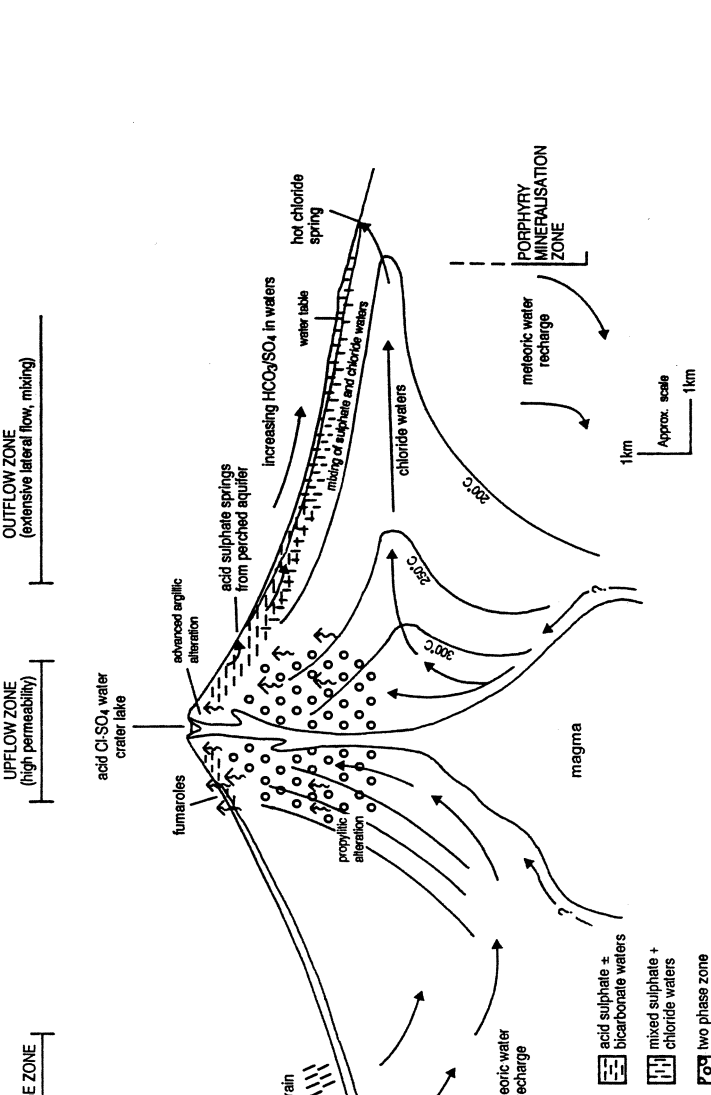

Figure 1.5. Conceptual structure of liquid-dominated geothermal systems in a high-relief setting. Note the deep two-phase zone and the extensive lateral flow compared to systems in a low-relief setting.

high relief. Two-phase or steam zones are present but are not as thick as in high-relief systems (described below). However, these steam zones can increase in depth when fluid removal on exploitation of the system exceeds natural fluid recharge, as has happened at Wairakei, New Zealand. Oxidation of hydrogen sulphide gas in the steam, together with condensation or mixing of the steam with ground waters, produced acidic sulphate waters. Condensation of carbon dioxide, which is less soluble than hydrogen sulphide, produces bicarbonate-rich waters which are often found on the margins on the field. Because of the low relief over these systems, chloride water hot-springs, sulphate water hot-springs, bicarbonate water hot-springs, fumaroles and steaming ground often occur in relatively close proximity to one another. These types of system are found in New Zealand, USA, East Africa and Iceland, and many occur in tectonic rift settings.

High-relief (Fig. 1.5)

Common in island-arc settings with characteristic andesitic vulcanism, the steep topography over these systems prevents the chloride fluid from reaching the surface. Large lateral flows, often over 10km, are not unusual. Over this distance the chloride fluid can be diluted with groundwater or mix with descending sulphate waters and steam condensates. These acid waters are produced in a two-phase zone often several hundred metres deep, where steam condenses and/or mixes with groundwaters. Fumaroles, steaming ground and acidic sulphate-water hot-springs are common surface discharge features near the upflow zone. The springs are fed from the condensate layers which lie near the surface, perched above the chloride water flows. These acid waters can also flow laterally to emerge down-slope as hot-springs, or descend into the system through fractures to mix with the ascending chloride waters. Examples of these systems are found in Indonesia, Taiwan, Japan and the Philippines.

Vapour-dominated systems (Fig. 1.6)

Fumaroles, steaming ground and acid sulphate-water hot-springs are the characteristic discharge features of these systems. The reservoir is composed of steam (with gases), although saline, boiling water feeding steam into the reservoir probably occurs at depth. Vapour-dominated reservoirs show a relatively constant temperature with depth of about 236°C, (the temperature of maximum enthalpy of saturated steam; Appendix 1). The pressure profile of the reservoir is controlled by steam (steam-static) and is similarly relatively constant with depth. The system is convecting with the steam upflow rising from depth and flowing laterally along the

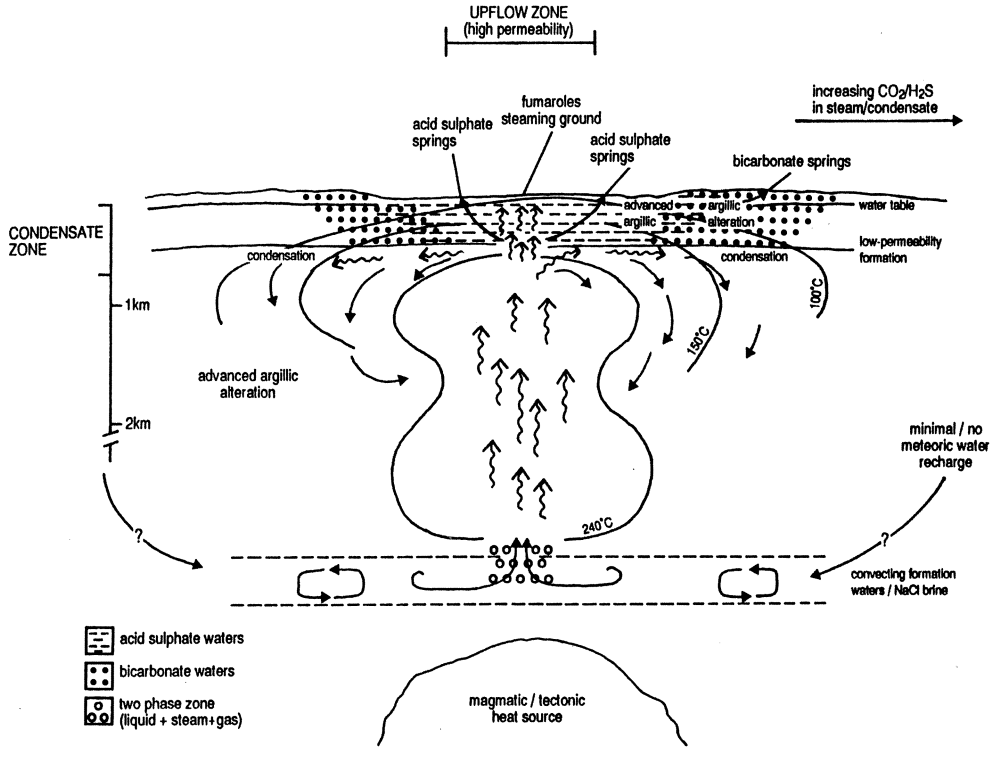

Figure 1.6. Conceptual structure of vapour-dominated geothermal systems. Note the consistency of the temperature-depth profile and the cycling of steam, through condensation, in the system.

base of the capping low-permeability rock horizon. The steam cools as it flows and eventually condenses and descends into the deep reservoir for recirculation. As less-soluble gases remain concentrated in the steam phase more readily than the more-soluble gases, the chemistry of the steam changes with the lateral flow and condensation (Chapter 3). Oxidation of hydrogen sulphide in the steam will produce acid condensates which dissolve the host rock, thereby increasing the size of the steam reservoir as the system matures. Vapour-dominated systems are much less common than liquid-dominated systems and only three have been well characterised: The Geysers, California, USA; Larderello, Italy and Kawah Kamojang, Indonesia.

CHAPTER 2

WATER CHEMISTRY

2.1 WATER TYPES

The most common type of fluid found at depth in high-temperature geothermal systems is of near-neutral pH, with chloride as the dominant anion. Other waters encountered within the profile of a geothermal field are commonly derived from this deep fluid as a consequence of chemical or physical processes. These waters, the characteristics of which are described below, are classified according to the dominant anions. Although not a formal genetic scheme, this descriptive classification does permit some generalisations to be made on the likely origins of the waters. Examples of the composition of the different water types are given in Table 2.1.

Chloride

Occurrence. This water type, also termed "alkali-chloride" or "neutral-chloride", is typical of the deep geothermal fluid found in most high-temperature systems. Areas which contain hot, large-flow springs with the greatest Cl concentration are fed more directly from the deep reservoir, and identify permeable zones within the field. However, these areas may not necessarily overlie the major upflow zone since the local topography can exert a significant control on the hydrology, as shown in Chapter 1.

Surface features. Chloride fluid is commonly discharged from hot springs and pools of good flow, and from most geysers. The water in deep pools appears clear and blue-green in colour - a distinctive features of chloride waters.

Chemistry. Chloride is the dominant anion, and usually attains concentrations in the thousands of mg/kg range, up to about 10,000 mg/kg. Less commonly, Cl levels exceed 100,000 mg/kg in more saline systems (eg. Salton Sea, California, USA). In such systems formation waters or seawater may have mixed with the original chloride fluid. Other main constituents include sodium and potassium (often in a ~10:1 concentration ratio), as the principal cations, with significant concentrations of silica (higher concentrations with increasing temperature at depth) and boron. Sulphate and bicarbonate concentrations are variable, but are commonly several orders of

magnitude less than that of chloride. The pH is invariably slightly acidic or alkaline, ie. near-neutral, at the temperature of measurement. Carbon dioxide and much lower levels of hydrogen sulphide, are the main dissolved gases. In fields with a high gas content, the chloride fluids may contain high levels of bicarbonate and boil at greater depths (Chapter 1). However, the high concentration of Cl prevents any confusion between these waters and the bicarbonate or dilute chloride-bicarbonate waters described below.

Alteration. Argillic-propylitic, with the following characteristic minerals: silica (amorphous silica, cristobalite, quartz) albite, adularia, illite, chlorite, epidote, zeolites, calcite, pyrite, pyrrhotite and base-metal sulphides. Sub-surface silicification is common.

Deposits. The discharge features are invariably surrounded by silica sinter, which provides a guide to extinct hot springs, pools and geysers, and to subsurface temperatures in excess of ~200°C. High-gas fields with significant bicarbonate concentrations can deposit an intimate mixture of sinter and travertine.

Application. These are the only spring waters which can be used with confidence in geothermometry. Hot, chloride springs of good flow usually indicate a highly permeable feed zone (eg. fault, eruption breccia pipe or conduit).

Sulphate

Occurrence. Also known as "acid-sulphate waters", these are invariably superficial fluids formed by the condensation of geothermal gases into near-surface, oxygenated groundwater. The gases, with steam and other volatiles, were originally dissolved in the deep fluid but separated from the chloride waters following boiling at depth. They are found on the margins of a field some distance from a major upflow area, at topographic levels high above the water table, in perched water tables and over boiling zones. Although usually found near the surface (<~100m), sulphate waters can penetrate to depth through faults into the geothermal system. Here they are heated, take part in rock alteration reactions and mix with the ascending chloride fluids (eg. many fields in the Philippines)

Surface features. These acid waters are often found in turbid (cloudy) pools or mud pools but may also occur as springs. As the separated steam contains a significant proportion of the enthalpy of the deep fluid, the steam-heated waters may boil at the water table to produce boiling mud pools and steaming ground. These hot, acid waters can dissolve rocks to form large collapse craters and caves (eg. Waiotapu, New Zealand) which often tend to plunge into the ground at an oblique angle rather than have a vertical aspect.

Chemistry. Sulphate is the principal anion, and is formed by the oxidation of condensed hydrogen sulphide

$$H_2S_{(g)} + 2O_{2(aq)} = 2H^+_{(aq)} + SO_4^{2-}{}_{(aq)}.$$

This reaction, and the condensation of carbon dioxide,

$$CO_{2(g)} + H_2O_{(l)} = H_2CO_{3(aq)} = H^+_{(aq)} + HCO_3^-{}_{(aq)} = 2H^+_{(aq)} + CO_3^{2-}{}_{(aq)}$$

produces protons, creating acid waters. The oxidation of hydrogen sulphide to sulphate ions produces a minimum pH of about 2.8. If waters are significantly more acidic than this (pH<2.0), a magmatic gas contribution is likely (see sulphate-chloride waters, below). Chloride occurs in trace amounts. Bicarbonate is either absent or at low concentrations since in very acid waters the dissolved carbonate is usually lost from solution as carbon dioxide gas (back-reaction of above equilibrium). Other volatile constituents which separate from the deep fluid on boiling may also condense into these waters (eg. NH_3, As, B) and attain significant concentrations. Near-surface reactions between the acid waters and the surrounding county rocks may leach silica and metal cations (Na, K, Mg, Ca, Al, Fe etc.) which can thereby attain high concentrations in the waters.

Alteration. Acid-sulphate waters react rapidly and leach the host rocks to produce advanced argillic alteration, with kaolinite, halloysite, crystobalite and alunite as diagnostic minerals. Extensive leaching of surface lithologies by these waters, or acidic steam, can produce silica residue. This must be differentiated from silica sinter, which is a product of depositional, not alteration, processes. Anhydrite, hematite, dickite, jarosite, pyrite, goethite-hematite mixtures and native sulphur are also commonly found.

Deposits. No extensive deposits usually form around springs discharging sulphate waters, though native sulphur, alunite and other sulphates may be present.

Application. Since the concentration of silica and most cations is only the product of near-surface leaching, such steam-heated waters cannot be employed in geothermometry as the concentrations of the dissolved constituents bear no relation to mineral-fluid equilibria in the reservoir. As gases migrate more directly to the surface than waters, the spatial distribution of acid-sulphate features and acid-alteration may identify areas overlying a permeable boiling zone. However, some caution is required in such interpretation, since the presence of a horizon which is impermeable to both waters and gases will cause lateral flow of both phases; under such circumstances the presence of acid discharge features may only indicate a thinning of this migration barrier.

Bicarbonate

Occurrence. These waters, which include those termed CO_2-rich fluids and neutral bicarbonate-sulphate waters, are the product of steam and gas condensation into poorly-oxygenated sub-surface groundwaters. Such fluids can occur in an umbrella-shaped perched condensate zone overlying the geothermal system, and are common on the margins of fields. Bicarbonate waters found in non-volcanogenic, high-temperature systems (eg. Turkey and Africa) are more problematic in origin and may constitute the deep reservoir fluid.

Surface features. Warm to hot springs and cool "soda" springs.

Chemistry. The waters are of near-neutral pH as reaction with the local rocks (either in the shallow reservoir or during lateral flow) neutralises the initial acidity of these waters (see above carbonate equilibrium). Loss of protons in such reactions produces near neutral waters with bicarbonate and sodium as the principal constituents. Sulphate may be present in variable amounts, with chloride at low concentrations or absent (Mahon et al., 1980a). These waters are highly reactive, and their corrosive action on well casings needs to be taken into account in the development of a field (Hedenquist and Stewart, 1985).

Alteration. Argillic alteration, with clays (kaolin, montmorillonite) and mordinite; some calcite and silicification may also occur.

Deposits. Extensive deposits of travertine ($CaCO_3$) can form around bicarbonate springs, and can be indicative of subsurface temperatures of below ~150°C. Aragonite can form if the surface discharge and cooling is very rapid.

Application. Although such fluids may discharge from equilibrated shallow and deep aquifers within high-temperature systems, they are of doubtful use in geothermometry. The geothermometer equations described in Section 2.5 have been derived from data on chloride fluid equilibria and their application to a completely different fluid type is questionable. Application of the NaKCa geothermometer to Na-HCO_3 fluids has been described as "troublesome" (Fournier, 1989a). Certainly, where these waters are formed by steam-heating/condensation, their chemistry is unrelated to equilibria in the deep reservoir fluid, making geothermometry inappropriate.

Sulphate-chloride

Occurrence. These waters can form by several processes, and the following have been suggested:

a) mixing of chloride and sulphate waters at variable depths

b) near-surface discharge and oxidation of H_2S in chloride waters

c) near-surface condensation of volcanic gases into meteoric waters
d) condensation of magmatic vapour at depth
e) passage of chloride fluids through sulphate-bearing sequences (eg. evaporites) or lithologies containing native sulphur.

Of these, waters formed by process (a) are probably the most usual, and it is these which are discussed below unless otherwise stated.

Surface features. Warm to hot springs.

Chemistry. These waters are typically of pH 2-5, with chloride and sulphate in approximately equal proportions. Waters formed by processes (c) and (d) can be recognised by the very high concentrations of Cl, SO_4 and, most diagnostic, high F. These waters may also be unusually acidic with pH 0-2; however, rock-water neutralisation reactions can raise the pH and mask this characteristic feature.

Alteration. A mixture of propylitic to advanced argillic-argillic; kaoline, silica residue, cristobalite, alunite, chlorite, calcite, adularia, anhydrite, pyrophyllite, smectites, goethite-hematite mixtures.

Deposits. May deposit poorly-developed, thin sinter and sulphate minerals. Waters that have passed through native sulphur at depth (process e) may remobilise the mineral and deposit distinctive yellow sulphur around the spring.

Application. It is often stated that as these fluids are a mixture containing the deep chloride fluid, geothermometry can therefore be applied with confidence. This is an erroneous argument since the composition of the mixed water will probably contain silica, sodium, potassium and other cations contributed by the acid component, and this will distort the results of solute geothermometry. Any application of geothermometers to mixed fluids must therefore be interpreted with caution.

Dilute chloride-(bicarbonate)

Occurrence. These waters are formed by the dilution of chloride fluid by either groundwater or a bicarbonate water during lateral flow. They are probably restricted to the margins of major upflow zones and outflow structures of high-temperature systems. They are often discharged from springs in low-temperature systems.

Surface features. Warm to hot springs.

Chemistry. Near-neutral waters, typically, pH 6-8 with chloride as the major anion with bicarbonate present but in variable concentrations.

Alteration. Chloride fluid type alteration assemblage, but poorly developed.

Deposits. Possibly a weak development of sinter or amorphous silica and/or travertine, perhaps acting as a cement to local lithologies, but often little or no deposits occur around the springs.

Application. If the chloride waters have only been diluted by groundwater, then geothermometry may be applicable. However, some discretion is needed since dilution will affect the silica geothermometer and the addition of bicarbonate may cause problems with the Na-K-Ca technique. In addition, during lateral flow, Li can be lost by adsorption and Mg can be added by near-surface reactions throwing into question the reliability of the Na/Li and K/Mg methods. Even if the application of geothermometers is suspect, the spatial distribution of these springs is important in understanding the hydrology of the system. In this respect it is important to recognise waters of this type as "dilute-chloride" and not refer to them as "bicarbonate" waters which are genetically very different. This point is made because the term "bicarbonate water" is often used in some reports in a casual manner to mean any spring waters containing significant bicarbonate, but not necessarily steam-heated in origin.

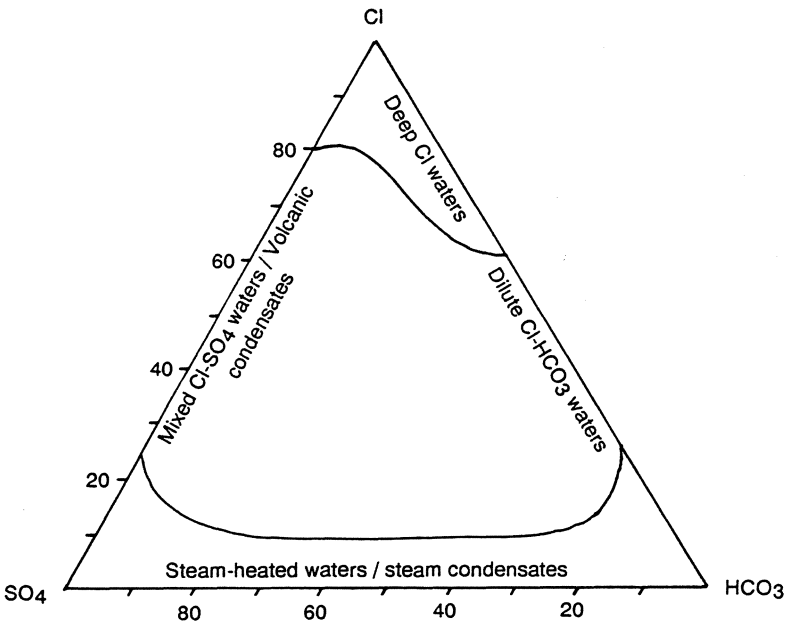

Figure 2.1. Ternary plot used to classify geothermal waters based on the relative proportions of chloride, sulphate and bicarbonate ions.

Table 2.1. Geothermal water discharge chemistry.

Field/ spring	t (°C)	pH (25°C)	Na	K	Mg	Ca	B	SiO_2	SO_4	HCO_3	Cl
			----------	----------	----------	----------	(mg/kg)	----------	----------	----------	----------
Chloride waters											
Wairakei, N.Z.											
Champagne Pool	99	8.0	1070	102	0.4	26	22	294	26	76	1770
Well 44 (surface)	-	8.4	1320	225	0.03	17	29	690	36	19	2260
Tauhara Spa, N.Z.											
Spring	95	8.0	820	59	--- 24 ---		24	169	62	44	1342
Ohaaki, N.Z.											
Ohaki Pool	95	7.1	860	82	0.1	2.5	32	338	100	679	1060
Cerro Prieto, Mexico											
Spring N29	89	7.6	5160	664	4.6	357	-	73	31	65	8790
Tongonan, Philippines											
Spring	98	8.3	1990	211	0.4	86	35	278	74	7	3397
Bacon-Manito, Philippines											
Pawa Spring	66	6.6	814	147	8.9	68	-	182	37	118	1418
Hveragerdi, Iceland											
Well G3 (surface)	-	9.6	212	27	<0.01	1.5	0.62	480	61	55	197
Seawater mixing											
Savusava, Fiji											
Spring	99	6.7	1100	45	3	1618	-	151	227	28	5392
Efate, Vanuatu											
E. Takara spring	66	7.0	4740	20	38	2560	-	215	170	-	10700
Morere, N.Z.											
Pool	62	6.7	6100	100	137	3900	-	28	25	21	16600
Puna, Hawaii											
Well 3 (30m)	89	6.4	2025	193	56	79	-	156	325	30	3684
Reykjanes, Iceland											
Well 8 (surface)	-	8.6	14920	2105	1.8	2320	12.2	898	44	2	28700
Seawater	-	8.2	10760	399	1290	411	4.5	5	2710	142	19350
Sulphate waters											
Waiotapu, N.Z.											
Spring	99	2.2	32	6.6	0.8	4.0	2	308	338	<1	6
Ngawha, N.Z.											
Tiger Bath	72	2.7	28	3.0	2.4	6.0	22	18	344	<1	37
Yellowstone, USA											
Norris Pool	70	2.2	27	24.0	1.0	2.6	1.5	364	482	<1	6
Tongonan, Philippines											
Kapakuhan Spring	65	2.9	17	10.4	5.3	102	0.1	130	582	<1	4
Bacon-Manito, Philippines											
Damoy Spring	25	2.8	13	4.2	7.9	17.2	0.3	112	334	<1	11.3
Vella Lavella, Solomon Is.											
Paraso Pool	48	2.5	1.3	0.6	1.8	2	-	168	1288	59	113
Bacon-Manito, Philippines											
Naghaso Lake	65	3.1	2890	360	3.4	200	24.9	328	42	-	4907

Table 2.1. Geothermal water discharge chemistry (continued).

Field/ spring	t (°C)	pH (25°C)	Na	K	Mg	Ca	B	SiO_2	SO_4	HCO_3	Cl
			(mg/kg)								
Bicarbonate											
Ohaaki, N.Z.											
Well 6 (surface)	-	7.4	435	39	90	180	1.2	180	15	2284	28
Well 32 (surface)	-	8.0	140	24	1.7	6.6	0.7	380	8	390	40
Ngawha, N.Z.											
Hotel well (120m)	58	7.4	131	10	37.2	94	12	128	48	704	67
Kamojang, Indonesia											
South spring	-	7.0	47	16	27	73	1.4	200	74	836	5
Well 9 (320m)	-	7.1	217	45	29	24	1.6	190	42	606	6
Well 8 (600m)	-	7.1	622	15	4.8	32	4.7	195	1400	342	13
Bali, Indonesia											
Angsri 1a	52	8.8	52	14	37.8	41	0.8	112	7	434	20
Angsri 1b	48	8.9	106	40	79.5	4.2	4.8	166	139	380	52
Belulang	48	8.9	217	67	203	1.8	4.1	142	133	1240	99
Njuling	38	8.8	266	84	158	2.4	8.4	157	17	879	373
Bacon-Manito, Philippines											
Balabagon	59	7.2	103	30	19.5	30	0.5	182	20.4	423	64
Kizildere, Turkey											
Well 14 (surface)	99	7.8	1172	117	1.2	6	25.6	268	778	2502	112
Spring	100	9.0	1260	125	0.1	1.2	23	185	750	2560	103
Sulphate-chloride											
Vanua Levu, Fiji											
Waiqele spring	96	6.5	200	4	0.02	156	-	73	550	26	147
Rotokawa, N.Z.											
Spring	65	2.4	990	102	11	11	45	340	520	144	1433
Volcanic gas condensates											
Mt Ruapehu, N.Z.											
Crater Lake	45	1.0	920	107	1430	1130	-	-	11375	<1	11496
	45	1.2	1110	202	1590	1540	15	585	16300	<1	12650
White Is, N.Z.											
Pool	-	2.0	7670	1000	7310	2560	6	180	10500	<1	61840
Kamiyama Cone, Japan*1											
Well (34m)	99	1.2	5000	-	4000	400	116	-	84000	-	68800
Biliran Is., Philippines*2											
Spring	80	1.4	475	163	24	44	90	-	9616	-	7651
Vanua Lava, Vanuatu*3											
Spring E11	87	1.4	144	35	27	120	50	380	3450	-	1345
Sulphur spring	83	1.5	170	44	2.0	112	-	540	2017	-	1080
Tatun, Taiwan*4											
Well 19 (95m)	161	2.0	146	58	53	205	46	419	3165	-	1620

Table 2.1. Geothermal water discharge chemistry (continued).

Field/ spring	t (°C)	pH (25°C)	Na	K	Mg	Ca	B	SiO_2	SO_4	HCO_3	Cl
			---------- (mg/kg) ----------								
Dilute chloride-bicarbonate											
Mokai, N.Z.											
North springs	-	6.3	245	13.0	1.2	9.4	3	130	8	155	274
	-	6.6	250	13.2	1.3	9.2	4	197	8	170	364
South spring	-	6.1	175	9.9	2.1	11.7	-	118	9	102	39
Rotokawa, N.Z.											
South bank springs	85	7.4	270	22	1.4	23	11.4	144	72	226	309
	90	6.6	380	32	0.8	30.0	16.3	182	103	173	477
North bank spring	65	7.1	210	21	0.63	12.8	2.9	260	59	282	155

Notes

- = no analysis; *1Fe 3770, Al 7140; *2Fe 371, Al 425; *3Fe 660, Al 682; *4Fe 778, Al 225

Additional compilations of water chemistry appear in Ellis and Mahon (1977) and Fournier (1981)

A diagnostic plot of water chemistry

Several graphical plots intended to classify geothermal waters have been presented in the literature. However, many of these divide the waters into several types which have little or no genetic or interpretive significance. The simple Cl-SO_4-HCO_3 ternary plot (Fig. 2.1) is to be preferred as it permits the identification of the above water types, and therefore some degree of genetic interpretation. It is easily constructed on triangular graph paper from the analytical data as follows:

1) sum the chloride, sulphate and bicarbonate concentrations

$$Cl + SO_4 + HCO_3 = \Sigma$$

2) calculate the relative proportion of each component of this sum as a percentage

$$\%Cl = (Cl/\Sigma)100$$
$$\%SO_4 = (SO_4/\Sigma)100$$
$$\%HCO_3 = (HCO_3/\Sigma)100$$

Note that in this diagram bicarbonate represents the total concentration of all carbonate species in the water. Alternatively, the plot can be generated from the data entered onto a spreadsheet computer program with a ternary plot template (Mustard and Richardson, 1990).

The plot aids the identification of the various water types, and assists in recognising waters which are most suitable for geothermometry (those closest to the Cl apex). Further, if data from the whole field area are plotted, then from the spatial position of spring and well discharges on the diagram, mixing trends and sub-surface flow directions can be identified.

2.2 PROCESSES AFFECTING WATER COMPOSITION

This section examines the chemical and physical processes which influence the composition of the geothermal fluid in the reservoir and as it ascends to the surface. The chemical processes centre around mineral-fluid reactions, both dissolution and deposition, while the dominant physical process is boiling, although conductive cooling and mixing are also important.

Mineral-fluid equilibria

The rock leaching experiments mentioned in Chapter 1 demonstrated that the common dissolved constituents in the deep chloride reservoir fluids fall into two groups based upon their solubility behaviour.

Soluble group species (Cl, B, Br, As, Cs) which readily pass into solution, often before appreciable alteration of the host rock has occurred. These tend to remain in solution and are considered to be unreactive or *conservative* species. This is really only true for Cl as the other species can be involved in near-surface reactions, notably with clay minerals.

Common rock-forming species (eg. SiO_2, Na, K, Ca, Mg etc) whose solubilities are controlled by temperature dependent mineral-fluid equilibria and only enter the solution after alteration of the host minerals.

Mineral-fluid equilibria therefore play a fundamental role in determining the chemistry of the discharge fluids. The reactions which take place are a function of the

temperature, pressure, salinity and host rocks of the geothermal system. There are two types of mineral-fluid reactions which need to be considered: dissolution-precipitation or solubility equilibria (eg. quartz, calcite) and ion-exchange equilibria (eg. Na and K between feldspars and micas). Relevant aspects of these reactions are therefore also considered in Sections 2.3 and 2.5. The product of mineral-fluid reactions is an assemblage of secondary alteration minerals. Hydrothermal alteration assemblages and their formation are discussed in more detail by Browne (1978) and Giggenbach (1981, 1984, 1988).

Solubility reactions

These determine how much of a particular species can enter and remain in solution before precipitation occurs. Examples of mineral solubilities which play a major role in determining geothermal fluid composition include quartz, calcite and anhydrite. Temperature is the dominant control on mineral solubility in geothermal systems, but changes in pH, pressure or salinity can also have an effect. In most geothermal systems, the solubility of minerals follows one of three behaviour patterns:

1) mineral solubility increases with increasing temperature (eg. alkali metal chlorides)
2) mineral solubility decreases with increasing temperature; known as *retrograde* solubility (eg. gypsum, anhydrite, calcite)
3) mineral solubility increases with increasing temperature but only to a maximum value and then decreases with further temperature rises (eg. silica).

Silica and calcite equilibria are particularly important in geothermal systems as they govern the amount of SiO_2 and Ca in solution, and are two of the main causes of scaling in wells.

Silica: The solubility of any silica mineral (quartz, chalcedony etc.) can be written as

$$SiO_{2(s)} + 2H_2O_{(l)} = H_4SiO_{4(aq)} = H_3SiO_4^-{}_{(aq)} + H^+{}_{(aq)}$$

and the solubility constant is given by

$$K_{SiO2} = a_{H4SiO4}$$

Silicic acid is a weak acid and dissociates to yield hydrogen ions. If the pH of the solution is increased (ie. becomes more alkaline) then the solubility of silica will also increase as the hydrogen ions are consumed by reactions such as

$$HCO_3^-{}_{(aq)} + H^+{}_{(aq)} = H_2CO_{3(aq)} = H_2O_{(l)} + CO_{2(g)}$$

The solubility of silica, and its temperature dependence is fully discussed in Sections 2.3 and 2.5.

Calcite: Geothermal reservoir fluids are commonly close to saturation with respect to calcite (Arnorsson, 1989). Calcite is not, however, found in some fields where temperatures exceed ~300°C. The solubility of calcite can be expressed by the equation

$$CaCO_{3(s)} + H_2O_{(l)} + CO_{2(g)} = Ca^{2+}_{(aq)} + 2HCO_3^-{}_{(aq)}$$

Calcite solubility therefore increases with increasing P_{CO_2} (up to mCO_2 ~ 1mole/kg, Fournier, 1985). The lowering of P_{CO_2} on boiling, as carbon dioxide is lost to the steam phase, increases the pH of the solution and leads to supersaturation and precipitation of calcite. As carbon dioxide has a minimum solubility around 160-180°C, boiling near this temperature can lead to greatest calcite saturation. Further boiling, after CO_2-degassing, lowers the temperature of the liquid phase, and leads to an increase in calcite solubility (the solubility of calcite increases with decreasing temperature, Fig. 2.2). It is for this reason that calcite deposition is most intense around boiling zones within geothermal systems - a useful guide in the interpretation of epithermal mineralisation, but a serious scaling problem if boiling occurs in wells in the exploitation of a geothermal resource. Cooling of a solution, by boiling or conduction, leads to greater undersaturation with respect to calcite and other carbonate minerals. To summarise, calcite solubility is increased by: decreasing temperature (Fig.2.2), increasing CO_2 partial pressure (Fig.2.2) and increasing salinity (Fig.2.3).

Ion-exchange reactions

These involve the transfer of ions between two or more aluminosilicate minerals and control the ratios of cations in solution, including H+. This means that solution pH can be buffered by a silicate mineral assemblage. Observations on geothermal alteration assemblages show that the majority of secondary minerals are formed by reactions such as:

albite - K-feldspar

$$NaAlSi_3O_{8(s)} + K^+_{(aq)} = KAlSi_3O_{8(s)} + Na^+_{(aq)}$$

$$K = a_{Na}/a_K$$

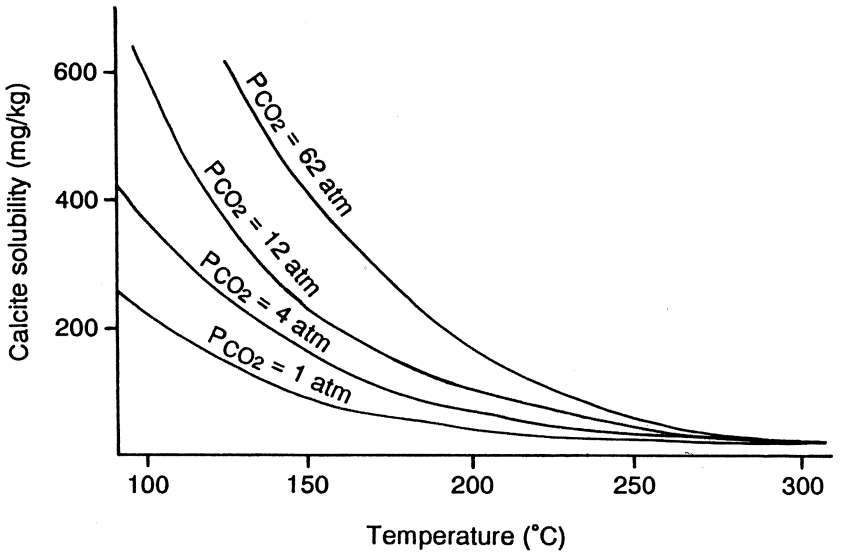

Figure 2.2. Changes in the solubility of calcite ($CaCO_3$) in water with temperature and the partial pressure of carbon dioxide.

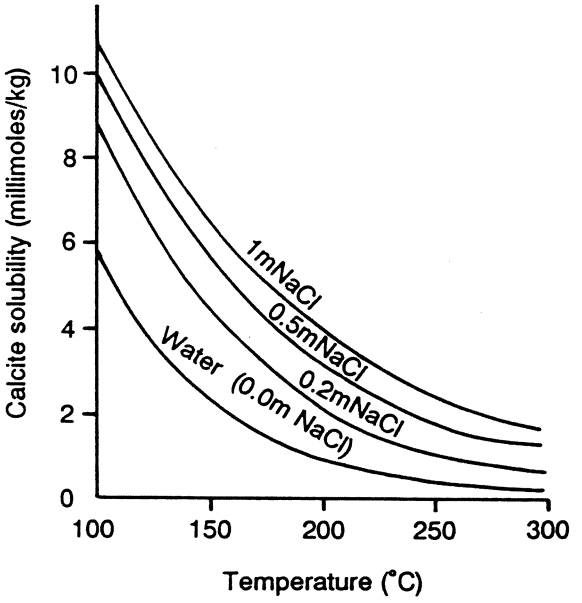

Figure 2.3. Changes in the solubility of calcite ($CaCO_3$) in water with temperature and salinity at P_{CO_2} = 12 atm.

K-feldspar - K-mica + quartz

$$3KAlSi_3O_{8(s)} + 2H^+_{(aq)} = KAlSi_3O_{10}(OH)_{2(s)} + 6SiO_{2(s)} + 2K^+_{(aq)}$$

$$K = a_K/a_H$$

wairakite - Ca-montmorillonite + quartz

$$1.17CaAl_2Si_4O_{12}.2H_2O_{(s)} + 2H^+_{(aq)} = Ca_{0.17}Al_{2.33}Si_{3.7}O_{10}(OH)_{2(s)} + SiO_{2(s)} + 2H_2O_{(l)} + Ca^{2+}_{(aq)}$$

$$K = a_{Ca}/a_H^2$$

The above equations show reactions between minerals and the liquid phase. Reactions can however also occur between minerals and gases, and the reaction of iron sulphide with hydrogen and hydrogen sulphide illustrates mineral-gas buffering reaction:

pyrite-pyrrhotite

$$FeS_{2(s)} + H_{2(g)} = FeS_{(s)} + H_2S_{(g)}$$

$$K = P_{H_2S}/P_{H_2}$$

Activity diagrams

In addition to writing the equilibrium or mass action constant for reactions such as those shown above, it is also possible to calculate the free energy change (ΔG) for each reaction using the expressions

$$\Delta G_{reaction} = \Delta G_{f,products} - \Delta G_{f,reactants}$$

and

$$\Delta G = -RT\ln K$$

Values for the free energies of minerals and aqueous species at different temperatures can be obtained from tables of thermochemical data (eg. Helgeson et al., 1978). These calculations can be used to construct mineral stability or activity diagrams such as that shown in Fig. 2.4. The construction of these diagrams is described by Henley et al. (1984). However, in both interpreting and drawing activity diagrams, several points should be remembered:

- the enclosed areas show the conditions under which the minerals are stable
- the slope of the boundary lines depends on the stoichiometry of the reaction

- the position of the boundary lines is determined by the equilibrium constant, which in turn is determined by the free energy change of formation of the reactant and products

These diagrams enable comparisons to be made between the observed mineral assemblage and the fluid chemistry which can be useful in evaluating any chemical changes as the fluids evolve (eg. Browne and Ellis, 1970). They are, however, only tools to aid interpretation and must make geological sense! Where significant discrepancies between predicted and observed stabilities exist, the possible reasons for the differences may lie in the data quality. In this respect, several points are relevant:

- the reliability of the diagram is dependent upon the quality of the thermodynamic data
- minerals with complex and variable compositions (eg. clays) are poorly represented by a single ΔG_f value
- grain size and crystallinity can also influence ΔG_f values
- diagrams are only valid for fixed conditions of temperature, and solute concentration

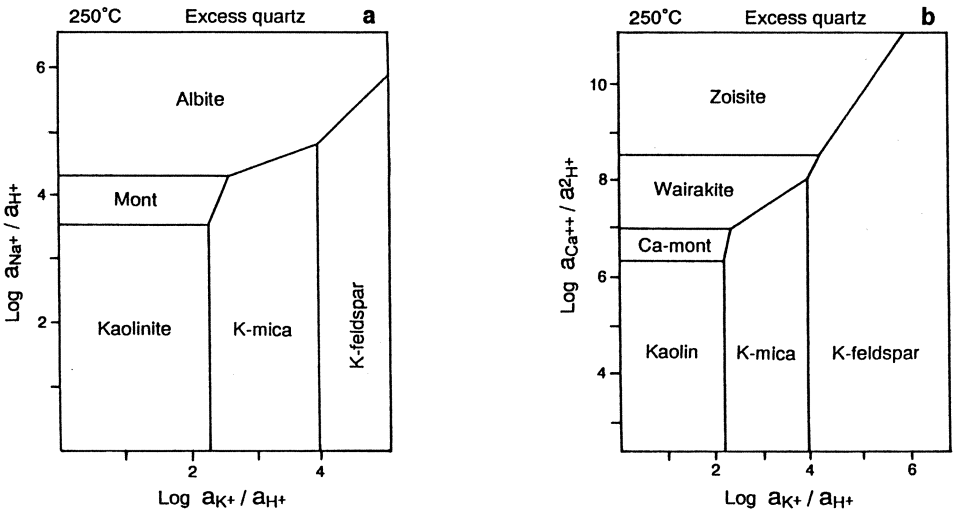

Figure 2.4. Mineral stability or activity diagrams (from Henley and Brown, 1985). (a) for the system Na_2O-K_2O-Al_2O_3-SiO_2-H_2O; (b) for the system CaO-K_2O-Al_2O_3-SiO_2-H_2O. The diagrams are drawn for conditions at 250°C with excess quartz present. They show the conditions under which each mineral is stable, and can be used to predict what happens to mineral stability if, for example, a_{H+} decreases.

Computer programs have been written which will calculate activity diagrams for the temperatures and minerals of interest. These programs can also calculate the speciation of solutes (eg. Arnorsson et al., 1982) under reservoir (ie. reaction) conditions.

Boiling (adiabatic) cooling

When a geothermal fluid rises to the surface it may boil due to reduced hydrostatic pressure; where the flow rate is high, cooling can be considered to be approximately adiabatic. On boiling, gases and other volatile species partition into the vapour ("steam") phase and move independently of the residual liquid water phase. This loss of steam, and therefore mass, produces a proportional increase in the concentration of the dissolved aqueous constituents. This change in concentration can be determined from mass-balance calculations (Section 2.6). The reactions discussed above give some indication of the dramatic change in fluid chemistry caused by boiling. For example, upon boiling, carbon dioxide is lost from the liquid phase and this creates a rise in liquid pH, an increase in silica solubility, and an initial fall in calcite solubility. The amount of steam formed from a given deep fluid varies sightly depending upon whether phase separation occurs in a single step, or continuously as the pressure is reduced (Chapter 3; Fournier, 1979b; Truesdell et al., 1977).

Springs which discharge waters which have cooled only by boiling are most useful for geothermometry and mixing-model applications. This is because the waters have had little time to engage in rock-water reactions, and the composition of the discharge closely reflects that of the reservoir fluid after correction for steam-loss. Such springs can be recognised by a high mass flow rate (> ~1-3 L/s), and temperatures at, or near, the local boiling point.

Conductive cooling

If a fluid ascends to the surface only slowly, it may have sufficient time to lose heat by conduction to the cooler host rocks. As no steam will have been lost by boiling, then the concentration of chloride will be about the same as in the reservoir feeding the spring. The concentration of other solutes would be the same as that in the reservoir too if the water did not react with the rocks as it ascended. Unfortunately, rock-water reactions, both with the primary minerals and secondary alteration products, are likely to occur as the water moves to the surface at a slow rate. This gives plenty of time for reactions to take place and change the original composition of the water. It is therefore important to be able to recognise springs

discharging conductively cooled waters, as these are unsuitable for geothermometry. Characteristic features include a low flow rate (<~0.5L/s) and groups of springs all with similar chloride concentrations, but different temperatures

Mixing (dilution) with other waters

The deep geothermal fluid may mix with cold groundwater before being discharged in a spring or well. Since such meteoric waters are usually less saline than the geothermal fluid, this process is also known as ***dilution***. In the interpretation of spring and well water chemistry it is important to recognise mixed fluids, and criteria which can indicate that dilution by meteoric water has occurred have been developed by Fournier (1979, 1981) and Arnorsson (1985); see box below.

Although dilution of the deep fluid with cold meteoric waters is the situation most commonly considered, mixing with steam-heated and other shallow-reservoir thermal waters can also occur. In such cases mixing may be indicated by plots of Cl vs SiO_2 and Cl vs SO_4. To be confident in any interpretation of mixing, groups of springs should be examined (rather than looking at the chemistry of isolated discharges) and the results related back to the spatial (geographic) distribution of the springs. These mixing-dilution processes are often best illustrated by the use of mixing models (Section 2.4).

2.3 INTERPRETATION OF WATER CHEMISTRY

In the interpretation of water chemistry, it is important to realise that not all springs will yield reliable information about the conditions at depth. As discussed above, hot or boiling chloride springs with a strong outflow have invariably experienced the least contamination, and are therefore most suitable for reservoir-related investigations. It is useful however, to record the composition of spring discharges across the whole field, since the spatial distribution of different water types can reveal details on sub-surface processes and hydrology. Early reviews of water chemistry, and how it may be interpreted, provide valuable insights into the development of key ratios which act as indicators to sub-surface conditions and processes. Accounts by Ellis (1970), Mahon (1970, 1976), Mercado (1970), Tonani (1970), Truesdell (1976) and White (1970) are still worth reading as they cover aspects of interpretation often not explained in more recent literature.

Criteria for the recognition of mixed fluids

1. high concentration of silica relative to the discharge temperature
2. variations in chloride concentrations of boiling springs too great to be explained by steam loss alone
3. low pH relative to the water salinity (often 6-7 for Cl<100mg/kg)
4. high total carbonate, if mixing preceded boiling and the deep geothermal fluid temperature exceeds 200°C
5. low Ca/H^+ ratio compared to that of the geothermal fluid
6. water undersaturated with respect to calcite
7. high Mg concentration
8. cool springs with large flow rates which are too great to be compatible with conductive cooling
9. temperatures indicated by geothermometers much higher (>50°C) than measured temperatures (eg. Fournier et al., 1979)
10. systematic meteoric/seasonal (temporal) variations in spring compositions and temperature (eg. Fournier, 1989b).
11. plots of conservative elements for a group of springs show a near-linear relationship (eg. Cl vs B)
12. variations in oxygen and hydrogen isotopes (eg. $\delta^{18}O$ vs δD; Cl vs $\delta^{18}O$)
13. variations in major cation concentrations (especially K) due to leaching and/or adsorption after mixing. (Can be significant where mixing prevents boiling resulting in $CO_2(aq)$ being converted to HCO_3)

pH

The pH of surface geothermal waters is principally determined by the loss of carbon dioxide on boiling which causes the solution to become progressively more alkaline. However, pH is also influenced by the fluid salinity and temperature and by mineral buffers. The pH of the reservoir fluid can be calculated by several methods; these are discussed, along with other calculations on reservoir chemistry, in Section 2.6.

Temperature

The value of neutral pH varies with temperature, as the pH scale is based on the ionisation of water, a temperature-dependent equilibrium. This is particularly

important when considering whether a fluid is acidic or alkaline at reservoir temperatures. At normal ambient temperatures, pH7 is considered as the neutral pH. This is convenient, if not absolutely correct, and is so commonly used that it is often forgotten that neutral pH varies with temperature. At the surface, neutral pH may be about pH7, but in the high-temperature reservoir it will lie around pH5.5, which means that high-temperature fluids with pH>~5.5 will be alkaline. The reason for this shift in the neutral pH can be explained by considering the water dissociation equilibrium on which the pH scale is based.

$$H_2O_{(l)} = H^+_{(aq)} + OH^-_{(aq)}$$

$K_w = a_H.a_{OH}$

This is a temperature dependent equilibrium. The amount of water which dissociates is very small, and the reaction lies strongly to the left. For example,

$K_w = 10^{-13.99}$ at 25°C

Rather than use such an inconvenient notation, the dissociation is often expressed in terms of pK_w where

$pK_w = -\log K_w$ and therefore at 25°C

$pK_w = 13.99$ a much more convenient way to express K_w.

Values of the water dissociation constant (as pK_w) 0 - 300°C							
t°C	0	10	25	50	75	100	125
pK_w	14.94	14.54	13.99	13.27	12.71	12.26	11.91
t°C	150	175	200	225	250	275	300
pK_w	11.64	11.44	11.30	11.22	11.20	11.22	11.30
Neutral pH at any temperature = $pK_w/2$							

Neutral pH occurs when the activity of both the hydrogen and hydroxyl ions are balanced, ie.

$a_H = a_{OH}$

therefore as $K_w = a_H.a_{OH}$, this mean that *at neutral pH*

$K_w = a_H^2$ or

$pK_w = 2(-\log a_H)$

as $pH = -\log a_H$, this can be substituted into the equation to give

$pK_w = 2pH_{neutral}$

re-arranging this expression, then the neutral pH is determined from

$$pH_{neutral} = pK_w/2$$

As values of pK_w for 0 - 300°C have been determined (see box), neutral pH at any temperature can be found by dividing pK_w by 2. For a fluid with a given salinity, an increase in temperature will produce a lower pH as more water dissociates.

Salinity

Mineral-fluid reactions can buffer the fluid pH by consuming protons. One such equilibrium is the alteration of K-feldspar to K-mica and quartz:

$$3KAlSi_3O_{8(s)} + 2H^+_{(aq)} = KAlSi_3O_{10}(OH)_{2(s)} + 6SiO_{2(s)} + 2K^+_{(aq)}$$

$$K = a_K/a_H$$

Other similar reactions are shown below and in Section 2.2. If the salinity of the fluid increases (ie. higher concentrations of Na, K, Cl etc.), then the law of mass action dictates that the above equilibrium will shift to the left. This shift will increase the amount of H^+ in solution, thereby causing a fall in fluid pH (Ellis, 1968, 1969). Although these reactions are written assuming aluminium is immobile in solution (not true), it is convenient to accept this limitation to illustrate the pH-salinity relationship. All other factors (eg. temperature) being equal therefore, greater fluid salinity produces a lower pH.

Gas content

As gases are lost from solution on boiling, the pH of the residual liquid increases. This is largely due to the consumption of hydrogen ions as carbon dioxide exsolves into the steam phase. The reaction can be expressed by the equilibrium:

$$HCO_3^-{}_{(aq)} + H^+_{(aq)} = H_2CO_{3(aq)} = CO_{2(g)} + H_2O_{(l)}$$

As carbon dioxide is lost from the liquid, the equilibrium will move to the right, consuming protons and thereby increasing the solution pH.

Mineral buffers

The fluid pH (hydrogen ion activity) can be buffered by reactions with silicate minerals. Examples of such mineral-buffering reactions include (Fournier, 1985):

wairakite - Ca-montmorillonite + quartz

$$1.17CaAl_2Si_4O_{12}.2H_2O_{(s)} + 2H^+_{(aq)} = Ca_{0.17}Al_{2.33}Si_{3.7}O_{10}(OH)_{2(s)} + SiO_{2(s)} + 2H_2O_{(l)} + Ca^{2+}_{(aq)}$$

analcime - Na-montmorillonite + quartz

$$2.33NaAlSi_2O_6.H_2O_{(s)} + 2H^+_{(aq)} = Na_{0.33}Al_{2.33}Si_{3.7}O_{10}(OH)_{2(s)} + SiO_{2(s)} + 2H_2O_{(l)} + 2Na^+_{(aq)}$$

K-mica - kaolinite

$$2Al_3Si_3O_{10}(OH)_{2(s)} + 3H_2O_{(l)} + 2H^+_{(aq)} = 3Al_2Si_2O_5(OH)_{4(s)} + 2K^+_{(aq)}$$

Common solutes

The deep reservoir chloride fluids of most geothermal systems tend to have similar dissolved constituents (solutes). However, solute concentrations will vary greatly, and these differences are due to variations in temperature, gas content, heat source, rock type, permeability, age of the system and fluid source or mixing (eg. with seawater).

Anions: Cl^-, HCO_3^-, SO_4^{2-}, F^-, Br^-, I^-

Cations: Na^+, K^+, Li^+, Ca^{2+}, Mg^{2+}, Rb^+, Cs^+, Mn^{2+}, Fe^{2+}

Neutral: SiO_2, NH_3, As, B, Noble gases

In general, both in text and tabulation of analyses, the following notes apply:

- the charge on the species is dropped for convenience.
- bicarbonate (HCO_3^-) often represents "total carbonate" (ie. $[HCO_3^- + CO_3^{2-} + CO_{2(aq)}]$, note that $CO_{2(aq)}$ is also written as H_2CO_3).
- boron may also be expressed as HBO_2^-, H_2BO_3

Chemical behaviour of common species

Neutral Species

Silica (SiO_2)

Silica concentrations in the geothermal fluid are controlled by the solubility of the different silica minerals and are usually <700 mg/kg, with values of 100-300 mg/kg being typical. Fournier and co-workers have examined the solubility of various silica species for over thirty years (Fournier, 1983; Fournier and Marshall, 1983; Fournier and Potter, 1982a,b; Fournier and Rowe, 1966; Morey et al., 1962) while Rimstidt and Barnes (1980) have studied the kinetics of silica dissolution and precipitation. A review of silica geochemistry is given by Fournier (1985). Silica can

occur in various forms or polymorphs (quartz, chalcedony, cristabolite, opal, amorphous silica) each of which shows slight variations in solubility (Fig. 2.5). The behaviour of quartz and amorphous silica are of most interest in geothermal studies as these determine the dissolution and precipitation of silica, although chalcedony is important in some systems (e.g. Iceland). In unusual circumstances, where the pathway changes to expose the fluid to volcanic glass or rocks rich in cristobalite, these very soluble silica polymorphs will control the concentration of silica in solution until they are dissolved, thereby distorting any silica geothermometry temperatures. The approximate solubility of silica minerals in liquid water at the vapour pressure of solution at a given temperature can be calculated from the geothermometry equations presented in Section 2.5. Equations for silica solubility as a function of pressure, salinity and specific volume of the solvent are given in Fournier (1985).

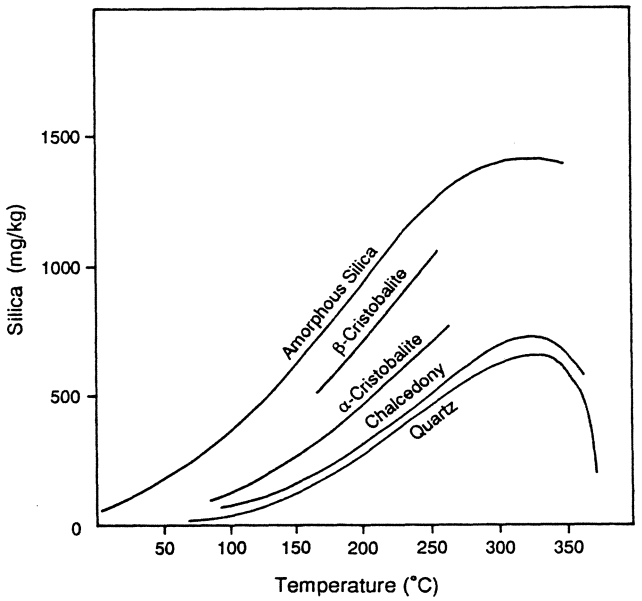

Figure 2.5. Variations in the solubility of silica phases in water at the vapour pressure of solution with temperature. A = amorphous silica; O = opal-CT; Cr = a-cristobalite; Ch = chalcedony; Q = quartz. Note that opal-CT was initially incorrectly identified as b-cristobalite (Fournier, 1985).

At depth, in reservoirs with temperatures in excess of 180°C, and even for many above 90°C, the concentration of silica in solution is determined by the solubility of

quartz (Fournier, 1985). However, as chalcedony has a higher solubility then quartz, this is often found to control silica concentrations in solutions at reservoir temperatures below about 140°C. The solubility of quartz, in liquid water at the vapour pressure of solution, increases from 6.1 mg/kg at 20°C to a maximum of 770.1 mg/kg at 340°C, and then falls to 299.6 mg/kg at 374°C, the critical point of water (Fournier and Potter, 1982a). This maxima in quartz solubility is illustrated as a function of enthalpy in Fig. 2.6. Increases in the salinity of the solution cause only slight decreases in the solubility of silica minerals at temperatures to 300°C (Fournier and Marshall, 1983). Pressure also has little effect up to about 300°C, but can influence quartz solubility above this temperature. For example, at 300°C when the pressure is increased from the vapour pressure of the solution to 1000 bars, the solubility of quartz increases by about 36% (Fournier, 1985).

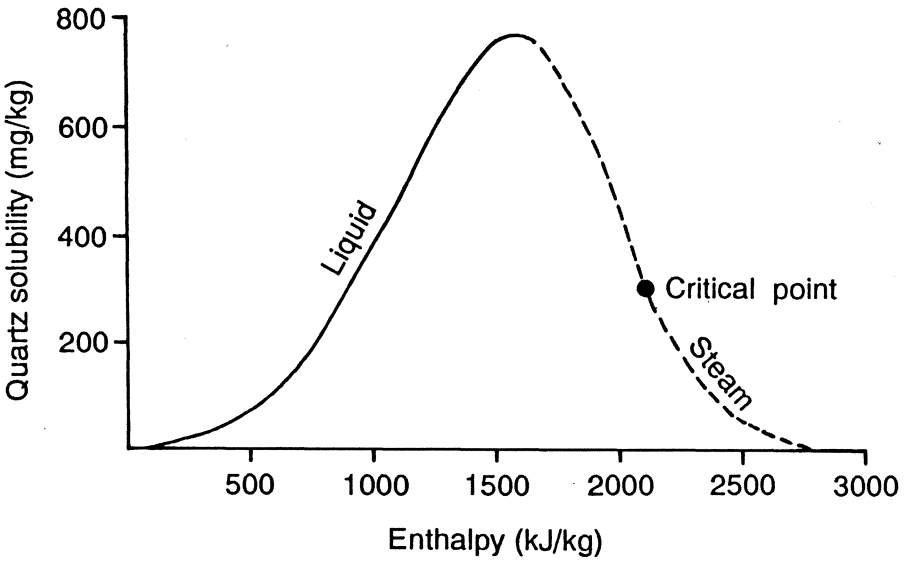

Figure 2.6. Changes in the solubility of quartz in water at the vapour pressure of the solution with enthalpy.

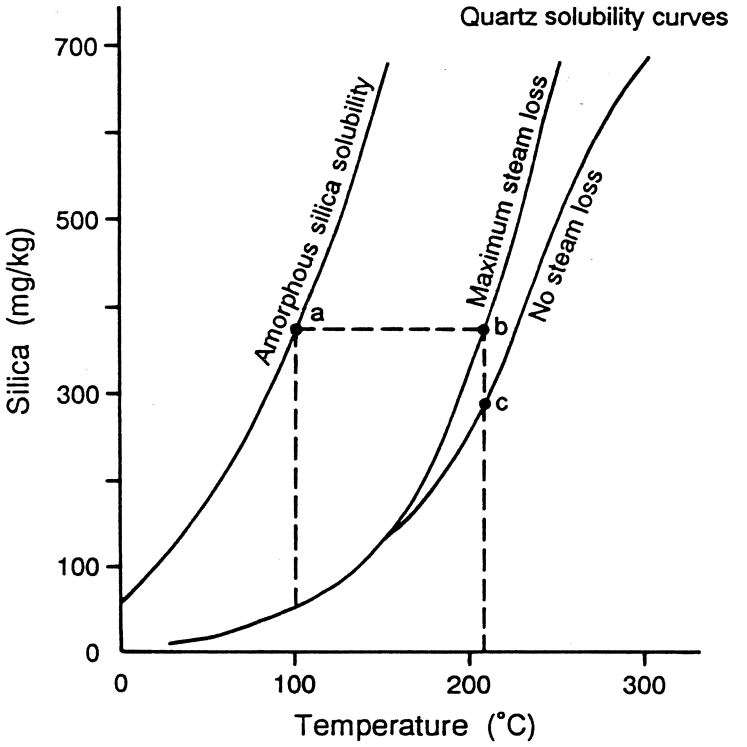

Figure 2.7. Solubilities of amorphous silica and quartz (curve Q_C) at the vapour pressure of the solutions with respect to temperature. Curve Q_B is a correction to curve Q_C and shows the concentration of dissolved silica that would be present after flashing (boiling) to 100°C from the initial fluid temperature (ie. from point c to point b). The dashed line (a-b-c) shows the concentration of silica in the reservoir, and the reservoir temperature of 210°C, for a spring boiling at 100°C and depositing silica. Springs depositing silica sinters must therefore discharge from a reservoir with temperatures in excess of 200°C.

The dissolution and precipitation of silica are kinetically rapid processes, and as quartz solubility below 340°C greatly decreases with falling temperature (from 770mg/kg at 340°C to about half this concentration, 336mg/kg at 220°C), it is likely that as the fluid ascends to the surface and cools by conduction or boiling, silica will deposit at depth in the fluid channels. This coating of silica can effectively seal the wall rock from any further reaction with the fluid, preventing leaching, mineral

alteration and the establishment of chemical and isotopic fluid-rock equilibrium. Silica precipitation may also be prompted by cooling induced by mixing of the hot fluid with cooler waters in the upper sections or on the margins of the field (Mahon et al., 1980a).

The deposition of amorphous silica at the surface requires silica supersaturation with respect to quartz. As high-temperature reservoir fluids ascend, they cool and pass from saturation with respect to quartz (and undersaturation with respect to amorphous silica) to supersaturation with quartz and eventually with amorphous silica. Rapid cooling caused by boiling is the most usual process to cause silica supersaturation, but other processes such as mixing and reaction with volcanic glass can have the same result. If a fluid ascends rapidly to the surface, the concentration of silica in the water will be increased through boiling and loss of steam. Assuming little or no deposition of silica on ascent, then the water discharging from the boiling spring (100°C) will be just saturated with respect to amorphous silica when reservoir temperatures are at 210°C or more (see Fig. 2.7). Thick sinters only form around springs which discharge water at, or close to, boiling point (ie. about 80-100°C), their presence therefore (from Fig. 2.7) indicates reservoir temperatures in excess of about 200°C. Of course, soft amorphous silica does deposit from warm springs, but these do not produce hard sinters. Fig. 2.7 shows that for even minor amounts of amorphous silica to deposit, the reservoir temperature must be at least ~110°C.

Ammonia (NH_3)

Ammonia, either as the gas (NH_3) or the solute (ammonium ion, NH_4^+) is a common, though relatively minor, constituent of geothermal fluids. High levels of NH_3 can be the product of steam heating, as the gas condenses out of the vapour phase and high NH^{4+}/B ratios have been used to indicate the amount of steam heating of near-surface fluids, the ratio increasing with increased steam-heating (Duchi et al., 1987a,b) However, high concentrations can also be found in deep fluids associated with sedimentary horizons. Check the B, I and SO_4 concentrations to see which cause is most likely. The ammonium ion can substitute for potassium alteration minerals.

Arsenic (As)

Recent work by Ballantyne and Moore (1988) and Webster (1989) has shown that arsenic occurs in the reduced As(III) state in the reservoir fluid, and that As(III) is also present in hot spring waters. Once all the available sulphide has been oxidised to

sulphate, then As(V) appears in the hot spring discharges together with As(III). However, the concentration of As(V) is small; Webster (1990) reports that 97-100% of the arsenic in New Zealand hot spring discharges is present as As(III). In solution, arsenic occurs predominantly as the uncharged species, arseneous acid (H_3AsO_3), and as arsenic acid (H_3AsO_4).

Boron (B)

Also expressed as boric acid H_3BO_3 or HBO_2^-, boron is an important diagnostic species in geothermal studies. Spring and well discharges of chloride fluids usually contain 10-50mg/kg B, but very high concentrations of boron (~800-1000 mg/kg) are found in waters associated with organic-rich sedimentary rocks. Waters from andesitic host rocks have higher boron levels than those associated with other volcanics. The Cl/B ratio is often used to indicate a common reservoir source for waters. However, some caution is required in applying this interpretation, since waters from the same reservoir can show differences in this ratio. These differences can be induced by a change in lithology at depth over a field (eg. the introduction of a sedimentary horizon), or by the adsorption of B onto clays during lateral flow. In some sedimentary-hosted reservoirs, boron can be contributed by the leaching of evaporitic sequences.

Noble gases

The noble gases (argon, Ar; helium, He; krypton, Kr; neon, Ne; xenon, Xe) are largely of atmospheric origin, being contributed to the geothermal system through the meteoric recharge waters. Surface waters and rain dissolve and attain equilibrium with the atmospheric gases in a matter of minutes (Mazor, 1977). The amount of the atmospheric gases dissolved depends upon the ambient temperature, salinity and air pressure ie. the altitude. Argon, Kr and Xe show a significant temperature dependence, but this is less marked with He and Ne. Noble gas solubility decreases with increasing total dissolved salts, but as most geothermal systems contain only dilute fluids this effect can be neglected (but not, of course, if sea-water or formation waters are involved in the system). Seasonal and diurnal changes in barometric pressure have a negligible effect on gas solubilities (Mazor, 1977). Helium and argon can also be radiogenic in origin: ^4He is formed by the decay of uranium and thorium, while the decay of ^{40}K produces ^{40}Ar. The isotopes enter into the fluid by rock-water reactions, direct magmatic input or by leakage of the gases from the mantle. The gases remain in the liquid phase until boiling occurs, after which they enter quantitatively into the steam phase and the residual waters become heavily depleted in

noble gases. The concentration of the gases dissolved in spring and well discharges can therefore be used as indicators of a meteoric origin for the geothermal fluids, of near-surface mixing and of boiling episodes and can aid recognition of a past thermal history for cold spring waters (Mazor, 1977).

Argon: Argon from the atmosphere displays a $^{40}Ar/^{36}Ar$ ratio of 295.6; thermal waters which show a greater value contain radiogenic ^{40}Ar.

Helium: As dissolved atmospheric helium cannot exceed ~ 5 x 10^{-8} cm^3 STP He/ cm^3 water (Mazor, 1977), greater concentrations are attributed to the addition of radiogenic ^4He.

Radon, Rn: This is the heaviest noble gas. It differs from the others in that it is radioactive, and is only radiogenic in origin. Several isotopes of radon exist, but ^{222}Rn is the longest-lived with a half life of 3.8days. It forms part of the ^{238}U-^{206}Pb series, and itself decays by alpha-particle emission to polonium-218.

Cations

Sodium and potassium (Na^+, K^+)

The concentration of these cations is controlled by temperature dependant mineral-fluid equilibria, which form the basis of the Na/K geothermometer (Section 2.5). Sodium is the major cation in geothermal reservoir fluids, with concentrations of ~200-2000 mg/kg. Potassium is also a major cation, but is present at lower levels than sodium. As a rough guide, K concentrations are typically about a tenth those of Na. The Na/K ratio is a useful guide to high-temperature zones (lower ratio, higher temperature). Iso-Na/K lines often correlate with iso-Cl lines, and can be interpreted in the same manner. Lower Na/K ratios (~<15) tend to occur in waters which have reached the surface rapidly, and are therefore associated with upflow structures or more permeable zones. Higher ratios are indicative of lateral flow, near-surface reactions and conductive cooling.

Lithium, rubidium, caesium (Li^+, Rb^+, Cs^+)

Collectively termed the "rare alkalis", these elements are regarded as part of the soluble or conservative species group, and are often used with Cl and B to characterise waters from common sources. They are however, readily incorporated into secondary, alteration minerals and often show a decrease in concentration with increasing migration to the surface, and with increased lateral flow. Typical concentration levels are around Li <20 mg/kg, Rb <2 mg/kg, Cs<2 mg/kg. Lithium is

taken up into chlorite, quartz and probably also onto clays in near-surface reactions causing an increase in the B/Li ratio with increasing lateral flow (Duchi et al., 1987a,b). Adularia and illite show a slight uptake of caesium, but the element is particularly concentrated into zeolite minerals such as wairakite. Rubidium is concentrated into illite and to a lesser extent, adularia, but may also be adsorbed onto clays and zeolites (Goguel, 1983).

These elements attain greatest concentration (of the order of 1-10 mg/kg) in areas with host rocks of rhyolitic and andesitic composition (including sedimentary environments with similar rock chemistry), and are significantly lower (~ <0.1 mg/kg) in fluids from basaltic areas (Ellis, 1979).

Calcium (Ca^{2+})

Calcium concentrations are controlled by minerals of retrograde solubility ($CaCO_3$, eg. calcite; $CaSO_4$, eg.anhydrite; CaF_2, fluorite), and to a lesser extent by Ca-rich aluminosilicates. Factors which affect the solubility of these minerals will also influence the level of Ca in the geothermal fluid. P_{CO_2} is particularly important in this respect, and calcite often precipitates in response to a loss of CO_2 on boiling. Calcium concentrations are usually at low levels in high-temperature fluids (<~50 mg/kg), but increase with both acidity and salinity. The Na/Ca ratio can be used in a similar way to the Na/K ratio, to indicate upflow zones, with the highest values indicating a more direct feed from the reservoir.

Magnesium (Mg^{2+})

Magnesium levels in high temperature geothermal fluids are usually very low (0.01-0.1 mg/kg), as Mg is readily incorporated into secondary, alteration minerals such as illite, montmorillonite and especially chlorite. Higher concentrations can indicate near-surface reactions leaching Mg from the local rock, or dilution by groundwater which can be relatively Mg-rich.

Aluminium (Al^{3+})

In chloride waters aluminium occurs at very low levels (<~0.02mg/kg) and is usually not detectable. Reservoir fluid concentrations are generally <2mg/kg. Although often regarded as an immobile species, the common co-precipitation of aluminium with silica, and the accumulation of the metal in sinters demonstrates this assumption to be false. By contrast, acid waters often contain several hundreds of mg/kg Al through rock leaching.

Iron (Fe^{2+}, Fe^{3+})

The concentration of iron in chloride fluids is invariably very low (0.001-1.0 mg/kg) although the concentration increases with increasing salinity and acidity. In high temperature systems (>180°C) the deep fluid is in equilibrium with pyrite. Below this temperature iron equilibria are controlled by pyrrhotite and marcasite which will become supersaturated and precipitate on boiling or cooling of the fluid. Marcasite may recrystallise to pyrite. Boiling can also lead to the precipitation of iron oxide minerals such as goethite, lepidocrocite and maghemite (Gunnlaugsson and Arnorsson, 1982). The dominant iron species below ~150°C are Fe^{2+} and $FeOH^{+}$, above this temperature $Fe(OH)_4^-$ predominates (Gunnlaugsson and Arnorsson, 1982). Elevated levels of iron in surface chloride-fluid discharges are significant and indicate or near-surface leaching of iron from minerals by acidic waters which have mixed with the chloride fluid. Contamination from well casings and wellhead equipment is usually insignificant (Gunnlaugsson and Arnorsson, 1982).

Manganese (Mn^{2+}, Mn^{4+})

A trace constituent in geothermal waters, manganese concentrations rarely exceed 0.01mg/kg. Manganese oxides are deposited from hot springs, and modern examples have been reported from Japan and the USA deposited from waters containing in excess of 5mg/kg Mn. Ancient hot-spring oxide deposits have also been described (Nicholson, 1990).

Anions

Fluoride (F^-)

The fluoride content of geothermal fluids is usually <10 mg/kg. Its concentration is limited by the retrograde solubility of fluorite, and is influenced by rock-water reactions where it may occur as a trace ion in micas. It usually occurs at low concentrations in high temperature fluids, unless high P_{CO_2} in the deep fluid removes the available Ca as calcite deposits, leaving excess F. High F concentrations are therefore often associated with low Ca levels. Unusually high F levels can be produced by the condensation of volcanic gases (HF) into meteoric waters, in this case it is invariably accompanied by very high Cl and SO_4 levels. Higher fluoride concentrations occur in areas with volcanic rocks (rhyolite, pumice and obsidian) than in those with sedimentary host lithologies (Mahon, 1964).

Chloride (Cl^-)

High chloride concentrations in springs indicate waters fed directly from the deep reservoir, with minimal mixing or conductive cooling. Low Cl levels in waters (which do not show steam-heating characteristics - see below) from a hot or boiling spring are characteristic of groundwater dilution. Iso-Cl lines (ie. concentration contours) can be used to delineate the upflow areas (higher Cl), the margins of the system and zones of groundwater inflow (lower Cl). Such maps can be useful for the identification of prospective well sites particularly when tied in with geophysical and geological surveys (eg. low-resistivity areas and fault zones). As the most conservative element in geothermal waters, Cl is an important diagnostic solute and is frequently used in ratios with other elements in the interpretation of water chemistry; for example, to eliminate boiling or dilution effects (eg: Cl/B, Cl/As, Cl/HCO_3). Concentrations can range from <10 to >100,000 mg/kg, but values of the order of 1000mg/kg are more typical in chloride-type waters.

Bromide (Br^-)

Usually at very low levels in geothermal fluid, except where seawater is a component of the geothermal fluid. Br/Cl and Br/I ratios can be used as indicators of seawater mixing.

Iodide (I^-)

Attains greatest concentrations in waters associated with organic-rich sedimentary rocks, although it can be contributed by organic matter in shallow near-surface reactions.

Bicarbonate (HCO_3^-)

The total dissolved carbonate concentration, as well as that of the individual species (HCO_3^-, CO_3^{2-}, H_2CO_3 or $CO_{2\text{-}aq}$) is determined by the partial pressure of carbon dioxide in the deep fluid (P_{CO_2}) and the solution pH. Loss of carbon dioxide during boiling raises the solution pH (ie. the water becomes more alkaline) by consuming protons through the reactions, all of which move to the right on loss of carbon dioxide:

$$CO_{2(aq)} = CO_{2(g)}$$
$$H_2CO_3 = H_2O + CO_{2(aq)}$$
$$HCO_3^- + H^+ = H_2CO_3$$
$$CO_3^{2-} + H^+ = HCO_3^-$$

At pH~6-10 bicarbonate is the dominant species; at lower pH values carbonic acid (H_2CO_3) dominates and at a more alkaline pH carbonate is the dominant ion. All the dissolved carbonate is present as carbonic acid at pH 3.8 or less, but as bicarbonate ions around pH 8.

Reactions between the dissolved carbon dioxide and the host rocks form HCO_3, the concentration of which is therefore influenced by permeability and lateral flow. As a consequence, boiling springs fed directly from the reservoir tend to have the lowest HCO_3 concentrations. This enables the HCO_3/SO_4 ratio to be used as an indicator of flow direction. The flow of a fluid away from the upflow yields greater opportunity for rock-water reaction and therefore increased production of HCO_3. This, combined with the loss of H_2S by rock-water reactions with increased lateral flow, leads to an increase in the HCO_3/SO_4 ratio away from the upflow zone.

Sulphate (SO_4^{2-})

The sulphate concentration is usually low in deep geothermal fluids (<50 mg/kg), but increases with increasing oxidation of the hydrogen sulphide. High concentrations of sulphate in surface waters (at levels greater than or approximately equal to, the Cl concentration) are usually the result of steam condensation into near-surface waters.

Chemical indicators of physico-chemical processes

The following section summarises the diagnostic features of the water chemistry, described in earlier sections of this Chapter, and the chemical profile of geothermal systems illustrated in Chapter 1. The chemical guides described below are the consequence of, for example, the different solubilities of solutes in the liquid or vapour phase; the temperature dependence of mineral-water reactions; mixing reactions; deposition reactions etc. To aid interpretation, the background to these guides should be appreciated; they should not be applied blindly and without thought for the active processes which create the geochemical patterns. Note that where ratios are mentioned, these are *atomic or molecular ratios*. These are calculated from the solute concentration and the formula weight (fw) of the solute:

eg. Cl/B ratio = $C_{Cl(mg/kg)} / C_{B(mg/kg)} \times (fw_B/fw_{Cl})$

Common source reservoir: similar Cl/B, Cl/Br, Cl/As, Cl/Cs ratios

Dilution by groundwater: iso-Cl maps (areas of low Cl), iso-Na/K maps (areas of low Na/K); high Mg

Dilution by seawater: very low Cl/Mg, Cl/(Mg+Ca); Cl/Mg~10; Cl/Br~660; Cl/SO_4~20; Ca/Mg~0.3

$$\%\text{seawater} \sim (Cl_{\text{geothermal discharge}} - Cl_{\text{meteoric water}})/Cl_{\text{seawater}}$$

Field margins: iso-Cl, iso-Na/K maps (lowest values)

Flow direction: decreasing Cl/B with flow; increasing B/Li with flow

Rock types: high B, I, NH_3, CO_2: organic-rich, sedimentary; high Li, Cs, Rb: rhyolite or rock with similar chemistry, and andesites; high F: rhyolite, pumice, obsidian, granitoids; high Br: higher in sedimentary than volcanic rocks; low Li, Cs: common in basaltic areas; high B: andesites

Steam heating: high SO_4, NH_3, B, HCO_3, particularly enriched over deep boiling zones and high permeability areas; low pH, Cl; high NH^{4+}/B

Upflows/high permeability/boiling/high temperature zones: iso-Cl maps (high Cl); low Na/K, Na/Ca, Na/Rb, Na/Li, Mg/Ca; high Cl/F, Cl/Mg, Cl/SO_4, $Cl/(HCO_3+CO_3)$, Na/Ca, Na/Mg ratios; low Ca, Mg, F, SO_4; high SiO_2

Statistical analysis of water chemistry

There have been few serious applications of advanced statistical methods to geothermal water chemistry, yet those that have been undertaken indicate that the methods show promise and are worthy of further study. Mazor and Manon, (1979) and Ghomshel et al. (1986) used correlations between species to indicate common sources and losses of ions in solution. Although useful, these studies lacked the quantitative approach afforded by more advanced multi-variate methods, such as principal component analysis, factor analysis and cluster analysis. Salvania and Nicholson (1990) and Veldeman et al. (1990) applied these techniques to well and spring water chemistry respectively.

Veldeman et al. (1990) found that cluster analysis distinguished waters from cold and thermal springs, and also separated mixed waters. Salvania and Nicholson (1990) looked at the weirbox chemistry of wells from different fields in New Zealand. Wells within the same field, but fed from different aquifers were effectively distinguished. However, the chemistry of the major-species was too similar to consistently discriminate between the deep reservoirs. Additional work using the trace element composition may be more successful. Factor analysis enables the

relative contributions of ions from different sources to be recognised more quantitatively than is possible using correlation coefficients (Salvania and Nicholson, 1990; Veldeman et al., 1990). Salvania and Nicholson (1990) have suggested that upon further quantification, this method could be used as a mixing model to identify the relative contributions of ions from different sources (Fig. 2.8).

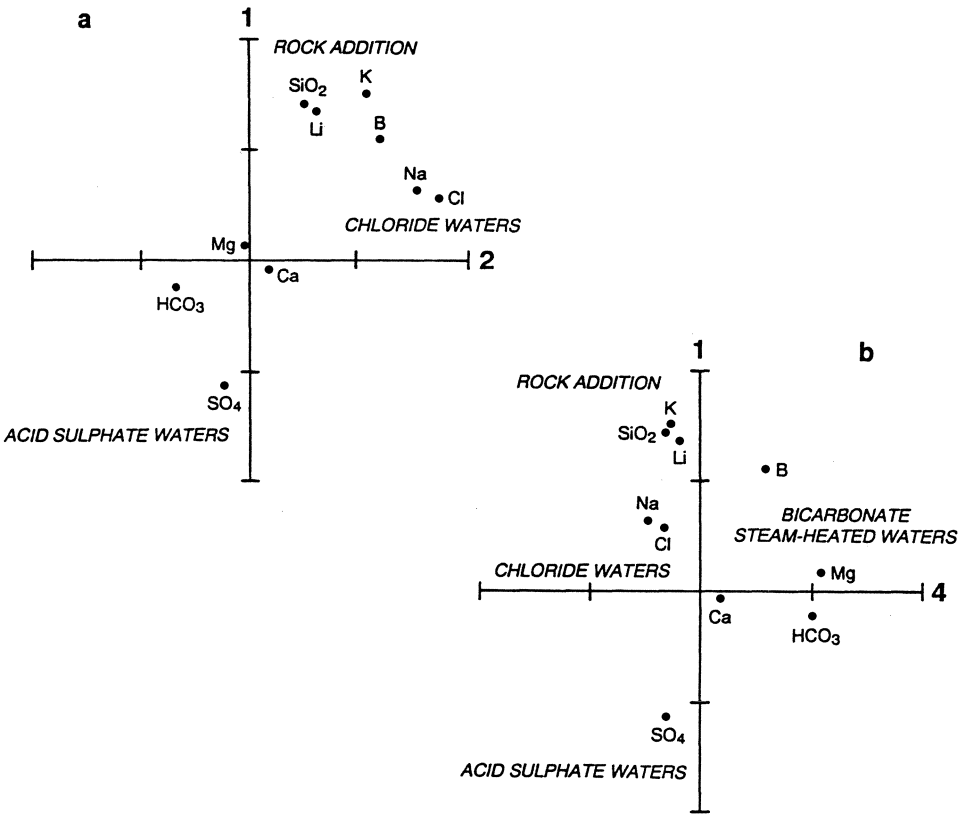

Figure 2.8. R-mode factor analysis on geothermal well chemistry. (a) Factor 1 vs Factor 2; (b) Factor (1) vs Factor 4. Each factor is considered to represent a source of solutes to the final discharge waters (as shown), and these diagrams may be developed into new mixing models (from Salvania and Nicholson, 1990).

These studies are still in the early stages of development, but show promise for advanced applications to both spring and well water chemistry. For example, temporal variations within well discharge chemistry have not been statistically examined. Using the above methods, it should be possible to identify individual dilution or mixing events within a large data set of the discharge chemistry of a single well over a long period of time. This could be done for each well to aid the development of evolving hydrological models of a field under development.

2.4 MIXING MODELS

Mixing models are an effective tool in all stages of geothermal development. They enable the processes acting upon a well discharge to be monitored over time, and are particularly useful during the early stages of evaluating the heat potential and flow structures of a new geothermal resource. Enthalpy-chloride and enthalpy-silica mixing models have found widespread usage, and are therefore considered in detail. However, other models using the carbonate concentration of the discharge have also been suggested, and these are also discussed.

Enthalpy - chloride diagrams

Enthalpy-chloride diagrams are of great value in understanding the hydrology of a geothermal field. They are simple to construct and can effectively define trends in sub-surface processes (boiling, dilution-mixing and conductive-cooling), and inter-relationships between groups of springs or wells within a field. They are also used to estimate reservoir fluid salinities and temperatures, thereby providing a useful check on geothermometry calculations. In this respect, they are particularly useful where the hot-spring waters are mixed, or have re-equilibrated in a shallow reservoir. In this situation it is not possible to obtain information about the deep reservoir by the simple application of geothermometers. Enthalpy-chloride diagrams can often overcome this limitation, and are also of value when dealing with a high enthalpy reservoir which exceeds the upper limits of geothermometry (Arnorsson, 1985; Fournier, 1979; Fournier et al., 1979; Truesdell and Fournier, 1976).

Note: As in most geochemical studies, it is essential that "background" values are obtained, in this case for chloride and enthalpy, to assist in the interpretation of the results. Local meteoric waters (streams, lakes, etc) should therefore always be included in any sampling programme)

Features of the diagram

Enthalpy scale: The specific enthalpy of water as a saturated liquid or vapour (steam). Expressed in kJ/kg, J/g or calories/g (Fig. 2.9a).

Temperature scale: This is often plotted for convenience, to aid interpretation of the figure, and shows the enthalpy-equivalent temperature of liquid water (Fig. 2.9a).

Chloride scale: The chloride content of well or spring water expressed in mg/kg (Fig. 2.9a).

Steam point and steam lines: The steam point is plotted at 2775 kJ/kg. However, it is important to realise that the enthalpy of steam varies with temperature and this value is merely taken as a convenient point which is valid for most situations. Figure 1.1 illustrates how the enthalpy of steam and liquid water varies with temperature, and selected values for the steam point at temperatures from 100°C to 374°C (the critical point of water) are shown on Figure 2.9b. Look at these figures and the steam tables in Appendix 1; notice how around 230-240°C the enthalpy values are constant, and in fact vary by only 2kJ/kg over the temperature range 218-250°C.

As enthalpy is assumed to be conservative, then following steam separation, the enthalpy of the parent fluid must lie on a line joining the hot-spring water position "HS" to the steam point (Fig. 2.9a). These are termed the steam lines, and are approximately straight lines for reservoirs with fluid temperatures up to 330°C. Above this temperature the curvature (which is present to some degree in steam lines at all temperatures) becomes pronounced and will lead to errors in the use of the graph if ignored. This is illustrated in Figure 2.9b for a reservoir fluid containing 1200mg/kg Cl. Examples are worked for the fluid boiling at 250°C, 350°C and 370°C; notice how the errors in the estimated chloride content of the boiled hot spring increase as the curve progressively departs from linearity as the critical temperature of water is approached. The parent fluid for each spring willplot on the steam line at an enthalpy calculated from geothermometry applied to the spring water. The position of the feed fluid to well discharges can be plotted in the same way, by using geothermometry or direct measurements to determine the enthalpy of the parent fluid.

Meteoric waters box: Meteoric waters which dilute the geothermal fluid are usually low in temperature (enthalpy) and chloride, and plot in the bottom left-hand corner of the diagram (Fig. 2.9a). The special case where the low-temperature diluting water has a high chloride concentration (eg. seawater) is discussed below.

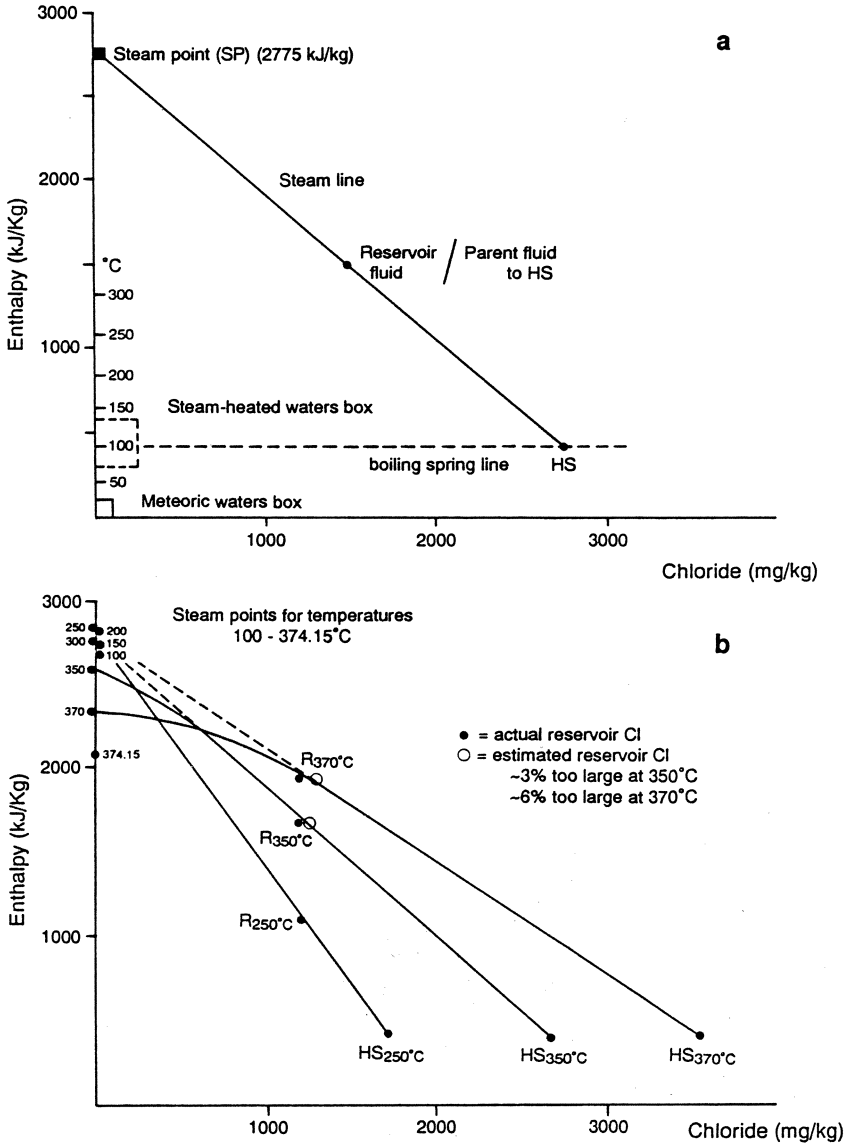

Figure 2.9. Enthalpy-chloride diagrams. (a) Example of a H-Cl diagram showing the component features of the plot. (b) Steam lines calculated for a reservoir fluid with 1200mg/kg Cl at 250°C, 350°C and 370°C. Notice that steam points for 150-300°C are very close, and little error will be introduced by adopting 2775kJ/kg as the standard steam point. However, at greater temperatures the curvature of the lines increases as the critical point is approached, introducing errors in the estimated reservoir chloride content if the standard steam point is used for these higher temperature reservoirs.

Steam-heated waters box: Steam-heated waters are low in chloride, but can be of a high temperature; consequently these waters plot above the meteoric waters (Fig. 2.9a).

Boiling-spring line: This line is often included to show the enthalpy at which water boils at the altitude of the field under study. At sea-level (1atm or 1.013 bars), this line will be at 100°C or 419.0 kJ/kg (Fig. 2.9a). The presence of the line readily identifies non-boiling springs which have been included in the figure, a point which can be important in interpretation.

Trends

When a geothermal fluid separates, the steam phase has a greater enthalpy content than the residual liquid phase. Loss of steam is therefore associated with a loss of mass and reduction in enthalpy. Figure 2.10a illustrates the general directions of steam-gain/loss (boiling), conductive-heating/cooling and mixing processes for an arbitrary geothermal fluid "X". These trends, which are described in more detail below, should be kept in mind when interpreting enthalpy chloride diagrams.

Steam gain: Fluid gains steam, enthalpy increases but chloride content decreases due to increase in fluid mass.

Steam loss: Fluid *boils* with subsequent loss of steam (and therefore mass and enthalpy), chloride increases due to lower mass of residual water ("evaporative concentration").

Conductive heating: Fluid gains heat from the surrounding rocks, enthalpy increases but chloride concentration remains constant.

Conductive cooling: Fluid loses heat to the surrounding rocks, enthalpy decreases but chloride concentration remains constant.

Mixing: Geothermal fluid mixes with cooler and more dilute meteoric waters or steam-heated waters, producing a decrease in the enthalpy and chloride content. As the total dissolved solids (TDS) content of meteoric waters is usually less than that of geothermal fluids, this process is also referred to as *dilution.* This term is acceptable, but remember that not all constituents may be diluted like chloride, and some may increase in concentration on mixing (eg. Mg, SO_4, HCO_3).

Figure 2.10b illustrates these processes with respect to a reservoir fluid "R". Areas in which steam-heated waters and meteoric waters typically plot are shown, and linked to "R" by a *mixing (dilution) line.* This line illustrates where the parent fluid of a spring, or a well fluid, will plot after mixing, the exact point depending upon the

relative proportions of diluting fluid and reservoir fluid. The proportion of hot water to cold meteoric water in the mixture is proportional to the relative position of the discharge on the dilution line (percentage hot-water component are marked on Fig. 2.10b). If the reservoir fluid cools conductively, then it will plot at lower and lower enthalpies, but retaining a constant chloride concentration (points C1, C). If however, the fluid cools adiabatically, that is by boiling, then the discharged water will plot at a lower enthalpy, but higher chloride concentration eg. at point HS, which is typical of a hot spring discharge. Note that HS plots on a line linking the reservoir fluid "R" to the steam point "SP"; providing that nothing else happens to the water, all fluids which have boiled will be related to their parent fluid in this way. As we will see, this relationship is very useful when it comes to interpreting hot-spring and well data.

Finally, before looking at some examples, remember that the enthalpy-chloride content of a fluid can often be obtained by a number of different processes, or sequences of processes. This is illustrated in Figure 2.10c for a spring or well discharge represented by "X", "P" is the parent fluid, "M" is an intermediate mixed fluid, while "B" represents a boiled intermediate water. Composition "X" can therefore be obtained by three different process routes:

mixing then boiling (route P-M-X)
conductive cooling (route P-X)
boiling then mixing (route P-B-X)

Which route is correct can only be decided by looking at the overall chemistry of the water (eg. the volatile content as indicated) and the physical features of the discharge (to evaluate whether adiabatic or conductive cooling is most likely).

Applications

Boiling springs and well discharges provide the most reliable information for the interpretation of the enthalpy-chloride diagram. Springs at temperatures below boiling can be used, but as these may have deposited silica prior to discharge, the silica geothermometer should not be used in the following procedure.

Procedure

Plot the chloride concentration and enthalpy of local meteoric waters as point "M".

Plot chloride concentration and enthalpy of the hot springs, HS_X.

Draw a straight line joining HS_X to the steam point.

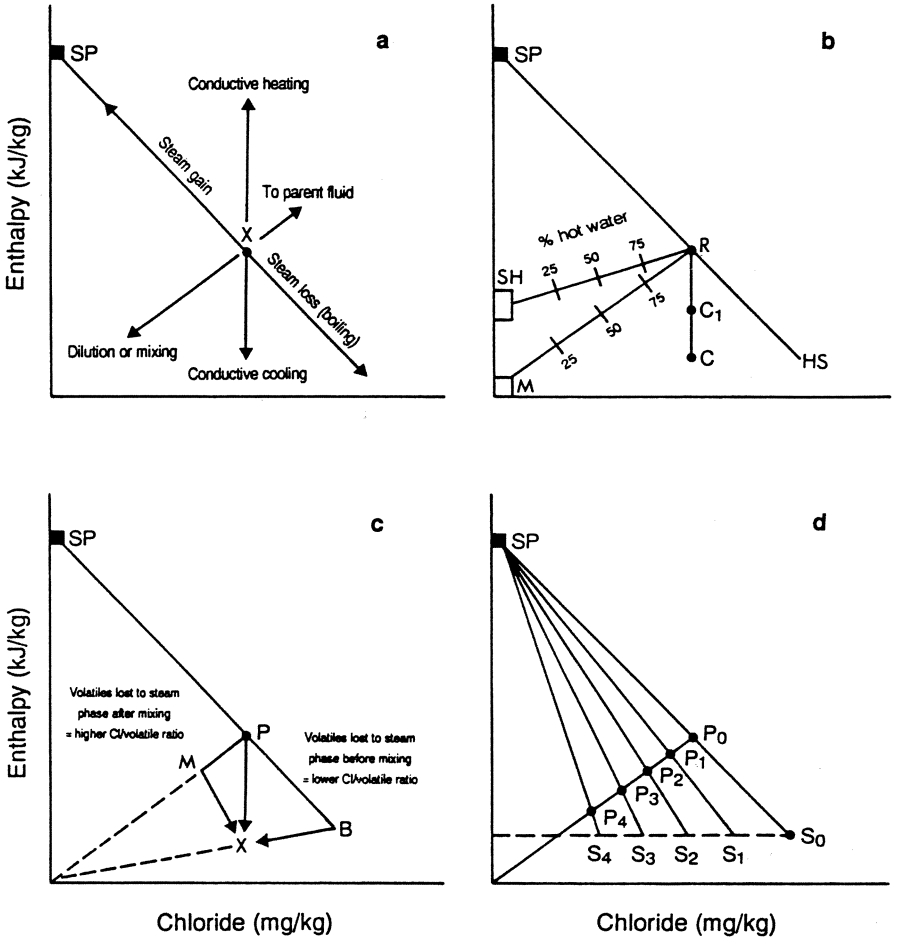

Figure 2.10. (a) Directions of trends and processes acting on an arbitrary geothermal fluid, X, as they would appear on an enthalpy chloride plot. (b) Dilution and cooling trends for a reservoir fluid, R. Mixing with steam-heated waters, R-SH, and groundwater, R-M leads to a reduction in both enthalpy and chloride content of the reservoir fluid (percentage values for the hot-water component are marked on the dilution lines). The chloride concentration is constant when the reservoir fluid cools by conduction, R-C_1-C, but is increased on adiabatic cooling (boiling), R-HS. (c) Possible alternative routes from the parent fluid, P, of a spring discharge, X: dilution by groundwater followed by boiling, P-M-X; conductive cooling, P-X; or boiling followed by dilution with groundwater, P-B-X. (d) Dilution of the parent fluid, P_0, with groundwater to produce P_1-P_4 which then act as parents to spring discharges S_1-S_4. The location of P_1-P_4 is determined from geothermometry on the spring waters (see *Case 1* in text for a full description of the diagram).

Calculate the temperature of the parent fluid feeding spring HS_X by geothermometry and convert this to enthalpy using steam tables (Appendix 1). This gives point P_X.

Plot P_X on this line at the calculated enthalpy. This gives the chloride concentration of P_X correcting for steam loss.

Plot the steam point ("SP") at 2775 kJ/kg.

If well-discharge data are available, these can be plotted too. In this case, geothermometry can be applied to the discharge or, if the separation pressure is known the position of the parent fluid on the steam line can be calculated from either the discharge enthalpy or chloride concentration using the heat-mass balance equation (Section 2.6).

Examples

The following examples illustrate the various applications and interpretations of enthalpy-chloride diagrams. Cases 1-3 use the diagram to interpret hot-spring discharges, Case 4 is based on well discharges, while Case 5 shows the special case of geothermal fluid mixing with meteoric water which has a high chloride concentration (eg. seawater, formation waters).

Case 1. Dilution with groundwater (Fig. 2.10d): Hot-spring waters are plotted as S_0-S_4. Using the silica geothermometer, the temperature of the parent fluid for each spring is estimated; these plot as points P_0-P_4. Notice that these points lie on a line which joins the meteoric water point, M. This is the meteoric water dilution or mixing line. The intersection of this line with the steam line of spring S_0 (the hot-spring with the higher chloride concentration) represents the enthalpy and chloride composition of the parent fluid, P_0. Spring S_0 is used since it is assumed to have undergone maximum boiling with no, or minimal, dilution; if several springs show this same maximum chloride concentration, we can be confident that this represents the undiluted thermal water, particularly if the springs have high flow-rates. In this example, P_0 also represents the composition of the reservoir fluid, R (Fig. 2.10d). However, remember that this is not necessarily so, particularly with high temperature reservoirs. (See Fig. 2.11a and Case 4 for examples where P_0 is not the reservoir fluid).

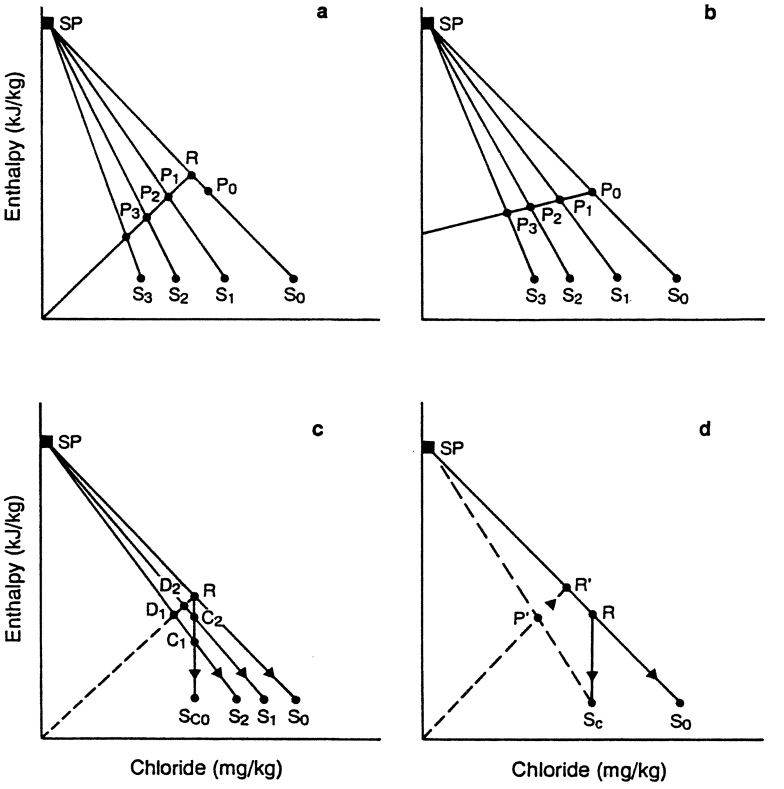

Figure 2.11. (a) An example of an enthalpy-chloride plot where geothermometry on the spring discharge, S_0, suggests a parent fluid, P_0, which does not correspond to the higher reservoir temperature, R. This can occur, for example, when using the silica geothermometer for high-temperature reservoirs where silica has been lost by the fluid before surface discharge. The correct reservoir temperature is indicated by the trend of the diluted parent waters P_1-P_3 (see *Case 1* and *Case 4* in text). (b) Dilution of the parent fluid, P_0, with steam-heated waters (*Case 2* in text). (c) In this example, the reservoir fluid, R, has not been diluted (Case 3 in text). The composition of the spring discharge waters is achieved by conductive cooling only, S_c, by adiabatic cooling (boiling) only, S_0, or by a combination of these processes (S_1, S_2). Note that springs S_c and S_0 show minimum and maximum chloride concentrations respectively. (d) If conductively cooled spring discharges from high-temperature reservoirs are not recognised, and mistaken for boiled waters then the estimated reservoir temperature will be in error. In this example, reservoir fluid, R, cooled conductively to discharge at spring S_c, and boils to discharge at S_0. S_0 and S_c are joined to the steam point by steam lines. Parent fluid P' is assumed to be derived by dilution of a reservoir fluid, R', which is plotted at the intersection of the dilution trend and the S_0 steam line. R' does not represent the true reservoir fluid, which in this example is of a lower enthalpy and higher chloride concentration.

Case 2. Dilution with steam-heated waters (Fig. 2.11b): This example is similar to that in Case 1, except that parent fluids P_1-P_3 have been diluted by steam-heated waters, and therefore fall on a different dilution line to those above. As in Case 1, parent fluid P0 has not been diluted and also represents the reservoir fluid.

Case 3. No dilution (Fig. 2.11c): Where you can be confident that the hot-springs plotted have not been diluted; then springs S_1 and S_2 must have obtained their different chloride concentrations by, for example, variable amounts of boiling and conductive cooling (C_1, C_2). This enables the temperature and salinity of the reservoir fluid to be estimated by a different method. The steam line is drawn as before, linking the steam point to S_0 (highest chloride spring). The intersection, R, of this line with a vertical line from S_c (lowest chloride spring) will then represent the reservoir conditions. This method assumes that S_0 has cooled only by boiling (thereby increasing the chloride concentration to its maximum value), while S_c has cooled only by conductive cooling (keeping the chloride concentration constant, at the reservoir value which will be a minimum). Note that whatever the example, springs which discharge waters that have cooled conductively must be identified since serious errors could arise in estimating the composition of the geothermal fluid if they are mistaken for boiled waters (eg. Fig. 2.11d).

Case 4. Plotting well discharge chemistry (Fig. 2.12a): The weirbox and/or total-discharge (TD) composition of well fluids can be plotted, as well as hot-spring waters. In this example, the weirbox compositions have been corrected for steam loss (by mass balance calculations knowing the separation pressure; see Section 2.6) and the TD composition plotted (W_1-W_3). Notice that W_1-W_3 plot on a steam-heated water dilution line, showing that the fluids feeding these wells have mixed by varying amounts with superficial thermal waters. This dilution line intersects the steam line of the undiluted, boiling spring S_0 at R. P_0 represents the composition of the parent fluid feeding spring S_0 as calculated by geothermometry. Notice that in this case P_0 is not coincident with R, and plots at a lower enthalpy. This is due to the failure of the geothermometer to indicate temperature greater than about 250°C due to rapid re-equilibration as the fluid rises to the surface.

Case 5. Dilution with high-chloride water (Fig. 2.12b): Usually, meteoric water has a lower chloride concentration than the geothermal fluid. However if, for example, mixing with sea-water occurs, then the boiling-dilution relationships can be difficult to sort out since the dilution and steam lines will now both be in the same direction.

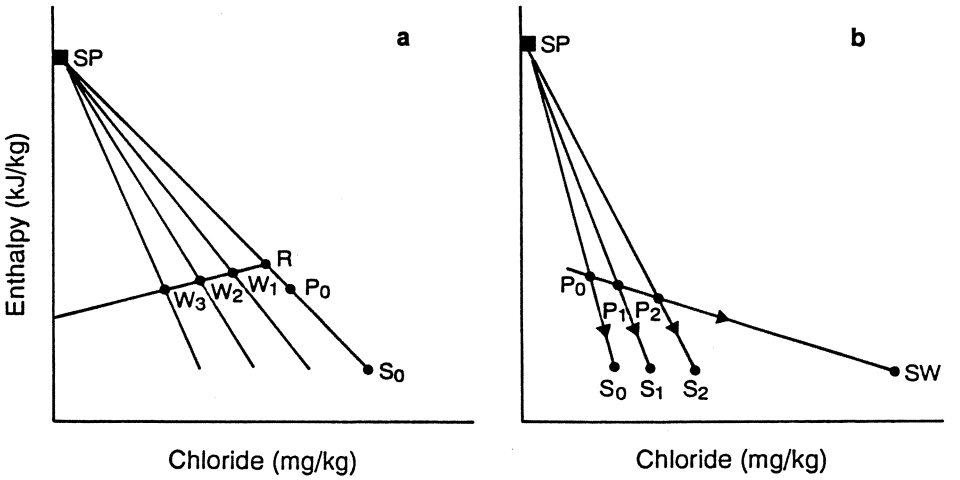

Figure 2.12. (a) Plot of well discharges, W_1-W_3, fed by reservoir fluid, R, diluted by steam-heated waters (*Case 4* in text). P_0 represents the parent fluid feeding boiling spring S_0 as determined by geothermometry, it is not coincident with the true reservoir or parent fluid, R, due to a breakdown in the geothermometer at high temperatures; cf. Fig. 2.11a. (b) Dilution of a parent fluid, P_0, with a high-Cl water such as seawater, SW (*Case 5* in text). Notice that dilution and boiling trends are now in the same direction, making interpretation of spring chemistry difficult.

This situation is illustrated in Figure 2.12b, where SW represents seawater, compare this with Figure 2.10d. The composition of the parent fluid P_0 can be estimated by the intersection of the seawater mixing line with the steam-line drawn through the *minimum chloride spring* S_0 (assumes S_0 has a chloride concentration elevated through boiling only, and not by mixing with high-chloride seawater). If the diluent has a chloride concentration similar to that of the hot-spring waters, then mixing

relationships cannot be distinguished on this diagram, and some other dissolved species would have to be used.

Conclusion

Many of these above dilution-mixing, boiling and conductive cooling trends are reflected in changes in the chemistry of the spring or well discharges which provide a useful comparison. Trends determined from enthalpy-chloride diagrams should be related back to the spatial distribution of the wells/springs in the field. This can help identify, for example, sub-surface flow directions, the existence of several shallow reservoirs feeding different groups of springs and areas of cold, groundwater inflow.

Enthalpy-silica diagrams

Enthalpy-silica diagrams provide a simple technique to estimate the temperature of the hot-water component of mixed waters. The method is based on heat and silica balance and its successful application is dependant upon three basic assumptions (Fournier and Truesdell, 1974; Truesdell and Fournier, 1977):

- there is no loss of heat after mixing
- the solubility of quartz controls the silica content of the reservoir fluid
- there is no deposition or dissolution of silica once the geothermal fluid has left the deep reservoir, ie. before or after mixing.

The second assumption is invariably valid, since it is known that deep geothermal fluids are saturated with respect to quartz, while careful selection of the springs used in the method (high temperature, large flow rate) will reduce any errors from the first assumption. Problems can arise when dealing with very-high enthalpy systems (> ~275°C). Quartz precipitates rapidly from such fluids, thereby breaking the third assumption and creating errors in the temperature calculation. The method can be applied to two mixing models:

- no steam or heat loss before mixing
- steam loss (adiabatic cooling) before mixing.

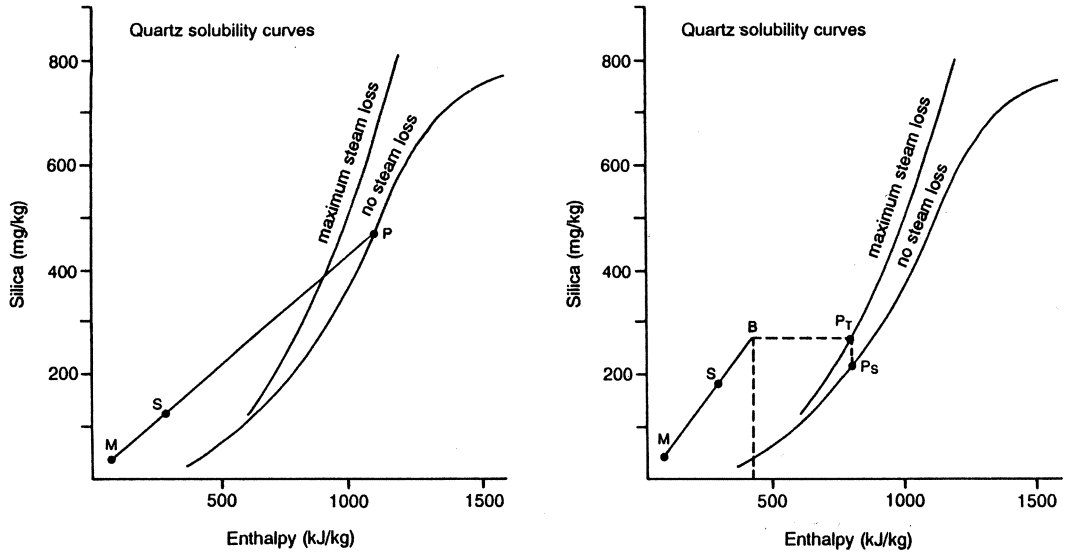

Figure 2.13. Enthalpy-silica mixing model showing quartz solubility curves for no steam loss and maximum steam loss on boiling (see Fig. 2.7). (a) Model 1, assumes no steam or heat loss before mixing. A line joining the composition of local meteoric waters, M, with the hot-spring composition, S, intersects the quartz solubility, no steam loss curve at P, which represents the composition of the parent geothermal water prior to mixing. (b) Model 2, steam and heat lost before mixing. The temperature and silica content of the parent fluid (P_T and P_S respectively) are determined by joing M and S to intersect at B a vertical line drawn at the temperature at which boiling is assumed to have occurred (100°C, 419kJ/kg in this case). From B a line parallel to the enthalpy axis intersects the quartz solubility maximum steam loss curve at P_T, indicating reservoir temperature. A vertical line from P_T intersects the quartz solubilty no steam loss curve at P_S, indicating the silica concentration in the reservoir fluid.

Procedure

Model 1: No steam or heat loss before mixing

Determine the temperature and silica content of local meteoric waters.

Convert temperatures to enthalpies using steam tables and plot as point "M" on Figure 2.13a.

Determine the temperature and silica content of the hot spring.

Convert the temperature to enthalpy and plot as point "S" on Figure 2.13a.

Draw a line through M and S to intersect the quartz solubility curve at point "P" (Fig. 2.13a).

Point "P" represents the enthalpy and silica content of the parent hot-water component before mixing. The temperature of the water can then be determined from steam tables, while the fraction of hot water in the mixed discharge is determined by dividing the distance M-S by M-P.

Model 2: Steam and heat loss before mixing

Plot the enthalpy and silica content of the meteoric and hot-spring water as described above (points M and S).

Draw a line through M and S and extend this to the enthalpy of the temperature at which steam is assumed to have been lost before mixing (eg. at 100°C, point B on Fig. 2.13b).

Draw another line from B parallel to the abscissa to intersect the maximum steam-loss curve at point P_T. This point represents the enthalpy of the parent hot-water component before boiling and mixing, while point P_S shows the original silica content of this fluid.

The fraction of the hot-water component (after steam loss) in the spring discharge is derived by dividing distance MS by MB. The fraction "X_S" (by weight) of original fluid lost as steam before mixing can be calculated from: $X_S = 1 - (SiO_2 \text{ at } P_S) / (SiO_2 \text{ at } P_T)$.

Correction. This model assumes that steam separation occurs at 100°C and 1 atm, enabling us to use the maximum steam-loss curve on Figure 2.13b. If however steam was lost at a higher temperature, then this curve will not be valid as the fluid will not have lost *all* its steam. An intermediate curve, between the maximum steam-loss and quartz solubility curves, must then be employed for precise work. The relative

position of this curve can be calculated from: the enthalpy of liquid water at 100°C ($H_{L,100}$), the enthalpy of liquid water read from the quartz solubility curve at a given value of silica ($H_{L,SiO2}$), and the enthalpy of liquid water at the actual temperature of steam loss ($H_{L,B}$) (Truesdell and Fournier, 1977). The relative distance from the intermediate curve to the quartz solubility and maximum steam loss curves is proportional to $(H_{L,SiO2} - H_{L,B}) / (H_{L,B} - H_{L,100})$.

Similarly, if steam is lost at pressures less than 1atm (ie. at high altitude) then the maximum steam-loss curve will move slightly to the left of that shown for 1 atm in Figure 2.13b. Generally, however, the effect of altitude is insignificant (Truesdell and Fournier, 1977).

Reservoir temperature

Under ideal conditions the temperature and silica content of the hot-water component derived from enthalpy-silica diagrams may represent that of the reservoir fluid (eg. Fournier, 1989b). The technique therefore provides an interesting comparison with estimates of reservoir temperature derived from enthalpy-chloride diagrams and geothermometry.

Carbonate - silica/chloride

In addition to the established enthalpy-chloride and enthalpy-silica mixing diagrams, a further model has been proposed by Arnorsson (1985). This employs the relationship between dissolved silica and total carbonate (expressed as ΣCO_3) in high-temperature systems (Fig. 2.14), and is useful in estimating reservoir temperature where mixing prevents boiling.

When a geothermal fluid boils, the carbon dioxide partitions into the vapour phase producing a residual liquid which is depleted in carbonate. However, if dilution occurs before boiling and prevents degassing of the fluid, then the resultant discharge will retain the dissolved carbon dioxide and consequently have a high $\Sigma CO_3/SiO_2$ ratio. This relationship is expressed as a mixing diagram (Fig. 2.14) which can be used to distinguish boiled waters from mixed or conductively-cooled discharges, and to estimate the temperature of the parent fluid. Such temperature estimates are made by drawing a line through the data points below the curve (ie. mixed and conductively-cooled waters) and extending this to intersect the equilibrium curve at

point P_0. This point represents the silica and total carbonate composition of the deep, hot water component. The silica concentration of this fluid, P_{0,SiO_2}, is then used in the quartz geothermometer to obtain the temperature of the parent fluid.

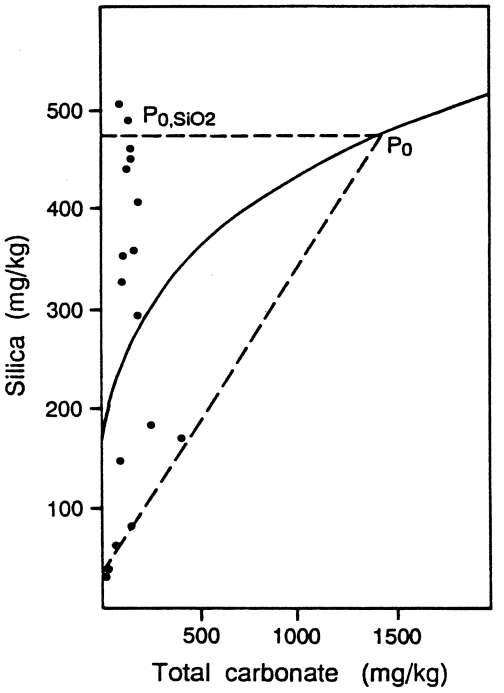

Figure 2.14. Silica-carbonate mixing model. Waters plotting above the silica-carbonate equilibrium line represent boiled waters, those below the line represent mixed waters which have not boiled. The intersection of the dashed line, which encloses the spring waters, with the equilibrium line indicates the composition of the parent fluid, P_0. From this the silica content of the parent fluid, P_{0,SiO_2} is determined and, by geothermometry, the reservoir fluid temperature is calculated.

This model is a useful complement to the enthalpy-silica, enthalpy-chloride diagrams and deserves more consideration than it has received. The principal limitation to using the model is practical. To produce meaningful results it is

essential that the discharge waters are sampled carefully to prevent atmospheric carbon dioxide contamination, and analysed accurately to ensure that correction is made for other weak acids in solution (Arnorsson, 1985). Such procedures are frequently not adopted on a routine basis.

Fournier (1989b) employed a bicarbonate-chloride mixing diagram applied to fluids from the Yellowstone National Park geothermal system, and used this to distinguish mixed, boiled and conductively-cooled fluids. Clearly dissolved carbonate is a potentially valuable tool in identifying processes active within a geothermal system.

2.5 SOLUTE GEOTHERMOMETERS

Geothermometers enable the temperature of the reservoir fluid to be estimated. They are therefore valuable tools in the evaluation of new fields, and in monitoring the hydrology of systems on production. In the following section, geothermometers based on mineral solubility (silica) and exchange reactions (Na-K; Na-K-Ca etc.) will be considered; gas and isotope geothermometers are discussed in Chapters 3 and 4, respectively. Solute geothermometers are based on temperature-dependent mineral-fluid equilibria and their successful application relies on five basic assumptions (Ellis, 1979; Fournier, 1977; Fournier et al., 1974; Truesdell, 1976; White, 1970):

1) The concentration of the elements or species to be used in the geothermometer is controlled only by a temperature-dependent mineral-fluid reaction.
2) There is an abundance of the minerals and/or dissolved species in the rock-fluid system for the reaction to occur readily.
3) The reaction attains equilibrium in the reservoir.
4) There is rapid flow to the surface with no re-equilibration after the fluid leaves the reservoir, ie. no near-surface reactions.
5) There is no mixing or dilution of the deep fluid (this assumption can be circumvented if the extent of dilution/mixing can be evaluated).

In other words, the reaction must be rapid enough to establish equilibrium in the reservoir but, to ensure the reservoir composition is retained in the discharge water, it should not be so rapid that it re-equilibrates as the fluid migrates to the surface.

All too frequently the geothermometry equations are applied automatically to all springs sampled, with little consideration given to which springs or geothermometers are most appropriate. This often leads to a range of unreliable results which show little agreement. Like any tool, geothermometers must be used correctly, and the following points highlight some common errors to avoid.

Data quality: Sampling and analysis of the waters should be precise and accurate, following standard procedures. An ionic balance is a useful check on the accuracy and completeness of an analysis (see Part II).

Spring selection: Not all hot springs are equally valid for geothermometry, and a priority, or weighting, should be established. Hot (ideally boiling) springs with a high chloride concentration and a good flow rate (> 1 L/s) provide the most reliable results. There waters will have risen to the surface rapidly, with minimal opportunity for rock-water reactions or re-equilibration to occur. Superficial, acid waters which have leached rocks in near-surface reactions are useless for geothermometry as their composition is a function of these reactions, and does not reflect that of the deep fluid. Warm, bicarbonate rich, dilute chloride waters may provide indications of shallow temperatures, but are of little real use in geothermometry. Springs should therefore be ranked by highest flow rate, highest temperature and highest chloride concentration. The Cl-HCO_3-SO_4 water classification diagram (Fig. 2.1 ternary plot) or the K-Na-Mg plot of Giggenbach (1988) (see below) can be used to select the waters most suitable for geothermometry.

Host rocks: The second assumption is fundamental to the correct application of geothermometers; ie. that in the reservoir host-rock there is an abundance of the mineral involved in the geothermometry reaction. There is little point, for example, in applying the quartz geothermometer to a fluid from a pure limestone reservoir as there will be little or no quartz for the fluid to react with. It is therefore important to consider the mineralogy of the host rocks before applying geothermometers.

Geothermometer selection: Disagreement between geothermometers should not be greeted with dismay. While it is re-assuring to obtain similar estimates of reservoir temperatures from different geothermometers, the reality is that geothermal systems are complex and many sub-surface processes can produce differences in geothermometry results. However, under these circumstances the different properties

and limitations of each geothermometer can provide clues to the hydrology of the system.

eg. geothermometers record the temperature of the *last equilibrium* (which is *not* necessarily that of the deep reservoir); differences between geothermometers may therefore be a function of the different reaction rates of their equilibria, with the last temperature of equilibration being different for each geothermometer.

eg. the silica geothermometer is based on absolute concentration, not concentration ratios, and is therefore influenced by boiling and dilution more than the alkali geothermometers.

Well discharges: The ease of sampling well discharges and the rapid flow of fluid to the surface overcome some of the problems associated with hot-spring waters, but can introduce a few of their own. Downhole samples may have lost some steam relative to the deep fluid, and this can be difficult to quantify. Discharged waters can also be contaminated with condensates flowing down the well.

Silica

The relationship between the silica content of well discharges and the reservoir temperature was recognised by Mahon (1966). Over the past thirty years, Fournier and co-workers have developed this observation, together with an improved knowledge of the solubility of silica species (Sections 2.2, 2.3), into a more rigourous geothermometry relationship (Morey, et al. 1962; Fournier and Rowe, 1966; Fournier, 1983; Fournier and Marshall, 1983; Fournier and Potter, 1982a,b). Geothermometry equations (valid up to about 250°C) have been developed for the different forms of silica (see box).

Silica geothermometer equations	
Quartz, no steam loss	$t°C = [1309/(5.19 - \log SiO_2)] - 273$
Quartz, maximum steam loss at 100°C	$t°C = [1522/(5.75 - \log SiO_2)] - 273$
Chalcedony	$t°C = [1032/(4.69 - \log SiO_2)] - 273$
α-Cristobalite	$t°C = [1000/(4.78 - \log SiO_2)] - 273$
β-Cristobalite	$t°C = [\ 781/(4.51 - \log SiO_2)] - 273$
amorphous silica	$t°C = [\ 731/(4.52 - \log SiO_2)] - 273$
where $t < 250°C$, and	
SiO_2 = concentration of silica (mg/kg)	

A limiting temperature for silica geothermometry tends to be about 250°C, since above this temperature silica dissolves and precipitates very rapidly - too rapidly for the silica concentration in solution to remain constant as the fluids are discharged to the surface. However, for situations such as rapidly discharging wells tapping a high-temperature reservoir, Fournier and Potter (1982a,b) have developed a geothermometry relationship which can be used above 250°C:

$$t°C = -k_1 + k_2SiO_2 - k_3SiO_2^2 + k_4SiO_2^3 + k_5 \log SiO_2$$

where $t < 330°C$, and
$k_1 = 4.2198 \times 10^1$
$k_2 = 2.8831 \times 10^{-1}$
$k_3 = 3.6686 \times 10^{-4}$
$k_4 = 3.1665 \times 10^{-7}$
$k_5 = 7.7034 \times 10^1$
SiO2 = concentration of silica (mg/kg)

As the geothermometer is dependent on an absolute concentration, rather than a ratio of concentrations, it is affected by physical processes such as boiling and dilution. These processes need to be recognised and, where possible, corrections should be made through the use of alternative geothermometry equations or the silica mixing model (Section 2.4). Note also that silica can be added by mixing with acidic

near-surface fluids. Under such circumstances, the silica content of the discharged mixed water will not be representative of the reservoir concentration, and geothermometry temperatures will be misleading.

Figure 2.15 illustrates the solubility of quartz in water and co-existing steam at the vapour pressure of the solution up to the critical point as defined by the above equation. This describes the solubility of quartz above ~250°C more precisely than the earlier expressions. The equation is, however, only valid for dilute solutions, as the solubility of quartz in saline solutions above 300°C shows a different behaviour to that described by this expression.

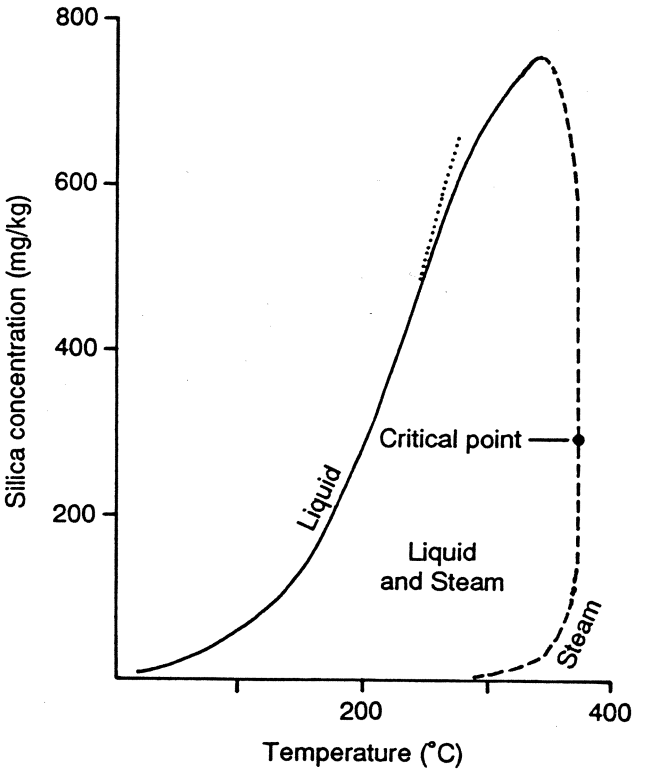

Figure 2.15. The solubility of quartz in water at the vapour pressure of the solution calculated from Fournier and Potter (1982a,b). The dashed line shows the deviation of the standard quartz geothermometry equation from the quartz solubility curve.

Na/K geothermometer

The Na/K geothermometer has steadily evolved over the past thirty years from the initial observation that low Na/K ratios were indicative of high temperatures at depth, to increasingly more precise calibration of the temperature dependence of this ratio. In high-temperature systems, the temperature-dependent variation of sodium and potassium in geothermal waters is due to ion exchange of these elements between co-existing alkali feldspars according to the reaction

$$\underset{\text{(albite)}}{\text{Na-feldspar}} + K^{+}_{(aq)} = \text{K- feldspar} + Na^{+}_{(aq)}$$

Na/K geothermometer equations	
$t°C = 856/[\log (Na/K) + 0.857] - 273$	Truesdell (1976)
$t°C = 883/[\log (Na/K) + 0.780] - 273$	Tonani (1980)
$t°C = 933/[\log (Na/K) + 0.993] - 273$	(25-250°C) Arnorsson (1983)
$t°C = 1319/[\log (Na/K) + 1.699] - 273$	(250-350°C) Arnorsson (1983)
$t°C = 1217/[\log (Na/K) + 1.483] - 273$	Fournier (1979b)
$t°C = 1178/[\log (Na/K) + 1.470] - 273$	Nieva & Nieva (1987)
$t°C = 1390/[\log (Na/K) + 1.750] - 273$	Giggenbach (1988)
where	
$t > \sim 120°C$	
Na, K = concentration of sodium and potassium (mg/kg)	

Experimentally-derived geothermometry equations based on the Na/K ratio were derived by White (1957, 1965), Ellis and Mahon (1967), Ellis (1970), Truesdell (1976), Fournier (1979a) and Giggenbach (1988). The equations shown below work well for reservoirs with temperatures in the 180-350°C range (Ellis, 1979), but break down at lower temperatures, notably at less than 120°C. At these temperatures the sodium and potassium concentrations are influenced by other minerals, such as clays,

and are not controlled only by the feldspar ion-exchange reaction. Although many equations have been proposed, they all give similar results above 300°C, and below this temperature only the equations of Fournier (1979b) and Giggenbach (1988) give significantly different (higher) results than the other equations.

The rate of re-equilibration of the Na-K exchange is slower than for both the silica dissolution-precipitation and K-Mg exchange equilibria. The geothermometer is superior in that the equilibrium conditions at depth are preserved in the solution for longer as it ascends to the surface. It is therefore able to indicate ("remember") higher temperatures from deeper levels. Further, as a concentration ratio, it is less affected by dilution and boiling than silica, providing little Na or K is added to the reservoir fluid through the diluting water. It does however, give anomalously high temperatures when applied to ammonia-rich waters that have reacted with organic-rich sedimentary horizons (Fournier, 1989a).

Na-K-Ca geothermometer

It was found that temperatures calculated from the Na/K geothermometer were generally too high when applied to waters high in Ca, particularly in lower temperature systems. The reason for this is thought to be that under these conditions Ca, Na and K compete in ion-exchange reactions with silicate minerals, thereby upsetting the simple Na-K-feldspar equilibrium discussed above. To overcome this, Fournier and Truesdell (1973) derived the empirical Na-K-Ca geothermometer which, they suggest, should be employed over the Na/K geothermometer when $[Ca^{1/2} / Na] > 1$ (with concentrations in molal units).

The equation presented below is slightly more involved than those previously discussed and requires further explanation in its application. The procedure is as follows (concentrations in mg/kg):

1) Calculate $[\log (Ca^{1/2} / Na + 2.06]$; if this is positive, calculate the temperature, t°C, using $\beta=4/3$.
2) If $t < 100$°C use this temperature.
3) If however, $t > 100$°C or $[\log (Ca^{1/2} / Na + 2.06]$ is negative, then use $\beta=1/3$ to calculate the temperature.

In formulating the geothermometry equation Fournier and Truesdell (1973) assumed:

- excess silica is present (generally acceptable for reservoirs hosted by volcanic and clastic-sedimentary lithologies).
- aluminium is conserved in the solid phase (known to be untrue, but considered acceptable since Al is invariably a very minor constituent in the deep geothermal fluid).
- protons involved in hydrolysis reactions are balanced over the net reaction ie. there is no pH change (probably not widely valid, but this is a necessary practical assumption to avoid the incorporation of a pH factor into the equation which could not easily be corrected for).

The geothermometer gives reliable results when applied to waters from high-temperature reservoirs (>~180°C), but breaks down t lower temperatures. Factors which affect the geothermometer include the partial pressure of carbon dioxide in solution, P_{CO_2}; interfering exchange reactions with other ions, notably Mg; and the precipitation of calcite with loss of carbon dioxide from solution on boiling.

As the absolute concentration of Ca in waters is controlled by carbonate minerals, the P_{CO_2} level will influence strongly the concentration of Ca. This factor was recognised by Fournier and Truesdell (1973) who stated that the geothermometer would still be reliable when applied to CO_2-rich fluids, providing no carbonate mineral had deposited after the fluid left the reservoir, otherwise falsely high temperatures could be obtained. It was also realised that given the influence of CO_2, boiling (creating a loss of CO_2, causing calcium carbonate minerals to precipitate) and dilution with CO_2-bearing groundwaters would affect the geothermometer.

Na-K-Ca geothermometer equation

$$t°C = 1647/\{\log (Na/K) + b[\log(Ca^{1/2} / Na) + 2.06] + 2.47\} - 273$$

where
$t > 70°C$
Na, K and Ca = concentrations of sodium, potassium and calcium (mg/kg)
$\beta = 4/3$, if $t < 100°C$
$\beta = 1/3$, if $t > 100°C$

Mg-correction to the Na-K-Ca geothermometer

1) Calculate the Na-K-Ca temperature, t°C, as described above. If $t < 70°C$ no correction is required, if $t > 70°C$ proceed as follows.

2) Calculate $R = [Mg/(Mg+0.61Ca+0.31K)] \times 100$ using concentrations in mg/kg.

3) If $R > 50$, ignore the calculated Na-K-Ca temperature and assume that the temperature of the water at depth is approximately the same as the temperature of the water measured in the field.

4) If $R = 5$ to 50, calculate the correction from:
$\Delta t_{Mg} = 10.664 - 4.7415 \log R + 325.87(\log R)^2 - 1.032 \times 10^5 (\log R)^2/T_{NaKCa} - 1.968 \times 10^7 (\log R)^2/T^2_{NaKCa} + 1.605 \times 10^7 (\log R)^3/T^2_{NaKCa}$

5) If $R < 5$, calculate the correction from:
$\Delta t_{Mg} = -1.03 + 59.971 \log R + 145.05(\log R)^2 - 36711(\log R)^2/T_{NaKCa} - 1.67 \times 10^7 \log R/T^2_{NaKCa}$

6) If the value calculated for Δt_{Mg} is negative or <1.5, do not apply the correction.

7) Finally, subtract the value of Δt_{Mg} from the Na-K-Ca calculated temperature to obtain the Mg-corrected temperature.

It was problems such as these that led to Paces (1975) developing a correction term involving P_{CO_2} to permit the geothermometer to be applied reliably to temperatures below 75°C. Pope et al. (1987) found that the geothermometer could be applied to dilute-chloride fluids, but was not reliable when applied to bicarbonate waters. Above 200°C, P_{CO_2} generally varies systematically with temperature, and the geothermometer yields reliable results. However, below 200°C, Fournier (1989a) suggests that the geothermometer is only applied with caution to bicarbonate-rich

waters as these may have fluid compositions far from the trends established for chloride-fluids, and the application of this geothermometer may not therefore be appropriate.

Falsely high temperatures are indicated by the geothermometer when applied to low-temperature waters relatively rich in Mg (ie. Mg > ~ 1mg/kg). In an attempt to overcome this, Fournier and Potter (1979) devised the Mg-correction to the Na-K-Ca geothermometer (see box).

The Na-K-Ca geothermometer has been criticised on theoretical grounds, namely that it depends on a common temperature dependence of two independent reactions of Na-K exchange and Na-K-Ca exchange (Arnorsson et al., 1983; Benjamin et al., 1983). However, the fact remains that despite the empiricity of the geothermometer, it has proved to be a useful tool in geothermal exploration when used within its limitations. In low-temperature environments (<100-120°C), and/or with fluids relatively rich in CO_2 or Mg, this geothermometer should be used with discrimination. Under such circumstances, more reliable results may be obtained with the K-Mg geothermometer.

Na/Li geothermometer

Earlier observations by Ellis and Wilson (1960) and Koga (1970) had shown that the lowest Na/Li values corresponded to the hottest portions of the geothermal field. Following this, Fouillac and Michard (1981) examined the relationship between Na and Li concentrations with temperature in explored geothermal systems, surface waters and experimental rock-water reactions. They demonstrated an empirical relationship between log Na/Li and $^1/_T$ for dilute, Cl < 0.2m (~7,000 mg/kg), and more saline Cl > 0.3m (> 10,000 mg/kg) waters. A further relationship was subsequently suggested by Kharaka et al. (1982). Separate independent relationships between Li and Na concentration and temperature were also shown to exist, with Li being more temperature dependant than Na. While these latter relationships could also be employed as geothermometers, they would be affected by dilution/mixing and boiling processes (as they use absolute concentrations, not ratios) and are therefore probably superfluous.

A theoretical basis for the Na/Li geothermometer has not been established. As lithium minerals are rare, it is unlikely that the Li enters the aqueous phase following

an equilibrium reaction with a lithium mineral. Ion-exchange reactions at depth may be the answer. Nonetheless, the Na/Li geothermometer does seem to be effective in low to high temperature systems and when applied to both sedimentary- and volcanic-hosted reservoirs, and was considered by Minissale and Duchi (1988) to be the most reliable geothermometer applied to a carbonate reservoir of central Italy. Perhaps this is not too surprising since the original data from which the relationship was derived included waters of varied origins and temperatures.

Na/Li geothermometer equations

$t°C = 1000/[\log (Na/Li) + 0.389] - 273$ Cl<0.3m
Fouillac & Michard (1981)

$t°C = 1195/[\log (Na/Li) + 0.130] - 273$ Cl>0.3m
Fouillac & Michard (1981)

$t°C = 1590/[\log (Na/Li) + 0.779] - 273$
Kharaka et al. (1982)

where
Na, Li = concentrations of sodium and lithium in molal units (Fouillac & Michard's equations) or mg/kg (Kharaka et al.'s equation)

The Na/Li ratio of the deep fluid is thought to be preserved on ascent to the surface. However, if lateral flow is significant then low-temperature sub-surface reactions could change this ratio, with adsorption of Li onto clays or alteration products being likely.

K/Mg and Li/Mg geothermometers

As exchange reactions with Mg appear to be rapid at low temperatures, the K/Mg and Li/Mg ratios are taken to be representative of the conditions of the last rock-water reaction prior to discharge. However, the Mg content of geothermal waters decreases as temperature increases, so waters with elevated Mg concentrations will have been involved in low-temperature water-rock equilibria, probably in a near-surface environment. The K/Mg geothermometer was first presented by Giggenbach et al. (1983), and later discussed in detail by Giggenbach (1988), while the Li/Mg geothermometer was proposed by Kharaka and Mariner (1989).

K/Mg and Li/Mg geothermometer equations
$t°C = 4410/[\log [K/(Mg)^{1/2}] + 14.00] - 273$ Giggenbach (1988)
$t°C = 2200/[\log [Li/(Mg)^{1/2}] + 5.470] - 273$ Kharaka & Mariner (1989)
where
K, Mg, Li = concentrations of potassium, magnesium and lithium (mg/kg)

The K/Mg geothermometer was first applied to waters from a low-enthalpy reservoir of 120-140°C which had not attained equilibrium with alkali feldspars thereby negating the use of the Na/K and Na-K-Ca geothermometers. However, from the K and Mg activities it was considered that the fluids were in equilibrium with K- and Mg-bearing clay minerals, enabling these solutes to be employed in a geothermometry. The equation relating K and Mg concentrations with temperature is only presented by Giggenbach et al. (1983) but the derivation is later shown by Giggenbach (1988).

The geothermometers are valid from 50-300°C, and are of greatest use in the study of low to intermediate systems when equilibrium has not been attained between the fluid and the complete mineralogical assemblage of the host rock.

Na-K-Mg geothermometer

A ternary plot of $Na/1000-K/100-Mg^{1/2}$ has been proposed by Giggenbach (1988) as a method to determine reservoir temperature (Fig. 2.16), and to recognise waters which have attained equilibrium with the host lithologies. Fournier (1990) observed that the temperatures and compositions at which this "full" equilibrium is attained will vary significantly with the form of the Na/K geothermometer equation which is taken as correct and the mineralogy of the reservoir rocks. He states that the diagram is most useful in determining which waters are most suitable for geothermometry, eliminating those which are only partially equilibrated owing to dilution/mixing or near-surface rock-water reactions.

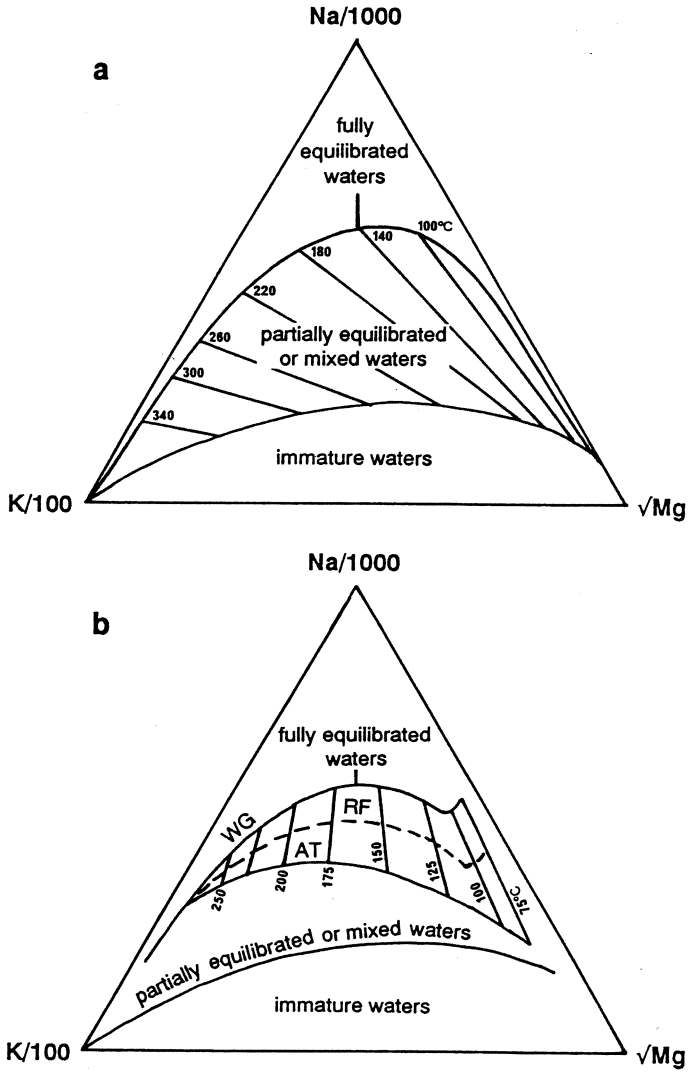

Figure 2.16. Ternary plot used to determine reservoir temperature and to recognise equilibrated waters suitable for geothermometry. (a) The original diagram proposed by Giggenbach (1988). (b) Revised plot of Fournier (1990) showing variations in the "full equilibrated line" as determined by variations in the Na/K geothermometry equation used (WG - Giggenbach, 1988; RF - Fournier, 1979b; AT - Truesdell, 1976).

Ca/Mg and SO_4/F geothermometers for carbonate reservoirs

In an attempt to overcome the limitations of the alkali geothermometers when applied to the carbonate/evaporite-hosted geothermal fields of Italy, Marini et al. (1986) proposed two geothermometers based on Ca-Mg and SO_4-F relationships. In these fields, calcite, anhydrite and dolomite are the principal components of the host lithologies, together with authigenic quartz and fluorite mineralisation.

The geothermometers are derived from theoretical considerations of two mineral-fluid equilibria: calcite-dolomite for the Ca/Mg geothermometer, and anhydrite-fluorite for the SO_4-F geothermometer. Application of these relationships to geothermal well fluids demonstrated that the SO_4/F geothermometer seems most reliable, while the Ca/Mg system is affected by Ca-mineral precipitation. In a study on geothermometry in a carbonate reservoir, Minissale and Duchi (1988) felt that the SO_4/F relationship underestimated the deep temperature, and proposed that the Na/Li geothermometer was more reliable. Clearly, more work needs to be done to fully evaluate these potential geothermometers.

2.6 CALCULATING RESERVOIR FLUID CHEMISTRY

As a reservoir fluid ascends to the surface and boils, volatile species (eg. CO_2) are concentrated in the separated vapour or steam phase. Solutes, however (eg. Cl), remain in the residual liquid phase and, as they are now dissolved in a smaller mass of liquid, become more concentrated after steam loss. It is possible to calculate back to the concentration of gases and solutes in the pre-boiled fluid if the chemistry and enthalpy of the well discharge is known. The first step in the calculation involves the determination of the fraction of steam which separated from the fluid on boiling. This is done using the heat and mass balance equation.

Heat and mass balance equation

Assuming that steam separation is adiabatic (ie. heat lost to the surroundings is negligible and no heat is gained by the fluid) then the distribution of the reservoir enthalpy between the liquid and vapour phases can be expressed by

$$H_{res} = yH_v + xH_l$$

where

H_{res} = enthalpy of the reservoir fluid
yH_v = enthalpy of the separated steam
xH_l = enthalpy of the residual liquid water

y = mass fraction of the fluid which separates as steam

x = mass fraction of the fluid which remains as liquid

Similar equations can be written for any conserved quantity, not just enthalpy. This means that the concentration of species, including isotopes, in the reservoir fluid can be calculated from the equation

$$C_{i,res} = yC_{i,v} + xC_{i,l}$$

where

$C_{i,res}$ = concentration of species "i" in the reservoir fluid

$yC_{i,v}$ = concentration of species "i" in the separated steam

$xC_{i,l}$ = concentration of species "i" in the residual liquid water

y = mass fraction of the fluid which separates as steam

x = mass fraction of the fluid which remains as liquid

Concentrations are expressed in *molal* or similar mass units (mg/kg).

These equations can be simplified by replacing the liquid fraction, x, by (1-y) as follows. The sum of the two mass fractions is unity,

therefore $x + y = 1$

and $x = (1-y)$

Substituting the expression for x into the above equations gives the following heat and mass balance equations:

$$H_{res} = yH_v + (1-y)H_l$$

$$C_{i,res} = yC_{i,v} + (1-y)C_{i,l}$$

Steam fraction calculation

The steam fraction, y, must be known before the concentration of components in the reservoir fluid can be determined. It is calculated using the heat balance equation with an estimate of the reservoir temperature (eg. from geothermometers) and the separation pressure or temperature.

$$H_{res} = yH_v + (1-y)H_l$$

where

H_{res} = reservoir enthalpy from estimates of reservoir temperature

H_v and H_l = enthalpy of vapour and liquid at the separation pressure or temperature determined at the well head. In single stage steam separation the reservoir fluid often "flashes" to steam at the surface at 100°C and 1 bar (absolute) and the enthalpies at this condition are used in the expression.

Note: Temperatures and pressures are converted to enthlapy values using steam tables (Appendix 1). The pressure read from gauges (bars gauge, b.g) is not the same as the absolute pressure (bars absolute, b.a.). Bars gauge is equal; to the pressure in bars absolute minus the ambient pressure (taken as 1 b.a.):

$$\text{b.g.} = \text{b.a.} - 1$$

As the steam fraction is then the only unknown in the expression, the equation can be solved and y calculated.

In "multiple steam separation", steam is separated from the well discharge at two or more consecutive pressures. In such cases the steam fraction needs to be calculated for each stage in the separation.

Weirbox composition

It is common practice to recalculate well discharges to "weirbox" conditions (ie. 0 b.g.) regardless of the true separation pressure. This provides a common basis for comparing the discharge chemistry of wells between and within fields, and of the same well over a long period of time. If separation has occurred at a pressure above 0 b.g., then the solute concentration can be recalculated to weirbox conditions using the mass balance equation

$$C_{\text{weirbox 0,bg}} = C_{\text{separation pressure p,bg}} / (1-y_{\text{p-0,bg}})$$

Note that $y_{\text{p-0,bg}}$ is the steam fraction which results from flashing the liquid from the separation pressure (p, bars gauge) to 0 b.g., and is calculated as shown above.

Reservoir fluid composition

The concentration of species in the reservoir before steam loss can be calculated from the mass balance equation after the steam fraction has been determined. Many solutes which are concentrated in the liquid phase (eg. Cl) can be regarded as essentially insoluble in the steam phase and the equation simplified to

$$C_{i,res} = (1-y)C_{i,l}$$

$C_{i,l}$ is determined by analysis of the discharge water, y is known from the earlier calculation, so $C_{i,res}$ can be determined.

For precise work, and for components which are soluble in both the liquid and steam phases, both the steam and the water discharged by the well must be analysed to determine $C_{i,l}$ and $C_{i,v}$ and the reservoir composition calculated from the complete mass balance equation

$$C_{i,res} = yC_{i,v} + (1-y)C_{i,l}$$

The results of these calculations are termed the "total discharge composition".

Total discharge (TD) composition

As shown above, the total discharge composition of a well is obtained by combining the chemistry of both the steam and liquid phases using the mass balance equation. Under ideal conditions this would represent the actual reservoir fluid composition. However, there are other factors which can influence the chemistry of the well discharge, such as:

- the addition of heat to the fluid from the wall rocks or
- the addition of steam to the discharge from surrounding formations.

Under such circumstances the additional heat added to the fluid creates "excess enthalpy" discharges which distort the calculations of steam fraction and reservoir fluid composition. It is often not known that such enthalpy additions have been made to the fluid, particularly in the early stages of field development, so rather than automatically assume the calculated composition is definitely that of the reservoir, the term "total discharge (T.D.) composition" is used to indicate that this is a composition calculated from the discharge enthalpy. The T.D. composition can also be used as a common basis to compare well chemistry, as well as the weirbox composition, but the possibility of excess enthalpy discharges distorting the comparisons must be remembered.

Reservoir fluid pH

The temperature and composition of the reservoir fluid can be determined from geothermometers, mixing models and the chemistry of well discharges. In addition, the pH of the reservoir fluid is an important parameter, but is one which cannot be directly measured. Instead, it can be estimated from calculations based on equilibria reactions. Two simple methods provide reasonable estimates of reservoir-fluid pH.

Method 1: carbonate equilibria

$$H_2CO_{3(aq)} = HCO_3^-{}_{(aq)} + H^+{}_{(aq)}$$

$$K = a_{HCO_3}\, a_H / a_{H_2CO_3}$$

The above equilibrium describes the dissociation of dissolved carbon dioxide into bicarbonate and hydrogen ions. The equilibrium constant for this reaction can be re-written substituting the activity of the ions by their concentrations (m) multiplied by the appropriate activity coefficient (γ).

$$K = \gamma_{HCO_3}\, m_{HCO_3}\, \gamma_H\, m_H / \gamma_{H_2CO_3}\, m_{H_2CO_3}$$

This can be re-arranged by taking logarithms and substituting (- pH) for (log [γ_H m_H])

$$\log K = \log (\gamma_{HCO_3}/\gamma_{H_2CO_3}) + \log (m_{HCO_3}/m_{H_2CO_3}) - pH$$

Log K (at the reservoir temperature) can be obtained from data tables; the activity coefficients vary with temperature and ionic strength and are calculated from the Debye-Huckel equation. Concentrations (molal units) are obtained from the total discharge composition of the well. This leaves the pH of the reservoir fluid (at the reservoir temperature) as the only unknown which can then be calculated. Remember that at reservoir temperatures, neutral pH<7 (Section 2.3).

Method 2: calcite dissolution equilibria

$$CaCO_{3(s)} + 2H^+{}_{(aq)} = Ca^{2+}{}_{(aq)} + H_2O_{(l)} + CO_{2(aq)}$$

$$K = a_{Ca}\, a_{CO_2} / a_H$$

The solubility of calcite can be expressed by the above equilibrium. If calcite appears in cores or cuttings of the reservoir lithology, then it can be assumed that the reservoir fluid is in equilibrium with calcite and the following procedure can be adopted to estimate reservoir fluid pH.

As in the above method, the equilibrium constant is re-written in terms of concentration and activity coefficients; logarithms are taken and pH substituted to give the expression

$$\log K = \log (\gamma_{Ca}\, \gamma_{CO_2}) + \log (m_{Ca}\, m_{CO_2}) + 2pH$$

As before, values of K are taken from tables, g values are calculated and concentrations, m, are determined from the total discharge composition, leaving pH as the only unknown.

These two methods depend for their accuracy on the quality of both the thermodynamic data and the chemical analyses. Even with the best quality data however, both methods still can only give a close approximation of reservoir pH as they do not take into account the reaction between the carbonate equilibria and other weak acids in solution. An alternative, more rigourous method of calculating reservoir pH was developed by Glover (1982), and this incorporates the effect of other weak acids in the fluid. In addition, reservoir pH is often incorporated into calculations of solute speciation within the reservoir. These calculations are undertaken by computer programs which draw on thermodynamic data sets (eg. Helgeson et al., 1978). Several programs are presented by Henley et al. (1984) but others are also available, such as that developed by Arnorsson et al. (1982). This latter paper is particularly recommended as it provides a good overview of the approach and calculations typical of speciation programs.

CHAPTER 3

GAS CHEMISTRY

3.1 INTRODUCTION

The following gases, with steam, are invariably present in geothermal discharges from both natural features and wells: CO_2, H_2S, NH_3, N_2, H_2, CH_4. These gases are often collectively referred to as the "non-condensible gases". Despite the near ubiquitous presence of these species, the exploration and evaluation of geothermal systems has traditionally placed greater emphasis on the sampling, analysis and interpretation of water chemistry, with gas chemistry rarely considered in the same detail. The greater care which gas sampling requires, coupled with the variability of gas compositions within a field and the sensitivity of gas equilibria to pressure, vapour-liquid separation processes and temperature has led to a lack of confidence in the interpretation of gas chemistry relative to water compositions. However, improved analytical procedures and an increasing database of geothermal gas compositions, particularly from well discharges, mean that it is possible to give gas chemistry the detailed consideration it deserves in all phases of the geothermal resource development.

The terms "steam", "gas" and "vapour" are all used in the literature on geothermal systems. It is usual for the vapour phase to be called the steam phase; this is not strictly correct but is so well-established that to try to correct the usage would be futile, and indeed this colloquial usage will be continued in this text. This imprecise terminology arises from the fact that the vapour phase is composed predominantly of steam (water vapour) with a small proportion of gas (only a few percent of the total). Although the proportion of gas within the steam discharge is small, the concentration of the gases together with the gas/steam and steam/water ratios can yield important information on the subsurface conditions, and on the behaviour of a field during exploitation.

Geothermal steam is produced by boiling of the fluid at depth. The vapour phase so produced can migrate to the surface vertically, whereas the residual water

often migrates laterally from the boiling zone. If the water finally emerges at the surface, it can be many kilometres away from the upflow zone, particularly in mountainous terrain. Under such circumstances, a knowledge of variations in gas discharge chemistries can yield more information on the structure of the system than that which can be obtained from distant hot-springs.

3.2 DISCHARGE FEATURES

Fumaroles: Since without any well discharge data the composition of the deep fluid is unknown, initial investigations tend to use the gas chemistry of fumaroles over a field on a comparative basis to recognise flow structures. Large fumaroles with a high mass discharge offer the most reliable data on the composition of sub-surface steam (ie. the steam wells will produce). In such cases, the large flow rate is assumed to be indicative of a rapid and direct migration to the surface, with correspondingly less time for near-surface rock-steam and condensation reactions to occur.

Kaipohan: A relatively new term, proposed by Bogie et al. (1987), to describe areas of diffuse cold geothermal gas emission, invariably surrounded by argillic alteration and dead vegetation. Kaipohan differ from steaming ground in that the area is cold, and that only gas is evolved, the steam content of the original discharge having condensed at depth to form a perched aquifer. The water in this aquifer must be near-saturation with respect to the geothermal gases (dominantly CO_2 and H_2S) to permit further diffusion of the gases to the surface. To form, kaipohan require the presence of a low-permeability formation and/or an area of steep, typically andesitic, terrain combined with a low water table and high gas flux. Although kaipohan are difficult to sample, unless the gas bubbles through a cold (meteoric) water pool, recognition of these features can be significant in understanding the hydrology of a system as they often occur over or close to the upflow zone.

Solfataras: Two definitions are in use. In one, the term solfatara, is used to describe a fumarole with sulphur dioxide and/or hydrogen sulphide in the discharge. Alternatively, the term is used for steam discharge areas which contain steaming ground and fumaroles.

Steaming ground: Steam produced by the underground boiling of a geothermal water reservoir commonly migrates to the surface independent of the liquid phase. This

steam (with gases) often discharges into the atmosphere through an area of steaming ground. Such an area typically shows extensive argillic alteration, dead or low vegetation cover and has temperatures at boiling point a few centimetres below the surface. *Hydrothermal eruption craters, acid springs* and *mud pots* may also be present. Unless specific discharge vents are present, or the gases discharge through a pool, areas of steaming ground are less amenable to sampling than fumaroles and commonly show air contamination. If the ground temperature is at boiling point a few centimetres below the surface, then holes can be dug and samples obtained, through collection can be slow.

Hot pools: Gas discharges from hot pools can be readily collected, with sampling as close to the discharge vent as possible. However, it should be remembered that even in deep pools some contamination by atmospheric gases can occur.

Well discharges: Results from well steam discharges greatly assist in the interpretation of fumarole chemistry, since they enable gas/steam ratios at the initial boiling stage, steam/water ratios and the gas content of the reservoir fluid to be calculated. This data gives greater confidence to the interpretation of fumarole chemistry in terms of flow direction and upflow areas.

3.3 PROCESSES AFFECTING STEAM COMPOSITION

The composition of the steam discharge is affected by several factors:

- the temperature and pressure of the geothermal reservoir
- the gas content of the reservoir fluid
- the solubility of a gas in the liquid phase
- the mass distribution coefficient of gases between the liquid and vapour phases
- the pressure and temperature of steam separation (as the mass distribution coefficients are temperature dependant)
- the chemistry of steam in the reservoir (if a two-phase system)
- the proportion of the mass of the original reservoir fluid which converts to steam
- the chemistry of steam produced by boiling of the reservoir fluid
- the stage at which steam is separated (early steam contains a higher proportion of gases than later-separated steam)

- reactions in the steam phase as it ascends, eg. condensation, oxidation, rock-steam reactions, contamination by air or organic matter degradation products (NH_3, CO_2, CH_4)

In a single-phase, hot-water reservoir, steam is formed as a consequence of reducing pressure as the fluid migrates to the surface. Under these circumstances, the steam chemistry, either at a fumarole or well discharge, is a direct consequence of the reservoir fluid composition. A more complex situation exists in two-phase reservoirs; these contain both vapour and liquid phases in equilibrium. In this case the steam discharged at the surface will be a composite mixture of the reservoir vapour plus steam produced by boiling of the ascending liquid phase. Under these circumstances, the gas chemistry of the discharge will not reflect the gas-gas or gas-liquid equilibria present in the reservoir. Examples of the composition of steam discharged from fumaroles and wells over liquid-dominated and vapour-dominated fields are presented in Table 3.1.

Geothermal system

The interaction of at least some of the above factors will create differences in gas composition between different types of geothermal field: for *high-temperature systems* carbon dioxide with lesser amounts of hydrogen sulphide are the main gases, together often representing over 90% of the gas content. Minor and variable amounts of other gases including ammonia, hydrogen, methane and nitrogen may also be present together with trace quantities of oxygen, the noble gases, hydrocarbons and the volatile species of boron, fluorine, arsenic and mercury. These gases are also found in *low-temperature systems*, however the relative proportions of the gases can be different from that shown in high-temperature fields: nitrogen and methane, for example, may be the principal gases rather than carbon dioxide and hydrogen sulphide. Fumaroles over *magmatic systems* show a very different chemistry and are characterised by the presence of significant amounts of hydrogen chloride, hydrogen fluoride and sulphur dioxide, together with variable amounts of the geothermal gases. It is important to be familiar with the chemistry of magmatic vapours and condensates to distinguish them from geothermal steam discharges.

Solubility

The solubility of a gas in the liquid phase of a geothermal fluid governs the extent to which it fractionates into the vapour phase on steam formation. For the common geothermal gases, the solubility order is (least soluble) $N_2<O_2<H_2<CH_4<CO_2<H_2S<$

NH_3 (most soluble). The solubility of the more soluble common geothermal gases is discussed by Ellis (1962), Ellis and Golding (1963) and Mahon et al. (1980b). Figure 3.1 illustrates the changes in the vapour-liquid distribution coefficient (an indicator of relative solubility) for carbon dioxide, hydrogen sulphide and ammonia over the temperature range of geothermal systems. As can be seen, gas solubility increases with temperature and the relative differences between carbon dioxide and hydrogen sulphide are approximately consistent over 200 - 260°C, with hydrogen sulphide 2-3 times more soluble (Ellis, 1962; Glover, 1970). Carbon dioxide and hydrogen sulphide solubilities decrease with increasing fluid salinity, an effect which is greatest at higher temperatures. However, given that most geothermal fluids are relatively dilute, this effect can be neglected and the values for the solubility of the gases in pure water taken as valid for these studies (Mahon et al., 1980b). Ammonia is consistently more soluble than the other two gases (~10 times greater than H_2S and ~20 times more soluble than CO_2 at 260°C), but these relative differences in solubility decrease rapidly towards the critical point of water, 374°C (Fig. 3.1; Ellis, 1962).

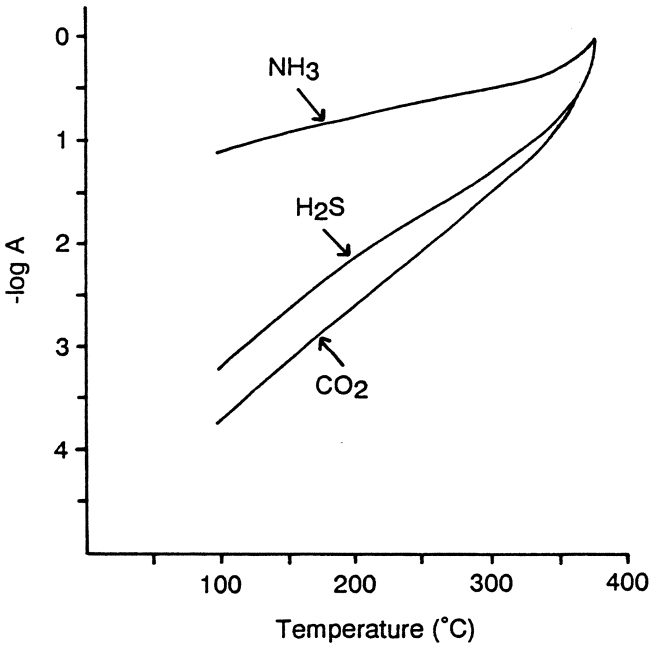

Figure 3.1. Changes in solubility (as measured by the vapour-liquid mass distribution coefficient, log A_{gas}) with temperature for carbon dioxide, hydrogen sulphide and ammonia up to the critical point. Note how differences in solubility diminish as the critical point is approached.

Mass distribution co-efficients

Solubility can be expressed in terms of the distribution of a gas between the vapour and liquid phases. This partitioning is described by the mass distribution coefficient,"A", which is defined by the expression:

$$A_{gas} = (n_{gas}/n_{H_2O})_{liquid} / (n_{gas}/n_{H_2O})_{vapour}$$

where n = number of moles of gas or water in the liquid and vapour phases. In other words, the mass distribution coefficient is defined by the concentration of gas in the liquid phase (C_l) divided by that in the vapour phase (C_v). Note that molar, molal, weight or other similar mass units can be employed in this ratio.

$$A_{gas} = C_l/C_v$$

from the mass balance equation

$$C_{TD} = yC_v + (1-y)C_l$$

where

C_{TD} = gas concentration of the total discharge

y = the steam fraction

(1-y) = the water fraction

substituting $A_{gas}.C_v$ for C_l

$$C_{TD} = yC_v + (1-y)A_{gas}.C_v$$

which can be rearranged as

$$C_{TD} = C_v [y + A_{gas}(1-y)]$$

The temperature-dependent equations for the mass distribution coefficient have been defined and are listed below. With A_{gas} known, it is possible therefore, for given temperature, to calculate the concentrations of a gas in the liquid and vapour phases using the above equations. Note however, that the gas composition in the total discharge is needed. This in turn requires a knowledge of the steam/water ratio, something which is invariably only available from well discharges.

Equations of Giggenbach (1980):			valid range (t°C)
$\log B_{CO_2}$	=	4.7593 - 0.01092t	100 - 340
$\log B_{H_2S}$	=	4.0547 - 0.00981t	100 - 340
$\log B_{CH_4}$	=	6.0783 - 0.01383t	100 - 340
$\log B_{H_2}$	=	6.2283 - 0.01403t	100 - 340
$\log B_{N_2}$	=	6.4426 - 0.01416t	100 - 340
$\log B_{NH_3}$	=	1.4113 - 0.00292t	100 - 340

Equations of Saracco and D'Amore (1989):

$$\log B_{gas} = a + bt$$

gas	a	b	valid range (t°C)
CO_2	5.035833	- 0.0132920	20 - 99
	4.895136	- 0.0117540	100 - 149
	4.769526	- 0.0109610	150 - 320
	5.393368	- 0.0129470	321 - 350
	13.173940	- 0.0352110	351 - 374
H_2S	4.600467	- 0.0143630	20 - 99
	4.377379	- 0.0120250	100 - 149
	4.044170	- 0.0097980	150 - 330
	7.988000	- 0.0213300	331 - 350
H_2	6.868929	- 0.0211210	20 - 99
	6.432524	- 0.0163230	100 - 149
	5.968130	- 0.0133010	150 - 320
	8.422500	- 0.0210500	321 - 350
	16.315200	- 0.0435420	351 - 374
CH_4	6.597095	- 0.0173380	20 - 99
	6.399970	- 0.0159020	100 - 149
	6.080947	- 0.0138746	150 - 340
	12.649167	- 0.0331500	341 - 359
	16.859010	- 0.0450120	360 - 374
CO	6.688962	- 0.0175880	20 - 99
	6.449000	- 0.0148500	100 - 140
	6.286525	- 0.0137290	141 - 320
	6.831643	- 0.0154640	321 - 350
	21.930700	- 0.0586160	351 - 374

It is not very convenient to use A_{gas} to describe the solubility of a gas as this co-efficient has very small values. It is more practical instead to use $1/A_{gas}$, and this has been given the notation "B" by Giggenbach (1980); ie.

$$B_{gas} = 1/A_{gas} = C_v/C_l$$

Alternatively, at relatively low gas concentrations, this equation can be simplified by expressing concentration not in mole ratios (n_{gas}/n_{H_2O}) but by the mole fraction, X_{gas}, ie. $X_{gas} = n_{gas}/(n_{H_2O} + \Sigma n_i)$

where Σn_i = the sum of the mole concentrations of all gases.

When $\Sigma n_i << n_{H_2O}$ (ie. low gas system),

then $X_{gas} \sim n_{gas}/n_{H_2O}$

and $B_{gas} = X_{gas,vapour}/X_{gas,liquid}$.

Giggenbach (1980) and Saracco and D'Amore (1989) have presented equations relating the mass distribution coefficient to temperature for carbon dioxide, hydrogen sulphide, ammonia, methane, hydrogen, nitrogen and carbon monoxide (see boxes).

Henry's Law coefficients

Gas solubility can also be expressed in terms of the Henry's Law coefficient, Kh, which increases with decreasing solubility. Henry's Law relates the partial pressure of a dissolved gas, P_{gas}, and the mole fraction of the gas in solution, X_{gas}:

$$Kh_{gas} = P_{gas}/X_{gas}$$

	Kh (bars/X_{gas})		
t (°C)	CO_2	H_2S	NH_3
25	1660	551	1.0
50	2880	899	2.7
100	5245	1555	14.5
125	6150	1703	28.1
150	6670	1829	49.1
175	6860	1959	78.8
200	6620	2042	119.0
250	5340	1934	233.0
300	3980	1645	413.0

This can be related to the mass distribution coefficient (another measure of solubility) by the expression:

$$Kh_{gas} = B_{gas}(P_v/Z_v)$$

where P_v = the water vapour pressure

Z_v = compressibility factor for pure saturated steam (ignoring the effects of dissolved gases) and

$$Z_v = P_v V_v/nRt$$

where n = the number of moles

V_v = the molar volume of steam in m^3

T = temperature in Kelvin

R = the gas constant (8.309×10^{-5} m^3bar/deg.mole)

Substituting for Z_v gives the expression:

$$Kh_{gas} = nB_{gas}RT/V_v$$

Figure 3.2 shows the variation in Kh with temperature for carbon dioxide. As can be seen, the relationship is not linear, and the coefficient attains a maximum value (minimum solubility) around 175°C. Henley et al. (1984) presented the following data (recalculated from the results of Ellis and Golding, 1963; and Glover, 1982) which illustrates the variation in Kh with temperature for hydrogen sulphide and ammonia as well as carbon dioxide in pure water. $Kh(H_2S)$ passes through a maxima around 200°C, but $Kh(NH_3)$ increases with increasing temperature. Temperature-dependent relationships for Henry's Law constants for gases in pure water have been established by Nehring and D'Amore (1984) for the upper temperature range, as shown in the box below.

$\log Kh_{CO2}$	=	5.31328 - 0.00306T	t>200°C
$\log Kh_{H2}$	=	7.34835 - 0.00563T	t>150°C
$\log Kh_{CH4}$	=	7.35698 - 0.00590T	t>150°C
$\log Kh_{H2S}$	=	4.00871 - 0.00142T	t>150°C
$\log Kh_{N2}$	=	7.56180 - 0.00567T	t>150°C
$\log Kh_{NH3}$	=	- 0.21173 + 0.00488T	t>150°C

Steam formation

As a geothermal fluid migrates to the surface, a reduction in the confining pressure within the geothermal system will cause the vapour phase to separate from the liquid phase (ie. the fluid boils). The depth at which this occurs depends upon several factors, notably the temperature and gas-content of the system (the boiling point-depth curve; influences upon this relationship are discussed in Chapter 1). The steam produced by boiling of subsurface waters is discharged at fumaroles and over steaming ground and, as noted, is very different in composition from magmatic steam discharged by active volcanoes (Table 3.1).

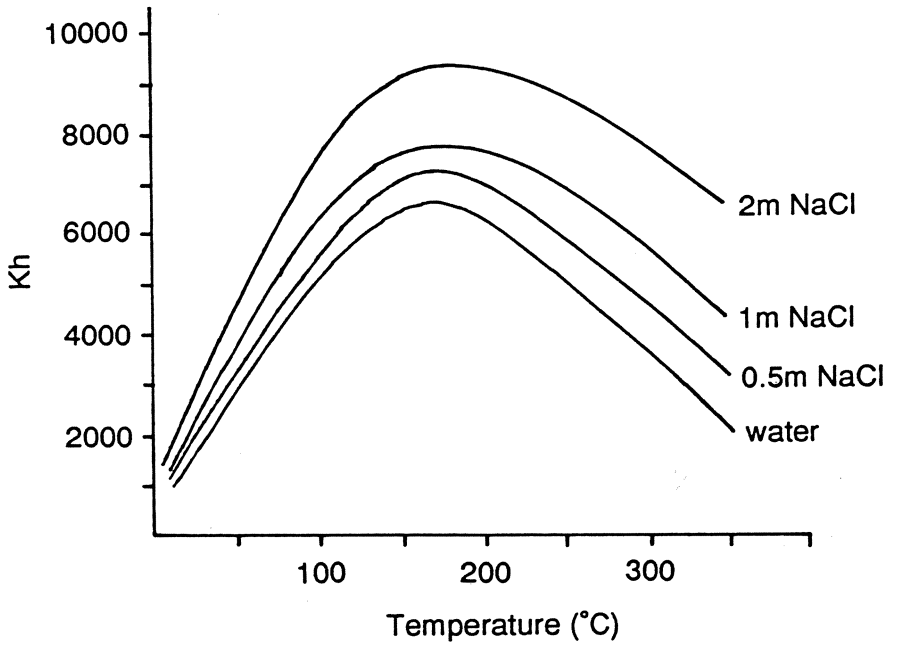

Figure 3.2. Variation in Henry's Law constant, Kh, with temperature for carbon dioxide at fluid salinities of 0 to 2m NaCl. Note that maximum values for Kh (CO_2 solubility minima) occur at around 175°C.

Gases are more soluble in steam than in the original fluid. After boiling, the residual liquid is therefore depleted in gas relative to the original fluid composition, although portions of all gases (especially the more-soluble species CO_2, H_2S, NH_3) will be retained in the liquid phase. Since, at a given temperature, each gas has a

Table 3.1. Geothermal gas discharge chemistry.

Field/ feature	Separation pressure (bg)	Enthalpy (kJ/kg)	Steam fraction (y)	Total gas in steam (mmol/mol steam)	CO_2	H_2S	CH_4	H_2	N_2 +Ar	NH_3
					(millimoles/mole total gases)					
Wells: liquid dominated systems										
Wairakei, N.Z.										
Average	1	1135	0.3	0.2	917	44	9	8	15	6
Tauhara, N.Z.										
Well 1	8.8	1120	0.2	1.2	936	64	-	-	-	-
Ohaaki, N.Z.										
Well 22	10	1169	0.19	10.04	956	18.4	11.8	1.01	8.89	4.65
Ngawha, N.Z.										
Well 4	1.87	966	0.19	24.5	945	11.7	28.1	3.0	2.1	10.2
Cerro Prieto, Mexico										
Well 19A	6.6	1182	0.289	5.88	822	79.1	39.8	28.6	5.1	23.1
Tongonan, Philippines										
Well 103	7.6	1615	0.414	2.95	932	55	4.1	3.6	1.2	4.3
Reykjanes, Iceland										
Well 9	19.0	1154	0.135	0.248	962	29	1	2	6	-
Wells: vapour dominated systems										
The Geysers, USA										
Average	-	2793	1.0	5.9	550	48	95	150	30	125
Larderello, Italy										
Average	-	2804	1.0	20.0	941	16	12	23	8	8
Fumaroles										
Wairakei, N.Z.										
Karapiti	-	(115°C)	1.0	1.7	946	23	7.4	10	11	2.6
Larderello, Italy										
Average	-	(100°C)	1.0	30.0	923	20.6	14	26	10.7	-

Data from Ellis and Mahon (1977) and Henley et al. (1984)

different mass distribution coefficient, the gas ratios in the steam will differ from those in the original fluid. The ratio (less-soluble gas / more-soluble gas) will increase in steam since a greater proportion of the less-soluble gas will enter the vapour phase. The gas concentrations in steam will fall as more steam is formed, and the (less-soluble gas / more-soluble gas) ratio will similarly decrease (eg. CO_2/H_2S) as the proportion of the more-soluble gas increases relative to the less-soluble gas. Steam evolving from a hot-water flow will therefore show an evolution in chemistry with distance from the source. Relative to early-formed steam, later-formed steam has the following characteristics (Glover, R.B., pers. comm., 1991):

- lower gas concentrations
- lower CO_2/H_2S ratios
- lower CO_2/NH_3 ratios
- lower H_2S/NH_3 ratios
- higher CO_2/H_2 ratios

Two extreme processes of steam separation may occur: single-stage and continuous (Raleigh) steam separation. Multiple-stage steam separation represents an intermediate condition. In a single-stage process, equilibrium in reactions is maintained; in Raleigh separation the products of a reaction are continuously removed and the process is driven to completion, ie. gases are quantitatively removed from the residual liquid.

Single stage

The loss of gases from the liquid phase on steam separation is illustrated in Figure 3.3 for the equilibrium, single-stage separation process. From this diagram it can be deduced that steam produced early in the separation process is enriched in carbon dioxide and hydrogen sulphide. The residual liquid rapidly becomes depleted in these gases after only a few percent steam separation; differences in the amount of gas retained by the liquid are a function of the relative solubilities of the gases. Since, of the three gases considered, CO_2 is the least soluble it enters the vapour phase more readily than H_2S or NH_3. Other less soluble gases, such as N_2 and CH_4, will pass into steam even more rapidly than CO_2. Steam formed later in the separation process by boiling of the residual liquid will therefore show increasingly lower and lower gas concentrations. Also, given the increase in gas solubility with higher temperatures, lower concentrations of gases will be found in steam which separates from fluids at higher temperatures than those which boil at lower temperatures ie. for a given percentage of steam formation, the concentration of gases in steam separated from a

260°C fluid will be less than in steam formed from a 240°C fluid (Glover, 1970). Gases will therefore be depleted more rapidly in the residual liquid at lower temperatures. Ammonia, the most soluble geothermal gas, is retained in the liquid phase to a much greater extent, with a decrease in the ammonia concentration by only about 3% for every 1% of steam separated (Ellis, 1962).

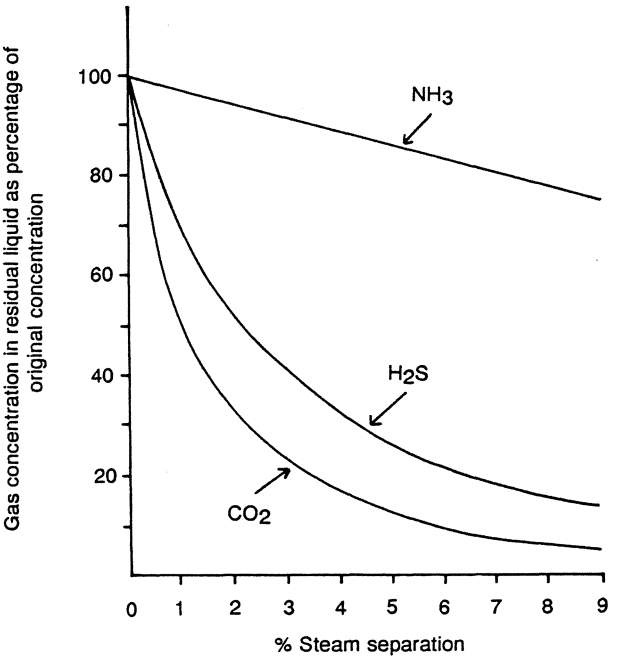

Figure 3.3. Proportion of gases remaining in the liquid phase following equilibrium single phase steam separation from a 260°C fluid. Gas proportions are calculated as percentages of (gas concentration in the residual liquid phase after separation) / (gas concentration in the fluid before separation). Note the rapid depletion of gases from the liquid phase on initiation of steam separation. Steam produced in the early stages of separation ("early steam") will therefore contain a large proportion of the available gases.

Continuous separation

The above discussion centred on equilibrium or single-stage separation. In continuous separation equilibrium is assumed but in infinitely small steps, ie. this is the limiting condition of multi-stage separation (see below). The gases are removed as they form and the residual liquid becomes depleted much more rapidly, for a given steam fraction, than in single-stage separation with gas concentrations in the liquid approaching zero after only a few percent steam separation (Ellis, 1962). As the gases are removed from the system, the equilibrium reactions continuously move towards the vapour phase

eg. $$CO_{2(aq)} = CO_{2(g)}.$$

The process of continuous separation can be described by the equation (Henley et al., 1984):

$$C_l/C_{TD} = ye^{-B_{av}}$$

where

y = the cumulative steam fraction removed

B_{av} = an average distribution coefficient for a *small* temperature interval

Multiple-stage separation

Multiple-stage separation represents an intermediate case, where steam forms in equilibrium with the liquid phase and is subsequently removed prior to further steam formation. This process was examined in detail by Glover (1970), who demonstrated that multi-stage separation reduces the gas content of the liquid more rapidly than single-step equilibrium separation. The difference in the gas content of the residual liquid between these processes is related to the solubility of the gases, with less soluble species removed most rapidly. The effect on CO_2 is therefore more marked than on H_2S (Fig. 3.4), which in turn shows greater effect than NH_3.

If steam separation over a small temperature interval only is being considered, then for n steps, each removing a fraction of the steam, y, an average mass distribution coefficient, B_{av}, can be used (Henley et al., 1984).

$$C_{TD}/C_l = [1 + y(B_{av} - 1)]^n$$

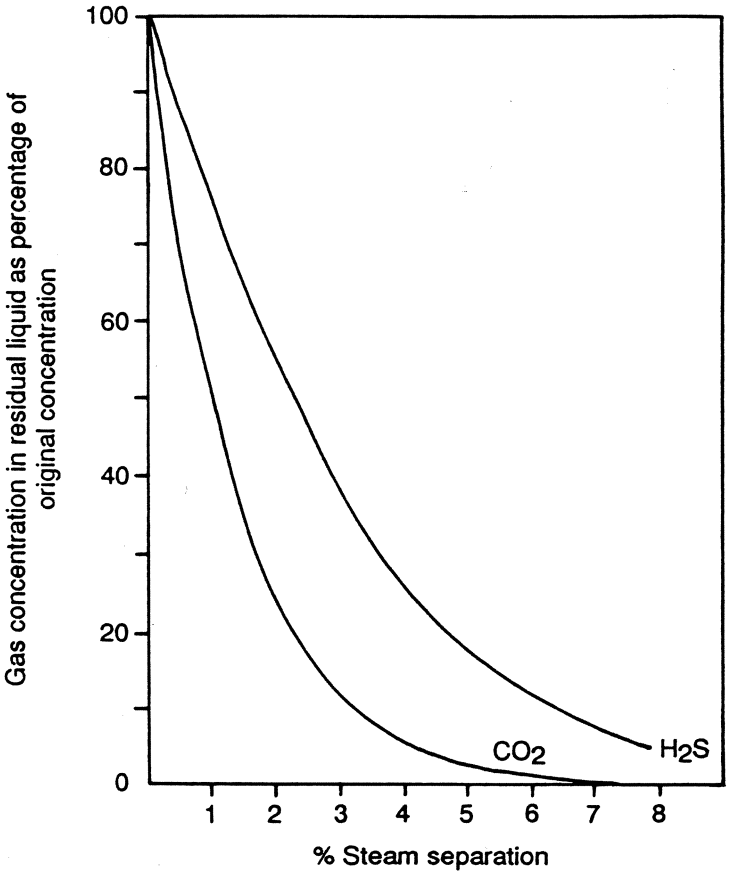

Figure 3.4. Proportion of gases remaining in the liquid phase following multiple-phase steam separation from a 260°C fluid (Glover, 1970). Gas proportions are calculated as percentages of (gas concentration in the residual liquid phase after separation) / (gas concentration in the fluid before separation). Note the rapid depletion of gases from the liquid phase on initiation of steam separation, and that this depletion becomes more complete than for single-stage separation (Fig. 3.3). Steam produced in the early stages of separation ("early steam") will therefore contain a large proportion of the available gases.

Condensation

As steam approaches the surface it may, on contact with cooler host rocks, condense to a liquid phase which can accumulate to form a perched aquifer. Regardless of whether a secondary aquifer forms, the condensation of part of the steam phase will increase the proportion of gas to steam (high gas/steam ratio) remaining in the vapour phase. The steam condensate will dissolve some of the more soluble gases (eg. ammonia, boron, arsenic), removing them from the vapour. The twin effects of steam condensation and (partial) removal of the more-soluble gases in the condensate, increases the proportion of the less-soluble gases in the remaining steam. Gas ratios will therefore also be affected by differences in the relative solubilities of the gases.

Oxidation

Oxidation of the fluid lowers the H_2S concentration as the gas is oxidised to sulphate, and therefore increases the CO_2/H_2S ratio.

Rock-steam reactions

Steam can react with the rocks which it passes through. The most notable effects of such reactions are the removal of hydrogen sulphide, hydrogen and ammonia. However, wall-rock reactions can also add gases to the steam phase. Carbon dioxide can be contributed from the decomposition of carbonate minerals, and thermal degradation of organic matter can yield additional carbon dioxide, methane and ammonia. Radioactive decay of minerals within the host rocks can additionally cause helium, argon and radon to enter the steam discharge.

Mineral equilibria and buffering

The concentration of the gases in the steam phase may be controlled, or buffered, by mineral assemblages within the host rocks. It has been suggested that oxygen and sulphur fugacities are controlled by elemental carbon (graphite) and pyrite - pyrrhotite - magnetite mineral buffers respectively (D'Amore and Nuti, 1977; Nehring and D'Amore, 1984; Giggenbach, 1987). Giggenbach (1980) however, argues that graphite does not control the content of CO_2, H_2 or CH_4 in geothermal discharges. He further suggests that since pyrrhotite and magnetite are not common minerals in geothermal systems, they are unlikely to buffer H_2S-H_2 concentrations, and that at temperatures below 300°C, iron-bearing alumino-silicates (such as chlorite or epidote) with pyrite are more likely candidates, a point acknowledged by Nehring and D'Amore (1984).

Seismicity

Microseismicity induced by exploitation releases steam plus other gases (He, CH_4, N_2) into a geothermal system. Such activity created zones of high He at Larderello (D'Amore and Truesdell, 1984), and elevated levels of these gases, with H_2 and CO_2, have been reported in areas of natural seismic activity (D'Amore and Panichi, 1987; Sugisaki, 1987; Sugisaki and Sugiura, 1986).

Contamination

Soil air will contain oxygen, nitrogen and other trace atmospheric gases and these can be entrained in the steam discharge as it passes through the soil profile. These contaminants can also be added to a sample during the sampling process. If contamination is suspected, a correction to the gas concentrations can be effected from the oxygen concentration in the sample and the known proportions of atmospheric gases relative to oxygen.

3.4 INTERPRETATION OF GAS CHEMISTRY

As with the water-soluble constituents, geothermal gases can be conveniently divided into two groups:

- *reactive* gases (eg. H_2O, CO_2, H_2S, NH_3, H_2, N_2, CH_4) which take part in chemical equilibria and provide information on the sub-surface conditions such as temperature
- *inert* or *conservative* gases (eg. the Noble gases, hydrocarbons other than methane) which act in an analogous manner to chloride in that they do not take part in chemical reactions. They can be used to provide information on the source of the gases.

The two main geothermal gas equilibria are the methane breakdown or Fischer-Tropsch reaction,

$$CH_4 + 2H_2O = CO_2 + 4H_2$$

and the ammonia breakdown reaction

$$2NH_3 = N_2 + 3H_2$$

All constituents are in the gaseous phase, and the equations are written to favour the products at higher temperatures.

Behaviour of common geothermal gases

Carbon dioxide (CO_2)

This is the most abundant gas in geothermal systems, often representing over 85% by both volume and weight of the total gas content of a discharge (Mahon, et al., 1980b). The gas can be produced by thermal alteration of carbonate rocks and minerals, from the degradation of organic matter within sedimentary rocks at depth or in near-surface reactions, and from solutes in meteoric waters (notably the conversion of $HCO_{3(aq)}$ to $CO_{2(g)}$ on boiling) or it can be, in part, of a magmatic origin. The influence of carbon dioxide on the overall chemistry and hydrology of a geothermal system should not be under-estimated. Water chemistry, density and pH, boiling point-depth relationships, rock alteration and the deposition of secondary minerals and scale are all controlled to some degree by the concentration of carbon dioxide (Mahon, et al., 1980b).

As shown in Figure 3.5, for a given temperature the fluid in a reservoir will boil at greater depths the greater the carbon dioxide concentration. Low-gas systems will show only a minimal change from the boiling point-depth relationship for pure water. However, a high-gas reservoir fluid (>~2 wt% CO_2) will boil at greater depths than a low-gas fluid of the same temperature. The effect of the gas on the depth at which boiling first occurs is greatest in the range 150-200°C, where the solubility of carbon dioxide passes through a minimum. The depth to first boiling may be further increased if free carbon dioxide exists above the liquid phase. Mahon et al. (1980b) consider that this can cause a CO_2-H_2O froth to form, lowering the density of the fluid and increasing the depth to a given temperature within the system. The overall effect of a high CO_2 content is therefore to reduce the geothermal gradient profile within a system. Further, temperature reversals in wells may not be due to the inflow of colder water into the system, but result from gas separation from the fluid lowering the temperature of the residual liquid (Mahon et al., 1980b).

The partial pressure of carbon dioxide increases with increasing temperature (Arnorsson et al., 1982). The value of P_{CO_2} at the point of gas equilibrium can be calculated by the expression derived by (Chiodini and Cioni, 1989):

$$\log P_{CO_2} = 3.573 - 46/T - \log(X_{H_2}/X_{CO_2})$$

This model, which is almost independent of temperature, assumes that P_{H_2O} is fixed by the presence of liquid water and can be applied both to fumaroles and well discharges (Chiodini and Cioni, 1989).

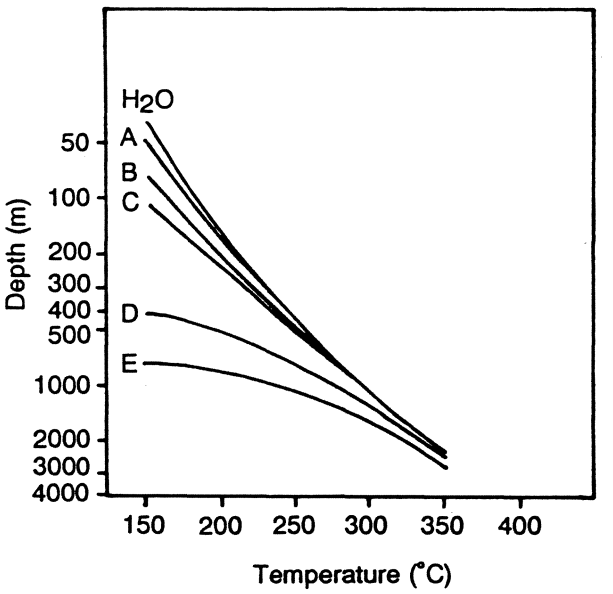

Figure 3.5. Changes in the boiling-point - depth profile with increasing carbon dioxide content. Note how the depth of first boiling for waters at a given temperature increases with increasing carbon dioxide concentration (Mahon et al., 1980b).

The pH of the fluid is buffered by CO_2/HCO_3 equilibria, and loss of CO_2 through boiling causes a change in the solution pH to more alkaline values (Ellis, 1962). The gas is less soluble than hydrogen sulphide and ammonia (Ellis, 1962; Ellis and Golding, 1963).

Hydrogen sulphide

This common gas may be produced by alteration of the reservoir rocks or from a magmatic source. It is reactive and is removed on reaction with wall rocks to form iron sulphides. Although this appears to be a slow process, the gas is lost through such reactions over time, increasing the CO_2/H_2S ratio with increased migration. Hydrogen sulphide is 2-3 times more soluble than carbon dioxide (Ellis, 1962).

Ammonia

This is the most soluble of the geothermal gases. High concentrations of ammonia can be the result of alteration of organic matter in sedimentary rocks at

depth, or in the near-surface environment. On migration to the surface the gas may be removed as a consequence of reaction with wall rocks, by adsorption onto clay alteration products or by solution into steam condensate. Although relatively soluble, ammonia increasingly partitions into the steam phase as temperature decreases; therefore as the geothermal water cools, more ammonia will be evolved.

Hydrogen

A highly reactive gas, hydrogen is readily removed on reaction with wall rocks. It is commonly lost over time and with increased migration (Arnorsson and Gunnlaugsson, 1985), and this enables the hydrogen and H_2/CO_2 content of discharges to be used to recognise flow directions and upflow zones.

Methane

Of all the hydrocarbon gases, methane is the one most commonly encountered. High concentrations of methane can be produced by the alteration of sedimentary rocks at depth, particularly if organic-rich, and it is not unusual for methane to be a principal constituent in gas discharges from sedimentary-hosted low-temperature systems. As discussed in Chapter 4, there is some debate over the methane formation reaction mechanism. The Fischer-Tropsch reaction

$$CO_2 + 4H_2 = CH_4 + 2H_2O$$

is commonly considered to be that most likely (Hulston and McCabe, 1962, Nehring and D'Amore, 1984); although a reaction between hydrogen and carbonaceous material has also been suggested (Gunter and Musgrave, 1971, Panichi et al., 1978). More recent work by Hulston and Lyon (1991) on the origin of methane in New Zealand geothermal systems found evidence of mixing of methane from two sources in the Mokai field. However, they could not determine whether an organic or biogenic source for New Zealand geothermal methane was most likely.

Nitrogen

As the principal atmospheric gas, most nitrogen in geothermal systems is derived from that dissolved in the meteoric recharge waters, although it can also be of magmatic origin. However, the original source of nitrogen in magmatic discharges is uncertain. It may be derived from the degradation of organic matter in the crust when it comes into contact with the magma. Nitrogen tends to assume greater proportions in low-temperature systems where it can be the major gaseous component.

Noble gases

The atmospheric noble gases (helium, He; neon, Ne; argon, Ar; krypton, Kr and xenon, Xe) are contributed to the geothermal fluid by the meteoric recharge waters and additionally for He and Ar, by rock leaching reactions (Chapter 2). Although radiogenic He can make a significant contribution to the overall concentration of the gas, and can in fact be the main source; radiogenic Ar has little impact on the total Ar content of the gas discharge. Argon can therefore be used as a conservative species in ratios, in much the same way that chloride is in water chemistry. On boiling, the gases all strongly partition into the steam phase. Above 280°C little fractionation between the gases occurs, since at these temperatures the solubilities of the gases, as shown by Henry's Law constants, converge (Mazor and Truesdell, 1984).

Oxygen

The presence of oxygen in a gas sample often indicates contamination either by soil air or during the sampling procedure (check O_2/N_2 ratio in sample with that of air). Oxygen concentrations in uncontaminated samples are near or below detection limits, as the deep fluid is reducing with P_{O_2} typically around 10-35 bars.

Hydrogen halides (HF, HCl)

In water-dominated systems with chloride waters at depth, virtually no hydrogen halides will be found in the vapour phase. However, steam produced by boiling of acidic geothermal waters or derived from magmatic sources can contain significant concentrations of free HF and HCl, both of which are readily dissolved by near-surface waters or steam condensates.

Volatile metals and non-metals

Arsenic: Arsenic can enter the vapour phase as arsenous acid, $As(OH)_3$ (EPRI, 1985). Only in very high-temperature systems is arsenic likely to be more than a trace constituent. As with boron, it will be readily removed from the vapour phase by steam condensation and mixing with groundwaters. Across a field, therefore, the highest arsenic concentrations should correspond to high permeability zones.

Boron: The volatility of boron increases with increasing temperature, and although originally derived by rock leaching and concentrated in the liquid phase, significant quantities of boron can be transported as a vapour. The principal volatile boron species is boric acid (H_3BO_3 or $B(OH)_3$), although BF_3 may also be present in gases evolved from acidic, high-fluoride fluids (EPRI, 1986). Boron is readily dissolved by steam condensate or near-surface steam-heated waters, in which it can

attain elevated concentrations notably when steam inflow is approximately equalled by evaporation (Glover, 1988; Tonani, 1970). Boron is therefore lost from the vapour phase with increased migration and shows highest concentrations in upflow zones (D'Amore and Truesdell, 1984). The following relationship between temperature and the boron distribution coefficient (for t = 150-320°C) has been derived by Glover (1988):

$$t°C = 456 + 149.5 \log K_D$$

where $K_D = C_{steam}/C_{water}$

Mercury: Mercury vapour and gaseous HgS can both contribute to the mercury content of the steam discharge. The hydrogen sulphide concentration of the deep fluid appears to play an important role in controlling mercury emissions, with less mercury vapour being produced with increasing H_2S concentrations (EPRI, 1987).

Tritium

Deep geothermal fluids with long residence times commonly contain little tritium compared with modern surface waters (Chapters 2 and 4). Steam produced from these waters will be similarly tritium-poor compared to steam formed from waters with shallow, more recent circulation paths. The tritium content of steam can therefore be used to differentiate between deep and shallow sources of the steam, and to recognise mixing between steam from both deep and shallow sources (D'Amore at al., 1977).

Indicators of physico-chemical processes

The following indicators extract and summarise the characteristics of geothermal gases and the active processes in gas addition and removal discussed above. As with diagnostic solute ratios, the indicators should not be followed blindly, but used in conjunction with an understanding of the processes which these trends represent. Note that correct interpretation of gas chemistry is often reliant upon large changes in gas ratios over a field; small, irregular variations with no obvious trend are difficult to interpret and may not be significant. The following indicators refer to chemical changes in steam flows. Where steam is continually evolving from a hot-water flow, differences in the chemistry of early-formed and late-formed steam (Section 3.3) will be superimposed on these trends.

Permeable/upflow zones

Fumaroles with high gas concentrations and the lowest CO_2/H_2S, CO_2/NH_3 and CO_2/H_2 are fed by steam with the most direct route to the surface. These are likely to be closest to the underlying hot-water source. This can assist in the location of drill sites. However, in mountainous terrain such sites may not be the best for drilling as the reservoir may be at an impractical drilling depth. Under such circumstances, drill sites lateral to the upflow zone, in the direction of flow, may be a more practical option.

Flow direction

Gas is lost from the deep fluid on boiling; the more the fluid migrates, the greater the amount of near-surface boiling and hence the lower the gas content of the steam. Further, ammonia, hydrogen and hydrogen sulphide are removed from steam by such processes as wall-rock reactions and solution into steam condensate. The further steam travels from the reservoir, the lower the absolute gas concentrations and the greater the CO_2/H_2S, CO_2/NH_3 and CO_2/H_2 ratios. Note also that as condensation removes water vapour from the steam flow, the total-gas proportion in the vapour phase (gas/steam ratio) will increase with increasing condensation.

Distance travelled from the upflow/boiling zone

Gases dissolved in the reservoir fluid prefer to enter the vapour phase whenever possible; this is shown by their distribution coefficients and relative solubilities. When the fluid boils, the initial few percent of steam formed contains the majority of the dissolved gases. The residual liquid is therefore highly depleted in dissolved gases, and later stages of steam separation will contain increasingly lower concentrations of gases. Steam formed in the early stages of boiling is characterised therefore by a higher gas content (ie. higher gas/steam ratio). Low CO_2/H_2S ratios, with low total gas contents and high enthalpy values may indicate several stages (or continuous) steam loss prior to discharge (Ellis, 1962) and a concomitant increase in the distance of lateral migration from the upflow zone. Steam discharge chemistry can thus be used to deduce which fumarole is closest to the upflow zone, and to select suitable drilling sites.

Source of gases

Radiogenic He: The He/Ar ratio is characteristically several orders of magnitude greater than the atmospheric value of 5.7×10^{-4}. The helium content of fluids will increase with increasing residence time.

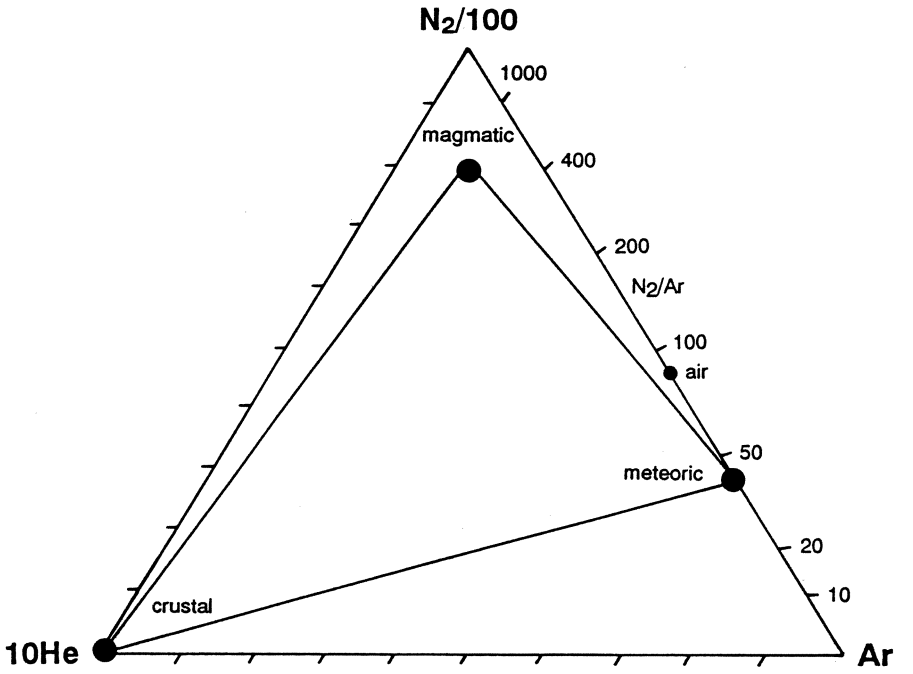

Figure 3.6. Mixing model to illustrate the relative contribution of magmatic, meteoric and crustal sources of gases in geothermal discharges.

Non-atmospheric N_2: A N_2/Ar ratio greater than the range 38 (for air-saturated water) to 84 (free air). A high ratio suggests decay of organic matter.

Meteoric: Molar ratios characteristic of a meteoric source include N_2/Ar = 38, He/Ar < 0.001.

ir contamination: Invariably indicated by the presence of oxygen in the sample, vith $N_2/Ar = 84$ and $He/Ar = 5.7 \times 10^{-4}$.

lagmatic input: Magmatic steam produced by active volcanoes (and their ondensates) can be recognised by high HCl, HF and SO_2 (Giggenbach, 1987). Iowever, any magmatic input into a geothermal system may be less obvious, but ould be indicated by high N_2 concentrations and N_2/Ar ratios around 800-2000. Compare with ammonia and methane signatures since the decomposition of organic-ich sediments can also yield high nitrogen contents. Helium is outgassed from the nantle and may therefore be diagnostic of a magmatic input with $He/Ar \sim 0.1$. Iowever, as young volcanic rocks may also contain mantle-driven helium, it can also nter the geothermal fluid by rock leaching (Truesdell et al., 1984).

lixing diagram: The proportions of N_2, He and Ar have been combined by Giggenbach (1980) to produce a diagnostic ternary plot to aid identification of the ominant source of the gases (Fig. 3.6).

eservoir rock type

High ammonia and carbon dioxide levels can indicate sedimentary rocks at epth. High levels of helium can be indicative of rocks bearing significant levels of ranium and thorium-bearing minerals.

ecomposition of near-surface organic matter

Indicated by high levels of ammonia, nitrogen, carbon dioxide, methane and ther hydrocarbons; high N_2/Ar and CH_4/Ar ratios.

ligh temperature reservoir

High hydrogen, boron, arsenic and mercury concentrations, and high H_2/H_2S atios are indicative of high subsurface temperatures (D'Amore and Panichi, 1987; Soga and Noda, 1976; White, 1970).

team gain by well discharge

If early-formed steam enters a well, the discharge will show a high gas content elative to the enthalpy of the well. The addition of gas-poor, late-formed steam owever, will dilute the concentration of gases in the original steam and result in a ischarge that shows a low gas content for its enthalpy (Glover, 1970).

3.5 GAS GEOTHERMOMETERS

The majority of gas geothermometers require that the gas/steam and, for a hot-water reservoir, the steam/water ratios are known (D'Amore and Panichi, 1987). Since steam and the corresponding water phase rarely discharge at the surface together, these ratios cannot be determined for hot springs or fumaroles. This has therefore limited the application of most gas geothermometers to well discharges. The exceptions to this are the empirical geothermometer of D'Amore and Panichi (1980), based on the CO_2-H_2S-H_2-CH_4 system, and the CO, CO_2 and H-Ar geothermometers; these can be applied to both natural and well steam discharges.

CO_2-H_2S-H_2-CH_4 geothermometer (D'Amore & Panichi)

D'Amore and Panichi (1980) proposed an empirical geothermometer to overcome the problem of unknown gas/water ratios, enabling estimates of the reservoir temperature to be made from a knowledge of CO_2, H_2S, H_2 and CH_4 concentrations in natural discharges. They made four, arbitrary assumptions which, the authors admit, are not applicable to all fields.

1) Elemental carbon (graphite), carbon dioxide and hydrogen react to form methane:

$$C_{graphite} + CO_{2(g)} + H_{2(g)} = 2CH_{4(g)} + 2H_2O_{(g)}$$

2) Anhydrite and pyrite react to form hydrogen sulphide:

$$CaSO_{4(anhydrite)} + FeS_{2(pyrite)} + 3H_2O_{(g)} + CO_{2(g)} = CaCO_{3(s)} + 1/3\ Fe_3O_{4(g)} + 3H_2S_{(g)} + 7/3\ O_{2(g)}$$

3) The partial pressure of oxygen is related to temperature by:

$$\log P_{O2} = 8.20 - 23643/T$$

4) The partial pressure of carbon dioxide is related to the proportion of carbon dioxide in the total gas content of the discharge:

if $CO_2 < 75\%$ $\quad P_{CO2} = 0.1$

if $CO_2 > 75\%$ $\quad P_{CO2} = 1.0$

if $CO_2 > 75\%$ & $CH_4 > 2H_2$ & $H_2S > 2H_2$ $\quad P_{CO2} = 10$

If these assumptions are valid, then the geothermometry equation is:

$$t°C = \{24775 / [2\log(CH_4/CO_2) - 6\log(H_2/CO_2) - 3\log(H_2S/CO_2) + 7\log P_{CO2} + 36.05]\} - 273$$

Giggenbach (1980) has criticised the premise behind the first and second assumptions, stating that graphite and anhydrite do not play a role in controlling the concentrations of geothermal gases, and that therefore the geothermometer is unsound.

A better estimate can be obtained by using an iterative calculation (Glover, R.B., pers. comm., 1991). This is done by first guessing P_{CO_2} and calculating the temperature. The CO_2 content at that temperature (enthalpy) is calculated assuming adiabatic steam separation has occurred to give the surface CO_2 concentration. Using the calculated CO_2 concentration in the deep fluid and Henry's Law ($P_{CO_2} = x_{CO_2}.H_{CO_2}$), the P_{CO_2} is then calculated, and this is used to calculate a new temperature. This iterative process is followed until P_{CO_2}, steam fraction and CO_2 concentration agree at the calculated fluid temperature.

CO-based geothermometer

A new geothermometer has been recently developed by D'Amore et al. (1987) and Saracco and D'Amore (1989). This utilises a series of equations, derived from gas equilibria, to calculate the reservoir temperature and only requires that the concentrations of CO_2, H_2S, H_2, CH_4 and CO in the dry gas of the discharge are known. It does not require a knowledge of gas/(total water) ratios and can therefore be applied to fumarole and hot-pool discharges. The geothermometer, which is valid over the range 140-370°C, assumes that chemical equilibrium is attained at depth in the system CO_2-H_2S-H_2-CH_4-CO-Fe_3O_4-FeS_2; and that the deep gas composition is retained until discharge. Gas/steam ratios do not have to remain constant (D'Amore et al., 1987). A computer program to solve the sets of equations is described by Saracco and D'Amore (1989); as well as providing the reservoir temperature, this program also calculates the steam fraction, gas/water ratio, P_{CO_2}, P_{O_2} and P_{S_2}. In addition, Chiodini and Cioni (1989) have presented a gas geothermometer based on the reaction

$$CH_{4(g)} + 3CO_{2(g)} = 4CO_{(g)} + 2H_2O_{(l)}$$

Their geothermometry equation is:

$$\log (X^4_{CO}/X^3_{CO_2}.X_{CH_4}) = 8.065 - 13606/T$$

CO_2-geothermometer

Developed by Arnorsson et al. (1983) this geothermometer is reported not to be affected by condensation processes (as carbon dioxide is the dominant gas) and has been applied to both fumaroles and well discharges above 100°C. Valid above 180°C, the upper limit of the geothermometer is determined by the stability of calcite within the system and is therefore around 300°C. D'Amore and Panici (1987) consider that the geothermometer can only be applied to geothermal systems in volcanic areas. The equation, with CO_2 in moles/kg steam, is:

$$\log CO_2 = 37.43 + 73192/T - 11829 \times 10^3/T^2 + 0.18923T - 86.187 \log T$$

H_2-Ar geothermometer

Geothermometers employing hydrogen-ratios have been suggested by Arnorsson and Gunnlaugsson (1985): CO_2/H_2 and H_2S/H_2. The sensitivity of these ratios to secondary effects such as condensation has been commented upon by Giggenbach and Goguel (1989). Furthermore, Taran (1986) has argued that geothermometers employing CH_4 and NH_3 are actually reflecting hydrogen reactions, and he developed a geothermometry expression based on hydrogen content. This was subsequently developed by Giggenbach and Goguel (1989) into the H_2-Ar geothermometer. The use of a ratio, rather than absolute hydrogen concentration, removes problems arising from secondary effects (dilution, boiling, condensation). Furthermore, as both gases are very insoluble, the geothermometer is less likely to be influenced by differences in the relative solubilities of the two gases (as happens with CO_2/H_2 and H_2S/H_2 combinations). The following equation is applicable to fumarole and well discharges, but it is essential that no argon is introduced by air contamination, and this may be the limiting factor in the application of the geothermometer. Using molar gas concentrations, the equation is:

$$t°C = 70\,[2.5 + \log (X_{H_2}/X_{Ar})]$$

gas/Σwater-based geothermometers

To use the following geothermometers the gas/Σwater (ie. total water or gas/steam and steam/water) ratio must be known. Depending upon how the geothermometry equations have been derived, and the source of the thermodynamic data used in the derivation, several variations on some geothermometry equations

have been presented (Henley et al., 1984). The equilibria on which the equations are based are presented below together with the geothermometry equations. These assume a single-phase reservoir: corrections must be applied where two-phase reservoir conditions exist (Henley et al., 1984). The following geothermometry equations are taken from Nehring and D'Amore (1984).

Methane breakdown (Fisher-Tropsch) geothermometer

Based on the thermal breakdown of methane.

$$CH_{4(g)} + 2H_2O_{(g)} = CO_{2(g)} + 4H_{2(g)}$$

$$\log X_{CH_4} - 4\log X_{H_2} - \log X_{CO_2} = 13419/T + 4\log Kh_{H_2} + \log Kh_{CO_2} - \log Kh_{CH_4} - 21.78$$

Hydrogen-CO_2 geothermometer

Based on the dissociation of water, and graphite controlling oxygen fugacity.

$$2H_{2(g)} + O_{2(g)} = 2H_2O_{(l)}$$

$$C_{(graphite)} + O_{2(g)} = CO_{2(g)}$$

$$\log X_{H_2} - 1/2 \log X_{CO_2} = 8.11 - 4501/T - \log Kh_{H_2} - 1/2 \log Kh_{CO2}$$

Ammonia breakdown geothermometer

Based on the dissociation of ammonia.

$$1/2\ N_{2(g)} + 3/2\ H_{2(g)} = NH_{3(g)}$$

$$1/2 \log X_{N_2} + 3/2 \log X_{H_2} - \log X_{NH_3} = 5.76 - 2617/T + \log Kh_{NH_3} - 1/2 \log Kh_{N_2} - 3/2 \log Kh_{H_2}$$

Hydrogen sulphide geothermometer

Based on pyrite-magnetite controlling sulphur fugacity and graphite controlling oxygen fugacity.

$$3FeS_{2(pyrite)} + 2H_{2(g)} + 4H_2O_{(l)} = Fe_3O_{4(magnetite)} + 6H_2S_{(g)}$$

$$C_{(graphite)} + O_{2(g)} = CO_{2(g)}$$

$$\log X_{H_2S} + 1/6 \log X_{CO_2} = 10.58 - 5071.8/T - 0.79\log T - \log Kh_{H_2S} - 1/6 \log Kh_{CO_2}$$

CHAPTER 4

ISOTOPE CHEMISTRY

4.1 INTRODUCTION

Elements are defined by differences in the number of protons in the nucleus (atomic number, *Z*). The isotopes of an element therefore have the same atomic number, but are distinguished on the basis of different atomic masses (mass number, *A* = number of protons + number of neutrons). These differences in atomic mass are caused by the gain or loss of neutrons. Isotopes of an element display slight differences in their chemical and physical behaviour. However, these differences are so slight that for most elements chemical reactions do not lead to a measurable separation of the isotopes. Such separation is only significant in the lighter elements where a difference of one or two neutrons represents a significant fraction of the total atomic mass. It is this property of mass fractionation that is employed in the application of stable isotopes to hydrological studies.

Stable isotopes do not decay naturally and are employed in geothermal studies to recognise processes or the origin of waters and gases. Isotopes of hydrogen (^{1}H, ^{2}H or D-deuterium), carbon (^{12}C, ^{13}C), oxygen (^{16}O, ^{18}O) and sulphur (^{32}S, ^{34}S) are those most commonly applied to geothermal investigations.

Radioactive isotopes, however, decay naturally by the emission of α or β particles (helium nuclei: 2p + 2n, and electrons respectively) sometimes with γ photons (high-energy X-rays), and in doing so change to nuclei of different elements. These nuclei are termed *daughter products* or *radiogenic* isotopes. Examples used in geothermal investigations include ^{3}H (T-tritium), ^{131}I, ^{222}Rn; these isotopes are most useful in dating or tracer studies.

Notation

Extensive use of fractions or ratios is made in isotope chemistry and this requires the introduction of some new terms. At first sight these may appear confusing but the notations soon become familiar and are necessary to avoid having to constantly use lengthy and clumsy expressions. The isotopic mass ratio in the sample, R_x, is always written with the heaviest isotope as the numerator (ie. $^{18}O/^{16}O$ and D/H). The need for this notation arises from the way in which isotopes are measured by a mass spectrometer. This instrument determines the ratios of abundance of the different isotopes in a sample, not the concentration. However, it is difficult to determine the absolute ratio accurately and not practical to do so when analysing large numbers of samples on a routine basis. To overcome this, the isotopic ratio in the sample is compared to that in a well-defined standard which is simultaneously analysed. This gives rise to the expression:

$(R_x - R_{std})/R_{std}$ which can also be written $(R_x/R_{std}) - 1.$

Convenient units of measurement for these isotopic ratios are parts per thousand (ppt) usually called per mille (‰, cf. percent) and given the notation delta (or "del"):

$$\delta_x\,(‰) = \{(R_x/R_{std}) - 1\} \times 1000 \quad \text{or} \quad 10^3 + \delta_x\,(‰) = 10^3\,(R_x/R_{std})$$

To enable isotope reactions to be used quantitatively, isotopic equilibrium between components must be established. This is related to the chemical equilibrium, but does not necessarily proceed at the same rate. As a consequence, chemical equilibrium between components may be established quicker than isotopic equilibrium, or vice versa. For example, chemical equilibrium between $CO_{2(g)}$ and liquid water is attained more rapidly than oxygen isotope equilibrium (Fritz and Fontes, 1980).

The equilibrium constant for isotopic exchange is derived from the reaction equation in the usual manner; for example, consider the exchange of two isotopes of element A between two compounds, AB and AC:

$$^1AB + {}^2AC = {}^2AB + {}^1AC$$

the equilibrium constant is denoted by

$$K = (a^2_{AB}\, a^1_{AC}) / (a^1_{AB}\, a^2_{AC})$$

where a = the activities of the reactant and products. However, as the activity coefficients of isotopic species of the same component are almost equal, then

concentration units can be employed instead. Using concentrations and rearranging the expression, the equilibrium constant is equal to the ratio of the isotope ratios in AB and AC:

$$K = ({}^{2}A/{}^{1}A)_{AB} / ({}^{2}A/{}^{1}A)_{AC}$$

The equilibrium constant, K, is related to the isotope fractionation factor, α, by

$$\alpha = K^{(1/n)}$$

where n is the number of atoms exchanged in the reaction. It can be seen from this that K and α are identical when only one atom in each molecule is exchanged. In the above example therefore:

$$\alpha = ({}^{2}A/{}^{1}A)_{AB}/({}^{2}A/{}^{1}A)_{AC}$$

or, in more general terms

$$\alpha = R_x/R_y$$

(in the above case x represents compound AB and y represents compound AC).

It is more practical to write an expression that relates α to the measured δ values. This can be done by dividing both R_x and R_y by R_{std}, multiplying both by 10^3 and substituting the expression for δ:

$$\alpha_{x,y} = (10^3 + \delta_x)/(10^3 + \delta_y) \qquad \text{or} \qquad 10^3(\alpha_{x,y}-1) = (\delta_x - \delta_y)/(10^3 + \delta_y)$$

This is an exact relationship. However, some approximations can be made to simplify the expression: $\delta_y << 10^3$ and can be neglected; $\alpha \sim 1$ for the majority of reactions of interest, and therefore $\ln\alpha \sim (\alpha-1)$. With these simplifications, the above equation reduces to:

$$10^3 \ln \alpha_{x,y} = \delta_x - \delta_y$$

The subtraction of δ-values in two phases is often expressed as $\Delta(x\text{-}y)$. In terms of relative enrichments or depletions in the isotopes of a given element, the δ expression is written so that an increase in δ corresponds to a relative enrichment in the heavier isotope, ie. an increase in $\delta^{18}O$ represents a shift towards a greater ^{18}O-content in the sample. Enrichment (or depletion) factors, ε, are given by $(\alpha-1)$; so for the enrichment of an isotope in compound x relative to compound y, the enrichment factor is expressed as

$$\varepsilon_{x,y} = (\alpha_{x,y} - 1)10^3 \text{ , or alternatively by}$$

$$\Delta_{x,y} = (\alpha_{x,y} - 1)10^3$$

Standards

To enable δ values to be reliably determined it is necessary to have standards with well-defined isotope ratios. Those most commonly used in geothermal work are commonly denoted by the abbreviations SMOW, PDB and CD, and deserve some explanation. Fritz and Fontes (1980) and Gonfiantini (1978) provide more detailed reviews of these and other standards used in stable isotope studies.

SMOW; ^{18}O, D: The composition of standard mean ocean water, as defined by Craig (1961), now replaced by Vienna-SMOW, an artificial mixture with an isotopic composition close to average ocean water. This is used as a standard for oxygen and hydrogen determinations.

$^{18}O/^{16}O$ = $(2005.2 \pm 0.45)10^{-6}$

D/H = $(155.7 \pm 0.05)10^{-6}$

PDB; ^{13}C, ^{18}O: Commonly used as a standard for carbon isotopes and, rarely, for oxygen isotope determinations, PDB is a carbonate derived from a belemnite found in the Pee Dee Formation of South Carolina, USA.

$^{13}C/^{12}C$ = $(11\,237.2 \pm 2.9)10^{-6}$

$^{18}O/^{16}O$ = $(2067.1 \pm 2.1)\,10^{-6}$

CD; ^{34}S: The standard for sulphur analyses is the mineral troilite (FeS) from the Cañon Diablo meteorite (also abbreviated to CDT).

$^{34}S/^{32}S$ = 45004.5×10^{-6}

4.2 GEOTHERMAL APPLICATIONS OF ISOTOPES

Stable isotopes

Origin of geothermal waters

Prior to the development of isotopic analytical techniques, it was uncertain whether geothermal waters had a magmatic or meteoric origin. However, Craig (Craig et al., 1956; Craig 1963) demonstrated that the δD content of geothermal waters is similar to that of local meteoric water, while the $\delta^{18}O$ value of the geothermal water is more positive than meteoric water (Fig. 4.1). Such an isotopic signature indicated that any magmatic contribution must be small (5-10% of the total fluid, otherwise the δD values of geothermal and meteoric water would not be

similar) and that the bulk of the geothermal fluid must be of meteoric origin. This model of geothermal systems recharged by local meteoric water was further supported by the leaching experiments of Ellis and Mahon (1964), mentioned in Chapter 1.

Since, at low temperatures, both ^{18}O and D fractionate into the condensed phase, water vapour in the atmosphere becomes increasingly depleted in these heavier isotopes on precipitation and progressive movement towards the poles, to greater altitudes and inland, away from the ocean. The $\delta^{18}O$ value of meteoric waters at any locality is therefore dependent upon latitude, altitude and distance from the ocean. This variation is systematic, and Craig (1961) showed that on a global scale the hydrogen-oxygen isotopic signature for fresh-waters could be defined by

$$\delta D = 8\delta^{18}O + 10.$$

The line defined by this equation is termed the *meteoric water line* (Fig. 4.1). Local variations of this equation do exist: although the slope is usually constant at 8, the

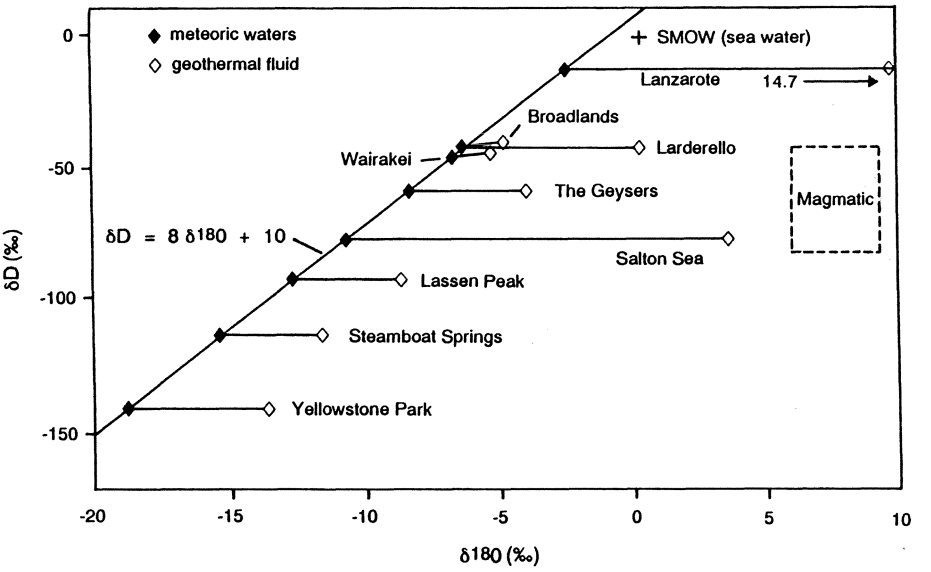

Figure 4.1. Oxygen isotope shifts of geothermal fluids relative to local meteoric waters.

deuterium intercept can differ from 10, for example the composition of meteoric waters in New Zealand is defined by $\delta D = 8\delta^{18}O + 13$ (Stewart and Taylor, 1981). This relationship provides a useful baseline for geothermal studies in helping to evaluate recharge areas and delineate sub-surface processes as discussed below. Note that in cases where the recharge water is derived from a greater altitude and/or some distance away from the geothermal system, an apparent deuterium shift will be present (eg. Iceland, Arnason, 1977b; El Tatio, Giggenbach, 1978; Broadlands-Ohaaki, Hulston, 1983; Fig. 4.1). The composition of juvenile or magmatic waters, however, is not known, but has been proposed by White (1974) to have a range of isotope content, with $\delta^{18}O$ +6 to +9‰ and δD –40 to –80‰.

Processes influencing fluid isotopic composition

Reaction with the host rocks at depth alters the original isotopic signature of the meteoric water to that characteristic of geothermal waters. However, this can be then further changed by several sub-surface processes as the geothermal water rises to the surface. Typical trends in changing isotopic composition under the influence of these processes are illustrated in Figure 4.2.

Rock-water reactions: The enrichment of ^{18}O in geothermal fluids relative to local meteoric water (the *oxygen isotope shift*, Fig. 4.1) is caused by rock-water reactions at depth. These lead to an exchange of oxygen, with the heavier isotope preferentially concentrating in the liquid phase. No corresponding shift is seen in the δD signature as there is little hydrogen in the rocks relative to that in the water, and the water/rock ratio is too high for the hydrogen content of the rock to constitute a significant fraction of the total hydrogen present. Any exchange reactions are therefore relatively minor, and do not significantly change the deuterium content of the geothermal fluid from that of the original meteoric water.

The extent of oxygen isotope shift is dependent on the original composition of the meteoric water and that of the rocks, the mineralogy of the rock, the reservoir temperature, the residence time of the fluid, the surface area of the rock available for reaction; ie. the permeability and porosity, the age of the system, and the rock-water ratio. If a geothermal system is old and/or has a high water-rock ratio, then the host rocks will have reacted extensively with the fluid and will approach equilibrium with respect to oxygen exchange. Under these circumstances, only a small shift in $\delta^{18}O$ will be seen (eg. Wairakei with a $\delta^{18}O$ shift of about +1‰).

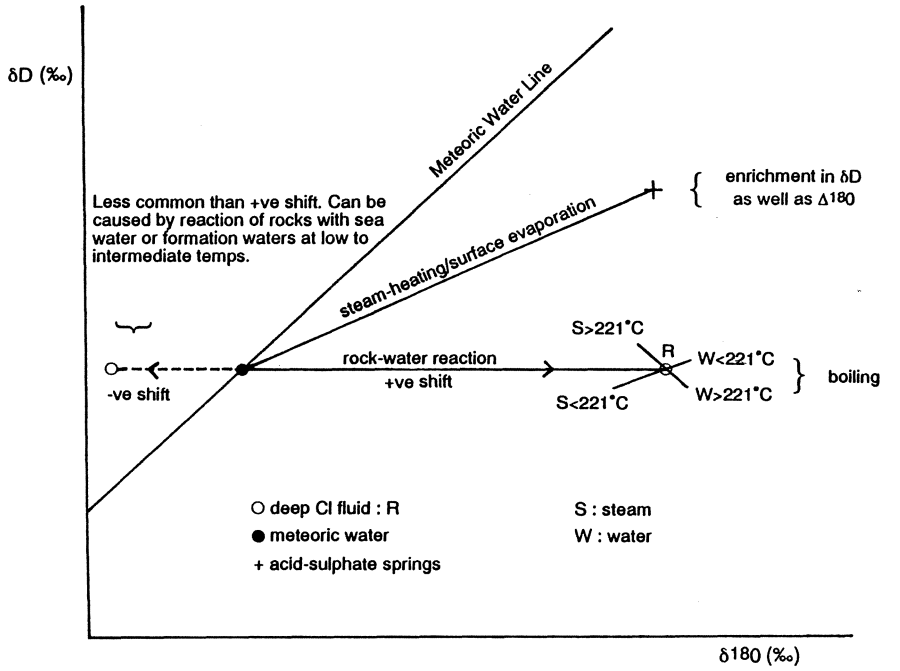

Figure 4.2. Schematic trends in isotopic signature of meteoric water and geothermal fluids with active processes. Note that the temperature of boiling influences the isotopic composition of the resultant steam (S) and water (W) phases due to a variation in the fractionation behaviour of D with temperature which changes at 221°C (see text for further details).

Boiling: As a geothermal fluid ascends to the surface it must lose heat, and will cool by conduction to the host rocks, by mixing with cooler water, or by loss of steam – boiling. Changes in the isotopic signature of discharge water and steam associated with boiling have been considered by Arnason (1977a), Giggenbach (1971) and Truesdell et al. (1977). Just as the chemical composition of the fluid changes on boiling, so too does the isotopic composition as the isotopes partition into the liquid or vapour phases. The exact changes that boiling will produce depends upon the temperature at which boiling occurs and the temperature of water-steam separation (Truesdell et al., 1977). Note that these are not necessarily identical, as water and

steam can travel together for some time prior to separation, permitting fractionation and steam-water isotopic equilibrium to be rapidly established. Below the critical point (374°C for pure water), ^{18}O is concentrated into the liquid phase, with fractionation increasing at lower temperatures. Hydrogen isotopes behave differently: below 221°C, D increasingly fractionates into the liquid phase with decreasing temperature; above 221°C to the critical point, D concentrates into the vapour phase reaching a minimum value at 280°C (Truesdell and Hulston, 1980). This fractionation behaviour causes changes in the isotopic composition of a fluid on boiling, with greatest changes occurring on single-step steam separation (Truesdell et al., 1977). Procedures to correct the isotopic composition for steam separation are described in Section 4.3.

Conduction: Conductive cooling itself will not alter the ^{18}O or D content of the fluid. However, as fluids which have cooled by conduction often have low flow rates and lengthy flow paths, then some ^{18}O exchange may take place in near-surface rock-water reactions.

Mixing: Mixing with meteoric waters will alter the isotopic signature of the geothermal fluid. Most meteoric waters have lower ^{18}O-contents than geothermal fluids; as a consequence, the mixed waters will have lower $\delta^{18}O$ values than the original geothermal fluid. Isotope mixing models, $\delta^{18}O$-Cl and δD-Cl, can be used to recognise when dilution/mixing and boiling processes are active (Panichi and Gonfiantini, 1978; Truesdell et al., 1977; Truesdell and Hulston, 1980). Seawater has a high D and ^{18}O content, and this can be employed by using $\delta^{18}O$-Cl and δD-Cl plots to identify the intrusion of seawater into a geothermal system.

Steam heating/Surface evaporation: Acidic steam heated waters show an enrichment in ^{18}O and D relative to meteoric waters, which is caused by evaporation at the surface or at shallow depths (Craig, 1963). At the surface, this enrichment is additionally influenced by isotopic exchange with atmospheric water, the composition of which will also vary between localities (Giggenbach, 1978). Sulphate waters are usually of little use in providing information on the deep chloride fluid, but the isotopic composition of associated fumaroles can be used to deduce the composition of the reservoir fluid (Truesdell and Hulston, 1980; Giggenbach and Stewart, 1982; Lyon and Stewart, 1985), and to illustrate the presence of magmatic steam (Kiyosu, 1985).

Geothermometry

As shown above, isotope fractionation is related to the equilibrium constant, and is similarly temperature dependent. In general, $\ln\alpha$ is directly proportional to $1/T^2$; therefore as the temperature increases, the value of $\ln\alpha$ decreases and tends to zero at high temperatures. Isotopic fractionation is therefore greater at lower temperatures. If, for a given reaction, the variation of α with temperature is known, then it should be possible to evaluate the temperature of equilibration by measuring the differences in isotopic composition of the reactants. This is the basis for isotope geothermometry, and these expressions are discussed further in Section 4.3. Compilations of fractionation factors are listed by Friedman and O'Neill (1977) and Lyon and Hulston (1984).

Reservoir monitoring

Variations in $\delta^{18}O$ and δD have been used to demonstrate increasing dilution or recharge over time within a system on exploitation, and for modelling regions of steam upflow (eg. Larderello, Panichi and Gonfiantini, 1978; The Geysers, Truesdell et al., 1987).

Radioactive isotopes

Dating: water age/residence time

Tritium and ^{14}C are commonly used in dating the residence time of waters in cold water aquifers. Unfortunately, they are not so successful when applied to geothermal systems: geothermal fluid frequently has long residence times which take it beyond the limit of tritium determinations (^3H $t_{0.5}$ = 12.43 years). Although ^{14}C has a longer half-life ($t_{0.5}$ = 5730 years), age determinations are hindered by dilution with CO_2 produced from within the geothermal system. Argon-39, with $t_{0.5}$ = 269 years has been suggested as an alternative dating method suitable for geothermal waters, although this method has yet to be refined (Truesdell, 1976; Hulston, 1977). Tritium can be used in reservoir monitoring studies since an increase in the ^3H of geothermal discharges can be indicative of increasing dilution or a rapid recharge by meteoric waters. In this respect, ^3H-Cl diagrams can be used to illustrate groundwater mixing with geothermal waters (eg. Giggenbach et al., 1983; Gupta et al., 1976).

Tracers

Radioactive isotopes, introduced into the geothermal field, can be used to determine flow directions, geological (ie. structural and lithological) controls on subsurface flow and flow rates. Such tests can be a useful prelude to reinjection of waste water and an aid to reservoir modelling. McCabe et al. (1983) review the application of radioactive tracers to geothermal systems and the suitability of several isotopes for this purpose. They considered, on both logistical and scientific grounds, that ^{131}I ($t_{0.5}$ = 8 days) offered the best option despite the toxicity of this isotope.

4.3 ISOTOPE GEOTHERMOMETERS

Isotope fractionation, like many other equilibria, is a temperature dependent process and therefore has potential for use as a geothermometer. However, before the isotopic exchange reaction between phases can be employed as a geothermometer, certain conditions have to be met:

1) For exchange to occur, isotopes of the element in question must co-exist in two different components in the fluid and/or solid phases of the geothermal reservoir.
2) Isotopic equilibrium must be achieved between these components.
3) The rate of isotopic exchange must be sufficiently rapid to permit equilibrium to be attained in the residence time of the fluid, but should also be slow enough to prevent re-equilibration as the fluid ascends to the surface.
4) Temperature must be the dominant control on the fractionation equilibrium.
5) The degree of fractionation must show a regular relationship with temperature and be detectable.

In addition, mixing between identical components with different isotopic signatures should not occur, or should be evaluated and corrected, and sampling-storage techniques must not alter the isotopic ratios in the sample.

Isotopic exchange reactions achieve equilibrium at different rates. Some, such as the exchange of oxygen isotopes between water vapour and liquid water, occur within seconds and are therefore of no use as geothermometers. The estimated half-life ($t_{0.5}$) at 250°C for several exchange reactions is listed below (Hulston, 1977, 1983; Hulston and Lyon, 1991; Truesdell and Hulston, 1980). Most of the isotope exchange

reactions are used as geothermometers; the equilibration times for the silica, Na/K and Na-K-Ca geothermometers are also given for comparison. Reaction rates such as these indicate how rapidly a geothermometer will re-equilibrate in shallow reservoirs and as it ascends to the surface. Under ideal conditions, the different equilibration times for the geothermometers could help recognise the presence of more than one reservoir. Furthermore, since longer equilibration times mean that a geothermometer will have a longer "memory", the careful selection of geothermometers could indicate the temperatures at different depths within the system, and thereby document the thermal history of the fluid (Hulston, 1977).

Exchange	$t_{0.5}$ *(at 250°C)*
$\Delta^{18}O$ SO_4-H_2O	~1 year
$\Delta^{18}O$ CO_2-H_2O	1-100 secs
$\Delta^{18}O$ $H_2O_{(l)}$-$H_2O_{(v)}$	1-100 secs
ΔD H_2-$H_2O_{(l)}$	1-20 weeks
ΔD CH_4-H_2	1-20 weeks
ΔD $H_2O_{(l)}$-CH_4	1-1000 years
$\Delta^{13}C$ CH_4-CO_2	1000-10,000 years
$\Delta^{13}C$ CO_2-HCO_3	1-100 hours
$\Delta^{34}S$ SO_4-H_2S	>1000 years
SiO_2 geothermometer	1-100 hours
NaK geothermometer	0.3 years
NaKCa geothermometer	0.3 years

Isotope geothermometry equations

The general notation for the expression of isotopic ratios has been described above. The names of the different isotope geothermometers is usually written using the Δ-notation, whereas the geothermometry equations are often expressed in terms of α. However, since $\Delta_{x,y} \sim (d_x - d_y) \sim 10^3 \ln\alpha_{x,y}$, these are just different ways of expressing the same thing within the approximations outlined in the introduction to this chapter. An example using the ^{18}O-sulphate-water geothermometer should clarify the situation.

Expression	*meaning*
$\Delta^{18}O\ (SO_4\text{-}H_2O)$	the difference between $\delta^{18}O$ of the sulphate ion and $\delta^{18}O$ of water ie. $\delta^{18}O(SO_4) - \delta^{18}O(H_2O)$
$10^3 \ln\alpha$	$\delta^{18}O(SO_4) - \delta^{18}O(H_2O)$ ie. $\Delta^{18}O\ (SO_4\text{-}H_2O)$
α	$\frac{(^{18}O/^{16}O)SO_4}{(^{18}O/^{16}O)H_2O}$ or $\frac{10^3 + \delta^{18}O(SO_4)}{10^3 + \delta^{18}O(H_2O)}$

In general, isotope geothermometry equations have the form:

$$\Delta = A/T + B/T^2 + C$$

with T in Kelvin. The values of the constants are derived from experimentally determined values of the temperature-dependent fractionation factors, α. The equations are therefore revised as these figures are refined.

Oxygen isotope geothermometers

$\Delta^{18}O\ (SO_4\text{-}H_2O)$

The fractionation of oxygen isotopes between dissolved sulphate (and bisulphate) ions and liquid water has probably become the most widely used isotope geothermometer, and has been successfully applied to high-temperature, hot-water systems.

The geothermometer is based on experimentally derived oxygen fractionation data for the sulphate-water system (Lloyd, 1968; Mizutani and Rafter 1969; Mizutani, 1972). The kinetics of the oxygen exchange was shown by Lloyd (1968) to be dependent upon pH as well as temperature. However, McKenzie and Truesdell (1977) calculated that for a near-neutral-pH chloride reservoir fluid, pH did not significantly influence the fractionation equilibrium position provided residence times are in excess of the equilibration periods of 18 years for a 200°C fluid, or 2 years for a 300°C fluid. The longer residence times of the geothermal fluid would therefore invariably ensure that isotopic equilibrium is established. Moreover, these slow re-equilibration periods also ensure that no isotopic exchange will occur as the fluids rise to the surface. The isotopic composition of the surface discharges, and the temperatures obtained from the geothermometer, are therefore likely to reliably

Isotope geothermometry equations

$\Delta^{18}O$ (SO_4-H_2O)	=	$2.88\,(10^6 / T^2) - 4.1$		(iii)
		$3.251\,(10^6 / T^2) - 5.6$		(ii)
$\Delta^{18}O$ (CO_2-$H_2O_{(g)}$)	=	$7.849\,(10^3 / T) + 2.941\,(10^3 / T^2) - 8.87$		(i)
		$9.289\,(10^3 / T) + 2.651\,(10^3 / T^2) - 10.55$		(iv)
ΔD (H_2-$H_2O_{(l)}$)	=	$396.8\,(10^3 / T) + 11.76\,(10^3 / T^2) - 217.3$		(i)
ΔD (CH_4-H_2)	=	$181.269\,(10^6 / T^2) - 8.949\,(10^6 / T^2)^2 - 90.888$		
			>200°C	(iv)
		$288.9\,(10^3 / T) + 31.86\,(10^3 / T^2) - 238.28$		(i)
$\Delta^{13}C$ (CH_4-CO_2)	=	$15.25\,(10^3 / T) + (10^6 / T^2) - 9.56$		(i)
		$15.301\,(10^3 / T) + 2.361\,(10^6 / T^2) - 9.01$		
			100-400°C	(iv)
$\Delta^{34}S$ (SO_4-H_2S)	=	$6.04\,(10^6 / T^2) + 2.6$		(i)
		$5.07\,(10^6 / T^2) + 6.33$	200-320°C	(v)

T in Kelvin

Data sources:

(i) D'Amore and Panichi (1987)
(ii) Lloyd (1968)
(iii) Mizutani and Rafter (1969)
(iv) Panichi and Gonfiantini (1978)
(v) Robinson (1973)

reflect the equilibrium conditions in the reservoir. However, water discharged from a spring will not always have the same isotopic composition of the deep reservoir fluid. Boiling and dilution, mixing and atmospheric oxidation of hydrogen sulphide are all factors which can influence the H_2O-SO_4 oxygen isotopic signature and therefore the temperature estimates of the geothermometer. Although these processes can

complicate the interpretation, they do not necessarily preclude the application of the geothermometer as corrections can be applied.

Processes influencing $\delta^{18}O(H_2O)$

Physical processes can significantly affect the $\delta^{18}O(H_2O)$ value of the discharge water and must be taken into consideration. Specific, common examples are phase separation (boiling) or the addition of water from another source with a different isotopic signature (dilution). Since the exchange of oxygen between the liquid and vapour phases is a rapid, near instantaneous reaction, then steam loss will change the $\delta^{18}O$ figure of the discharge water to increasingly more positive (isotopically heavy) values. Dilution with isotopically light groundwaters however, will make the $\delta^{18}O$ value of the geothermal discharge increasingly negative.

Boiling: Single step steam loss. In this case the steam remains in contact with the water until it physically separates at a single depth, usually the surface. Isotopic equilibrium therefore exists between the water and steam, and fractionation takes place at the temperature of physical separation of these phases (ie. at the surface temperature for springs and wells discharging a two-phase mixture). The ^{18}O values of the steam and water can be used to calculate back to the isotopic signature of the reservoir fluid using the mass balance equations and the oxygen isotope fractionation factor. Arnason (1977b) and MacKenzie and Truesdell (1977) derived the following equation:

$$\frac{10^3 + \delta^{18}O(H_2O)_{res}}{10^3 + \delta^{18}O(H_2O)_s} = n + (1-n)\,(1/\alpha_{l,v})$$

or

$$\delta^{18}O(H_2O)_{res} \approx \delta^{18}O(H_2O)_s - (\alpha_{l,v} - 1)(1 - n) = \delta^{18}O(H_2O)_s - \varepsilon f_s$$

where

$\alpha_{l,v}$ = $(^{18}O/^{16}O)_{liquid} / (^{18}O/^{16}O)_{vapour}$

n = $(H_{v,s} - H_{l,res}) / (H_{v,s} - H_{l,s})$

ε = enrichment factor

f_s = steam fraction

and

$\delta^{18}O(H_2O)_{res}$	=	$\delta^{18}O$ value of the geothermal reservoir fluid
$\delta^{18}O(H_2O)_s$	=	$\delta^{18}O$ value of surface water
n	=	liquid fraction
$H_{v,s}$	=	enthalpy of steam at the spring temperature
$H_{l,res}$	=	enthalpy of liquid water at the reservoir temperature
$H_{l,s}$	=	enthalpy of liquid water at the spring temperature
$\alpha_{l,v}$	=	oxygen isotope fractionation between liquid water and water vapour

Over the temperature range 3-360°C $\alpha_{l,v}$ can be calculated from the equation (McKenzie and Truesdell, 1977):

$$10^3 \ln \alpha_{l,v} = 1.2051\,(10^3/T) + 0.7664\,(10^6/T^2) - 3.494$$

with T in Kelvin. This is considered to be the more common situtation.

Boiling: Continuous steam loss. Where steam physically separates and migrates independently from the liquid phase, isotopic fractionation occurs during boiling. Integrating the above single-step steam loss equation, Truesdell et al. (1977) derived the following expression for the limiting situation where steam continuously separates from the liquid phase

$$\ln \frac{10^3 + \delta^{18}O(H_2O)_{res}}{10^3 + \delta^{18}O(H_2O)_s} = \int_{H_{l,s}}^{H_{l,res}} (1 - 1/\alpha_{l,v}) \frac{dH}{(H_{v,s} - H)}$$

Conductive cooling: As for other solutes, conductive cooling with no steam loss does not change the isotopic composition of the water, and the geothermometry equation can be directly applied.

Dilution with groundwater: Dilution with meteoric waters, which have their own (lighter) oxygen isotope signature, will influence the $\delta^{18}O$ value of the reservoir fluid. Typically, the ^{18}O-enrichment of the deep fluid will be diluted to increasingly negative $\delta^{18}O$ values on mixing with the meteoric waters. As the $\delta^{18}O$ of the geothermal water is used in the geothermometry equation, the use of uncorrected $\delta^{18}O$ values from the diluted waters will produce erroneous results. The fraction of hot, geothermal water in the mixed discharge needs to be calculated and a correction can then be applied to the measured $\delta^{18}O$ figure. This hot water fraction, x, can be calculated from the application of solute geothermometry and mixing models

(discussed in Chapter 2) to the spring discharge, and this is used in determining the $\delta^{18}O$ value of the deep, hot water component using:

$$\delta^{18}O_{HOT} = \{\delta^{18}O_{spring} - (\delta^{18}O_{meteoric}\,[1\text{-}x])\} / x$$

Warm springs, good flow: Assume no steam loss before or after mixing. Use silica mixing model; no correction for steam loss required to $\delta^{18}O_{HOT}$ figure before application to the $\Delta^{18}O$ (SO_4-H_2O) geothermometry equation.

Boiling spring, good flow: Assume steam is lost only after mixing - not before. Use enthalpy-chloride mixing model to calculate x and H_{mix}: the enthalpy after mixing but prior to boiling. Apply either single step or continuous steam separation correction to calculate the effect of boiling (substitute H_{mix} for $H_{l,res}$), then calculate $\delta^{18}O_{HOT}$. If steam *is* lost before mixing, then application of the mixing model will yield geothermometry temperatures which are minimum values.

Processes influencing $\delta^{18}O(SO_4)$

As isotopic exchange of oxygen between dissolved sulphate and water is a relatively slow equilibrium, dilution and boiling alone should not significantly influence the $\delta^{18}O(SO_4)$ value of the discharge. However, if these processes lead to the addition of sulphate to the water, then clearly this will have an effect upon the overall isotopic signature of the dissolved sulphate. Factors affecting $\delta^{18}O(SO_4)$ which may be commonly encountered include: mixing with SO_4-bearing waters (eg. seawater, steam-heated waters); H_2S oxidation; dissolution of marine evaporites. A small range of calculated temperatures and a good agreement with other geothermometers suggests that the isotopic composition of the sulphate is not affected by these processes.

Mixing with SO_4-bearing waters; H_2S oxidation: These factors can be readily negated by careful selection of spring samples. In a given area, springs which have both the lowest sulphate concentrations *and* the highest Cl/SO_4 ratio, are most suitable for analysis. If springs over an area show the same maximum Cl/SO_4 ratio, but have different Cl and SO_4 concentrations, then this indicates groundwater dilution has occurred without oxidation of hydrogen sulphide, making spring selection less critical. If sulphate were produced by H_2S oxidation, then the sulphate concentration would be related to the amount of dissolved oxygen, and would therefore be

approximately constant and independent of Cl content (Fournier et al., 1979). Sulphate derived from the condensation and oxidation of volcanic gases show unusually light oxygen isotope ratios; such sulphates can also be reecognised by their sulphur isotopic ratio, enabling thermal discharges unsuitable for geothermometry to be recognised and eliminated (Sakai, 1977). Correct sampling procedures are also important to ensure that the integrity of the sample isotopic composition is preserved (see Chapter 7).

Dissolution of evaporite minerals; seawater mixing: These factors can be recognised by significant enrichments in ^{18}O and ^{34}S (and therefore "heavy" $\delta^{18}O(SO_4)$ and $\delta^{34}S(SO_4)$ values) in the dissolved sulphate (eg. McKenzie and Truesdell, 1977; Fournier et al., 1979; Giggenbach et al., 1983).

Geothermometry equation

Depending upon which experimental data are used, there are slight variations in the geothermometry equation developed:

$10^3 \ln\alpha_{(SO_4\text{-}H_2O)} = 3.2\,(10^6 / T^2) - 5.6$	Lloyd (1968)
$10^3 \ln\alpha_{(SO_4\text{-}H_2O)} = 2.88(10^6 / T^2) - 4.1$	Mizutani & Rafter (1969)

However, the two equations converge around 200°C, and are in reasonable agreement (within 10°C) over the temperature range 0-300°C (Panichi and Gonfiantini, 1978). The version of Mizutani and Rafter (1969) was adopted by Fournier (1981) and Henley et al. (1984), and appears to be the equation most widely used. This equation is valid for subsurface temperatures in the range ~140-350°C and may possibly be used down to 95°C (McKenzie and Truesdel, 1977; Truesdell, 1976). Remember though that low reservoir temperatures will require long residence times to establish isotopic equilibrium (~500 years at 100°C), making the geothermometer unsuitable for low-enthalpy systems unless residence times are extraordinarily lengthy.

$\Delta^{18}O$ (H_2O-CO_2)

Panichi et al. (1977), using Bottinga's (1969) fractionation factors, successfully developed this geothermometer on the Larderello system. The technique is valid over the range 100-300°C. To avoid isotopic re-equilibration during sampling, steam and carbon dioxide were cooled under liquid nitrogen during collection. The

geothermometer depends on the isotopic exchange of oxygen between carbon dioxide and water vapour, however, this exchange only takes place in the presence of liquid water (Truesdell and Hulston, 1980) and will not occur in the rising steam phase. Truesdell and Hulston (1980) argue that because of the oxygen exchange with liquid water, more reliable results are obtained using CO_2-$H_2O_{(l)}$ fractionation figures and not those for the CO_2-$H_2O_{(g)}$ exchange.

Hydrogen isotope geothermometers

Five common geothermal gases contain hydrogen (H_2O, H_2S, H_2, CH_4, NH_3), making four geothermometers based on the exchange of deuterium and hydrogen possible (Truesdell and Hulston, 1980). Bottinga (1969) and Richet et al. (1977) have calculated fractionation factors for the major gases, although no data is available for ammonia. Truesdell and Hulston (1980) point out that since hydrogen sulphide and ammonia are partially ionised in solution, any hydrogen exchange reaction would equilibrate too rapidly with water to be of use in geothermometry. As with geothermometers based on oxygen exchange reactions, similar corrections for boiling must be made to the hydrogen-based methods (Arnason, 1977a; Truesdell et al., 1977).

ΔD $(H_2$-$H_2O_{(l)})$

This geothermometer is based on the reaction

$$H_2O_{(l)} + HD_{(aq)} = HDO_{(l)} + H_{2(aq)}$$

and gave reliable results when applied to most Icelandic geothermal systems (Arnason, 1977a). In one case (Reykjanes) however, high temperatures where estimated possibly due to mixing of the oceanic-derived thermal fluid with cold meteoric waters. Other workers have found variable results with this technique, probably due to varying degrees of re-equilibration on ascent (Lyon, 1974; Sheppard and Lyon, 1981). As water is involved in this geothermometer, a correction for steam-liquid water fractionation should be made, similar to that for the sulphate-water geothermometer described above. However, this may be neglected due to the large $\Delta D_{(H2\text{-}H2O(l))}$ fractionation factor, the absence of any rock-water deuterium exchange and the small $\Delta D_{(H2O(g)\text{-}H2O(l))}$ fractionation at 220°C (Lyon and Hulston, 1984). An alternative to the quadratic geothermometry equation shown in the box is provided by

Lyon and Hulston (1984). Their equation is valid over the temperature range 100-600°C to within 2°C:

$$t°C = -191 + 325500/(\Delta D + 144)$$

ΔD (H_2-CH_4)

The original fractionation factors calculated by Bottinga (1969) yielded temperature estimates that were too high (Lyon, 1974). Subsequent revision of these factors provided a better agreement with the measured temperatures, and an equation valid for temperatures in excess of 200°C has been developed (Panichi and Gonfiantini, 1978).

ΔD ($H_2O_{(l)}$-CH_4)

Hydrogen exchange between methane and liquid water has potential as a geothermometer, but still requires precise calibration. An interim temperature scale has been proposed by Hulston (Hulston, 1978; Hulston, 1983; Truesdell and Hulston, 1980), and is discussed further by Lyon and Hulston (1984).

Carbon isotope geothermometers

$\Delta^{13}C$ (CO_2-CH_4)

The exchange of ^{13}C and ^{12}C in co-existing CO_2 and CH_4 gases have been used as a geothermometer, but with mixed success. The geothermometer assumes the gases are in equilibrium in the reaction

$$CO_2 + 4H_2 = CH_4 + 2H_2O.$$

Methane formed by this reaction is always depleted in ^{13}C relative to CO_2; initial fractionation factors were calculated by Craig (1953, 1957). These were used by Hulson and McCabe (1962) and gave reasonable estimates for the reservoir temperatures at Wairaki, New Zealand. However, revised fractionation factors presented by Bottinga (1969) yield calculated temperatures that are often significantly higher (ie. 50-200°C) than the measured reservoir temperature (Lyon, 1974; Panichi

et al, 1977; Panichi and Gonfiantini, 1978) throwing into doubt the validity of the geothermometer. There are a number of possible explanations for this apparent discrepancy. It has been suggested that the above reaction is invalid, and that the isotopic composition of methane is actually a product of the thermal degradation of organic matter (Gunter and Musgrove, 1971; Gunter, 1978; Nuti et al., 1980; DesMarais et al., 1981). Alternatively, the samples could be contaminated by carbon dioxide or methane from rocks in the upflow region. Equally, the two gases may be from different, unrelated sources, isotopic equilibrium was never attained and any correlation between calculated and measured temperatures is just coincidence (Panichi and Gonfiantini, 1978). Alternatively, however, this difference in calculated and measured temperatures may be simply due to the long equilibration time of the reaction. Attempts to determine this time from laboratory experiments have had mixed success. Little exchange seems to occur below 200°C, while Giggenbach (1982) has estimated an equilibration time of 20,000 years at 400°C, although Hulston (1983) considers that field evidence suggests that this is an over-estimation, and the reaction is faster than this. With such long reaction times the geothermometry temperatures probably actually reflect the conditions at depths below that reached by drilling (Hulston, 1977; Lyon and Hulston, 1984; Panichi et al., 1977) and beyond the exploitable reservoir. This latter suggestion is favoured by several authors and is supported by high temperatures in deep drill holes at Larderello, Italy and Ohaaki, New Zealand and agreement between different isotope geothermometers for New Zealand systems (Truesdell and Hulston, 1980). In addition to the geothermometry equation given in the box, the following expression can be used over the temperature range 150-500°C to calculate temperatures to within 2°C (Lyon and Hulston, 1984):

$$t°C = -173 + 15790/(\Delta^{13}C + 9.0)$$

$\Delta^{13}C$ (CO_2-HCO_3)

There are some inconsistencies at high temperatures in the fractionation data for carbon isotope exchange between CO_2 and bicarbonate (Malinin et al., 1967; Mook et al., 1974; Thode et al., 1965), and a compromise between the data has been proposed by Hulston (Hulston, 1978; Lyon and Hulston, 1984). There appears to be little re-equilibration in this reaction as the fluids rise to the surface (Truesdell and Hulston, 1980). Ellis and Mahon (1977) pointed out that bicarbonate ions decompose on reaction with weak acids in the geothermal fluids, thereby imposing a potential limitation to the application of this technique. Ellis (1979) notes however, that this

geothermometer may be of use when applied to alkaline waters as found in parts of Yellowstone Park, USA or Iceland.

Sulphur isotope geothermometer

$\Delta^{34}S$ (SO_4-H_2S)

Sulphur exchange between SO_4 and H_2S (and HS^- or HSO_4^-) is dependent on sulphur concentration, temperature and pH. The reaction is rapid under acidic conditions (a few days-weeks at 200-300°C), but is very slow (thousands of years) in an alkaline environment (Robinson, 1973; Truesdell and Hulston, 1980, Hulston, 1983). A knowledge of reservoir pH and sulphur concentration is therefore required for a sound estimate of equilibration time, but for systems with reservoir temperatures around 250°C with a fluid pH ~ 6 and a total sulphur content of about 10^{-4} mol/kg (eg. Wairakei, New Zealand) re-equilibration takes over one thousand years (Hulston, 1983). Fractionation factors have been calculated by Robinson (1973) and yield temperatures in excess of those measured, probably indicating that equilibration took place at depths, and temperatures, beyond those reached by drilling.

Part II

Exploration Techniques & Surveys

CHAPTER 5

EXPLORATION TECHNIQUES

5.1 INTRODUCTION

This chapter is an introduction to Part II, and provides an overview of exploration techniques for both active and extinct or fossil geothermal systems. The latter are of interest to geothermalists in charting the history of thermal activity in a region, and to economic geologists searching for epithermal gold deposits.

Active geothermal systems: The principal chemical methods used to identify, delineate and evaluate active geothermal systems are the subject of this book. Sampling and analytical methods are fully described in Chapters 6, 7 and 8.

Fossil geothermal systems: These are subdivided into "young", Tertiary and Quaternary (ie. Cainozoic), and "ancient" or Pre-Tertiary systems. This division is made because the types of survey most effective in investigating these systems changes as the state of preservation of the system deteriorates over time.

Geothermal system status - relevant survey
Active systems water, gas, soil, soil-gas, mineralogical (stream sediment, botanical)*
Fossil/epithermal systems *Tertiary and Quaternary ("young") systems:* soil, mineralogical (rock) *Pre-Tertiary ("ancient") systems:* rock, mineralogical
**Parentheses indicate less-useful techniques*

Geochemical surveys are well known in their application to mineral exploration, and several texts have been written on the subject. To provide a general background to the surveys and their interpretation the books by Levinson (1980) and Rose et al. (1979) are recommended, and that by Govett (1983) is also useful. Remember though that there are distinct differences in exploring for mineral deposits and for geothermal systems, and these must be reflected in the design and interpretation of the survey. It is this approach, one of attempting to recognise the (palaeo-) hydrology of a system, which is adopted here.

5.2 EXPLORATION SURVEYS

Active systems

Exploration and interpretation techniques applied to active geothermal systems form the body of this text, but are discussed here to provide an overview which will place the methods and procedures in context.

Water surveys

Also known as "hydrogeochemical" surveys, these are conducted on active geothermal features (hot springs and pools) and wells. Spring and well water samples are the main sampling medium of most geothermal investigations. The sampling and analytical methods are detailed in Chapter 6, while the interpretation of geothermal water chemistry is discussed in Chapters 2 and 4.

Surveys of freshwater courses (streams, lakes) may also be undertaken to detect leakage of geothermal water into the drainage system. These are useful when evaluating the total discharge of geothermal water, and heat loss, from a system. As with groundwaters, the near-surface flow of geothermal waters will be controlled by topography and geology, and it is not unusual to find geothermal waters emerging into stream banks and river or lake beds. Suck leakages will not be readily detected without a systematic survey of the local drainage features. To detect such leakages, the stream, river and lake waters are sampled throughout the prospective area, and conductivity, temperature and chloride determinations are made. An increase in any of these parameters is indicative of a geothermal discharge. It is useful to also determine, or estimate, the flow rate of the stream at the time of sampling. This enables the dilution of any geothermal discharge by increased rainfall to be evaluated,

and allows direct comparisons to be made with any future surveys as all determinations can be normalised to a given flow rate.

Gas surveys

These are undertaken on fumaroles, gas vents in pools, steaming ground and wells. The sampling and analysis of gas discharges is considered in Chapter 7, while the interpretation of gas chemistry is discussed in Chapters 3 and 4. Gas surveys are less popular than water surveys, largely because of the collection of gas samples can be more time consuming and is often thought to be more difficult. It is possible, however, to routinely carry out gas surveys and such an approach should be encouraged. The information obtained is does not duplicate that gained from the water surveys, and can greatly assist in the interpretation of the hydrology of a system.

Soil and soil-gas surveys

These are proven but often under-valued survey techniques whose principal use is to identify permeable zones within the field, and to delineate the margins of the system. In this regard they provide a useful comparison to geophysical surveys. Samples are taken on a grid pattern over the area of interest. In regional surveys exploring for the presence of a geothermal field, samples may be taken 1km or more apart, whereas over areas of known geothermal activity, sample spacing can be around 50-100m. In soil surveys, samples are taken in the field and returned to the laboratory for analysis. The determinations in soil-gas surveys, however, are invariably undertaken in the field. Although successful, these surveys are prone to variations in ambient conditions and can be correspondingly more difficult to interpret. Soil surveys do require the presence of an establish soil layer, preferably with significant organic matter content. Although the soil does not have to have formed in-situ (and it is this regard that geothermal soil surveys differ from mineral exploration surveys), it must have covered the geothermal system for sufficient time for geochemical anomalies to be established.

Mineralogical surveys

Mapping the aerial and vertical distribution of secondary minerals formed by the reaction of the host rocks with geothermal water and/or steam can provide clues to the thermal and hydrological history of the system. The assemblage of minerals formed by alteration and deposition from the waters is different for each type of geothermal water; diagnostic or typical minerals for each fluid type are given in

Chapter 2, where some typical water-rock alteration reactions are also examined. Certain minerals, notably clays and calc-silicates, act as guides to regions of high temperature and permeability (Browne, 1978). By examining the distribution of these key minerals in cores and surface outcrop, it can be deduced which type of fluid reacted with the rock and the regions of highest temperature. Note that it is not unusual for minerals characteristic of acidic sulphate water or steam alteration to overprint the chloride-water alteration assemblage if the geothermal reservoir water level fluctuated during the lifetime of the system.

Stream sediment surveys

Highly popular and successful in mineral exploration, these surveys are of limited used in geothermal exploration. The fine size fraction of the sediments (typically –80 mesh) is collected and analysed for key trace elements which indicate the presence of a geothermal system. These "pathfinder" elements are transported by the geothermal water (or gas) which leaks into the stream water through the steam bed or banks. As it does so, the species are adsorbed onto the clay minerals and organic matter of the sediments. Pathfinder species of most use in geothermal exploration are likely to be Hg, As, B, NH_3. Any anomalously high concentrations of such species on steam sediments must be interpreted in terms of their geographic and geological context, in much the same way as soil surveys are examined (Chapter 8) as not all variations will be of geothermal origin.

Rock surveys

Also commonly referred to as "lithogeochemical" surveys, these have found widespread and successful application in mineral exploration, notably for hydrothermal ore deposits. Lithologies over the prospective area are sampled systematically and analysed for distinctive trace element suites. The objective is to establish element patterns which will identify potentially mineralised areas. In this respect, rock chemistry can be an aid in investigating ancient or pre-Tertiary systems, but for active or young geothermal fields this traditional approach is less appropriate. In such young systems, the secondary alteration assemblage is commonly preserved, and far more information on the ancient fluid chemistry can be obtained from the mineralogy of the alteration assemblage and from fluid inclusion studies (eg. Henneberger and Browne, 1987) than can be obtained from the bulk rock chemistry.

Botanical surveys

Surveys based on the sampling and chemical analysis of plants ("biogeochemical" or "geobotanical") have not found application in geothermal investigations. Such surveys could be successful, but variations in the uptake of elements between plant species, and variations in the concentration of elements within different parts of the same plant, mean that highly trained samplers are required. Furthermore, any plant selected for sampling must have a widespread distribution over and beyond the area of interest in order to establish background levels. Geographic and geological factors will also need to be taken into consideration. It is difficult, therefore, to see how biogeochemical surveys could find routine application, except possibly in very localised investigations. The absence of vegetation and the presence of plants with stunted growth is, however, a common consequence of hot ground over or near geothermal areas. This can be a useful exploration guide, particularly during preliminary investigations using aerial photographs.

Fossil/epithermal systems

The links between geothermal systems and some types of epithermal gold mineralisation are now well established (eg. Henley, 1985). These similarities have been extensively discussed elsewhere (eg. Berger and Bethke, 1985; Henley et al., 1986) and it is not intended that this section should reiterate these reviews. Instead, to emphasise the importance of establishing the hydrological regime of a system, the application and interpretation of rock and mineralogical surveys to epithermal systems is placed in a geothermal context. This approach attempts to reconstruct the hydrology of the system and thereby identify the ancient thermal, chemical and hydrological setting of a given outcrop. As this approach can yield information on the fluid-rock interactions and thermal history of the field, it is potentially more successful to epithermal gold exploration than the base-metal-exhalative-deposit approach of searching for lithogeochemical haloes. In this regard, it is essential that the explorationist should be aware of the structure of active geothermal systems, the different fluid types and their respective deposits and the genetic significance of these fluids/deposits (Chapter 1, Chapter 2). There are two key objectives in gold exploration over ancient geothermal systems:

- to identify areas of chloride fluid discharge
- to locate permeable structures

Chloride fluids are the gold-transporting waters and are therefore of obvious interest and importance. Zones through which such fluids have passed are commonly silicified, with silica sinter deposited at the palaeo-surface. Areas of chloride fluid discharge may occur surrounded by an area of argillic alteration. Such an apparent anomaly can be explained by the fact that these fluids often rise to the surface through permeable structures which cut thorough zones of steam alteration. Overprinting of steam alteration over an area of silica deposition can also occur when a water table is lowered and can explain the intimate association of these two styles of alteration belonging to chloride and sulphate fluid types.

Permeable structures can contain zones of boiling and gold deposition. Such structures may not always attain the surface, or may be permeable to steam but not to water. In either case, volatile species can be transported in the steam phase to create anomalies in the secondary minerals overlying the permeable zone. Recognition of these ancient structures can therefore aid targeting zones of potential gold deposition.

Rock surveys

Although less suited to active geothermal systems, rock chemistry is useful in the identification of permeable or steam zones within young or ancient systems, and can therefore assist in reconstructing the palaeohydrology of the system. This is the most appropriate application of rock surveys in geothermal-epithermal investigations. Such a study should be conducted in conjunction with mineralogical determinations, since some normalisation to account for the heterogeneous nature of the sampling medium will be required. In interpreting the survey it should also be remembered that in the lifetime of a system, permeable zones will change, creating a series of anomalies. The more volatile species (Hg, B, As, NH_3, Sb) will become concentrated on secondary minerals over steam zones, and it is these which will be of most use. Under ideal conditions, anomalous concentrations of these species will indicate upflow and boiling zones: key targets in gold exploration. Elevated levels of the species will probably occur in the upper regions of the geothermal system as a whole, due to leakage of vapour and changes in the permeable regions over time. They can therefore also be used to delineate the areas of past hydrothermal activity and to assist in determining the level (depth) of preservation of the system (Henneberger, 1986; Nicholson, 1988; 1989).

Mineralogical surveys

The comments given above for mineralogical surveys over active fields, also apply to such surveys over fossil geothermal fields and epithermal mineralisation. In interpreting the relicts of a geothermal-epithermal system, it is useful to bear in mind the chemical and hydrological structure of geothermal fields (Chapter 1) and the different types of fluid with their characteristic alteration assemblage and mineral deposits. Such a working model at the outset of exploration will aid recognition of the structure of the system and the depth of preservation - essential when evaluating the gold potential of a prospect. This potential will be enhanced if the system has been preserved above the ancient boiling zone(s) - the depositional areas for gold. The value of identifying ancient geothermal deposits was demonstrated recently by the successful identification of gold prospects in Scotland and Australia (Nicholson, 1988, 1989; White et al., 1989).

Mapping the alteration assemblage in three dimensions will, as for active systems, develop the hydrological and thermal history of the field. In the early exploration stage however, recognition of the palaeosurface is a great asset to developing an exploration scheme. In this regard the identification of silica sinter is particularly important. The presence of a thick sinter deposit not only indicates a palaeosurface (and therefore a high level of preservation), but demonstrates the palaeo-reservoir temperature was in excess of ~200°C and marks areas of chloride water discharge (the gold-depositing fluid). The development of textural and geochemical criteria to distinguish silica sinters from other siliceous lithologies (including sub-surface silicification) has been addressed by Nicholson and co-workers (Nicholson, 1988, 1989; Nicholson and Aquino, 1989; Nicholson and Parker, 1990; Parker and Nicholson, 1990) and White et al. (1989).

It appears that thick sinter deposits commonly form around a biogenic framework of bacteriological and algal matter. Silica deposits and accumulates around this framework, rapidly gaining height or thickness and commonly forming a porous sinter. This biogenic material leaves characteristic textures in the sinter at both outcrop and thin-section scale. These take the form of striations and mushroom or stromatolite-like formations on the upper sinter surface, and columnar structures in cross-section. Banding, often continuous over several meters, may also be seen in cross-section. Under the microscope, rods and filaments, ranging from microns to 1mm in thickness, commonly appear, often in clusters, amidst a fine-grained silica groundmass. Where the sinter has deposited from a flowing water then ripples and

terraces form on the upper surface. These are invariably arcuate in section with the concave surface pointing away from the flow, towards the source of the discharge (ie. the long slope of the ripple points towards the source; Lloyd, 1972). Around hot pools sinter often forms upstanding banded circular rims and rounded overhangs facing into the pool, these features often show algal structures in thin section. Sinters do not need an algal framework to develop thick deposits, and the absence of such textures does not preclude a geothermal origin. Around geysers, for example, the water temperature is too hot for even thermophilic algae/bacteria and sinter deposits in hard, denser masses which display a diagnostic nodular texture known as "geyserite". This appears on the upper surface of the sinter as a mass of nodules, which range in scale from millimetres to several centimetres in diameter. Smaller nodules often form on larger examples. Coarse plant material, spores and pollen may be included within sinters and boxwork structures form on the silica rims surrounding hot pools.

Silica residue, formed by the leaching of a rock by acidic waters or steam to leave silica, must be distinguished from silica sinter. The deposits represent destructive (residue) and depositional (sinter) processes representative of different fluid types and different levels of the geothermal system. Silica residue is commonly porous and friable, and does not develop the characteristic textures of sinter. The presence of admixed sulphate-water minerals (eg. kaolin, alunite) is diagnostic of silica residue. Both residue and sinter age to quartz.

Sinter geochemistry may also provide a diagnostic criteria and aid to identification. Further work is still required in this area, but enrichments in the sinter chloride, boron, arsenic and antimony concentrations may be diagnostic. As discussed by Nicholson and Parker (1990) and Parker and Nicholson (1990), arsenic in sinters is probably present as sub-micron size particles of amorphous sulphide. High concentrations of As (~>100 mg/kg) and commonly associated metals (Sb, Tl, Hg) are likely to be a reliable guide to gold-bearing geothermal/epithermal systems. Any gold or silver associated with the amorphous sulphide phase will be diluted by the silica, making elements of the arsenic association more reliable pathfinder species. Although the absence of arsenic does not preclude a geothermal origin, it may indicate a gold-poor system.

Criteria for the recognition of silica sinter
Textures *Surface:* striations, mushrooms, banding, ripples, terraces, circular rims, overhangs, plant material, boxworks *Cross-section:* columns, plant material *Thin-section:* rods, filaments **Geochemistry** *Diagnostic(?):* enrichments in Cl, B, As, Sb *Au-potential:* high As-Sb-Tl-Hg

Soil and soil-gas surveys

Soil surveys can be usefully applied over young systems, using the procedures described above, to identify permeable zones and flow structures. However, given the diffusion of volatile species from the soil over time, such surveys would be less helpful if applied to ancient systems.

CHAPTER 6

WATER SURVEYS

Too often in the preparation and interpretation of geochemical surveys great emphasis is placed on the analytical methods used and recognition of any associated sources of error. However, before a sample can be analysed it must be collected, and it is this aspect of the analytical programme than can be neglected. Bad sampling techniques can invalidate a survey and are far more costly to correct than analytical errors. Laboratory errors or mistakes can often be corrected by reanalysis of the sample, but if the sample is contaminated or unrepresentative, the analytical result will lack significance, regardless of the accuracy and precision of the analytical method used. This is not usually discovered until after the samples have been analysed and the data interpreted on a field-wide basis, possibly necessitating a re-sampling programme: bad sampling techniques are very costly. It is therefore worthwhile to adopt standardised methods of water sampling. This includes standardising the equipment to be used, and the correct preparation of that equipment in the laboratory several days before any field surveys are undertaken.

6.1 PRE-FIELD LABORATORY PREPARATION

Collection bottles

Sample bottles can be made of a variety of glass and plastic materials, and not all are suitable for geothermal waters. The vessel must preserve the integrity of the sample until analysis and possible problems which must be considered include

- contamination of the water from the bottle material (eg. boron from borosilicate glass)
- contamination of the water by prolonged contact with atmospheric gases
- loss of volatiles through the vessel walls or through the cap seal
- loss of trace constituents by adsorption onto the vessel walls

To overcome these potential difficulties, the sample bottles should be non-contaminating, airtight, not gas-permeable and specially cleaned. This latter aspect will be returned to below. The geothermal water could be contaminated with inorganic constituents by glass vessels and these are therefore generally avoided.

They are also heavier and less robust than most plastics, and are therefore also practically less suitable. However, some plastics are gas permeable and can contaminate the sample with trace metals and organics. Coloured bottles should be avoided as the colouring agent can readily contaminate the sample.

Clearly no single material is suitable for all types of constituents and a mixture of plastic and glass vessels are used: glass for volatile and organic analyses, plastic for all other species. Teflon (ptfe) is robust and inert, and would be an ideal choice for the plastic bottles but is too expensive for routine use. High-density polythene bottles are a good compromise between cost and inertness. They should have an air-tight seal; this can be tested by capping the bottles and standing on them. The quality of the bottle will play a role in determining the final quality of the analyses. It is wise therefore to purchase bottles of known composition and life cycle from established specialist manufacturers such as Nalgene.

Glass bottles should have a butyl rubber tube, 10 - 20cm long, placed over the neck of the vessel. Water is placed in the vessel to fill the bottle and the tube, which is then sealed by a spring clip. Since butyl rubber is not readily gas permeable, this permits the waters to cool without creating and air space which would contaminate the sample.

The volume of the bottles required will vary with the sampling programme, and practical aspects of the difficulties of transport. However, 500mL bottles provide sufficient water for routine and duplicate determinations.

Bottle cleaning

Many methods have been used to clean both glass and plastic bottles for water sampling. The purpose of cleaning is to remove traces of previous samples, to leach any contaminants from the vessel walls and, for trace analysis, to help prevent adsorption of species onto the bottle walls. The following procedure has been used successfully for both cation and anion determinations, and is recommended for all glass and plastic sampling equipment (including the bottle caps).

1. Soak vessels for 24hrs in a 5% solution of Decon 90.
2. Wash bottles at least three times in deionised water.
3. Soak vessels for 24 hrs in 1M nitric acid.
4. Wash bottles at least three times in deionised water and cap.

Water Sampling Equipment Checklist
plastic bottles
glass bottles
1:1 nitric acid in a teflon dropper bottle
pH papers or
pH electrode (with batteries & buffers)
maximum thermometers
water baler
water dipper
1L plastic beaker
pole with clamp and nylon rope
plastic syringe
0.45μm filter membranes
filter holder
plastic tweezers
washbottle with deionised water
flow meter/stopwatch
general equipment
thick rubber gloves
towel
waterproof marker pen
notebook, pens, pencils, tape measure
maps, aerial photographs, compass,
camera with spare film and batteries
first-aid kit
additionally for pipeline and wells
Webre separator
high-pressure hot water cooler
Klyen downhole sampler

Steps (3) and (4) can be omitted if the bottles are only to be used to sample waters for major ion determinations. Decon 90 has been used by the author, but any laboratory surface cleanser of equivalent quality could be substituted.

Sampling equipment

A check list of field equipment for water sampling is given here for convenience. The use of the equipment is described in Section 6.3. The *pole* is useful for safely placing the water baler and thermometer into hot pools, away from the edge and without disturbing any particulate matter deposited on the sides of the pool. The *maximum thermometer* records the temperature of the water and this will remain fixed once the thermometer is removed from the pool or spring. A steel case partially covering the thermometer helps prevent breakage. Check the required immersion depth for an accurate reading to be obtained. *pH papers* are a rapid and convenient, but should cover a narrow range of pH values and be sensitive to 0.2pH units to be useful. A *pH electrode* can provide a more accurate determination, but as field instruments can drift rapidly, this must be regularly calibrated with buffers and must have an automatic temperature compensation control. A *water dipper* is used to sample springs, shallow pools or weirboxes and can be constructed by clamping a beaker to a pole. The *water baler* enables water to be sampled from various depths within a pool, which is helpful in obtaining a representative sample from the discharge vent if mixing within the pool is poor. Both plastic and steel vessels are available, examples used by the author are made by Zone Sampling Devises (steel) and Azlon (plastic), and are available in several volumes. The water should be filtered to remove particulate matter and this is conveniently done by passing water through a *filter* in a holder with a *plastic syringe*. The equipment is available as standard kits, Millipore equipment has been used by the author. The *nitric acid* used to acidify the sample should be of research-grade (not laboratory or analytical grade) or re-distiled to prevent contamination.

6.2 FIELD SURVEY

The location and difficulty of access will determine the nature of the initial and detailed surveys. A reconnaissance survey to gain an impression of the whole field and notable discharge areas is always useful. This would be followed up by a detailed mapping and sampling survey. As local weather conditions can influence the condition of the features and the ground conditions some local knowledge of the behaviour of the field is valuable from both a scientific and safety view. Sampling during the summer or dry season will reduce the influence of near-surface

groundwater mixing; while mapping discharge features in winter is made easier as more steam is visible.

Mapping springs

The time taken to make an accurate and detailed map of the geothermal features over an area is never wasted. The difficulty lies in balancing the differing needs of the amount of manpower and time available, with the level of accuracy and detail desired. A classic example of detailed field mapping is shown by Lloyd (1972) who prepared a plane-table map of individual features, cross-referenced to aerial photographs and photographs of the key features. Rarely is it possible to map an area in such detail. However, quality maps can be prepared using large-scale base maps or, if these are not available, enlarged aerial photographs. Features can be marked on the maps/photographs with a fine drawing pen, or by piercing a hole with a fine needle to show the location of the spring (Lloyd, 1972).

All features should be numbered. If local names exist for specific features, these can be included too. Names should not however, be used *instead* of a reference number as local names can change or become confused over time.

Field notes

It is essential for follow-up and monitoring work that springs examined and sampled in the initial survey can be recognised by subsequent field parties. Detailed field descriptions of the features, preferably with a photograph, cross-referenced to the geothermal-feature map are the key to successful feature identification. The parameters which should be recorded for each spring or pool are listed in the box below.

Field measurements

Physical parameters must be measured in the field, but it may also be necessary to determine key chemical concentrations as they may change on transportation to the laboratory. While such chemical determinations can be done beside each feature, it is more productive (and often more precise) to have determinations made by an analyst in a field laboratory a short distance away. In this way springs can still be sampled while determinations are being made routinely.

Geothermal feature mapping: Field notes	
feature name/number	cross-references to map
feature type	seepage/spring/pool/spouter/geyser
grid reference	cross-references to map
size of spring/pool	in metres
overflow/inflow	in litres/second
ebulation	yes/no; height; periodicity
geyser action	yes/no; height; periodicity
gas evolved	yes/no; small/moderate/large amount/odour
date/time	for future comparisons
physical measurements	temperature/flow rate
chemical measurements	pH/sulphide/bicarbonate/ammonia (see below)
deposits	colour, type, texture of residues/precipitates
water bottle numbers	cross-referenced to bottle label
gas bottle numbers	cross-referenced to bottle label
name of field worker	for any future queries
sketch	showing a scale, north, positions of deposits around feature, inflow/outflow, positions of gas discharge, sample points, measurement points
photograph	include in the photograph a label showing spring name/number, north and a scale

pH: Easy to measure pool-side using narrow range pH-paper or a portable pH-electrode. Ensure the electrode is regularly calibrated with buffers and has an automatic temperature compensation. The temperature at which the pH is determined should be recorded.

bicarbonate, sulphide, ammonia: Can change concentration on prolonged storage or contact with the atmosphere; determine using procedures described in Section 6.4.

chloride: Need not be determined in the field as chloride concentrations are stable, but can be a useful guide to recognise possible dilution/upflow areas and flow directions and therefore assist in the progressive planning of the survey.

temperature: Measure using a maximum-thermometer (note required depth of immersion for a correct reading) or electronically (many portable pH-electrodes

incorporate a temperature probe). Use the pole to ensure the maximum temperature at the discharge point is determined.

flow rate: Measure using a V-notch, a current meter or by surface measurement/estimation. Using a V-notch of angle θ, the flow rate, Q, is calculated using the formula (Lloyd, 1972; P.R.L. Browne, pers. com., 1988):

$$Q = 0.59\ (8/15)\ \tan(\theta/2)\ \sqrt{2g}\ h^{5/2})$$

where

h = the distance from the bottom of the "V" and the height of the water just before it falls over the notch in metres.

g = 9.81m/sec^2

Alternatively the time taken for a float to travel a set distance in the outflow channel is measured with a stop-watch and the cross-sectional area of the channel is determined. The flow rate is then estimated from:

flow rate (L/s) = [(channel length x width x depth) x 0.85] / time

Note that time is in seconds and that all dimensions are in decimetres (1dm = 10cm, and 1dm^3 = 1L). As the surface velocity of a stream or outflow is faster than the mean velocity of the discharge a correction factor (0.85) is applied to the expression. The actual value of the mean velocity would have to be determined using a flow meter, but 0.85 is an average figure.

Selection and prioritizing springs for sampling

Within a geothermal area some spring waters will yield more information about the deep reservoir conditions than others. It is important therefore to ensure that these springs are recognised and sampled in the survey.

Chloride springs with the following characteristics yield the most reliable information:

- high flow rate
- high temperature (boiling or near-boiling)
- high chloride concentration

Waters discharged with these characteristics are presumed to have had the most rapid ascent to the surface with minimal near-surface dilution or mixing. These are given the highest priority in sampling, and all springs with these features should be sampled.

Acid-sulphate and bicarbonate springs produced by steam-heating of groundwaters are generally unreliable guides to the subsurface conditions. The concentrations of the solutes in such waters are derived from near-surface rock-water reactions and bear little relation to the equilibrium reactions at depth.

Spring survey procedure

1) Map the springs in the geothermal area, distinguishing chloride, sulphate and bicarbonate springs were possible on appearance and pH. Note spring temperatures and flow rates (estimated or measured).
2) Sample all boiling or near-boiling chloride springs with high flow rates.
3) Ensure a representative selection of other types of hot springs are sampled throughout the area to give an indication of flow direction and dilution trends.

6.3 SAMPLING METHODS

Springs and pools

The temperature, flow rate and pH of the feature should be determined prior to sampling.

Place the water baler or dipper into the water and rinse twice. Fill the plastic beaker with water, this will be filtered and used to rinse the sample bottles.

Using the plastic tweezers place a 0.45μm filter membrane into the holder. Wetting the holder surface with deionised water from the wash bottle can help retain the membrane in position. Screw the holder closed ensuring that the O-ring is not trapped in the screw threads. Rinse the syringe with water.

Filter 50-100mL of water into each sample vessel, cap and rinse thoroughly. Rinse each bottle at least twice with the geothermal water.

Collect the sample for analysis. A complete analysis will require:

- one 500mL filtered, *unacidified* sample in a *plastic* bottle; for pH, TDS and anion determinations
- one 500mL filtered sample *acidified* to pH<3 in a *plastic* bottle; for silica and cation (especially trace metal) determinations and
- one 500mL filtered, *unacidified* sample in a *glass* bottle with butyl rubber tube seal; for volatile and atmosphere-sensitive (pH, H_2S, HCO_3, NH_3, SO_4) and organic species

and additionally if specifically required:

- one 100mL filtered, *unacidified* sample diluted 1+10 with deionised water in a *plastic* volumetric flask; for silica
- one 500mL filtered, *unacidified* sample in a *glass* bottle with oxidising solution (see below); for mercury
- one 100mL *unacidified* sample in a *glass* bottle; for ^{18}O and D
- one 1L *unacidified* sample in a *glass* bottle; for ^{3}H
- one 1L filtered, *unacidified*, sterilized sample in a *glass* bottle for ^{34}S and ^{18}O in sulphate

Fill the bottles to overflowing and cap.

The sample bottles should be dried with the towel and labelled, as shown, with a waterproof pen. The details should be cross-referenced into a note book and onto a map.

The bottles should finally be placed in self-sealing polythene bags to prevent contamination and to preserve the details on the label which may otherwise rub off on transportation.

Sample bottle label
geothermal field
spring/pool name/number
date of sampling
time of sampling
spring temperature (t°C)
pH_t
filtered/unfiltered
acidified/unacidified
bottle number

Notes

Samples should be acidified by adding 1:1 nitric acid drop-wise until the pH<3.

Samples with high silica concentrations in excess of about 300mg/kg may still deposit silica on standing. Under such circumstances the samples will have to be diluted with deionised water to bring the silica content below 300mg/kg and a sample specifically for silica determinations should be taken. For this, 10mL of filtered,

unacidified water should be pipetted into a 100mL plastic volumetric flask and made up to the mark with deionised water.

If the pool or spring is not deep, then samples for the analysis of volatile species should be rapidly transferred to the glass bottle to minimise reaction. Alternatively, deep pools can be sampled by immersing two glass bottles clamped together and linked by a butyl rubber hose. This enables the collection of a sample which has not been exposed to atmospheric contact (Ellis and Mahon, 1977).

Wells

Representative discharges from wells are collected from the weirbox at the base of the tower silencer, and from sample points along the pipeline. Downhole sampling determines whether chemical variations occur with depth and over time, and requires a specialised sampling vessel to preserve the sample composition as it is raised to the surface out of the well. To ensure that the discharge is representative of the reservoir fluid and is not contaminated with drilling fluids, the well should have been discharged at a high flow rate prior to sampling. In this regard a knowledge of the well history is useful, and the well characteristics should be monitored. Perameters which should be recorded for sampling and monitoring, both in the notebook and on the collection bottle, are detailed in the box below.

Weirbox

Samples taken from the weirbox of the silencer ("atmospheric sampling") should be at the local boiling point. Waters cooler than this can have been concentrated by evaporation or diluted by steam condensation, and corrections to the solute concentrations to allow for these processes would need to be made (although solute ratios would remain usable). The sampling procedure is the same as described above for springs and pools using a water dipper. The temperature of the weirbox water should be recorded.

Twin tower silencers are more readily sampled than horizontal silencers. Samples are physically more difficult to collect from horizontal silencers and suffer from variable condensation and evaporation effects which cannot be readily corrected (Ellis and Mahon, 1977; Klyen, 1982).

Well sample bottle label
geothermal field
well number
date of sampling
time of sampling
well head pressure (state bg or ba)
separation pressure (state bg or ba)
discharge enthalpy (if known)
flow rate
temperature (t°C)
$pH_{t°C}$
acidified/unacidified
filtered/unfiltered
bottle number

Pipelines

Sample points along a pipeline should be located at distances of six pipe diameters from the well head, and forty-two pipe diameters downstream from any restrictions (Klyen, 1982; Mahon, 1961). The water and steam phases of the discharge are separated using a portable Webre Cyclone Separator ("pressure sampling") which is attached to the sample points on the pipeline. Alternatively a steel, high-pressure, hot-water cooler can be used. An excellent, detailed and illustrated description of the operational procedures of both devises is given by Klyen (1982).

Downhole samples

Samples from down a well can identify variations in discharge chemistry with depth resulting from inflows and mixing, and can provide otherwise unobtainable samples representative of the reservoir fluid. Any downhole sampling device must be able to withstand high temperatures and pressures, low-pH fluids and highly saline fluids. It must also be reliable and preserve the downhole fluid composition on ascent to the surface. The Klyen Sub-surface Sampler fulfils these requirements and has gained widespread usage. The construction and operation of the sampler is described in detail by Klyen (1973, 1981, 1982).

Specialised sampling requirements

Sampling for mercury analysis

To reduce the loss of mercury from the sample, the volatile species are oxidised into an ionic form on collection with an "oxidising solution" in the bottle. Airtight, acid-washed glass or teflon 500mL bottles should be used for sample collection. For precise, low-level work these, and all other sampling equipment, should be cleaned by refluxing with concentrated nitric acid.

Solutions required: concentrated sulphuric acid; 6% K_2CrO_4 solution (prepared by dissolving 60g K_2CrO_4 in 1kg deionised water).

Procedure: Before leaving the laboratory, clean bottles should be filled with a mixture of 400mL deionised water, 50mL sulphuric acid and 50mL 6% K_2CrO_4 solution. It is convenient if the sulphuric acid and 6% K_2CrO_4 solution are taken into the field in cleaned 10mL glass tubes or vials.

At the sample site, the deionised water solution is emptied from the sample bottle, and this is then rinsed twice with the filtered (using the above methods) geothermal water which will be sampled. Empty a 10mL-vial of sulphuric acid into the sample bottle, followed by a 10mL vial of 6% K_2CrO_4 solution. Fill the sample bottle with filtered geothermal water using the standard procedure described above. It is wise to use goggles when doing this as the acid may "spit" when hot water is added to the bottle (Giggenbach and Goguel, 1989).

Note: Other oxidising solutions can be used; one alternative is composed of 6mL concentrated nitric acid, 6mL 5% $KMnO_4$ solution and 10mL 5% $K_2S_2O_8$ solution in the 500mL sample bottle (Kindle, 1989).

Sampling for isotope analysis

In all samples collected for isotopic analysis, atmospheric contact should be minimised as much as possible. Glass vessels should be used and must be airtight. The sample vessel described by Ellis and Mahon (1977), and mentioned above, for the collection of water free from atmospheric contact would be suitable if sampling from pools; but these features can suffer from evaporative effects and atmospheric mixing through convective circulation and are not the most suitable for isotope analysis. Well discharges can be sampled using the standard methods.

^{18}O and D: Springs with large flow rates discharging from a small vent should be chosen to minimise surface effects such as oxidation and evaporation (Truesdell and Hulston, 1980). Only 20mL is required for these analyses, but it is useful to collect 100mL to permit repeat determinations (Henley et al., 1984).

^{3}H: As the concentrations of tritium in geothermal waters is very low, large sample volumes are required, at least 500mL (preferably 1L) with minimal atmospheric contact.

^{34}S and ^{18}O in sulphate: Samples collected for sulphur isotope analysis, should be filtered and sterilised to stop any biological activity which would alter the sulphur isotopic composition of the sample. This is most readily achieved by the addition of formaldehyde (10mL/1L). Any hydrogen sulphide present must be prevented from oxidising, and can be fixed as CdS by the addition of $CdCl_2$ (Truesdell and Hulston, 1980). Surface and near-surface produced sulphate should be excluded by the selection of springs with minimum SO_4/Cl ratios. As about 25mg SO_4 are required for the analysis, the sample volume will need to be sufficiently large to provide this amount (Giggenbach and Goguel, 1989).

Sample storage

If quality, acid-washed bottles are used, then filtered, acidified samples can be stored for several months, possibly years, without deterioration, particularly if it is only the major constituents which are of interest. However, concentration by evaporation will occur on prolonged storage, and correction for this can be made by re-determining chloride and comparing this with the initial concentration. Unacidified samples can also be stirred, but acidification reduces the possibility of precipitation or algal growth. If samples with silica concentrations >300mg/kg are to be stored, they must be diluted with deionised water to reduce the silica content to <300mg/kg to prevent precipitation of silica.

6.4 ANALYTICAL METHODS

Introduction

This section describes procedures suitable for the analysis of geothermal waters. The methods detailed are not exhaustive and for some species alternatives may be available; anions, for example, can also be determined by ion chromatography. However, the techniques described have been successfully applied to geothermal waters and are suitable for routine analysis. In compiling this section I have drawn heavily upon the experience of staff at DSIR (New Zealand); both in discussions and from their analytical methods reports (Ellis et al., 1968; Giggenbach and Goguel, 1989). Standard procedures for water analysis are also given in APHA (1989, 1991), ASTM (1992), Kindle (1989) and Watson (1979). Good analytical laboratory

procedures and methods for the evaluation and treatment of errors have not been detailed, since these are standard practice and should be known by the analyst. If required, this information can be found in textbooks on analytical chemistry and the following are recommended: Fritz and Schenk (1979), Harris and Kratchvil (1981) and Vogel (1990) describe laboratory procedures, the theory and background to error treatment and the classical wet chemical methods of analysis, with some details on instrumental methods; Christian and O'Reilly (1986) and Willard et al. (1981) concentrate on instrumental methods of analysis.

Species-analytical method cross-reference

Under each entry the method of analysis is abbreviated on the right-hand edge of the page; for convenience the species determined by given techniques are listed here.

Volumetric (titrimetric) (VOL): HCO_3, CO_3; B; Cl; H_2S; I, Br
Colourimetric (spectrophotometric) (COL): SiO_2; SO_4
Gravimetric (GRAV): Total dissolved solids (TDS)
Ion-selective electrode (ISE): NH_3; F; pH
Atomic absorption spectroscopy (AAS): Al; As; B; Fe; Li; Mg; Hg; SiO_2
Atomic emission spectroscopy*, flame source (F-AES): Cs; Ca; K; Rb; Na; inductively coupled plasma source (ICP-AES): B**

Notes
* most AAS instruments have an emission mode
** ICP-AES can also be used for the majority of elements determined by AAS but is particularly recommended for boron.

Aluminium (Al) **AAS**

To prevent co-precipitation of aluminium with silica or iron hydroxides, samples should be filtered and acidified in the field. If silica concentrations are high, the samples should be diluted in the field with deionised water to reduce the silica concentration to <300 mg/kg.

Procedure

Stock standard solution (1000 mg/kg Al): 1g Al foil dissolved in 25mL of concentrated hydrochloric acid. A few drops of concentrated nitric acid and a small drop of mercury aid dissolution. As sample waters to be analysed have been acidified, the stock solution should be diluted to give 1kg of solution with 0.1M HNO_3.

Working standard solutions: Prepare by successive dilution of the stock solution with 0.1M HNO_3 to give the required concentrations (typically 100, 30, 10, 1 mg/kg).

AAS operating conditions: Hollow cathode lamp, wavelength 309.3nm, band pass 0.3nm, nitrous oxide-acetylene flame.

Method: Optimise the instrument to give maximum absorbance by adjusting the flame while aspirating the 30 mg/kg sample. Analyse the working standard solutions and plot a calibration graph of absorbance against concentration; this should be linear to about 30 mg/kg. Analyse the samples and determine the concentration from the calibration graph. If the Al concentration in the samples exceeds the linear portion of the calibration (>30 mg/kg), the samples should be diluted to bring the Al < 30 mg/kg.

Notes: Waters with low Al concentrations (<0.3 mg/kg) should be analysed using graphite furnace AAS. Alternatively, preconcentration of Al by solvent extraction using 8-hydroxyquinoline can be used in both colourimetric and flame-AAS methods.

Reference: Giggenbach and Goguel (1989).

Ammonia (NH_3) **ISE**

Ammonia in water exists as the ammonium ion (NH_4^+) which can be converted to nitrate or nitrogen by biological activity. Samples should therefore be preserved by filtration and acidification in the field.

Procedure

Principle: Dissolved ammonia is determined by an ammonia-specific gas-sensing electrode (eg. Orion 95-12). The procedure converts ammonium ion to free ammonia by the addition of sodium hydroxide to raise the pH to above 11

$$NH_4^+(aq) + OH^-(aq) = NH_3(g) + H_2O(l)$$

The gas diffuses across a hydrophobic gas-permeable membrane membrane at the base of the electrode until the partial pressure of ammonia of both sides of the membrane is equal. The pH change in the filing solution created by the re-dissolution

of the ammonia is detected by the electrode. This change is proportional to the ammonia concentration which can be determined by calibration.

Stock standard solution (1000 mg/kg NH_3): 3.141g dry ammonium chloride in 1 kg deionised water.

Working standard solutions: Successively dilute stock solution with deionised water to give desired working solution concentrations (eg. 100, 10, 5, 1, 0.5, 0.1 mg/kg NH_3)

pH-ionic strength adjustor solution (pH-IAS): 5M NaOH, 0.05M disodium EDTA, 10% methanol with a few drops of thymolphthalein indicator to give a deep blue colour showing pH>11. This solution ensures sample pH>11 to release ammonia for detection.

Method: Pipette 50mL of sample into a clean, dry plastic beaker containing a magnetic bead. Place beaker on a magnetic stirrer and stir at a constant rate. This rate should ensure efficient mixing, but should not form a vortex or bubbles in solution. Add 1mL pH-IAS and immediately insert the electrode into the solution ensuring that no air-bubbles are trapped under the electrode, and that the magnetic beads to not strike the electrode. Allow the electrode to achieve equilibrium for five minutes, and read the potential to the nearest 0.1mV. Take further readings every minute until two consecutive readings do not differ by more than 1.0mV. This is considered to be the equilibrium potential and is recorded. Remove electrodes from solution, rinse with deionised water and blot dry with a tissue; do not wide across the electrode membrane. Repeat this procedure with subsequent aliquots of the sample solution until two equilibrium potentials within 1.0mV are obtained. The mean of these two potentials is the mV-reading which will be used to determine the sample ammonia concentration from the calibration graph. The calibration graph is prepared using the above procedure on the standard solutions, which should be analysed in ascending order of ammonia concentration. Plot the calibration graph on semi-logarithmic graph paper with electrode potential (mV) on the linear scale and ammonia concentration (mg/kg) on the logarithmic scale. This should be linear to ~0.5 mg/kg NH_3 and show a difference of ~58mv per decade change in concentration.

Notes: Ammonia can be lost from the solution while waiting for the electrode to achieve equilibrium. To prevent this a plastic film (eg. Parafilm) should be placed over the beaker and around the electrode. Mercury and hydrogen sulphide may interfere if either are present at high concentrations. Mercury can be complexed by adding sodium iodide to sample aliquots, and hydrogen sulphide is removed by acidifcation and bubbling with air. Samples with an ionic strength in excess of 1M

should be diluted. In some circumstances the electrode shows significant drift; hourly calibration checks with a standard solution should be made.
References: Orion (1987), Walters et al. (1984).

Arsenic (As) **AAS**

AAS procedure 1: Direct determination
Stock standard solution (1000 mg/kg As): 1.320g dry As_2O_3 dissolved in 50mL concentrated hydrochloric acid, dilute to 1kg of solution with deionised water.
Working standard solutions: Successively dilute stock solution with deionised water to make 50, 20, 10, 5, 1, mg/kg working standard solutions.
AAS operating conditions: Electrodeless discharge lamp, simultaneous background correction with a deuterium lamp, wavelength 193.7nm, band pass 0.7nm, nitrous oxide-acetylene flame.
Method: Optimise the flame for minimum absorption on water aspiration. Prepare a calibration graph of absorbance against concentration with the standard solutions, and use to determine sample As concentrations.
Notes: Background correction must be performed, especially at low As concentrations (<1mg/kg). Arsenic concentrations in the range 2 - 50 mg/kg can be determined using the above method, but greater sensitivity is obtained using hydride generation which is recommended for samples with As < 10 mg/kg. ICP-AES is more sensitive than flame AAS enabling concentrations down to 0.07 mg/kg to be determined at 193.7 nm.
Reference: Giggenbach and Goguel (1989).

AAS procedure 2: Hydride generation
Principle: This method is more sensitive than direct determination and should be used where arsenic concentrations are <10mg/kg. Arsenic is transported to the flame as arsine gas (AsH_3) which decomposes readily in the hydrogen flame. This type of flame is used as it absorbs little light at the wavelengths of the determination. Arsine gas is produced by reaction between the sample and sodium borohydride in a generating vessel which is added to the spectrophotometer. Such vessels are commercially available. The arsine gas is fed directly to the flame in a stream of argon or nitrogen, and the signal observed is in the form of a peak. This is quantified by determination of the peak area.
Stock standard solution (1000 mg/kg As): 1.320g dry As_2O_3 dissolved in 50mL concentrated hydrochloric acid, dilute to 1kg of solution with deionised water.

Working standard solutions: Successively dilute stock solution with deionised water to make 10, 5, 1, 0.5, 0.1 mg/kg working standard solutions.
AAS operating conditions: Electrodeless discharge lamp, wavelength 193.6nm, band pass 0.5nm, hydrogen-argon flame.
Reagents: 1.5M HCl, 5% sodium borohydride solution: dissolve 8g sodium hydroxide pellets in about 50mL deionised water in a beaker, add 5g sodium borohydride, stir and dilute to 100mL; centrifuge solution and store.
Method: Place 25mL 1.5M HCl in the reaction vessel. Add 1mL of the sample/standard solution. Allow contents to mix then add 2.5mL sodium borohydride and leave for 40 seconds to react. Flush the arsine gas into the flame and record the absorbance peak on a chart recorder. Flush the reaction vessel with deionised water between samples. Prepare a calibration graph of absorbance against concentration with the standard solutions, and use to determine sample As concentrations.
Reference: Aggett and Aspell (1976).

Bicarbonate (HCO_3^-) **VOL**
Carbonate (CO_3^{2-})

Atmospheric contact on sampling should be minimised to preserve the carbonate equilibria is the sample. The water should be analysed in the field or rapidly taken to the laboratory after sampling.

Procedure
Principle: This is essentially an alkalinity titration corrected for the effects of other weak acids in solution, notably boric acid, silicic acid and ammonium ion. Water samples with pH > 8.3 contain carbonate as well as bicarbonate ions. The carbonate is converted to bicarbonate by titrating to pH 8.3. the bicarbonate is then converted to dissolved H_2CO_3 by titration to pH 3.8. This is removed as CO_2 by bubbling CO_2-free air or nitrogen through the sample. Back titration to the initial sample pH then corrects for the effects of the other weak acids in solution.
Reagents: Standardised 0.02M HCl, standardised 0.02M NaOH, buffer solutions pH4.0, pH9.0.
Method: Pipette 10mL of sample into a 50mL beaker containing a magnetic stirring bead. Place onto an insulated magnetic stirrer and determine the sample pH with the calibrated pH electrode and meter. If pH>8.3 follow the procedure outlined below. Titrate to sample pH = 3.8 with 0.02M HCl and record the volume of acid used (V_{HCl}). Remove dissolved carbon dioxide by bubbling CO_2-free air or nitrogen

through the sample for 10 minutes. Titrate back to the original sample pH with 0.02M NaOH and record the volume used (V_{NaOH}). Calculate the bicarbonate concentration (mg/kg) from:

$$[HCO_3^-] = 61016(0.02V_{HCl} - 0.02V_{NaOH})/10$$

If the initial sample pH is above 8.3 then CO_3^{2-} ions will be present in solution. These can be determined by titrating the sample to pH 8.3 using 0.02M HCl, record the volume used ($V_{C,HCl}$). Follow the above procedure, and calculate the concentration of carbonate (mg/kg) from:

$$[CO_3^{2-}] = 60092(0.02V_{C,HCl} - 0.02V_{NaOH})/10$$

The bicarbonate ion concentration then requires a correction for the carbonate concentration as follows:

$$[HCO_3^-] = [61016(0.02V_{HCl} - 0.02V_{NaOH})/10] - 1.015[CO_3^{2-}]$$

Notes: The pH values used in the method are selected from a knowledge of the distribution of carbonate (H_2CO_3, CO_3^{2-}, HCO_3^-) and other weak-acid species in aqueous solution.

Reference: Giggenbach and Goguel (1989).

Boron (B) **VOL/COL/AAS/ICP-AES**

Boron can be determined by wet chemical, AAS and ICP-AES methods. Each has its limitations, but ideally ICP-AES is the optimum technique, with low detection limits, good sensitivity and rapid sample analysis. Wet chemical methods are a better alternative to AAS methods, particularly at low (<10mg/kg) boron concentrations. A pre-concentration step, using gel chromatography, can be used prior to analysis for samples with a low boron content (Yoshimura et al., 1979). As laboratory glassware is commonly made from borosilicate glass, this should be avoided wherever possible and plastic labware used instead. Where the use of glass is unavoidable, it should be rinsed in nitric acid prior to use. Geothermal waters should not be stored in glass bottles, and laboratory cleaning agents should be boron free, particularly for low-level determinations.

VOL procedure: Mannitol titration

Principle: This technique is based the reaction of mannitol with dissolved boron (as boric acid) to yield hydrogen ions. This causes the pH of the solution to fall in proportion to the concentration of boron in solution which can be determined by titration of the hydrogen ions with a dilute alkaline solution. As carbon dioxide can buffer the pH change in solution, this must be removed to prevent loss of accuracy.

Reagents: 0.5M sulphuric acid, 1M and 0.02M standardised sodium hydroxide (CO_2-free), bromothymol blue indicator 1g/100mL 95% ethanol, mannitol powder.
Stock standard solution (1000 mg/kg B): 5.716g dry boric acid in 1kg deionised water.
Working standard solutions: Sequentially dilute the stock solution to make 4-5 working standard solutions, typically 60, 40, 20, 10, 5 mg/kg B.
Method: Take a known volume of sample (50mL for waters with B>5mg/kg, 250 mL for waters with B<5mg/kg) and place in a conical flask. Add a drop of brothymol blue, acidify with 0.5M sulphuric acid and add 1mL excess of the acid for every 50mL of water. The solution should be yellow in colour. Remove carbon dioxide from solution by bubbling CO_2-free air or nitrogen through the sample for 10 minutes, and then allow the solution to return to ambient temperature. Add a magnetic stirring bead to the flask, place on an insulated magnetic stirrer and with constant stirring, adjust the pH to exactly 7.30 using 1M and then 0.02M sodium hydroxide with a calibrated pH electrode and meter. The alkali should be added slowly as pH 7.30 is approached to permit the electrode to achieve equilibrium: a reading can be taken to be at equilibrium if it remains stable for one minute. The indicator changes colour from yellow to green as pH 7.30 is approached. Add 2.5g of mannitol for every 50mL of sample. The solution pH becomes more acidic and is titrated back to a stable reading of pH 7.30 using 0.02M NaOH. Perform this procedure on a black solution (using deionised water) and the standard solutions to construct a calibration graph.
Notes: The 0.02M NaOH should be held in a microburette with CO_2-absorbing reacts present (eg. "carbosorb"). The detection limit is 0.1mg/kg B.
References: DoE/NWC (1980), Giggenbach and Goguel (1989)

COL procedure: Azomethine-H spectrophotometric method
Principle: Boron reacts with azomethine-H to form a yellow complex, which is then measured by spectrophotometer. The intensity of the absorbance is related to the boron concentration. Interfering species are masked by the use of EDTA. The method is useful for boron concentrations up to 10mg/kg; waters with higher concentrations will have to be diluted.
Reagents: azomethine-H, ascorbic acid, di-sodium EDTA, glacial acetic acid, ammonium acetate.
Azomethine-H solution: 1.0g of azomethine-H with 2.0g ascorbic acid in about 70g of deionised water, warm to dissolve. Make up to 100mL in a volumetric flask. Store for 1-2 days only in a boron-free glass or a plastic bottle.

Buffer solution: 3.0g Na_2EDTA in 150g deionised water; add 125mL glacial acetic acid and 250g ammonium acetate, warm and stir to dissolve. Store in a boron-free glass or a plastic bottle.

Stock standard solution (1000 mg/kg B): 5.716g dry boric acid in 1kg deionised water.

Working standard solutions: Sequentially dilute the stock solution to make 4-5 working standard solutions, typically 20, 10, 5, 3, 1 mg/kg B.

Method: Pipette an aliquot of the water into a 25mL plastic volumetric flask. The ideal aliquot volume depends on the boron concentration in solution as follows: B 5-10mg/kg, 1mL; B 2-5mg/kg, 2mL; B 1-2mg/kg, 5mL; B 0.5-1mg/kg, 10mL; B<0.5mg/kg, 15mL. Add sufficient deionised water to make the volume up to 15mL. Add by pipette 5.0mL of the azomethine-H solution and 4.0mL buffer solution, swirl the flask to mix. Make up to the mark with deionised water. Mix, and store at <20°C for 20 minutes. Measure the absorbance of the solution at 420nm using 10mm cells with deionised water in the reference cell. Analyse a blank solution in the same manner and correct the results accordingly. The concentration of boron is determined from the calibration graph, which is prepared by analysing the standard solutions using the same procedure.

Notes: The coloured solutions should be kept below 20°C as the colour fades at higher temperatures. Standards and samples should be determined at the same temperature.

Reference: DoE/NWC (1980)

AAS procedure

Stock standard solution (1000 mg/kg B): 8.816 dry borax $(Na_2B_4)_7.10H_2O$) in 1kg deionised water.

Working standard solutions: Successively dilute stock solution with deionised water to make working standard concentrations of 500, 100, 50, 20, 10, 5 mg/kg.

AAS operating conditions: Hollow cathode lamp, wavelength 249.7nm, band pass 0.7nm, nitrous oxide-acetylene reducing flame with 50mm-high red zone.

Method: Analyse the working standard solutions and plot a calibration graph of absorbance against concentration; this should be linear to about 1500 mg/kg. Analyse the samples and determine the concentration from the calibration graph.

Notes: Boron sensitivity is poor by AAS, particularly at concentrations below ~10mg/kg. The success of the method depends on stable machine conditions, notably that of the boron lamp. Although useful at higher concentrations, AAS should be replaced by the wet chemical method at boron concentrations below ~20 mg/kg.

Reference: Giggenbach and Goguel (1989).

Bromide (Br^-) See *iodide*.

Caesium (Cs) **F-AES**

Procedure

Stock standard solution (100 mg/kg Cs): 0.1267 dry CsCl in deionised water to give 1kg of solution.

Working standard solutions: 2.5, 1.0 mg/kg made up by successive dilution of the stock with a matrix-matching solution containing 1000mg/kg Na and 100 mg/kg K.

AES operating conditions: flame emission mode, wavelength 852.1, bandpass 0.14nm, air acetylene flame.

Method: To suppress ionization K must be added to sample and standard solutions to attain a concentration of 1000 mg/kg (eg: add 0.01 mL of a saturated KNO_3 solution per mL of standard/sample solution). Analyse the working standard solutions and plot a calibration graph of emission against concentration. Analyse the samples and determine the concentration from the calibration graph.

Notes: A fuel-rich air-hydrogen flame can be used for chloride waters where Fe, Al, Ca and TDS concentrations are low. This permits Cs to be determined without the addition of K as an ionization suppressant. Background correction at 852.6nm eliminates spectral interferences.

References: Giggenbach and Goguel (1989); Goguel (1981).

Calcium (Ca) **F-AES**

Prior to the development of the F-AES method, calcium was determined with magnesium by wet chemical methods, as these could not distinguish the two metals, early analyses are often reported as "Ca+Mg".

Procedure

Stock standard solution (1000 mg/kg Ca): 2.497g dry $CaCO_3$ in 50mL deionised water. Add dropwise the minimum volume of 1:1 HCl required to dissolve the carbonate (~20mL), dilute to 1Kg with deionised water.

Working standard solutions: 40, 20, 10, 5, 1 mg/kg solutions made by successive dilution of the stock with a solution containing 1000mg/kg Na and 100mg/kg K. This Na-K solution is used to prepare the working standards in an attempt to make a closer

match to the matrix of the samples than could be provided by dilution with deionised water. This matrix-matching should be attempted with all trace constituents: the concentrations of Na and K can be varied as required to make a more appropriate match the concentrations in the samples.

AES operating conditions: flame emission mode of AA instrument, wavelength 422.7nm, bandpass 0.50-1.00nm, nitrous oxide-acetylene, fuel-rich + argon (~1L/min) flame with a 2-5mm high red zone. sample height 12mm above top of burner, 6mm diameter mask.

Method: Analyse the working standard solutions and plot a calibration graph of emission against concentration. Analyse the samples and determine the concentration from the calibration graph.

Notes: Concentrations in the range 0.01 to 100 mg/kg Ca can be determined using the above method provided ionization is suppressed.

Reference: Giggenbach and Goguel (1989).

Carbonate (CO_3^{2-}) See *bicarbonate.*

Chloride (Cl-) **VOL**

Procedure: Mohr titration

Principle: Chloride may be determined in neutral or slightly alkaline solution by titration with silver nitrate using potassium chromate as indicator. Chloride is precipitated as silver chloride, and the excess silver ions form silver chromate to yield a permanent red-coloured end-point. Sulphuric acid or calcium carbonate are added to bring the solution to near-neutral pH.

Reagents: standardised 0.1M silver nitrate solution, 5g potassium chromate solution in 100mL deionised water, phenophthalein indicator.

Stock standard solution (2000 mg/kg Cl): 3.297g dry sodium chloride in 1kg deionised water.

Method: Pipette a 25mL aliquot of the sample into a conical flask and add a few drops of phenophthalein indicator. Adust the sample pH with dilute sulphuric acid (1M) or calcium carbonate until the indicator just turns colourless (pH 8.3). Add 1mL of the potassium chromate solution as indicator and titrate with silver nitrate.

Notes: Suitable for samples with Cl>10mg/kg. The solution should be near-neutral, with acid samples neutralised by the addition of calcium carbonate. Addition of calcium carbonate has the advantage of providing a white suspension enabling the end-point to be clearly observed. It can therefore be advantageous to add this to all

samples. Note that bromide, iodide and sulphide are also titrated, but should introduce little error in the analysis of chloride-waters as Cl^- >> Br^-, I^-, S^{2-}. If sulphide is likely to be a problem then it should be removed by acidification of the sample with nitric acid and bubbling nitrogen through the solution.

Chloride determination by potentiometric titration is an alternative method described by Ellis et al. (1968) and Giggenbach and Goguel (1989).

Reference: Ellis and Mahon, 1977; Ellis et al., 1968; Vogel, 1990.

Fluoride (F^-) **ISE**

Procedure

Stock standard solution (1000 mg/kg F): 2.210g dry NaF dissolved in deionised water to 1kg.

Working standard solutions: 5, 1, 0.5, 0.1, 0.05, 0.02 mg/kg F^- solutions; higher concentrations (50, 20, 10mg/kg) may be required if analysing unusually high-fluoride waters.

Total ionic strength adjustment buffer (TISAB) solution: 58.0g sodium chloride, 57.0mL glacial acetic acid, 4.0g trans-1,2-diaminocyclohexane-N,N,N',N'-tetra-acetic acid (CDTA), 243.0g tri-ammonium citrate in 500mL deionised water. Add sufficient 10M NaOh to bring the solution pH to 5.4. Cool and quantitatively transfer to a 1L volumetric flask; dilute to the mark with deionised water.

Method: Pipette equal volumes of sample and TISAB into a clean, dry plastic beaker containing a magnetic bead. Cover and leave to decomplex for at least 20 minutes and preferably for 24 hours. Place beaker on a magnetic stirrer and stir at a constant rate. this rate should ensure efficient mixing, but should not form a vortex or bubbles in solution. Insert the electrodes into the solution ensuring that no air-bubbles are trapped under the electrodes and that the magnetic beads to not strike the electrodes. Allow the electrode to achieve equilibrium for five minutes, and read the potential to the nearest 0.1mV. Take further readings every minute until two consecutive readings do not differ by more than 0.5mV. This is considered to be the equilibrium potential and is recorded. Remove electrodes from solution, rinse with deionised water and blot dry with a tissue; do not wide across the electrode membrane. Repeat this procedure with subsequent aliquots of the sample solution until two equilibrium potentials within 0.5mV are obtained. The mean of these two potentials is the mV-reading which will be used to determine the sample fluoride concentration from the calibration graph.

The calibration graph is prepared using the above procedure on the standard solutions, which should be analysed in ascending order of fluoride concentration. It is not necessary to leave the standards to decomplex. Plot the calibration graph on semi-logarithmic graph paper with electrode potential (mV) on the linear scale and fluoride concentration (mg/kg) on the logarithmic scale. This should be linear to ~ 0.1mg/kg F with a detection limit of ~0.02mg/kg F for a new electrode, and show a difference of ~58mv per decade change in concentration. The calibration graph will depart from linearity at higher concentrations, and the detection limit will be raised, as the electrode ages.

Notes: All solutions should be stored in screw-top plastic bottles pre-soaked for one day in a 5% solution of Decon 90, and for a further day in dilute nitric acid. To reduce electrode drift, laboratory illumination should be constant at least one hour prior to, and during, the analysis. Sample and standard solutions should be analysed at the same temperature, and this should be fixed through the analysis (±0.5°C and preferably ±0.1°C). Insulate the magnetic stirrer from the beaker to prevent heat transfer to the solution. Geothermal waters containing exceptionally high levels of boron (>500 mg/kg), iron or aluminium (>35 mg/kg) may require pre-treatment, such as solvent extraction, to remove these species prior to analysis.

Reference: Nicholson (1983), Nicholson and Duff (1981a,b,c)

Hydrogen sulphide (H_2S) **VOL**

Samples for sulphide analysis must be collected specifically for this determination (see above) and should be analysed in the field laboratory, or within 24 hours of collection at most.

Procedure

Principle: This iodimetric titration is based on the reaction of hydrogen sulphide with iodine

$$H_2S + I_2 = 2H^+ + 2I^- + S$$

The excess iodine is then titrated with thiosulphate.

Reagents: 0.01N iodine solution, 0.01N sodium thiosulphate solution (prepare these fresh by dilution of 0.1N I_2 and 0.1N $Na_2S_2O_3$ stock solutions), 1M sulphuric acid, 5000 mg/L sodium starch glycollate solution.

Method: Place 20 mL 0.01N iodine solution in a conical flask and add 20mL 1M sulphuric acid. Add 100mL of the sample *to* the acidified iodine sample, not conversely. If the solution becomes pale, add a further 10mL of iodine solution.

Titrate with the thiosulphate solution using the starch solution as indicator. Record the volumes (mL) of iodine and thiosulphate solutions used and calculate the hydrogen sulphide concentration (mg/kg) from:

$$[H_2S] = [170(V_{I_2} - V_{Na_2S_2O_3}/100] - \text{Blank}$$

The blank titration is carried out using the above procedure on a degassed aliquot of the sample water. The blank aliquot is first acidified with hydrochloric acid, and the H_2S then removed by bubbling air through the sample.

Notes: Sulphide can also be determined using a silver/sulphide ion selective electrode, or colourimetrically. Calibration methods also have the difficulty of preparation and storage of reliable sulphide standard solutions. These can be prepared using sodium sulphite crystals, although oxygen contamination and the development of other sulphide species will occur and be a source of error. The solutions will rapidly deteriorate on storage (hours). Alternatively, standards can be prepared by bubbling hydrogen sulphide gas from a cylinder into distiled, deoxygenated water to produce a saturated solution about 0.1 molal in hydrogen sulphide. This can be standardised to determine the precise concentration. If kept under nitrogen these solutions can be stored for several months.

References: APHA (1989, 1991), Giggenbach and Goguel (1989), Webster (1989).

Iodide (I^-) **VOL**

Bromide (Br^-)

Ion chromatography is probably the best technique to determine these halides which are usually at low concentrations in geothermal waters. In the absence of such equipment the following titrimetric method can be used.

Procedure

Principle: Iodide is oxidised to iodate, KI is added after removal of excess bromide, and the iodine is liberated for titration. On a second aliquot bromide is retained and oxidised to bromate, while iodide is oxidised to iodate on addition of hypochlorite. Both are powerful oxidising agents and liberate iodine from KI. The iodine is titrated and the concentration of bromide determined by difference.

Reagents: 1:4 sulphuric acid; 273g sodium acetate in 1kg deionised water; 1:8 acetic acid; saturated bromine water; 50g sodium formate dissolved in hot water and diluted to 100mL with deionised water; potassium fluoride crystals; sodium chloride crystals (free from Br and I); 1:2 hydrochloric acid; calcium carbonate powder; potassium iodide crystals (free from iodate: test by dissolving a few crystals in water, acidify

with sulphuric acid and add starch solution, a blue colour indicates the presence of iodate); potassium hypochlorite solution prepared by dissolving 15.5g KOH in 250mL of deionised water and passing 8.75g chlorine from a cylinder with solution standing in an ice bath; 1g sodium molybdate in 100mL deionised water; standardised 0.01N sodium thiosulphate solution; starch and methyl red indicators.

Method: Solution A: Place 100mL of sample into a 250mL conical flask containing a drop of methyl red indicator. Acidify with the sulphuric acid, add 15mL sodium acetate, 5mL acetic acid and just sufficient bromine water to impart a yellow colour to the solution. Leave for 5 minutes. Add sodium formate until the yellow colour disappears, then add an additional 1mL of the formate solution.

Solution B: Place 100mL of sample into a 250mL conical flask and add sufficient sodium chloride to yield an overall chloride concentration of 30,000 mg/kg (3g/100mL). Add a drop of methyl red and neutralise the solution with the hydrochloric acid. Add 10mL potassium hypochlorite, 0.5mL hydrochloric acid and excess calcium carbonate. Heat to boiling and keep hot for eight minutes on a water bath. Add 2mL sodium formate and heat for a further eight minutes. Cool and add several drops of sodium molybdate solution.

In both Solutions A and B add 1g potassium iodide crystals and add 10mL sulphuric acid. Leave in the dark for five minutes and for each solution titrate the liberated iodine with 0.01N thiosulphate using starch as indicator. Ignore the return of the blue colour beyond the end-point. Record the volume of thiosulphate used for each solution (V_A, V_B)

$$I\ (mg/kg) = 211.5 \times V_A \times N_{thiosulphate}$$

$$Br\ (mg/kg) = 13320\ (0.01V_B - 0.01V_A) \times N_{thiosulphate}$$

Notes: Iron, manganese and organic matter interfere with the determination, and this should be removed prior to analysis by shaking 150mL of the sample with an excess of anhydrous calcium oxide. The sample should then be filtered and discarde the first 25mL of filtrate. Any iron precipitates which form at the final stage in solutions A or B should be removed by the addition of 0.5g potassium fluoride.

Reference: Ellis et al. (1968)

Iron (Fe) **AAS**

Samples should be filtered and acidified on collection to avoid precipitation of iron oxides on particulate matter, and to keep iron in solution.

Procedure

Stock standard solution (1000 mg/kg Fe): 1g iron metal in 20mL 5M hydrochloric acid and 5mL concentrated nitric acid, dilute to 1kg with deionised water.

Working standard solutions: Successively dilute the stock solution with deionised water to prepare working standards with concentrations of 200, 100, 10, 5, 1 mg/kg.

AAS operating conditions: Hollow cathode lamp, wavelength 248.3nm (Fe<5 mg/kg) or 371nm (Fe>5 mg/kg), bandpass 0.2-0.3nm, nitrous oxide-acetylene + argon (~1L/min) flame.

Method: Analyse the working standard solutions and plot a calibration graph of absorbance against concentration. Analyse the samples and determine the concentration from the calibration graph.

Reference: Giggenbach and Goguel (1989)

Lithium (Li) **AAS**

Although flame emission can be effectively used for Li, but the complexity of the calibration graph has made AAS the preferred method.

Procedure

Stock standard solution (100 mg/kg Li): 0.532g dry Li_2CO_3, add dropwise the minimum quantity of 1:1 hydrochloric acid required to dissolve the carbonate, dilute to 1kg with deionised water.

Working standard solutions: Prepare 25, 10, 5, 2.5, 0.5 mg/kg Li working standards by successive dilution of the stock with a Na-K matrix-matching solution containing 1000mg/kg Na and 100 mg/kg K.

AAS operating conditions: Hollow cathode lamp, wavelength 670.8nm, bandpass 0.50nm, air-acetylene flame.

Method: Analyse the working standard solutions and plot a calibration graph of absorbance against concentration, this is linear to about 2mg/kg. Analyse the samples and determine the concentration from the calibration graph.

Notes: Flame ionization effects are negligible in the air-acetylene flame, but chemical interference can be significant. This can be reduced by dilution of samples to Li<2mg/kg.

Reference: Giggenbach and Goguel (1989); Patterson (1980).

Magnesium (Mg) **AAS**

Procedure

Stock standard solution (1000 mg/kg Mg): 1.000g Mg ribbon in 50mL of 1:1 hydrochloric acid, dilute to 1kg with deionised water.

Working standard solutions: Prepare 20, 10, 5, 2.5, 1.0 0.5 mg/kg Mg working standards by successive dilution of the stock with a Na-K matrix-matching solution containing 1000mg/kg Na and 100 mg/kg K.

AAS operating conditions: Hollow cathode lamp, wavelength 285.2nm, bandpass 0.20 to 0.50nm, nitrous oxide-acetylene + argon (~1L/min), fuel-lean flame with 5mm high red zone, sample height 12 - 16mm above burner.

Method: Create the calibrate graph with the 0.5, 1.0, 2.5 mg/kg solutions and then analyse the samples. Samples with Mg>2mg/kg should be re-run with a 90° rotated burner with calibration using the higher standards (5-20mg/kg). Samples with Mg>20mg/kg should be diluted.

Notes: Sample height reduced interference from Al, Ca, SiO_2. With very low Mg concentrations (<0.01mg/kg) an AAS method using the air-actylene flame with strontium nitrate addition can be used. Alternatively, the samples can be analysed by ICP-AES with detection limits around 0.001mg/kg.

Reference: Giggenbach and Goguel (1989).

Mercury (Hg) **AAS**

Sampling waters for quantitative mercury analysis requires specialised techniques which are described in Section 6.3.

Procedure

Principle: Mercury (II) ions are reduced to elemental mercury vapour by stannous chloride in a reaction vessel, often a Dreschel bottle. This vapour is swept into the light path of the spectrophotometer by a stream of air or nitrogen and the absorbance of mercury measured. The signal is output to a chart recorder and the peak area of the absorbance peak is calculated.

Stock standard solution (1000 mg/kg Hg): 1.354g $HgCl_2$ in 1kg deionised water, store in a refrigerator.

Working standard solutions: 5, 2, 1, 0.5, 0.1 mg/kg prepared by successive dilution of the stock standard with deionised water, store in a refrigerator.

AAS operating conditions: Hollow cathode lamp, wavelength 253.7nm,

Reagents: 2% stannous chloride in hydrochloric acid (add 20.0g stannous chloride to 40mL 1:1 hydrochloric acid, dilute to approximately 100mL with deionised water, transfer to a 1L volumetric flask, add 5mL concentrated sulphuric acid and dilute to the mark with deionised water); concentrated nitric acid.
Method: Place 75mL of sample/standard solution into the Dreschel bottle and add 10.0mL 2% stanous chloride solution. Shake vigourously for two minutes then attach the bottle to the spectrophotometer air-line. Wait 15 seconds then open the tap to transport the vapour into the light path. Record the peak on the chart recorder. Flush the system with air prior to analysing the next sample. Prepare a calibration graph of peak area against mercury concentration.
Notes: A drying tube containing either glass wool or magnesium perchlorate removes aerosol droplets, which would interfere with the absorbance, from the mercury vapour before it enters the light path. This method is very sensitive to mercury and 0.0001 mg/kg Hg can be determined; it assumes that all the mercury is in an inorganic form. If other forms of mercury are present, these can be converted into the inorganic form by oxidation with potassium permanganate (DoE/NWC, 1978). To avoid excessive mercury concentrations in the "blank" solutions, research-grade chemicals should be used where possible, and all glassware should be acid washed. Ideally all apparatus, including the AAS set up, should be reserved only for mercury determinations.
Reference: DoE/NWC (1978).

pH **COL/ISE**

The pH of a sample should be recorded in the field at the temperature of the discharge ($pH_{t°C}$) and in the laboratory after cooling.

COL procedure

There are many different pH-indicator solutions which find common usage in volumetric procedures (Vogel, 1990) but these are of little use for the precise determination of the pH of a geothermal fluid. Papers which when immersed into the water display different pH-sensitive colours are a rapid method of determining solution acidity. The most appropriate are narrow-range papers which typically cover 2-3 pH-units in 0.1-0.2 increments. Although these lack the resolution of a pH-electrode (which can determine pH to 0.01 units) the simplicity of measurement and convenience ensures this remains a popular method of pH determination ideally suited to reconnaissance surveys.

Method: Immerse the paper in the water, ensuring all the graduated scale (if present) on the paper is covered. Align the paper colour to the calibrated scale to determine the pH.

ISE procedure

Several models of pH electrode and portable meters are available, but not all are suitable for geothermal water analysis. Ensure that the chosen electrode is capable of operating at temperatures up to 100°C and that there is automatic temperature compensation built into the electrode-meter system. A combination electrode is more convenient than a system with separate pH and reference electrodes. The Orion Ross pH electrode range is well suited to the analysis of geothermal waters. It has a rapid response time and minimal drift due to temperature differences, thereby reducing the need for regular recalibrations.

Method: Calibrate the electrode in pH 4.00 and pH 9.00 buffer solutions and perform regular calibration checks throughout the day as demanded by the drift characteristics of the electrode-meter system. Place the electrode into the water sample and leave until thermal equilibrium is established. The time for this to occur depends upon the electrode system, but can take several minutes. Record the pH to 0.01 pH-units together with the temperature of the water.

Potassium (K) **F-AES**

Procedure

Stock standard solution (1000 mg/kg K): 1.907g dry KCl in 1kg deionised water.

Working standard solutions: Dilute stock with 0.1M NaOH or using a 1000mg/kgNa-100mg/kgK matrix-matching solution to prepare working standard concentrations (typically, 200, 100, 50, 10, 5, 1 mg/kg).

AAS operating conditions: flame emission mode, wavelength 769.9nm, bandpass 1.0nm, air-acetylene, fuel-lean flame, 5mm mask.

Method: Ionization is significant and buffering by sodium at ten times the potassium concentration is needed. This can be achieved either by a 1:10 dilution of the sample with 0.1M NaOH, or by the naturally high sodium content of the geothermal fluid. In this latter case, the standards must be matrix-matched. Analyse the working standard solutions and plot a calibration graph of emission against concentration. This is not linear above 0.5mg/kg, however at higher concentrations a linear calibration graph can be obtained by plotting emission against √K-concentration. Analyse the samples and determine the concentration from the calibration graph.

Notes: A red-sensitive photomultiplier tube should be used or a filter to remove light from the 589nm Na line must be in place. For very high K concentrations and undiluted geothermal waters a less sensitive line with the following conditions can be used: 404.7nm (less intense line of doublet), bandpass 0.07nm, air-acetylene flame. Response is linear to 200mg/kg K but suffers from reduced precision at K<20mg/kg. Spectral interferences are minimal.
Reference: Giggenbach and Goguel (1989).

Rubidium (Rb) **F-AES**

Procedure
Stock standard solution (100 mg/kg Rb): 0.1415g dry RbCl in 1kg deionised water.
Working standard solutions: Prepare 2.5, 1.0, 0.5 mg/kg working standards by successive dilution of the stock with a Na-K matrix-matching solution containing 1000mg/kg Na and 100 mg/kg K.
AAS operating conditions: flame emission mode, wavelength 794.8nm, bandpass 0.14nm, air-acetylene flame.
Method: Ionization suppression by potassium is required, and is achieved using matrix-matched standards and the typical potassium concentrations in geothermal waters; otherwise potassium must be added to give a concentration of 1000mg/kg in solution. Analyse the working standard solutions and plot a calibration graph of emission against concentration. Analyse the samples and determine the concentration from the calibration graph.
Notes: Interference by potassium emission is reduced using the narrow bandpass, alternatively background correction measurements would have to be made. Contamination from Rb in potassium salts is common and may require correction.
Reference: Giggenbach and Goguel (1989).

Silica (SiO_2) **COL/AAS**

To preserve silica in solution samples should be filtered on collection and either acidified or diluted to bring SiO2<300mg/kg. Silica can be determined by colourimetric and AAS methods. Both are effective, although better precision and accuracy have been reported for the colourimetric method. However, samples analysed colourimetrically require some pretreatment to ensure total silica is determined to prevent polymerisation and precipitation on storage.

COL procedure

Principle: The method is based on the reaction of monomeric silica and molybdate at pH~1 to form a yellow silico-molybdate complex which absorbs at 410nm. The complex is not stable however, and will start to beakdown within an hour. For a total silica determination, any polymeric species must be broken down using an alkaline digestion. Iron (III) chloride and the molybdophosphate complex interfere by absobing at 410nm, and must be removed by the addition of oxalic acid.

Reagents: 100g/L ammonium molybdate, 1M sodium hydroxide, 75g/L oxalic acid, 0.5M HCl.

Stock standard solution (1000 mg/kg SiO_2): 4.73g of sodium meta-silicate ($Na_2SiO_3.9H_2O$) in 1kg deionised water. Alternatively, fuse 1.000g SiO_2 with 5g Na_2CO_3 in a pre-weighed platinum crucible with lid at 850°C in a muffle furnace. Place the hot crucible into a pre-weighed beaker with 50mL deionised water, warm and stir to dissolve. Add deionised water to 1kg.

Working standard solutions: Prepare 200, 150, 100, 50, 20mg/kg SiO_2 solutions by successive dilution of the stock standard.

Method: Alkaline digestion: add an aliquot (1-5mL) of standard or sample solution containing up to 1mg SiO_2 to a platinum crucible containing 5mL deionised water; add 0.5mL of 1M NaOH and heat for 10 minutes over a boiling water bath, cool. Place sample in a 50mL volumetric flask containing 10mL 0.5M HCl. Wash the crucible and add the washings to the flask to make up to ~40mL. Add 5mL of the ammonium molybdenate solution, shake and leave for 15 minutes. Add 2mL of oxalic acid, make up to the mark and read the absorbance at 410nm within 10 minutes. A calibration graph is prepared using the same procedure carried out on blanks and standard solutions.

Notes: Acidification of the sample in the field may not be sufficient to ensure reliable results, and a 10-fold dilution has been recommended. For geothermal waters with low iron and phosphate contents, the oxalic acid may be omitted. This also preserves the stabilily of the yellow colour, since oxalic acid aids the breakdown of the silico-molybdate complex.

Reference: Chemerys (1983), Giggenbach and Goguel (1989).

AAS procedure

Stock standard solution (2000 mg/kg SiO2): See above.

Working standard solutions: Prepare 500, 200, 100, 50, 10mg/kg SiO_2 solutions by successive dilution of the stock standard.

AAS operating conditions: Hollow cathode lamp (50mm diameter ideal), wavelength 251.6nm (SiO_2<200mg/kg) or 252.4nm (SiO_2>200mg/kg), bandpass 0.20nm, nitrous oxide-acetylene, fuel-rich flame with 50mm high red zone.

Method: Analyse the working standard solutions and plot a calibration graph of absorbance against concentration; this should be linear to about 200 mg/kg, above which the less sensitive line can be employed. Analyse the samples and determine the concentration from the calibration graph.

Notes: AAS is a reliable method for determining high silica concentrations (>200mg/kg) as it is not affected by the form of silica in solution. Greater precision and accuracy are reportedly achieved by shaking the samples for 30 minutes prior to analysis. Instrument and flame stability are essential. Frequent wavelength readjustments should be made, and a clean burner used.

Reference: Chemerys (1983), Giggenbach and Goguel (1989).

Sodium (Na) **F-AES**

Procedure

Stock standard solution (10 000 mg/kg Na): 25.421g dry NaCl in 1kg deionised water.

Working standard solutions: Successively dilute the stock solution with deionised water to prepare working standards of 2000, 1000, 100, 50, 10, 1 mg/kg.

AAS operating conditions: Flame emission mode, wavelength 819.5nm (most intense line of doublet), bandpass 0.14nm, air-acetylene flame. Low Na concentrations (<200mg/kg): wavelength 589.0-589.6nm doublet, bandpass 3-5nm, air-acetylene flame, 5mm mask.

Method: Analyse the working standard solutions and plot a calibration graph of absorbance against concentration; this should be linear to 2000 mg/kg. Analyse the samples and determine the concentration from the calibration graph. Using the low-Na conditions, the calibration graph is not linear.

The use of separate conditions for low-Na samples is necessary to eliminate spectral interferences which become significant when Na concentrations are <200mg/kg.

Reference: Giggenbach and Goguel (1989).

Sulphate (SO_4) **COL**

Any sulphide present in solution should be removed to prevent oxidation to sulphate. It is unlikely that this will be a problem with spring samples, but could

cause difficulties with well discharges low in sulphate but with appreciable dissolved hydrogen sulphide. Removal of sulphide is achieved by immediately acidifying the sample to pH<3 with a measured volume of 1:1 nitric acid and passing oxygen-free nitrogen through the sample. The dilution factor caused by the addition of the acid should be noted and the final determination corrected for this. It may be necessary to collect a separate 100mL sample for sulphate determination.

Procedure

Principle: A colourimetric technique, the method depends on the reaction of sulphate with barium chromate to precipitate barium sulphate, leaving chromate ions in solution which are then determined.

Reagents: Chromate suspension: 2.5g barium chromate in 10mL 1M HCl and 3mL glacial acetic acid diluted to 100mL; ammonia-calcium solution: 0.25g calcium carbonate in a minimum of 1M HCl until dissolved, boil to remove carbon dioxide, add 45mL concentrated ammonia solution, dilute to 100mL; 95% ethanol.

Stock standard solution (1000 mg/kg SO_4): 1.841g dry potassium sulphate in 1kg deionised water.

Working standard solutions: 200, 100, 50, 25mg/kg SO_4 prepared by successive dilution of the stock standard.

Method: Place 5mL aliquots of the sample into a 25mL volumetric flask containing 2mL of the chromate suspension. Shake, leave for several minutes then add 0.5mL of the ammonia-calcium solution. Shake and leave for several minutes before adding 10mL of ethanol. Shake, make up to the mark with deionised water, stopper and leave overnight for the particles to settle. Read the absorbance at 380nm. Blanks and standard solutions are analysed in the same manner and used to construct a calibration graph.

Notes: Avoid any sediment entering the spectrophotometric cells by using a dropper to remove the solutions from the volumetric flasks. Samples containing SO_4>250mg/kg should be diluted. Use 10mL aliquots for waters with SO_4<20mg/kg. If sulphate concentrations are very low (<~5mg/kg) the above method not be sufficiently sensitive and ion chromatography will have to be used. At such low concentrations, all traces of sulphide must be removed from the sample before it oxidises.

An alternative method where sulphate is gravimetrically determined after precipitation as barium sulphate is described by Vogel (1990).

Reference: Ellis et al. (1968), Giggenbach and Goguel (1989), Iwasaki et al. (1957).

Sulphide (S^{2-}) See *hydrogen sulphide*

Total Dissolved Solids (TDS) **GRAV**

This gives an indication of the salinity of the solution. It is not a quantitative measurement as volatile compounds, notably bicarbonate for geothermal waters, may be lost during the procedure. The quantity of dissolved solids can also be calculated by summing the concentrations (mg/kg) of the solutes. The determined and calculated values can be compared to obtain a mass balance evaluation of data quality (see below).

Procedure

A precisely measured mass of water, typically about 100.00g) is placed into a pre-weighed evaporating basin. The sample is evaporated to dryness and weighed. Place the sample into an oven at 110°C for two hours, then weigh. Repeatedly heat and weight the sample every 30 minutes until no further weight loss occurs. Record the dry weight of the sample as the TDS.

If desired the ash content of the sample can be determined by then placing the evaporating basin into a muffle furnace at 500-600°C. The sample is ignited for 30-60 minutes and then weighed. Repeat until a constant weight is obtained.

Reference: APHA (1989, 1991).

6.5 DATA QUALITY AND PRESENTATION

Quality control checks

The quality of the analyses should be regularly checked. If the analyses are performed in-house then this can be achieved by good laboratory practise, ensuring reliable standards and regular calibration checks together with the use of an in-house internal quality control solution. This solution is usually a bulk geothermal water sample which has been analysed regularly and whose composition is well known.

When using a commercial laboratory the geochemistry does not have direct control on the laboratory procedures or data quality, and this has to be determined independently. Problems can be avoided through good communication between the geothermal geochemist and the laboratory analytical chemist. Nonetheless, independent verification of data quality is essential and it should be common practise

to include the following quality-control solutions in a batch of samples sent for analysis.

Blanks: These are "samples" of deionised water which have been stored and treated (eg. filtered, acidified) in exactly the same way as the samples of geothermal water. This helps identify any source contamination through these treatments. They also help in identifying poor laboratory procedures such as solution carry-over from the previous sample.

Controls: These are solutions whose composition is well known. They can be made up from standard solutions or, more commonly are aliquots of a bulk geothermal water sample kept specifically for this purpose. These help recognise systematic errors in the batch of analyses.

Replicates: More than one aliquot of a few samples should be included in the batch. This enables poor precision and random errors to be recognised, and provides a reflection on the quality of the analytical techniques of the laboratory.

Blank, control and replicate solutions should form a significant proportion of the batch of samples sent for analysis, so that every fifth or tenth sample analyses should be a quality-control solution. Naturally, which solutions are geothermal samples and which are quality-control solutions should not be revealed to the commercial laboratory.

Ionic balance

The ionic balance, also known as the charge balance, of a solution is used as a check on the completeness and accuracy of an analysis of a geothermal fluid. It is not infallible however, since it only takes into account charged species. Errors in the analyses of uncharged species such as silica, boron and ammonia, for example, will not be indicated by the ionic balance. Furthermore, the method is also insensitive to errors in determinations of the minor or trace species. Nonetheless, it is a useful check on gross errors (analytical or transcription) in the analysis as a whole, but principally of the major charged species (Na, K, Cl, SO_4, HCO_3).

It is calculated by converting the concentration of all charged species from mg/kg to meq (see below), and summing the milliequivalents for both anions and cations. As a charged solution cannot exist in nature,

$$\Sigma\text{anions (meq)} = \Sigma\text{cations (meq)}.$$

There will be some slight variations in the balance, but the difference should not be greater than 5%. Calculate from either of the expressions:

$$[2(\Sigma\text{anions} - \Sigma\text{cations}) / (\Sigma\text{anions} + \Sigma\text{cations})]$$

or

$$\Sigma\text{anions}/\Sigma\text{cations}$$

Mass balance

Although not commonly determined the mass balance can provide a check on the completeness and quality of the major ion analyses. It is calculated by comparing the determined TDS values with the sum of the concentrations of the dissolved species. Like the ionic balance, the mass balance is dominated by th major constituent and will not show errors in the analysis of minor components. Furthermore, as volatiles are lost in the drying phase of TDS determinations, this test is unreliable for fluids with a high bicarbonate content. Calculate from:

$$\text{TDS (mg/kg)} / \Sigma \text{ solute concentrations (mg/kg)}$$

Units

The concentration of constituents dissolved in a geothermal fluid can be expressed in a number of ways. Chemists dealing with surface waters at ambient temperatures use moles/L and mg/L. As will be shown, these units are of little use when dealing with waters of varying temperatures and different salinities as they do not readily enable comparisons of solute concentrations to be made between, or across, geothermal fields. Geothermal chemists should use mg/kg units for general purposes and moles/kg for thermodynamic calculations. To help explain these differences, consider the definitions of units shown in the box.

mg/L, mg/kg, ppm

These units often appear to be used inter-changeably, as if they are just different ways of expressing the same thing. As you can see from the definitions, there are distinct differences between the units, it is just that these differences are minimal for dilute solutions at, or near, STP conditions (standard temperature and pressure) and water chemists can be more casual in their transfer between units. To understand this examine the following statements in conjunction with the unit definitions.

Solute concentration units
mg/L: milligrammes of solute per litre of solvent
mg/kg: milligrammes of solute per kilogramme of solvent
ppm: parts by weight of solute per one million parts by weight of solution (solvent plus solutes)
moles/L (mol/L), molarity (M): the number of moles of solute per litre of solvent
moles/kg (mol/kg), molality (m): the number of moles of solute per kilogramme of solvent
meq, milliequivalents: millimoles of positive or negative charge per kilogramme of solvent
Note that the solvent is usually water.

(i) For *dilute* solutions

$$\text{mass of solutes} << \text{mass of solvent}$$

therefore

$$\text{mass of solution} \sim \text{mass of solvent}$$

and

$$\text{ppm} \sim \text{mg/kg}$$

(ii) The density of the solvent = mass of the solvent (kg) / volume of the solvent (L), so

$$\text{mg/L} \times (1/\text{solvent density}) = \text{mg/kg}$$

But *at STP* the density of pure water = 1kg/L (by definition). As noted, water is the solvent here and therefore

$$\text{mg/L} \sim \text{mg/kg}$$

for a *dilute solution at STP*

$$\text{ppm} \sim \text{mg/L} \sim \text{mg/kg}$$

However, geothermal fluids are not always dilute and can have different salinities. So the mass of the solutes may make a significant contribution to the mass of the solution, in which case

$$\text{mass of solution} \neq \text{mass of solvent}$$

and ppm cannot be equated with mg/kg

$$\text{ppm} \neq \text{mg/kg}$$

Furthermore, as geothermal fluids are not at STP then the density and volume of water will no longer be unity, so

$$\text{mg/L} \neq \text{mg/kg}$$

for a *geothermal fluid*
ppm ≠ mg/L ≠ mg/kg

Summary: To enable solute concentrations to be comparable between well and spring discharges, and between different geothermal fields a unit which is unaffected by differences in temperature and salinity is needed. Variations in temperature negate the use of *mg/L*, and differences in salinity make *ppm* inappropriate. However, comparisons based on the mass of the solute and the mass of the solvent are not influenced by temperature or salinity variations and *mg/kg* should be the chosen unit for geothermal fluid chemistry.

Molarity, molality

As illustrated in the definitions, there are parallels between molarity (moles/L) and molality (moles/kg), and mg/L and mg/kg. Although molarity is commonly used in routine laboratory work, it is a volume-based, temperature-dependent unit and is therefore not suited to geothermal fluid analysis. Molality, like mg/kg, is not affected by temperature or salinity and is therefore used for equilibrium calculations. Note that moles/L or moles/kg are often abbreviated to mol/L and mol/kg, and that solute concentrations are described as molar or molal.

Milliequivalents

Equivalents (eq) and milliequivalents (meq) are less useful units than mg/kg or moles/kg. They measure the quantity of positively or negatively charged species in solution, and are mainly used in geothermal studies in the ionic balance of an analysis (see above). The concentration of the species is expressed in millimoles and

multiplied by the charge on the ion to obtain the number of milliequivalents. Equivalents are similarly calculated but using molar rather than millimolar concentrations.

Conversion of units

Methods to convert between units are summarised in the box. These expressions hold for most dilute geothermal solutions and introduce only small errors when dealing with saline solutions such as seawater. It should be noted however, that for the exact conversion of mg/kg or mg/L to molality additional terms (in **bold**) need to be added to the right hand side of the equations:

Unit conversions

ppm - mg/kg	mg/kg = ppm / (1 - TDS)*
mg/L - mg/kg	mg/kg = mg/L / (solvent density)
mg/kg - molality	mole/kg = mg/kg x 10^{-3} / formula wt.**
mg/L - molarity	mole/L = mg/L x 10^{-3} / formula wt.**
millimoles - moles	moles = millimoles x 10^3
mg/kg - meq	meq = [(mg/kg) / atomic wt.] x charge
meq - eq	equivalents = meq x 10^3

Notes

* TDS = weight of the total dissolved solids in solution in kg. Calculate by summing the concentrations of all species in solution.

** formula wt. = atomic weight for elements or the molecular weight for compounds (Appendix 2). See text for additional terms for exact conversions.

$$\text{mole/kg} = (\text{mg/kg} \times 10^{-3} / \text{formula wt.}) \times \mathbf{10^3 / (10^3 - [\Sigma mg/kg / 10^3])}$$

$$\text{mole/L} = (\text{mg/L} \times 10^{-3} / \text{formula wt.}) \times \mathbf{10^3\, V / (10^3 - [V\, \Sigma mg/L / 10^3])}$$

where

Σmg/kg and Σmg/L = the sum of the concentrations of all dissolved constituents in mg/kg or mg/L respectively

V = specific volume of the solution

Since in geothermal are often dilute, with salinities less than that of seawater, the terms in bold approach unity and can be neglected.

Tabulation of results

Good reporting practice

Given the cost of obtaining the samples and the analytical data, it is essential that this information is presented clearly, in full and without ambiguity. Unfortunately data presented in tables, even in published works, are often incomplete or poorly presented with inadequate explanation of symbols or abbreviations. Particular examples of common bad practice include:

Blank spaces in the table: These encourage transcription errors and it is often not clear whether blanks refer to a result below the detection limit, or simply the lack of a determination.

Ambiguous use of the abbreviation "nd": This is used for both "not determined" and "not detected", and the reader is commonly left to decide which.

Significant figures: Results are reported to significant figures which exceed the accuracy or precision of the analytical method. Indiscriminate use of spreadsheet programs with a two-figure decimal place default is a common source of this error.

It is however, easy to present data which can be clearly read without ambiguity. The following practices are recommended.

- the absence of a determination is indicated by a dash "-" in the column.
- a result below the detection limit of the technique is shown by "< dl" where "dl" represents the value of the detection limit for the analytical method (eg. < 1 mg/kg).
- the units of measurement for each determinand are stated.
- all abbreviations used in the table are explained either in the caption or as notes at the base of the table.
- the temperature (t°C) at which the pH was determined is clearly stated by the notation $pH_{t°C}$.
- all decimal figures are preceded by a zero to prevent transcription errors (eg. 0.43).

- results are reported to the number of significant figures which reflect the accuracy/precision of the determination, and this number remains consistent across the table for a given determinand.

Data presentation

It is useful to standardise on the data included in the table, and even the format of the presentation. Although the order of presentation of the determinations is not crucial, it is helpful to present the information in the following order: descriptive details, physical determinations, cation analyses, uncharged species determinations, anion analyses. The data recorded for spring/pool and well discharges would typically be as follows.

Springs/pools: geothermal field, spring/pool name/number, date/time, flow rate (L/s), t°C, $pH_{t°C}$, Na, K, Mg, Ca, B, SiO_2, NH_3, SO_4, HCO_3, Cl.

Wells: geothermal field, well number, date/time, H, separation pressure (bg), $pH_{t°C}$, Na, K, Mg, Ca, B, SiO_2, NH_3, SO_4, HCO_3, Cl.

Concentrations are expressed in mg/kg
H = discharge enthalpy (kJ/kg)
bg = bars gauge, add 1 bar to obtain the pressure in bars absolute (ba) for use in the steam tables

The above details only show analyses for the major components in geothermal water, but note that cations are reported following the Periodic Table in Group-Period order, so any minor species added later can follow this order; eg. Li would be placed before Na and Fe after Ca. The same rule would apply to reporting of additional halogens, with F before Cl and Br after Cl.

CHAPTER 7

GAS SURVEYS

7.1 PRE-FIELD LABORATORY PREPARATION

Sample flasks

An effective sealing valve is essential for any vessel used in gas sampling, as air contamination must be avoided. Hirabayashi (1986) describes a simple arrangement for gas sampling using a double-mouthed syringe. The simplicity of the equipment is attractive, but no details regarding the seals are provided and it appears that the mouth of the syringe is sealed by a screw clip; the preservation of sample integrity must be a concern with such apparatus. Giggenbach (1975) described a 300mL-volume cylindrical, round-bottom glass flask equipped with a Quickfit Rotaflo teflon stopcock. This valve is resistant to attack by acid gases, and preserves the seal despite large temperature variations during sample collection and storage.

Flask cleaning and preparation

Flasks should be cleaned with Decon 90 and deionised water using the procedure outlined in Section 6.1; an acid wash is not necessary.

The precise volume of each flask is calculated from the weight (to 0.1g) of the bottle when empty, and the weight when filled with deionised water. The flasks are labelled and the volume recorded or etched onto the flask. The flasks are then partially evacuated using an oil pump to aid the addition of sodium hydroxide solution.

A precisely known volume of carbon dioxide-free sodium hydroxide is added to the clean flasks to absorb the acid gases in the discharge. The concentration and volume of sodium hydroxide added depends on the gas composition of the discharge and the size of the collection vessel. However, for the 300mL flasks 50mL of 5M NaOH is usually adequate.

The flasks are then evacuated and weighed to 0.1g.

Preparation of CO_2 -free NaOH: The hydroxide solution should be free from dissolved carbon dioxide, and this can be readily prepared by dissolving 200g NaOH

in 400mL of freshly deionised water. Keep covered and allow to cool, some sodium carbonate may precipitate. Quantitatively transfer to a 1L volumetric flask and dilute with fresh deionised water (Giggenbach and Goguel, 1989).

Sampling equipment

In addition to the sample flasks described above, sample tubes are required to transfer the gases to the flask. These should not react with the gases, both to avoid contamination of the sample and to preserve the life of the equipment. Tubes, connectors and funnels (or domes) constructed of stainless steel or titanium are recommended although butyl rubber can be used for connectors (Finlayson, 1970; Giggenbach, 1975; Giggenbach and Goguel, 1989; Klyen, 1982).

Gas Sampling Equipment Checklist
300mL glass flasks with Rotaflo valve
sampling tubes, funnels, connectors
maximum thermometers
pole with clamp
large volume of water to cool flasks
thick rubber gloves
teflon tape
additionally for pipelines and wells
Webre separator
Klyen downhole sampler
general equipment
towel
waterproof marker pen
notebook, pens, pencils, tape measure
maps, aerial photographs, compass,
camera with spare film and batteries
first-aid kit

7.2 FIELD SURVEY

Mapping techniques and field notes applicable to geothermal field surveys have been discussed in Section 6.2, and these are similarly adopted for surveys of fumaroles and steaming ground.

Selection and prioritizing fumaroles for sampling

High temperature vents with a large, audible, flow rate are the ideal fumaroles for sampling. These are given first priority, with lesser discharges ranked on the basis of mass discharge and temperature. Steaming ground and gentle or weakly discharging vents are likely to be air-contaminated, and are only sampled if no other features are available.

7.3 SAMPLING METHODS

Fumaroles

Two techniques can be adopted: tubes can be inserted into the vent as far as possible, or a funnel with tubes attached can be placed over the fumarole. If the latter is used then the funnel should be stamped firmly into the ground and covered with soil. Whichever method is used, the vents should be permitted to discharge for several minutes to purge the tubes of air and to warm them to reduce condensation.

The flask is then attached to the tubes and the stopcock slowly opened to produce a rapid but steady flow. The bottles are held valve-downwards to permit the gases to flow through the hydroxide solution to absorb the acid gases. Swirling the flask and cooling it with water during sample collection aids condensation of the steam and absorption of the gases by the hydroxide. As the pressure within the flask approaches atmospheric, the flow of gases into the flask will slow. Sampling should cease when the bubbling stops or when the condensate fills about 90% of the bottle. The volume of condensate collected will depend on the concentration of the non-absorbed gases. With a fumarole of large flow rate, sampling will be complete in 10-15 minutes. The stopcock should be closed and retighted again after the bottle has cooled.

The bottle, already numbered from weighing in the laboratory, should be labelled and stored upright for transport.

In the laboratory, prior to analysis, the bottles are weighed once again to 0.1g.

If analyses for silica, boron, fluoride and ammonia are required, an additional sample is taken in a flask which has been evacuated but contains no sodium hydroxide solution. This is termed the *non-alkali condensate* sample.

Gas discharges from pools

In sampling gas vents in pools, it can be difficult to obtain a sample which has not been contaminated with air. This is best attempted by placing a funnel over the discharge vent at the base of the pool. The funnel can be made of stainless steel, titanium or teflon and is connected to the sample flask by the sampling tubes. In sampling from deep pools it may be easier to hold the funnel over the vent by clamping it to a long pole. If insuffient metal tubes are available, a butyl rubber hose can be used to link the funnel to the flask.

Gas bottle label
geothermal field
feature name/number
date of sampling
time of sampling
vent temperature (t°C)
bottle number

Gas discharges from pools often have a gentle flow, and under such circumstances sufficient gas must be permitted to pass to purge the tubes prior to sampling. This can be aided by sealing the end of the tube with a length of butyl rubber secured with a spring clip to permit the gas pressure to build before releasing to purge the tubes.

The sampling procedure is otherwise similar to that described above for fumaroles.

Wells

Wells that have a well-head separator, or dry-steam wells (no water) can be sampled directly, otherwise it is necessary to separate the water and steam phases.

Pipelines are sampled using a flask attached to the steam outlet of a Webre separator (Klyen, 1982). Note that to avoid collection of an unrepresentative sample, pressure

drop through the separator should be avoided, and there should be no water at the dry steam outlet. As a guide to the quality of the separation, the chloride content of the condensate can be determined; this should be negligible. *Downhole samples* are collected with the Klyen sub-surface sampler (Klyen, 1982).

Well gas bottle label
geothermal field
well number
date of sampling
time of sampling
well head pressure (bg or ba)
separation pressure (bg or ba)
discharge enthalpy (if known)
bottle number

General notes on sampling gases

A distinct clicking sound, produced by rapidly tilting the flasks, indicates the presence of a good vacuum.

The presence of a smell of hydrogen sulphide on opening the flask, and a condensate pH of less than 9 indicates that too little sodium hydroxide has been added to absorb all the acid gases. The solution pH should be greater than 10 for a reliable result, with pH 9 the absolute minimum (R.B. Glover, pers. comm. 1988).

If the carbon dioxide content of the steam is high, sodium carbonate may precipitate from the solution. This can be redissolved by the addition of deionised water in the laboratory.

The volume of sodium hydroxide added to the flasks can be reduced if the discharge is high in non-absorbed gases which will rapidly fill the vacuum space.

Sample storage

With well-maintained Rotaflo stopcocks, a vacuum or gas sample can be preserved in the flasks for over a year. However, if the sample is contaminated by air then the sulphide species will oxidise and be lost. Further, if carbon monoxide is to be determined, then there should be no excess of sodium hydroxide otherwise sodium formate ($NaHCO_2$) will form within days of collection (Giggenbach and Goguel,

1989). If CO determinations are required, the samples should therefore be analysed as soon as possible after collection.

7.4 ANALYTICAL METHODS

The gas sample in the flask is divided into two phases each of which is analysed separately:

residual gases, not absorbed by the hydroxide (Ar, CH_4, CO, H_2, He, N_2, O_2) and determined by gas chromatography

gases absorbed by sodium hydroxide (CO_2, H_2S) and determined by wet chemical analysis.

An additional sample of steam condensate should be collected in an evacuated flask with no hydroxide solution ("non-alkaline condensate") if determinations of minor and trace constituents (NH_3, H_3BO_3 and trace amounts of silica, fluoride, mercury, arsenic etc.) are required. These are determined using the same procedures as for water samples.

As extraction of the condensate without loss or contamination of the residual gases is difficult, the gases are determined first using gas chromatography. The following details of equipment and methods have been described by Ellis et al. (1968), Ellis and Mahon (1977), Giggenbach (1975), Giggenbach and Goguel (1989) and R.B Glover (pers. comm. 1988).

Mass/volume of steam condensate: Determined from the weight of the sample flask plus hydroxide solution before (W_{f+NaOH}, grams) and after sample collection ($W_{f+NaOH+s}$, grams) weighed to 0.1g. The mass of the sample (W_s) is given by:

$$W_s = W_{f+NaOH+s} - W_{f+NaOH}$$

The volume of the condensate, V_c (mL), can be measured following analysis of the residual gases by decanting the liquid from the flask into a graduate measuring cylinder and recording the volume of the liquid (V_l); from this has to be deducted the volume of the hydroxide solution added to the flask before sampling (V_{NaOH}).

$$V_c = V_l - V_{NaOH}$$

For low-gas samples, the mass change approximates to the volume of the condensate and $V_c \sim W_s$.

Volume of the flask (V_f): Determined from the weight of the flask empty (W_f) and when full of deionised water (W_{di}); as the density of the water is unity, volume and mass can be equated and the volume of the flask is given by:

$$V_f = W_{di} - W_f$$

Gas chromatographic determinations

Equipment

CH_4, He, H_2, N_2, O_2: separation on a 4.0m (1/8 inch outside diameter) column packed with molecular sieve 5A (50-80 mesh) at 30°C with argon as carrier gas at a flow rate of 20mL/min. A thermal conductivity detector gives high sensitivity for He and H_2, with lower sensitivity for the other gases.

Ar, CH_4, CO, N_2: separation on a 1.5m molecular sieve 5A column at 80°C with subsequent conversion of O_2 to water in 0.5m MS5A column at 220°C with hydrogen as the carrier gas at a rate of 20mL/min. Separation of Ar and O_2 is not necessary in this scheme. A thermal conductivity detector yields high sensitivity for these gases.

If any acid gases remain in the residual gas sample (eg. from not using sufficient hydroxide solution in the flask) these will gradually cause a deterioration in the molecular sieve column. The gases can be removed by using a liquid air bath or a pre-column of Chemosorb W on which concentrated sodium hydroxide has been adsorbed.

Calibration

The system is calibrated using a series of aliquots of pure gases at a known pressure which is determined by the manometer. A graph of peak area against moles of gas at standard temperature and pressure is then constructed for each gas. Alternatively, calibration graphs can be eliminated by multiplying the peak area of each gas by a "response factor" which takes into account the variations in the sensitivity of the detector for different gases (Deitz, 1967). For example, with argon carrier gas a thermal conductivity detector is almost 13 times more sensitive to hydrogen than nitrogen. Examples of the response factors for this system are: H_2 = 0.0780, O_2 = 0.787, N_2 = 1.0, CH_4 = 0.371 (R.B. Glover, pers. comm., 1988). Calculations are simplified if the gas concentrations are expressed in terms of pressure in millibars.

Volume/pressure/temperature/amount of the residual gases (V_{rg}, P_{rg}, T_{rg}, M_{rg}): Calculate the residual gases volume (V_{rg}, mL) from the volume of the flask and that of the total liquid in the flask (hydroxide and condensate):

$$V_{rg} = V_f - V_l$$

Note that when the residual gases pressure (P_{rg}, millibars) is determined, (by a manometer attached to the flask and gas chromatograph) the volume of the gas inlet system ("dead space", V_{ds}) between the flask and the manometer must be taken into account. The pressure of the gases is therefore measured in a volume equal to (V_{rg} + V_{ds}). The residual gas temperature (T_{rg}, Kelvin) is taken to be the laboratory ambient temperature. The amount of all the residual gases collected in the flask is calculated from:

$$M_{rg}\,(\text{millimoles}) = (V_{rg}/22.4)\,[(P_{rg} - p_w)/1013.25]\,(273/T_{rg})$$

where

p_w = water vapour pressure at T_{rg}

Calculation of the amount of each residual gas, (M_{gas}): This is derived from the partial pressure of the gas in the flask (P_{gas}) plus dead space volume (measured by the manometer-gas chromatograph system). As all gases will dissolve to some extent in the liquid phase within the flask, this amount has to be allowed for and added to the gas in the vapour phase. The amount dissolved depends upon the Henry's law constants, the gas involved, the gas temperature, the volumes of the liquid and vapour phases in the flask and the partial pressure (concentration) of the gas.

$$M_{gas}\,(\text{millimoles}) = P_{gas}\,[(V_{rg} + V_{ds})/22400] + (V_l/18K_{gas})$$

The second term allows for the gases dissolved in the liquid phase, where Kh_{gas} is the Henry's law distribution coefficient at 20°C. Kh_{He} = 142900, Kh_{H_2} = 65500, Kh_{Ar} = 36400, Kh_{O_2} = 39840, Kh_{N_2} = 78740, Kh_{CH_4} = 36100 (Giggenbach and Goguel, 1989).

The amount of water collected is calculated from the volume of the steam condensate (V_c):

$$M_{H_2O}\,(\text{millimoles}) = V_c\,(1000/18)$$

If the sample is high in gas content and relatively low in steam, then the amount of water must be calculated by subtracting the amount of all the gases from the weight of the condensate.

Wet chemical determinations

These are performed on the alkaline condensate in the order: H_2S, CO_2. Determinations for ammonia, boron, silica, fluoride, mercury, arsenic and other trace gaseous constituents which dissolve in the steam condensate, are made on the separate non-alkaline condensate sample using the same procedures as for the water samples (Section 6.4).

Hydrogen sulphide (H_2S) *VOL*

The method is essentially the same as that for water samples. Iodine loss from the sample during the analysis is a problem. This is due to the volatility of iodine in acidic conditions, and the heat generated by the addition of the alkaline condensate to the acidified iodine solution. Reproducibility is improved by refrigeration of all reagents and performing the titration in an ice bath (B.L. Lovelock, pers. comm., 1989).

Reagents: 0.01N iodine solution, 1M sulphuric acid, 0.01N sodium thiosulphate, starch indicator.

Method: Pipette 10mL of the iodine solution into a conical flask. Add 10mL 1M sulphuric acid, stirring slowly, and an aliquot of the alkaline condensate (V_a, typically 5-10mL). Titrate rapidly with the thiosulphate solution with starch as indicator. Record the volume of thiosulphate used ($V_{thio,s}$). Perform a blank titration using the same procedure without adding any sample; record the volume of thiosulphate used ($V_{thio,b}$). The iodine consumed by the hydrogen sulphide is equal to ($V_{thio,b}$ - $V_{thio,s}$).

Calculation: Concentration of H_2S in steam condensate (millimoles/100 moles steam) = $900\,(V_{thio,b} - V_{thio,s})\,(N_{thio}/V_a)\,(V_l/V_c)$.

where

N_{thio} = the normality of the thiosulphate solution.

V_c = the volume of condensate in the flask, mL.

V_l = is the total volume of liquid in the flask (condensate plus the hydroxide solution), mL.

The factor (V_l/V_c) corrects for the dilution of the condensate by the hydroxide solution added to the flask before sampling.

References: Giggenbach and Goguel, (1989), R.B. Glover (pers. comm., 1988), B.L. Lovelock (pers. comm., 1989).

Carbon dioxide (CO_2) *VOL*

Carbon dioxide can be determined using the method for bicarbonate described in Section 6.4, or the following potentiometric titration. All traces of hydrogen sulphide must be removed from the sample, otherwise it will interfere with the determination. This is achieved by oxidising the sulphide to sulphate by adding hydrogen peroxide to the sample, or by removing the sulphide through precipitation by the addition of silver nitrate. Peroxide oxidation ensures that other sulphur species are also removed, but requires that the samples are left overnight (Giggenbach and Goguel, 1989) and involves the incorporation of dilution factor. Precipitation of the sulphide with silver is an easier but more expensive option.

Reagents: 1N and 0.1N hydrochloric acid, 0.1N silver nitrate, buffer solutions pH4 and pH9.

Method: Place an aliquot of the condensate (V_a) into a small beaker. Add a stirring bead and place onto a magnetic stirrer, stirring at a constant rate. Insert a calibrated pH electrode and add silver nitrate until no further brown silver sulphide precipitates. Adjust the solution pH with the 1N hydrochloric acid, and add dropwise until the pH approaches 9. A white precipitate should develop as the acid is added; if not, add silver nitrate until the white precipitate appears. Add, dropwise, the 0.1N hydrochloric acid until the solution pH = 8.3. Titrate with 0.1N hydrochloric acid until the solution pH = 3.8; record the volume of acid used ($V_{HCl,s}$). A blank correction must be performed as the sodium hydroxide will have absorbed some atmospheric carbon dioxide during the preparation and filling of the flasks. This is performed using the same aliquot volume and method. Record the volume of acid used in the titration ($V_{HCl,b}$); this is subtracted from $V_{HCl,s}$ in the final calculation.

Calculation: Concentration of CO_2 in steam condensate (millimoles/100 moles steam) = $1800\,(V_{HCl,s} - V_{HCl,b})\,(N_{HCl}/V_a)\,(V_l/V_c)$.

where

N_{HCl} = the normality of the hydrochloric acid.

V_c = the volume of condensate in the flask, mL.

V_l = is the total volume of liquid in the flask (condensate plus the hydroxide solution), mL.

The factor (V_l/V_c) corrects for the dilution of the condensate by the hydroxide solution added to the flask before sampling.

Note: The volume of the aliquot used depends on the concentration of carbon dioxide in the condensate; sufficient aliquot volume is required to give a reproducible titration (~15-20mL in a standard burette, or ~5mL if a 10mL micro-burette is used).
References: Giggenbach and Goguel (1989); R.B. Glover (pers. comm. 1988).

Calculation of gas in the total discharge (TD_{gas})

If the enthalpy and pressure at sampling are known, then the steam fraction (y) and water fraction (1-y), and hence the gas in the total discharge, can be calculated.

$$TD_{gas} = (\text{gas in steam})\ y + (\text{gas in water})\ (1-y)$$

The second term can be neglected for sparingly soluble gases, or can be calculated from known distribution coefficients, or determined by analysis (eg. ammonia).

7.5 GAS CONCENTRATION UNITS

Units

Gas concentrations are commonly reported in several different units and it is necessary to know how these relate to one another and to be able to convert between units. Chemists, for example, find units based on the mole most helpful as these can be used in equilibria calculations; whereas engineers are more interested in weight-based units.

Conversion of units

Before introducing the conversions between units, a few reminders of definitions and constants will be useful (fwt = formula weight of a substance; STP = standard temperature and pressure).

1 mole = 1000 millimoles = fwt of a gas
1 millimole = 0.001 moles = fwt of a gas/1000
1 mole steam = 18g; 100 moles steam = 1800g
STP = 273.15 K, 760mmHg
760mmHg = 1013.25 millibars = 1 atmosphere
volume of 1 mole of gas at STP = 22.4L = 22400mL

An example of alternative ways of expressing the same analysis will illustrate the inter-relationships between units (Table 7.1).

Gas concentration units

mole-based units

millimoles/100 moles steam: amount of a gas (in millimoles) in 100 moles of steam

on a dry gas basis:

mole%: amount of a gas (moles) in 100 moles of total gas

millimole/mole dry gas: amount of a gas (moles) in 1 mole of total gas. This is also the individual gas faction, x_i.

weight-based units

g/tonne: amount of a gas (in grams) in 1 tonne of steam

mg/kg: mg of gas per kg steam

wt%: parts of gas (by weight) per 100 parts steam

fractions

total-gas fraction (gas/steam ratio), x_g: (sum of concentration of all gases in millimoles/100 moles of steam) / 100

individual gas fraction, x_i: see millimole/mole dry gas

mole fraction, X_i: moles of a gas, i/mole of steam, $X_i = (x_g\, x_i\, y)/10^6$, where y is the steam fraction.

Unit conversions

millimoles/100 moles steam - g/tonne steam: g/t = (millimoles gas/100 moles steam) (fwt gas x 1000) / (fwt steam x 100)

g/tonne steam - millimoles/100 moles steam: millimoles /100 moles steam = (g/t) (fwt steam x 100) / (fwt gas x 1000)

millimoles/100 moles steam - moles % ("dry gas basis"): moles % = [(millimoles gas /100 moles steam) / (sum of all gas concentrations in millimoles/100 moles steam)] x 100/1000

Table 7.1. Equivalent presentations of a gas analysis

Units	Steam fraction	Gas fraction	Gas concentration CO_2	H_2S	CH_4	N_2	NH_3
mg gas / kg steam							
	0.20		23 467	377.8	106.7	140	47.2
millimoles gas / 100 moles steam							
	0.20		960	20	12	9	5
millimoles gas / moles total gas							
	0.20	10.06*1	954	19.9	11.9	8.9	5
mole %							
	0.20	0.1006*2	95.4	1.99	1.19	0.89	0.5
			Total discharge composition (TD)				
millimoles gas/ kg TD							
			106.7	2.2	1.3	1.0	0.56
mole fraction (X_i)							
			1.9 x10^{-3}	4.0 x10^{-5}	2.3 x10^{-5}	1.8 x10^{-5}	1.0 x10^{-5}

*1 millimoles gas/mole steam

*2 molar gas/steam ratio

CHAPTER 8

SOIL AND SOIL-GAS SURVEYS

8.1 INTRODUCTION

Water and gas sampling of natural discharges are the most common types of survey over known geothermal areas. However, where discharge features are few and where the extent of the field is not known, soil and soil-gas surveys can prove helpful. These surveys can identify permeable regions in a field and possible upflow or boiling zones. They can also delineate the margins of a geothermal system, and therefore often complement geophysical surveys particularly where interpretation of geophysical data is difficult, eg. due to topographic effects.

There are two types of survey: soil and soil-gas. Each identifies areas of anomalously high concentrations of volatile species either in the soil itself, or in the soil-gas (also known as the soil atmosphere). In both cases, the anomalies are produced by vapour leaking from the underlying geothermal system. Such leakage will be greatest along permeable regions, especially faults, and may indicate directions of subsurface flow or possible upflow zones. As vapours can penetrate lithologies impermeable to water, anomalies which represent upflows can be many kilometres from any hot-spring discharges, particularly in mountainous terrain with high relief.

Standard procedures have yet to be adopted in many aspects of geothermal soil surveys. Furthermore, too many of the reported surveys are flawed either in execution or in reporting, and comparison between surveys is made difficult by the general lack of precise information on the analytical procedure, the context of the survey (topography, geology, known geothermal activity) and the anomaly recognition-interpretation criteria. This Chapter highlights aspects which need to be taken into consideration (and therefore reported) when undertaking a geothermal soil survey, and presents outlines of the analytical methods adopted to date.

8.2 SURVEY ORGANISATION

Any soil survey is composed of three stages: sampling, analysis and interpretation. Information from these stages combine to fulfil the three primary objectives of the survey: to identify target areas, to eliminate non-prospective ground and to eliminate false anomalies. The targets in geothermal surveys are permeable regions (to aid the location of drilling sites) and field margins. "False" anomalies are high concentrations formed by processes unrelated to geothermal activity. Before initiating a survey, several decisions need to be taken regarding the sampling and analytical programmes:

- which soil horizon or depth should be sampled?
- over what area, and how often, should samples be taken?
- what species should be determined in the sample?
- what size fraction should be examined?
- what decomposition or leaching procedure should be used?

Orientation survey

The answers to these questions may be predetermined by the type of survey (soil or soil-gas) and pathfinder species adopted, and experience gained from past surveys (either personal experience or reports from the literature). Often however, no such information is available, and the optimum sampling and analytical procedures have to be determined specifically for the survey area or region. This is commonly achieved by the use of a reconnaissance or orientation survey performed over a geographically (topography, drainage, climate, land-use) and geologically (lithologies, weathering/soil development, soil type) similar area. These are carried out in the same way as the soil/soil-gas survey (described below), and should aim to optimise or determine the following factors to achieve the best practicable contrast between background and anomalous concentration:

- sample spacing and sample depth/horizon
- soil size fraction taken for analysis
- extraction and analytical procedure
- most suitable exploration or pathfinder species
- typical range of background and anomalous values
- typical size of target areas (regional and local scale)
- identification of potential sources of false anomalies or contamination
- identification of features to be recorded by field samplers to aid interpretation

Sampling grid

Soil samples should be collected on a grid pattern to enable a reliable interpretation of any anomaly pattern. The spacing on the grid is determined by factors such as the target size, the topography and geology of the area, and the amount of funds and time available for the study. The grid should be orientated in such a way that it crosses major geological structures, such as faults and the regional strike, and does not parallel these features. It should be organised so that several samples are taken from soils overlying different lithologies and different topographies, and be sufficiently large to cover the entire prospective geothermal area. The sampling interval is also determined by the typical size of the anomaly, as at least two or three samples should lie within the anomaly. Regional reconnaissance grids used to search for geothermal areas may be 1x1km or 1x2km, but surveys over potentially prospective or known geothermal areas are usually 250x250m or 150x300m in size. More detailed, follow-up surveys can be conducted on sample grids as small as 10x10m, though 100x100m or 50x25m may be more typical. In organising a sampling grid, it is worth remembering that not all samples collected need be analysed. Rather than return to the field to perform a follow-up survey, it is often more economic to over-sample in the field, and routinely analyse only every third or fourth sample; intervening samples are only determined where potential anomalies have been identified.

Sampling grids should use a topographic map, or large-scale aerial photograph, as a base map onto which the sample sites are placed. The sites should be marked in the field (eg. with stakes), and accurately located on the base map. It is rarely possible to sample on a perfectly square or rectangular grid, but as long as the overall coverage of the grid is maintained this is not essential. It is far more important that field samplers mark the actual location of the sample, rather than pretend that the formal grid pattern was followed. The ideal way to lay out grid sampling lines is by using a theodolite and staff; but this is time consuming, and if an accurate base map is available then lines can be paced using a compass. Again, accurate location of the sample sites on the map is essential.

8.3 SOIL SURVEYS

Soil surveys have the advantage over soil-gas methods in that the anomalies develop over time by the adsorption of vapour-borne species onto components in the

soil, and are therefore not as subject to short-term variations in ambient conditions. Although species can be taken up by soil oxide and clay minerals, greater quantities are usually adsorbed by the soil organic matter, and it is this which is the preferred sampling medium. The most widely adopted volatile species for these surveys is mercury, but others which have proved successful include arsenic, antimony, boron and ammonia. Most surveys have been conducted over high-temperature, volcanic-hosted systems, but recent work has demonstrated that soil surveys are also effective over low-temperature, sediment-hosted fields (Liu and Nicholson, 1990, Nicholson et al., 1989). These authors demonstrated that ammonia and boron can be used as pathfinder species over low-temperature fields, but that Hg, As and Sb may not be effective across such systems.

Soil sampling

In profile, or cross-section, soils are divided into several layers or "horizons". Soil scientists recognise many different horizons, but for the purposes of these surveys it is necessary only to divide the profile into three: the near-surface, brown, friable, organic-rich layer is termed the "A" horizon; this is underlain by the clay-rich, yellow-brown to orange-brown "B" horizon; this in turn is underlain by weathering fragments of the parent rock, the "C" horizon. The thickness of each horizon depends on many factors, including climate, drainage and topography, and the precise characteristics of the soil profile will be determined in the orientation survey. In geothermal surveys, the best results have been achieved by sampling the organic-rich unit, or A horizon, as the volatile species accumulate more on organic matter than on clay minerals. Note that this is a major difference to mineral exploration soil surveys which use the B horizon. Successful geothermal surveys have been performed with sampling from the B horizon, but the background-anomaly contrast is weak and could result in some anomalies being missed. Under no circumstances should samples be taken on a constant-depth basis. As horizon thickness and development is not uniform over an area, this can (and almost certainly will) result in samples being taken from both the A and B horizons, making the survey difficult to interpret at best or at worst meaningless. Field samplers must therefore be trained to recognise the characteristic features of both A and B horizons, and to sample only from the former.

Sample preparation

Optimum methods of sample preparation are determined as part of the orientation survey, and can significantly affect the effectiveness of the survey. Most samples need to be dried, disaggregated, sieved and leached prior to analysis.

Drying: If paper sampling bags are used then this can be performed without removal of the samples from the bags. Soils in polythene bags will have to be transferred to a beaker or evaporating dish for drying; some care is required here not to confuse or mix samples. Soils are dried in an oven and regularly weighed until no further weight loss occurs. The temperature should be low, to prevent the loss of volatiles, and 35°C has proved to be successful.

Sieving: The samples are disaggregated with a pestle and mortar, and then sieved to eliminate the coarse fraction. In mineral exploration surveys, the -80 mesh (<0.15mm) size fraction is commonly used. No similar standard has been adopted in geothermal surveys, and some have used the -18 mesh fraction (<1mm). Coarser fractions will require larger aliquot masses to ensure reproducibility, but the effectiveness of the size fraction can be determined in the orientation survey. Although no systematic study has been performed on the relative merits of different size fractions for geothermal surveys, it appears that successful results can be achieved using <1mm, which is quicker to sieve than the -80 mesh fraction.

Leaching: Total decomposition techniques are undesirable in geothermal surveys as these are influenced by the underlying lithologies which will only add to the background "noise" of the survey. Since only species of geothermal origin are of interest, and these are adsorbed onto the soil particles, a selective decomposition or leaching procedure is all that is required. There are several methods which can be adopted, and where appropriate these are mentioned under the individual pathfinder species below. However, a general or standard leach which can be adopted uses cold, dilute hydrochloric acid.

Standard HCl leach: Add 10g of the dried, sieved soil sample to 100mL of 1M hydrochloric acid. Leach for one hour at room temperature with regular stirring. This will release adsorbed species from clay minerals, oxides and organic matter. However, it will also dissolve carbonate minerals and possibly also sulphide minerals. Some care is therefore required as such mineral decompositions will add to the "noise" of the survey or will create geology-related anomalies. These will have to be eliminated from geothermal-related anomalies during interpretation, and some knowledge of the soil types and soil mineralogy over the survey area will be helpful in this respect.

Ammonia

This is a new technique which was developed by Aredes and Nicholson (1990) over a low-temperature, sediment-hosted field. It should also be applicable to volcanic-hosted hot-water systems and to vapour-dominated fields. Anomalies highlighted fault zones and a potential upflow area, and these showed a good agreement with conclusions from earlier geophysical surveys.

Analytical procedure: Leach 10g of soil with 100mL 2M KCl solution for one hour with constant shaking. Leave to permit the soil particles to settle. Take 10mL aliquots of the solution for analysis by ammonia-selective electrode. The analytical method described in Section 6.4 is then followed.

Interferences: Degradation of localised concentrations of organic matter (such as animal waste, offal) buried in pits can produce localised high concentrations of ammonia.

Antimony

There have been few studies involving antimony, the most detailed being that of Zhu et al. (1986; 1989). Antimony anomalies overlapped those defined by Hg and As concentrations.

Analytical procedure: Zhu et al. (1986; 1989) used hydride generation as the analytical method, but details of sample leaching or digestion are not given. It should be possible to determine As and Sb on aliquots of the same soil leachate.

Arsenic

After mercury, arsenic has been the most studied element in soil surveys over geothermal areas. Anomalously high levels of As are commonly coincident with high concentrations of Hg and Sb (eg. Openshaw, 1983; Zhu et al., 1986; 1989).

Analytical procedure: The leachate is analysed for arsenic by hydride generation using the standard procedure described in Section 6.4.

Boron

The most detailed investigations into soil-boron concentrations over geothermal areas have been conducted by Liu and Nicholson (1990) and Zhu et al. (1986). Anomalies highlighted structural features and occurred over proposed upflow areas.

Analytical procedure: Leach 10g of soil with 100mL of deionised water at 70°C for one hour with constant shaking. Filter, and analyse aliquots of the leachate by the procedures described in Section 6.4. The ideal method of analysis, especially for a large number of samples, is ICP-AES (inductively coupled plasma source atomic

emission spectroscopy). Note that the standard hydrochloric acid leach can also be employed (substitute 1M HCl for the hot water, leaching takes place at ambient temperature), but is less effective than the water, resulting in lower boron concentrations in the leachate. Relative anomaly patterns will however remain the same regardless of the leachate, but background-anomaly contrast may be reduced (Liu and Nicholson, 1990).

Interferences: Boron anomalies can also be caused by thermal water passing through the soil, but these are easily recognised by the location of springs, the presence of high concentrations of other solutes (eg. Li) and the greater contrast of the water-formed anomalies compared to those formed by vapour-borne boron.

Mercury

Surface enrichments in mercury are not unusual around geothermal areas, and in some instances deposits of mercury minerals such as cinnabar have been formed. This element has been the subject of many investigations, and the success of its application to geothermal surveys over hot water and vapour-dominated systems is well documented (eg. Phelps and Buseck, 1980; van Kooten, 1987; Varekamp and Buseck, 1983). At the elevated sub-surface temperatures of geothermal systems, mercury strongly partitions into the vapour phase and is transported to the surface largely as elemental mercury vapour. This vapour is adsorbed onto organic matter and, to a lesser extent, clay minerals in the upper, low-temperature soil horizons, to create elevated concentrations of mercury.

Analytical procedure: Commercial instruments designed specifically for mercury determinations are available. The instrument most commonly used in soil surveys is produced by the Jerome Instruments Company and is based on the gold-film method (McNerty et al., 1972).

Gold film detector: The dried sample is placed in a quartz tube and heated to over 800°C. The amount of mercury is determined by the adsorption of the element onto one of two gold films. Differences in the resistivity of the films, due to mercury adsorption on one, can be calibrated. Detection limits can be less than 0.1 ppb.

Cold-vapour AAS: The standard procedure, described in Section 6.4, is adopted on the 1M HCl leachate of a soil sample. Alternatively the sample may be decomposed with sulphuric acid and hydrogen peroxide solution using the following method (Klusman and Landress, 1979). Place 1g of -80-mesh soil in a 25 x 200mm culture tube containing 10mL of concentrated sulphuric acid. Add two 1mL aliquots of 50% hydrogen peroxide solution, allowing time for reaction between aliquots. Heat gently (<95°C) to drive off excess peroxide. Immediately prior to analysis dilute

the sample to 50mL in a volumetric flask. Detection limits of this method are around 10ppb.

Interferences: Secondary local influences on soil-mercury concentrations include soil pH, clay minerals, iron and manganese oxides, and organic matter content. These, however, are minor influences which are swamped by any geothermal source of the element (Klusman and Landress, 1978, 1979; Klusman et al., 1977). False (non-geothermal) anomalies can be created by aqueous and wind-borne effluents from industrial activities in the region; a knowledge of local drainage and wind directions is important in such cases. Mercury anomalies have also been reported associated with road and track systems (Fletcher et al., 1986).

8.4 SOIL-GAS SURVEYS

Helium, followed by radon, have been the most popular species in soil-gas surveys. Carbon dioxide and mercury vapour have also been employed, but there are few examples of surveys of the sulphur gases in soils over geothermal areas (see Hinkle and Harms, 1978). All soil-gas surveys are more subject to local climatic influences than soil surveys. These influences, which include air and soil temperature, barometric pressure and soil moisture (Klusman and Jaacks, 1987), affect the concentration of a gas in the soil at any given instant. Surveys which measure the gas concentration at a sample point at a single instant are therefore most prone to distortion by the conditions at the time of analysis. This distortion can be particularly significant if the survey is conducted over several days or weeks across the field. Soil-gas surveys can be difficult to reproduce, and this will create problems for follow-up surveys, especially if these are conducted in different seasons. The success of soil surveys lies in the fact that these anomalies are developed over time, thereby smoothing out the effect of ambient sampling conditions. More reliable and reproducible results will be obtained in soil-gas surveys if the concentrations at each sample point are the result of sampling over a period of time (days or weeks), rather than a few minutes. Other factors which influence the migration of the gas to the surface, such as changes in the soil texture, or rock porosity, should be borne in mind when interpreting the results.

Soil-gas sampling

Soil-gas sampling, like soil sampling, is performed on a regular grid pattern over the prospective area. Unlike soil surveys, however, soil-gas samples are taken at

a constant depth (usually 1m) over the area. Procedures vary in detail with the exploration species selected, and are described below for each of the gases.

Carbon dioxide

There have not been many investigations which have used CO_2 as a pathfinder species to geothermal areas. Soil-gas CO_2 anomalies were compared with those defined by soil-Hg, Hg-vapour and radon by Koga et al. (1982): all showed a good agreement. Sheppard et al. (1990) compared soil-Hg, Hg-vapour and soil-gas CO_2 anomalies over three geothermal areas, with variable agreement between species. Several studies have examined CO_2 emissions through soils over active volcanoes (eg. Aubert and Baubron, 1988).

Analytical procedure: No single analytical method has become standard practice. Soil-gas is pumped through a steel tube from the base of a hole, typically 1m in depth and 10-25mm in diameter. Carbon dioxide is determined in situ with a gas chromatograph, infra-red analyser or mass spectrometer (Aubert and Baubron, 1988, Sheppard et al., 1990). The instruments are calibrated in the field, either by determination of air or by use of a reference standard. Replicate determinations are made until consistent gas compositions are attained in concurrent aliquots. Alternatively, CO_2 can be collected on molecular sieves packed into open glass jars which are inverted and buried in the soil for a fixed period of time (typically 6-8 weeks). After this time they are retrieved, sealed with screw-top caps and returned to the laboratory for analysis by gas chromatography (Hinkle and Harms, 1978).

Interferences: Carbon dioxide can be evolved by the thermal degradation of organic matter or carbonate minerals in host sediments. Variations in soil-gas CO_2 compositions should therefore be interpreted alongside a knowledge of any lithological changes across the survey area.

Helium

Soil-gas helium surveys have been successfully conducted over high and low-temperature geothermal systems (eg. Hinkle et al., 1978; McCarthy, 1983; McCarthy et al., 1982). The surveys have effectively delineated the margins of fields and isolated permeable fault zones which are exploited by the ascending gas.

Analytical procedure: In the most common technique of sampling, a 1m steel probe is inserted into the soil. The gas is extracted by a syringe attached to the probe through a rubber septum or seal, and discharged into airtight steel containers (Bergquist, 1979; Kahler, 1981). The probe is purged using the syringe prior to taking the sample. Alternatively a soil sample is taken in the usual manner, and

sealed in airtight metal containers. It is degassed in the laboratory by placing the containers into an ultrasonic cleaning bath for 20 minutes to disaggregate the soil. The samples are left for two weeks to permit the helium to be released from the soil in the container. The gas is extracted by syringe through a rubber septum which is glued onto the container just prior to extraction (Hinkle et al., 1978). The gas sample is analysed by mass spectrometry.

Interferences: Gases can diffuse more readily from sandy or coarse-grained soils, and helium concentrations would therefore be less than in clay-sized soils. Changes in the soil texture over an area should be noted to aid interpretation of the anomaly pattern. Variations in rock type, hydraulic gradient and diurnal changes in the soil-gas concentrations may influence the helium survey results, but were found to be insignificant by McCarthy (1983) and McCarthy et al. (1982). Seasonal climatic changes, notably air and soil temperature, do affect the soil-gas, and higher helium concentrations are found during the winter months (Klusman and Jaacks, 1987). The concentration of helium can be diluted by heavy discharges of other gases; under such circumstances more meaningful anomaly patterns can be produced by plotting helium-gas ratios (eg. He/CO_2).

Mercury vapour

The determination of Hg-vapour in soil-gases is not as popular as soil-Hg surveys. but the technique has been successfully applied to both water-dominated and vapour dominated systems (Koga and Noda, 1976; Koga et al., 1982; Noda, 1981). Sheppard et al. (1990), however, found the technique gave erratic results and was not as useful as soil-Hg or soil-gas CO_2 surveys.

Analytical procedure: The standard method now adopted is based upon the adsorption of Hg-vapour by a gold film, needle or wire (McNerny and Buseck, 1973). This is buried in the soil at a fixed depth of 1m for five days, retrieved and analysed in the laboratory (Noda, 1981). Alternatively, a set volume of soil-gas can be pumped over a gold trap, or through an oxidising solution which is later analysed (Koga and Noda, 1976; (McNerny and Buseck, 1973).

Interferences: The methods which collect Hg-vapour, directly (rather than permitting it to accumulate over several days) are subject to local climatic fluctuations, discussed above. Mercury vapour can also be emitted by ore deposits and volcanic activity. Any anomalies should therefore be interpreted in conjunction with a knowledge of the geology of the area.

Radon

Of the 27 radioactive isotopes of radon, only two have sufficiently long half-lives to be of use in soil-gas surveys: ^{222}Rn (radon) and ^{220}Rn (thoron) with half-lives of 3.8 days and 54.5 seconds respectively. These isotopes decay by alpha-particle emission, and it is the density of these particles which is measured in radon surveys, *not* the concentration of radon gas. Radon surveys have been successful in identifying fault zones and areas of high thermal gradients. However, they are time consuming as the procedure involves two visits to the site, and the clearing of vegetation along survey lines to permit holes to be dug for the detectors (Whitehead, 1981, 1984).

Analytical procedure: The usual method involves the burial of alpha-particle sensitive film to record the alpha-particle tracks; cellulose nitrate film, Kodak LR115 II, has found wide usage (Cox, 1980; Koga et al., 1982; Gutierrez-Negrin, 1985; Whitehead, 1984; Whitehead et al., 1983) A strip of the film, ~ $1cm^2$, is stuck to the bottom of a 250mL plastic cup which is then inverted and buried to depths of around 30-50cm. An air space should remain between the film and the soil after burial. This can be achieved by the use of a filter or plastic tube (Gutierrez-Negrin, 1985; Whitehead, 1981). Interpretation of the data is easier if the period of measurement is fixed and constant for all cups. The time period selected depends on the rock type and its uranium-thorium content, but is typically 1-6 weeks. This integrates the anomaly over time, reducing the effect of random ambient fluctuations. After collection, the film is etched in 2.5 M sodium hydroxide at 50-60°C for 2-3 hrs to emphasise the alpha-particle tracks, which are then counted under a microscope. Alternatively, the films can be mounted and projected onto a screen for track counting; this is a more rapid, but less precise, method than using the microscope. Results are expressed in tracks/area/time.

Interferences: As radon is part of the uranium and thorium decay series, the concentration of these elements in the underlying lithologies is important. Variations in rock type can therefore influence the anomaly pattern, and it may be necessary to establish background concentration levels for each rock and soil type. Being a soluble gas, radon can be dissolved in shallow groundwater, and local hydrological changes may therefore affect the gas concentration. Similarly, variations in rainfall over the study period will affect the results as moisture reduces the efficiency of the film to track registration (Whitehead, 1981). Local changes in vegetation can alter the porosity of the soil and affect the release of radon (Whitehead, 1981) over the study area. Seasonal variations in soil-gas radon can also be pronounced. Whitehead (1981) reports summer levels about ten times greater than those in winter.

8.5 DATA QUALITY, PRESENTATION AND INTERPRETATION

The standard procedures to ensure data quality (standards, blanks, duplicates) as described under water surveys (Chapter 6) are adopted. In addition, it is important to avoid systematic errors or bias in the analytical method creating false anomalies in the survey. This is readily avoided by not analysing the soils in the order collected along a sample line. Prior to sending the samples to the laboratory therefore, the soils are randomised and given laboratory reference numbers. Ensure that a complete and duplicate record is kept of the lab. no. - field no. cross-reference. Standard, blank, control and duplicate samples are also given lab. numbers, but the identity of these are not revealed to the analyst.

Presentation methods

The most common, and useful, way of presenting the results is in the form of a map on which the sample points, species concentration and iso-concentration lines, or contours, are drawn between the points. Such maps can include all the relevant survey information (see box) and can be readily compared to the topographic and geological maps when interpreting the data. In this respect, it is useful to have all three maps at the same scale, possibly as overlays. Concentration contour maps are easily read by the specialist and non-specialist alike and are the recommended form of presentation. An alternative, but effective method of representing concentration at a given point uses symbols of varying size (usually dots) to represent concentration ranges - the larger the dot, the greater the concentration. Concentration graphs or profiles along selected sample lines are also used. These are effective in emphasising permeable zones, but are really complementary to the contour maps.

Anomaly identification and interpretation

Deciding what the concentration contour interval should be (or the concentration range represented by the dots) is important as it will affect the anomaly pattern on the map. Three approaches can be adopted:

- concentrations are contoured at regular intervals which divide the concentration range into convenient even segments
- an anomaly is defined as the mean concentration plus the value of two standard deviations. Contours are drawn at this anomaly threshold and at convenient intervals above and below this value.
- the data set is divided into background and anomalous populations using cumulative frequency (probability) plots.

Data presentation on soil anomaly maps and captions
Map species determined, concentration units sample sites concentration at each site iso-concentration contours, with shading national grid reference or latitude/longitude scale bar north arrow **Caption** national location of the survey area size fraction, leaching method, analytical method used date of survey, names of field survey team, analyst
Note: To aid interpretation, the anomaly map has to be compared with topographic and geological maps, these should include the following data: **Topographic maps** streams, springs, lakes, swamps, bogs, topography, roads, buildings, fences, woodland, scrub **Geological maps** rock types, strike and dip, faults, mineralisation

The first approach is too empirical, and while it will recognise the highest anomalies, other significant elevated concentration patterns could be lost as the contour interval is arbitrarily selected. The "mean plus two s.d." method is often adopted with no real thought to its significance or the implications of the distribution of the data set. It is only really useful where only a single population can be identified in the data set. The third method is that which should be adopted. Cumulative frequency plots (also called probability plots) divide the results into groups ("populations"), typically: background values, anomalous values and a region

of overlap. They provide a more quantitative method of anomaly recognition and contour interval selection. The application of probability graphs to exploration soil surveys is described in detail by Sinclair (1974, 1981).

The background and anomaly thresholds defined, and the data illustrated on a map, it now remains for the anomaly pattern to be interpreted. Non-geothermal anomalies must be eliminated and prospective drilling targets identified if possible. The anomaly pattern should be compared to the topographic and geological maps. Any correlation between the anomaly pattern and the following factors should be checked:

- rock type
- soil type
- drainage area (look out for swamp and bog areas)
- topography (especially hill slopes/valley floors)
- man-made structures (roads, buildings)
- land use
- linear anomaly along sample lines; probably caused by not randomising the samples and systematic bias in the analytical method

Anomalies which consistently tie in with any of the above factors should be discounted as they are not of geothermal origin. It is common for geothermal vapours to exploit fault zones, and for unknown faults to be identified by these surveys, so linear anomalies which *cross* sample lines should not be discredited (this is why the orientation of the sample grid to cross major structures is important).

Ideally, any remaining anomalies are geothermal in nature and require interpretation. It is possible to identify permeable zones, upflow zones, flow directions and field margins through the relative concentrations of the exploration species. However, in reaching final conclusions about the anomaly pattern it is worth recapping factors which can influence anomaly development:

- the amount of the species available for transport
- the migration paths from depth to surface (related to geological structure, rock porosity and soil texture)
- the effectiveness of soil composition in retaining species (clay/organic-matter content)
- seasonal and climatic variations, especially rainfall.

- sealing of previously permeable zones and the creation of others (eg. by silicification or tectonic activity respectively) will alter the anomaly pattern, often causing well-defined but weak anomalies.
- landslip or coverage of a geothermal area by a new surface layer (soil/volcanic ash) will mask any anomaly until this can be extended up into the new surface horizon. This process can be rapid in active, high-temperature systems (a few days or weeks) but the duration for the re-establishment of equilibrium will depend upon the characteristics of the system and the overburden.

Anomaly development is thought to be a dynamic equilibrium, with geothermal vapours from depth replacing those evolved from the soil to the atmosphere. After cessation of hydrothermal activity the anomaly will continue to exist even though not replenished by vapour. How long the anomaly will last is not known, and probably depends on the individual characteristics of the soil profile and the species in question. However, it is expected that some proportion of the more volatile species will diffuse into the atmosphere. In this regard, the less volatile species (As, Sb, B and possibly Hg) may be more useful in surveys over young or fossil systems.

APPENDIX 1

STEAM TABLES

The following steam tables contain thermodynamic data for water at saturated vapour pressures and temperatures over the temperature range 0.01 - 374.136°C (Keenan et al., 1969).

Temp.	Pressure	Specific volume		Enthalpy		
°C	bars	cc/g		kJ/kg		
		vap.	liq.	vap.	liq.	evap.
0.01	0.01	206136	1.000	2501	0.01	2501
1	0.01	192577	1.000	2503	4.16	2499
2	0.01	179889	1.000	2505	8.37	2497
3	0.01	168132	1.000	2507	12.57	2494
4	0.01	157232	1.000	2509	16.78	2492
5	0.01	147120	1.000	2511	20.98	2490
6	0.01	137734	1.000	2512	25.20	2487
7	0.01	129017	1.000	2514	29.39	2485
8	0.01	120917	1.000	2516	33.60	2482
9	0.01	113386	1.000	2518	37.80	2480
10	0.01	106379	1.000	2520	42.01	2478
11	0.01	99857	1.000	2522	46.20	2475
12	0.01	93784	1.001	2523	50.41	2473
13	0.01	88124	1.001	2525	54.60	2471
14	0.02	82848	1.001	2527	58.80	2468
15	0.02	77926	1.001	2529	62.99	2466
16	0.02	73333	1.001	2531	67.19	2464
17	0.02	69044	1.001	2533	71.38	2461
18	0.02	65038	1.001	2534	75.58	2459
19	0.02	61293	1.002	2536	79.77	2456
20	0.02	57791	1.002	2538	83.96	2454
21	0.02	54514	1.002	2540	88.14	2452
22	0.03	51447	1.002	2542	92.33	2449
23	0.03	48574	1.002	2544	96.52	2447
24	0.03	45883	1.003	2545	100.7	2445
25	0.03	43360	1.003	2547	104.9	2442
26	0.03	40994	1.003	2549	109.1	2440
27	0.04	38774	1.003	2551	113.2	2438
28	0.04	36690	1.004	2553	117.4	2435
29	0.04	34733	1.004	2554	121.6	2433

Temp.	Pressure	Specific volume		Enthalpy		
°C	bars	cc/g		kJ/kg		
		vap.	liq.	vap.	liq.	evap.
30	0.04	32894	1.004	2556	125.8	2430
31	0.04	31165	1.005	2558	130.0	2428
32	0.05	29540	1.005	2560	134.1	2426
33	0.05	28011	1.005	2562	138.3	2423
34	0.05	26571	1.006	2563	142.5	2421
35	0.06	25216	1.006	2565	146.7	2419
36	0.06	23940	1.006	2567	150.9	2416
37	0.06	22737	1.007	2569	155.0	2414
38	0.07	21602	1.007	2571	159.2	2411
39	0.07	20533	1.007	2572	163.4	2409
40	0.07	19523	1.008	2574	167.6	2407
41	0.08	18570	1.008	2576	171.7	2404
42	0.08	17671	1.009	2578	175.9	2402
43	0.09	16821	1.009	2580	180.1	2400
44	0.09	16018	1.009	2581	184.3	2397
45	0.10	15258	1.010	2583	188.4	2395
46	0.10	14540	1.010	2585	192.6	2392
47	0.11	13861	1.011	2587	196.8	2390
48	0.11	13218	1.011	2589	201.0	2388
49	0.12	12609	1.012	2590	205.1	2385
50	0.12	12032	1.012	2592	209.3	2383
51	0.13	11486	1.013	2594	213.5	2380
52	0.14	10968	1.013	2596	217.7	2378
53	0.14	10476	1.014	2597	221.9	2376
54	0.15	10011	1.014	2599	226.0	2373
55	0.16	9569	1.015	2601	230.2	2371
56	0.17	9149	1.015	2603	234.4	2368
57	0.17	8751	1.016	2604	238.6	2366
58	0.18	8372	1.016	2606	242.8	2363
59	0.19	8013	1.017	2608	246.9	2361
60	0.20	7671	1.017	2610	251.1	2358
61	0.21	7346	1.018	2611	255.3	2356
62	0.22	7037	1.018	2613	259.5	2354
63	0.23	6743	1.019	2615	263.7	2351
64	0.24	6463	1.019	2617	267.9	2349
65	0.25	6197	1.020	2618	272.0	2346
66	0.26	5943	1.020	2620	276.2	2344
67	0.27	5701	1.021	2622	280.4	2341
68	0.29	5471	1.022	2623	284.6	2339
69	0.30	5252	1.022	2625	288.8	2336
70	0.31	5042	1.023	2627	293.0	2334
71	0.33	4843	1.023	2629	297.2	2331
72	0.34	4652	1.024	2630	301.4	2329
73	0.35	4470	1.025	2632	305.5	2326
74	0.37	4297	1.025	2634	309.7	2324
75	0.39	4131	1.026	2635	313.9	2321
76	0.40	3973	1.027	2637	318.1	2319
77	0.42	3822	1.027	2639	322.3	2316
78	0.44	3677	1.028	2640	326.5	2314
79	0.46	3539	1.028	2642	330.7	2311
80	0.47	3407	1.029	2644	334.9	2309
81	0.49	3281	1.030	2645	339.1	2306
82	0.51	3160	1.030	2647	343.3	2304
83	0.53	3044	1.031	2649	347.5	2301
84	0.56	2934	1.032	2650	351.7	2299

Temp.	Pressure	Specific volume		Enthalpy		
°C	bars	cc/g		kJ/kg		
		vap.	liq.	vap.	liq.	evap.
85	0.58	2828	1.032	2652	355.9	2296
86	0.60	2726	1.033	2654	360.1	2293
87	0.63	2629	1.034	2655	364.3	2291
88	0.65	2536	1.035	2657	368.5	2288
89	0.68	2446	1.035	2658	372.7	2286
90	0.70	2361	1.036	2660	376.9	2283
91	0.73	2278	1.037	2662	381.1	2281
92	0.76	2200	1.037	2663	385.3	2278
93	0.79	2124	1.038	2665	389.5	2275
94	0.81	2052	1.039	2667	393.7	2273
95	0.85	1982	1.040	2668	398.0	2270
96	0.88	1915	1.040	2670	402.2	2268
97	0.91	1851	1.041	2671	406.4	2265
98	0.94	1789	1.042	2673	410.6	2262
99	0.98	1730	1.043	2674	414.8	2260
100	1.01	1673	1.043	2676	419.0	2257
101	1.05	1618	1.044	2678	423.3	2254
102	1.09	1566	1.045	2679	427.5	2252
103	1.13	1515	1.046	2681	431.7	2249
104	1.17	1466	1.047	2682	435.9	2246
105	1.21	1419	1.047	2684	440.1	2244
106	1.25	1374	1.048	2685	444.4	2241
107	1.29	1331	1.049	2687	448.6	2238
108	1.34	1289	1.050	2688	452.8	2236
109	1.39	1249	1.051	2690	457.1	2233
110	1.43	1210	1.052	2691	461.3	2230
111	1.48	1173	1.052	2693	465.5	2227
112	1.53	1137	1.053	2695	469.8	2225
113	1.58	1102	1.054	2696	474.0	2222
114	1.64	1069	1.055	2697	478.2	2219
115	1.69	1037	1.056	2699	482.5	2217
116	1.75	1006	1.057	2700	486.7	2214
117	1.80	975.6	1.058	2702	491.0	2211
118	1.86	946.7	1.059	2703	495.2	2208
119	1.92	918.8	1.059	2705	499.5	2205
120	1.99	891.9	1.060	2706	503.7	2203
121	2.05	865.9	1.061	2708	508.0	2200
122	2.11	840.8	1.062	2709	512.2	2197
123	2.18	816.6	1.063	2711	516.5	2194
124	2.25	793.2	1.064	2712	520.7	2191
125	2.32	770.6	1.065	2713	525.0	2189
126	2.39	748.8	1.066	2715	529.2	2186
127	2.47	727.7	1.067	2716	533.5	2183
128	2.54	707.3	1.068	2718	537.8	2180
129	2.62	687.6	1.069	2719	542.0	2177
130	2.70	668.5	1.070	2720	546.3	2174
131	2.78	650.1	1.071	2722	550.6	2171
132	2.87	632.3	1.072	2723	554.9	2168
133	2.95	615.0	1.073	2725	559.1	2165
134	3.04	598.3	1.074	2726	563.4	2163
135	3.13	582.2	1.075	2727	567.7	2160
136	3.22	566.6	1.076	2729	572.0	2157
137	3.32	551.4	1.077	2730	576.3	2154
138	3.41	536.8	1.078	2731	580.5	2151
139	3.51	522.6	1.079	2733	584.8	2148

Temp.	Pressure	Specific volume		Enthalpy		
°C	bars	cc/g		kJ/kg		
		vap.	liq.	vap.	liq.	evap.
140	3.61	508.9	1.080	2734	589.1	2145
141	3.72	495.6	1.081	2735	593.4	2142
142	3.82	482.7	1.082	2736	597.7	2139
143	3.93	470.2	1.083	2738	602.0	2136
144	4.04	458.1	1.084	2739	606.3	2133
145	4.15	446.3	1.085	2740	610.6	2130
146	4.27	435.0	1.086	2742	614.9	2127
147	4.39	423.9	1.087	2743	619.2	2124
148	4.51	413.2	1.088	2744	623.6	2120
149	4.63	402.9	1.089	2745	627.9	2117
150	4.76	392.8	1.090	2746	632.2	2114
151	4.89	383.0	1.092	2748	636.5	2111
152	5.02	373.5	1.093	2749	640.8	2108
153	5.15	364.4	1.094	2750	645.2	2105
154	5.29	355.4	1.095	2751	649.5	2102
155	5.43	346.8	1.096	2752	653.8	2099
156	5.57	338.4	1.097	2754	658.2	2095
157	5.72	330.2	1.098	2755	662.5	2092
158	5.87	322.3	1.100	2756	666.9	2089
159	6.02	314.5	1.101	2757	671.2	2086
160	6.18	307.1	1.102	2758	675.5	2083
161	6.34	299.8	1.103	2759	679.9	2079
162	6.50	292.7	1.104	2760	684.3	2076
163	6.66	285.9	1.106	2761	688.6	2073
164	6.83	279.2	1.107	2762	693.0	2070
165	7.00	272.7	1.108	2764	697.3	2066
166	7.18	266.4	1.109	2765	701.7	2063
167	7.36	260.2	1.110	2766	706.1	2060
168	7.54	254.3	1.112	2767	710.5	2056
169	7.73	248.5	1.113	2768	714.8	2053
170	7.92	242.8	1.114	2769	719.2	2050
171	8.11	237.3	1.116	2770	723.6	2046
172	8.31	232.0	1.117	2771	728.0	2043
173	8.51	226.8	1.118	2772	732.4	2039
174	8.71	221.7	1.119	2773	736.8	2036
175	8.92	216.8	1.121	2774	741.2	2032
176	9.13	212.0	1.122	2775	745.6	2029
177	9.35	207.3	1.123	2775	750.0	2025
178	9.57	202.8	1.125	2776	754.4	2022
179	9.79	198.4	1.126	2777	758.8	2018
180	10.02	194.0	1.127	2778	763.2	2015
181	10.25	189.8	1.129	2779	767.6	2011
182	10.49	185.8	1.130	2780	772.1	2008
183	10.73	181.8	1.132	2781	776.5	2004
184	10.98	177.9	1.133	2782	780.9	2001
185	11.23	174.1	1.134	2782	785.4	1997
186	11.48	170.4	1.136	2783	789.8	1993
187	11.74	166.8	1.137	2784	794.3	1990
188	12.00	163.3	1.139	2785	798.7	1986
189	12.27	159.9	1.140	2786	803.2	1982
190	12.54	156.5	1.141	2786	807.6	1979
191	12.82	153.3	1.143	2787	812.1	1975
192	13.10	150.1	1.144	2788	816.5	1971
193	13.39	147.0	1.146	2789	821.0	1968
194	13.68	144.0	1.147	2789	825.5	1964

Temp.	Pressure	Specific volume		Enthalpy		
°C	bars	cc/g		kJ/kg		
		vap.	liq.	vap.	liq.	evap.
195	13.98	141.1	1.149	2790	830.0	1960
196	14.28	138.2	1.150	2791	834.5	1956
197	14.59	135.4	1.152	2791	839.0	1952
198	14.90	132.6	1.153	2792	843.4	1949
199	15.22	130.0	1.155	2793	847.9	1945
200	15.54	127.4	1.156	2793	852.4	1941
201	15.87	124.8	1.158	2794	857.0	1937
202	16.20	122.3	1.160	2794	861.5	1933
203	16.54	119.9	1.161	2795	866.0	1929
204	16.88	117.5	1.163	2796	870.5	1925
205	17.23	115.2	1.164	2796	875.0	1921
206	17.59	113.0	1.166	2797	879.6	1917
207	17.95	110.7	1.168	2797	884.1	1913
208	18.31	108.6	1.169	2798	888.7	1909
209	18.68	106.5	1.171	2798	893.2	1905
210	19.06	104.4	1.173	2798	897.8	1901
211	19.45	102.4	1.174	2799	902.3	1897
212	19.84	100.4	1.176	2799	906.9	1892
213	20.23	98.51	1.178	2800	911.5	1888
214	20.63	96.63	1.179	2800	916.0	1884
215	21.04	94.79	1.181	2801	920.6	1880
216	21.46	92.99	1.183	2801	925.2	1876
217	21.88	91.23	1.185	2801	929.8	1871
218	22.30	89.52	1.186	2802	934.4	1867
219	22.74	87.84	1.188	2802	939.0	1863
220	23.18	86.19	1.190	2802	943.6	1859
221	23.62	84.58	1.192	2802	948.2	1854
222	24.08	83.01	1.194	2803	952.9	1850
223	24.54	81.47	1.195	2803	957.5	1845
224	25.00	79.96	1.197	2803	962.1	1841
225	25.48	78.49	1.199	2803	966.8	1836
226	25.96	77.05	1.201	2803	971.4	1832
227	26.44	75.64	1.203	2804	976.1	1828
228	26.94	74.26	1.205	2804	980.8	1823
229	27.44	72.90	1.207	2804	985.4	1818
230	27.95	71.58	1.209	2804	990.1	1814
231	28.46	70.29	1.211	2804	994.8	1809
232	28.99	69.02	1.213	2804	999.5	1805
233	29.52	67.77	1.215	2804	1004	1800
234	30.06	66.56	1.217	2804	1009	1795
235	30.60	65.37	1.219	2804	1014	1791
236	31.15	64.20	1.221	2804	1018	1786
237	31.71	63.06	1.223	2804	1023	1781
238	32.28	61.94	1.225	2804	1028	1776
239	32.86	60.84	1.227	2804	1033	1771
240	33.44	59.76	1.229	2804	1037	1767
241	34.03	58.71	1.231	2804	1042	1762
242	34.63	57.68	1.233	2804	1047	1757
243	35.24	56.67	1.236	2803	1052	1752
244	35.86	55.68	1.238	2803	1056	1747
245	36.48	54.71	1.240	2803	1061	1742
246	37.11	53.75	1.242	2803	1066	1737
247	37.76	52.82	1.244	2802	1071	1732
248	38.40	51.90	1.247	2802	1076	1727
249	39.06	51.01	1.249	2802	1081	1721

Temp.	Pressure	Specific volume		Enthalpy		
°C	bars	cc/g		kJ/kg		
		vap.	liq.	vap.	liq.	evap.
250	39.73	50.13	1.251	2802	1085	1716
251	40.40	49.26	1.254	2801	1090	1711
252	41.09	48.42	1.256	2801	1095	1706
253	41.78	47.59	1.258	2800	1100	1700
254	42.48	46.77	1.261	2800	1105	1695
255	43.19	45.98	1.263	2800	1110	1690
256	43.91	45.19	1.266	2799	1115	1684
257	44.64	44.42	1.268	2799	1120	1679
258	45.38	43.67	1.270	2798	1124	1674
259	46.13	42.93	1.273	2797	1129	1668
260	46.89	42.21	1.276	2797	1134	1663
261	47.65	41.49	1.278	2796	1139	1657
262	48.43	40.79	1.281	2796	1144	1651
263	49.21	40.11	1.283	2795	1149	1646
264	50.01	39.43	1.286	2794	1154	1640
265	50.81	38.77	1.289	2794	1159	1634
266	51.63	38.12	1.291	2793	1164	1629
267	52.45	37.49	1.294	2792	1169	1623
268	53.29	36.86	1.297	2791	1174	1617
269	54.13	36.25	1.300	2791	1179	1611
270	54.99	35.64	1.302	2790	1185	1605
271	55.85	35.05	1.305	2789	1190	1599
272	56.73	34.47	1.308	2788	1195	1593
273	57.61	33.90	1.311	2787	1200	1587
274	58.51	33.34	1.314	2786	1205	1581
275	59.42	32.79	1.317	2785	1210	1575
276	60.34	32.24	1.320	2784	1215	1569
277	61.26	31.71	1.323	2783	1220	1563
278	62.20	31.19	1.326	2782	1226	1556
279	63.15	30.68	1.329	2781	1231	1550
280	64.12	30.17	1.332	2780	1236	1544
281	65.09	29.67	1.335	2778	1241	1537
282	66.07	29.19	1.338	2777	1246	1531
283	67.07	28.71	1.342	2776	1252	1524
284	68.07	28.24	1.345	2775	1257	1518
285	69.09	27.77	1.348	2773	1262	1511
286	70.12	27.32	1.352	2772	1268	1504
287	71.16	26.87	1.355	2771	1273	1498
288	72.22	26.43	1.359	2769	1278	1491
289	73.28	26.00	1.362	2768	1284	1484
290	74.36	25.57	1.366	2766	1289	1477
291	75.45	25.15	1.369	2765	1294	1470
292	76.55	24.74	1.373	2763	1300	1463
293	77.66	24.33	1.376	2761	1305	1456
294	78.79	23.94	1.380	2760	1311	1449
295	79.93	23.54	1.384	2758	1316	1442
296	81.08	23.16	1.388	2756	1322	1435
297	82.24	22.78	1.392	2755	1327	1427
298	83.42	22.40	1.396	2753	1333	1420
299	84.61	22.04	1.400	2751	1338	1412
300	85.81	21.67	1.404	2749	1344	1405
301	87.02	21.32	1.408	2747	1350	1397
302	88.25	20.97	1.412	2745	1355	1390
303	89.49	20.62	1.416	2743	1361	1382
304	90.75	20.28	1.420	2741	1367	1374
305	92.02	19.95	1.425	2739	1372	1366

Temp.	Pressure	Specific volume		Enthalpy		
°C	bars	cc/g		kJ/kg		
		vap.	liq.	vap.	liq.	evap.
306	93.30	19.62	1.429	2737	1378	1358
307	94.59	19.29	1.434	2734	1384	1350
308	95.90	18.97	1.438	2732	1390	1342
309	97.23	18.66	1.443	2730	1395	1334
310	98.56	18.35	1.447	2727	1401	1326
311	99.92	18.04	1.452	2725	1407	1318
312	101.2	17.74	1.457	2722	1413	1309
313	102.6	17.45	1.462	2720	1419	1301
314	104.0	17.16	1.467	2717	1425	1292
315	105.4	16.87	1.472	2714	1431	1283
316	106.8	16.58	1.477	2712	1437	1275
317	108.3	16.30	1.482	2709	1443	1266
318	109.7	16.03	1.488	2706	1449	1257
319	111.2	15.76	1.493	2703	1455	1248
320	112.7	15.49	1.499	2700	1461	1239
321	114.2	15.22	1.504	2697	1468	1229
322	115.7	14.96	1.510	2694	1474	1220
323	117.2	14.71	1.516	2691	1480	1210
324	118.8	14.45	1.522	2687	1486	1201
325	120.3	14.20	1.528	2684	1493	1191
326	121.9	13.95	1.534	2681	1499	1181
327	123.5	13.71	1.541	2677	1506	1171
328	125.1	13.47	1.547	2673	1512	1161
329	126.8	13.23	1.554	2670	1519	1151
330	128.4	13.00	1.561	2666	1525	1141
331	130.1	12.76	1.568	2662	1532	1130
332	131.7	12.54	1.575	2658	1539	1119
333	133.4	12.31	1.582	2654	1545	1109
334	135.2	12.09	1.589	2650	1552	1098
335	136.9	11.87	1.597	2645	1559	1086
336	138.6	11.65	1.605	2641	1566	1075
337	140.4	11.43	1.613	2636	1573	1064
338	142.2	11.22	1.621	2632	1580	1052
339	144.0	11.01	1.629	2627	1587	1040
340	145.8	10.80	1.638	2622	1594	1028
341	147.7	10.59	1.647	2617	1601	1016
342	149.5	10.39	1.656	2612	1609	1003
343	151.4	10.18	1.665	2606	1616	990
344	153.3	9.983	1.675	2601	1624	977
345	155.2	9.784	1.685	2595	1631	964
346	157.1	9.587	1.695	2589	1639	951
347	159.1	9.391	1.706	2583	1647	937
348	161.1	9.197	1.717	2577	1654	923
349	163.1	9.005	1.728	2571	1662	908
350	165.1	8.813	1.740	2564	1671	893
351	167.1	8.623	1.753	2557	1679	878
352	169.2	8.435	1.765	2550	1687	863
353	171.3	8.247	1.779	2542	1696	847
354	173.4	8.060	1.793	2535	1704	830
355	175.5	7.873	1.807	2527	1713	814
356	177.6	7.688	1.822	2518	1722	796
357	179.8	7.502	1.839	2510	1731	778
358	182.0	7.317	1.855	2501	1741	760
359	184.2	7.131	1.873	2491	1751	741

Temp.	Pressure	Specific volume		Enthalpy		
°C	bars	cc/g		kJ/kg		
		vap.	liq.	vap.	liq.	evap.
360	186.5	6.945	1.892	2481	1761	721
361	188.7	6.759	1.913	2471	1771	700
362	191.0	6.571	1.934	2459	1781	678
363	193.3	6.381	1.958	2448	1792	655
364	195.7	6.190	1.983	2435	1804	631
365	198.0	5.995	2.011	2421	1816	606
366	200.4	5.797	2.041	2407	1829	578
367	202.8	5.593	2.076	2391	1842	549
368	205.3	5.380	2.114	2374	1857	517
369	207.7	5.162	2.159	2354	1873	482
370	210.2	4.925	2.213	2332	1890	442
371	212.8	4.671	2.280	2306	1911	395
372	215.3	4.380	2.369	2274	1936	338
373	217.9	4.019	2.509	2229	1971	258
374	220.5	3.404	2.880	2140	2049	91
374.136	220.9	3.155	3.155	2099	2099	0

APPENDIX 2

ATOMIC WEIGHTS

Element	Symbol	Atomic number	Atomic weight	Element	Symbol	Atomic number	Atomic weight
Actinium	Ac	89	(227)	Mercury	Hg	80	200.59
Aluminum	Al	13	26.9815	Molybdenum	Mo	42	95.94
Americium	Am	95	(243)	Neodymium	Nd	60	144.24
Antimony	Sb	51	121.75	Neon	Ne	10	20.183
Argon	Ar	18	39.948	Neptunium	Np	93	(237)
Arsenic	As	33	74.9216	Nickel	Ni	28	58.70
Astatine	At	85	(210)	Niobium	Nb	41	92.906
Barium	Ba	56	137.34	Nitrogen	N	7	14.0067
Berkelium	Bk	97	(247)	Nobelium	No	102	(254)
Beryllium	Be	4	9.0122	Osmium	Os	76	190.2
Bismuth	Bi	83	208.980	Oxygen	O	8	15.9994
Boron	B	5	10.811	Palladium	Pd	46	106.4
Bromine	Br	35	79.909	Phosphorus	P	15	30.9738
Cadmium	Cd	48	112.40	Platinum	Pt	78	195.09
Calcium	Ca	20	40.08	Plutonium	Pu	94	(244)
Californium	Cf	98	(249)	Polonium	Po	84	(210)
Carbon	C	6	12.01115	Potassium	K	19	39.102
Cerium	Ce	58	140.12	Praseodymium	Pr	59	140.907
Cesium	Cs	55	132.905	Promethium	Pm	61	(145)
Chlorine	Cl	17	35.453	Protactinium	Pa	91	(231)
Chromium	Cr	24	51.996	Radium	Ra	88	(226)
Cobalt	Co	27	58.9332	Radon	Rn	86	(222)
Copper	Cu	29	63.54	Rhenium	Re	75	186.2
Curium	Cm	96	(245)	Rhodium	Rh	45	102.905
Dysprosium	Dy	66	162.50	Rubidium	Rb	37	85.47
Einsteinium	Es	99	(254)	Ruthenium	Ru	44	101.07
Erbium	Er	68	167.26	Samarium	Sm	62	150.35
Europium	Eu	63	151.96	Scandium	Sc	21	44.956
Fermium	Fm	100	(252)	Selenium	Se	34	78.96
Fluorine	F	9	18.9984	Silicon	Si	14	28.086
Francium	Fr	87	(223)	Silver	Ag	47	107.870
Gadolinium	Gd	64	157.25	Sodium	Na	11	22.9898
Gallium	Ga	31	69.72	Strontium	Sr	38	87.62
Germanium	Ge	32	72.59	Sulfur	S	16	32.064
Gold	Au	79	196.967	Tantalum	Ta	73	180.948
Hafnium	Hf	72	178.49	Technetium	Tc	43	(99)
Helium	He	2	4.0026	Tellurium	Te	52	127.60
Holmium	Ho	67	164.930	Terbium	Tb	65	158.924
Hydrogen	H	1	1.00797	Thallium	Tl	81	204.37
Indium	In	49	114.82	Thorium	Th	90	232.038
Iodine	I	53	126.9044	Thulium	Tm	69	168.934
Iridium	Ir	77	192.2	Tin	Sn	50	118.69
Iron	Fe	26	55.847	Titanium	Ti	22	47.90
Krypton	Kr	36	83.80	Tungsten	W	74	183.85
Lanthanum	La	57	138.91	Uranium	U	92	238.03
Lawrencium	Lw	103	(257)	Vanadium	V	23	50.942
Lead	Pb	82	207.19	Xenon	Xe	54	131.30
Lithium	Li	3	6.942	Ytterbium	Yb	70	173.04
Lutetium	Lu	71	174.97	Yttrium	Y	39	88.905
Magnesium	Mg	12	24.312	Zinc	Zn	30	65.37
Manganese	Mn	25	54.9380	Zirconium	Zr	40	91.22
Mendelevium	Mv	101	(256)				

Numbers in parentheses indicate mass number of most stable known isotope.

REFERENCES

Aggett, J. and Aspell, A.C., 1976. The determination of arsenic (III) and total arsenic by atomic-absorption spectroscopy. Analyst, 101, 341-347.

APHA, 1989. Standard methods for the examination of water and waste water, 17th edition. America Public Health Association, American Water Works Association, Water Pollution Control Federation, Washington, 1624pp.

APHA, 1991. Supplement to the 17th edition of Standard methods for the examination of water and waste water. America Public Health Association, American Water Works Association, Water Pollution Control Federation, Washington, 150pp..

Aredes, S. and Nicholson, K., 1990. Ammonia in soils: A new technique in geothermal exploration. Geotherm. Res. Council Trans., 14, 1371-1376.

Arnason, B., 1977a. The hydrogen-water isotope applied to geothermal areas in Iceland. Geothermics, 5, 75-80.

Arnason, B., 1977b. Hydrothermal systems in Iceland traced by deuterium. Geothermics, 5, 125-151.

Arnorsson, S., 1983. Chemical equilibria in Icelandic geothermal systems. Implications for chemical geothermometry investigations. Geothermics, 12, 119-128.

Arnorsson, S., 1985. The use of mixing models and chemical geothermometrs for estimating underground temperatures in geothermal systems. J. Volcanol. Geotherm. Res., 23, 299-335.

Arnorsson, S., 1989. Deposition of calcium carbonate minerals from geothermal waters - theoretical considerations. Geothermics, 18, 33-39.

Arnorsson, S. and Gunnlaugsson, E., 1985. New gas geothermometers for geothermal exploration - Calibration and application. Geochim. Cosmochim. Acta, 49, 1307-1325.

Arnorsson, S., Sigurdsson, S. and Svavarsson, H., 1982. The chemistry of geothermal waters in Iceland. I. Calculation of aqueous speciation from 0°C to 370°C. Geochim. Cosmochim. Acta, 46, 1513-1532.

Arnorsson, S., Gunnlaugsson, E. and Svavarsson, H., 1983. The chemistry of geothermal waters in Iceland. II. Mineral equilibria and independent variables controlling water compositions. Geochim. Cosmochim. Acta, 47, 547-566.

ASTM, 1992. Annual Book of ASTM Standards. Sections 11.01, 11.02, Water. American Society for Testing Materials, Philadelphia, USA.

Aubert, M. and Baubron, J-C., 1988. Identification of a hidden thermal fissure in a volcanic terrain using a combination of hydrothermal convection indicators and soil-atmosphere analysis. J. Volcanol. Geotherm. Res., 35, 217-225.

Ballantyne, J.M. and Moore, J.N., 1988. Arsenic geochemistry in geothermal systems. Geochim. Cosmochim. Acta, 52, 475-483.

Banwart, W.L., Tabatabai, M.A. and Bremner, J.M., 1972. Determination of ammonia in soil extracts and water samples by an ammonia electrode. Comm. Soil Sci. and Plant Analysis, 3, 449-458.

Benjamin, T., Charles, R. and Vidale, R., 1983. Thermodynamic parameters and experimental data for the Na-K-Ca geothermometer. J. Volcanol. Geotherm. Res., 15, 167-186.

Berger, B.R. and Bethke, P.M. (eds), 1985. Geology and geochemistry of epithermal systems. Reviews in Economic Geology, 2, Society of Economic Geologists, 298pp.

Bergquist, L.F., 1979. Helium: An exploration tool for geothermal sites. Geotherm. Res. Council Trans., 3, 59-60.

Bischoff, J.L., Radtke, A.S. and Rosenbauer, R.J., 1981. Hydrothermal alteration of greywacke by brine and seawater: roles of alteration and chlorite complexing on metal solubilities at 200°C and 350°C. Econ. Geol., 79, 659-676.

Bogie, I., Lawless, J.V. and Pornuevo, J.B., 1987. Kaipohan: an apparently nonthermal manifestation of hydrothermal systems in the Philippines. J. Volcanol. Geotherm. Res., 31, 281-292.

Bottinga, Y., 1969. Calculated fractionation factors for carbon and hydrogen isotope exchange in the system calcite-carbon dioxide-graphite-methane-hydrogen-water vapour. Geochim. Cosmochim. Acta, 33, 49-64.

Browne, P.R.L., 1978. Hydrothermal alteration in active geothermal fields. Ann. Rev. Earth Planet. Sci., 6, 229-250.

Browne, P.R.L., 1979. Minimum age of the Kawerau geothermal field, North Island, New Zealand. J. Volcanol. Geotherm. Res., 6, 213-215.

Browne, P.R.L., 1987. Hydrothermal alteration processes and their recognition. Pre-congress workshop on mineralisation and volcanicity. Pacific Rim Congress, Queensland University, 98-149.

Browne, P.R.L. and Ellis, A.J., 1970. The Ohaki-Broadlands geothermal area, New Zealand: Mineralogy and related geochemistry. Am. J. Sci., 269, 97-131.

Chemerys, J.C., 1983. Comparison of analytical methods for the determination of silica in geothermal water. J. Volcanol. Geotherm. Res., 16, 57-63.

Chiodini, G. and Cioni, R., 1989. Gas geobarometry for hydrothermal systems and its application to some Italian geothermal areas. Appl. Geochem., 4, 465-472.

Christian, G.D. and O'Reilly, J.E. (eds), 1986. Instrumental analysis. Allyn and Bacon, Boston, 933pp.

Cox, M.E., 1980. Ground radon survey of a geothermal area in Hawaii. Geophys. Res. Lett., 7, 4, 283-286.

Craig, H., 1953. The geochemistry of stable carbon isotopes. Geochim. Cosmochim. Acta, 3, 53-92.

Craig, H., 1957. Isotopic standards for carbon and oxygen and correction factors for mass spectrometric analysis of carbon dioxide. Geochim. Cosmochim. Acta, 12, 133-149.

Craig, H., 1961. Isotopic variations in meteoric waters. Science, 133, 1702-1703.

Craig, H., 1963. The isotopic geochemistry of water and carbon in geothermal areas. In: Tongiorgi, E. (ed.), Nuclear geology in geothermal areas, Spoleto, 1963. Consiglio Nazional delle Ricerche, Laboratorio di Geologia Nucleare, Pias, 17-53.

Craig, H., Boato, G. and White, D.E., 1956. Isotopic geochemistry of thermal waters. National Acad. Sci. National Research Council Publication 400, 29-38.

D'Amore, F. and Nuti, S., 1977. Notes on the chemistry of geothermal gases. Geothermics, 6, 39-45.

D'Amore, F. and Panichi, C., 1980. Evaluation of deep temperatures of hydrothermal systems by a new gas-geothermometer. Geochim. Cosmochim. Acta, 44, 549-556.

D'Amore, F. and Panichi, C., 1987. Geochemistry in geothermal exploration. In: Economides, M. and Ungemach, P. (eds) Applied geothermics, Wiley & Sons, New York, 69-89.

D'Amore, F. and Truesdell, A.H., 1984. Helium in the larderello geothermal fluid. Geothermics, 13, 227-239.

D'Amore, F., Celati. R., Ferrara, G.C. and Panichi. C., 1977. Secondary changes in the chemical and isotopic composition of the geothermal fluids in Larderello field. Geothermics, 5, 153-163.

D'Amore, F., Fancelli, R., Saracco, L. and Truesdell, A.H., 1987. Gas geothermometry based on CO content - Applications in Italian geothermal fields. Proc. 12th Workshop on Geothermal Reservoir Engineering, Standord University, USA, 247-252.

Deitz, W.A., 1967. J. Gas Chromatog., 5, 68-70. Cited by Ellis et al., 1968.

Del Moro, A., Puxeddu, M., Radicati di Brozolo, F. and Villa, I.M., 1982. Rb-Sr and K-Ar ages on minerals at temperatures of 300°C-400°C from deep wells in the Larderello geothermal field (Italy). Contrib. Mineral. Petrol., 81, 340-349.

DesMarais, D.J., Donchin, J.H., Nehring, N.L. and Truesdell, A.H., 1981. Molecular carbon isotopic evidence for the origin of geothermal hydrocarbons. Nature, 292, 826.

DoE/NWC, 1978. Mercury in waters, effluents and sludges by flameless atomic absorption spectrophotometry. Methods for the examination of waters and associated materials. The Standing Committee of Analysts, The Department of the Environment/National Water Council, HMSO, London, 35pp.

DoE/NWC, 1980. Boron in waters, effluents, sewage and some solids 1980. Methods for the examination of waters and associated materials. The Standing Committee of Analysts, The Department of the Environment/National Water Council, HMSO, London, 35pp.

Duchi, V., Minissale, A.A., and Prati, F., 1987b. Chemical composition of thermal springs, cold springs, streams and gas vents in the Mt Amiata geothermal region (Tuscany, Italy). J. Volcanol. Geotherm. Res., 31, 321-332.

Duchi, V., Minissale, A.A., Ortino, S. and Roman, L., 1987a. Geothermal prospecting by geochemical methods on natural gas and water discharges in the Vulsini Mts volcanic district (Central Intaly). Geothermics, 16, 147-157.

Ellis, A.J., 1962. Interpretation of gas analysis from the Wairakei hydrothermal area. N.Z. J. Sci., 5, 434-452.

Ellis, A.J., 1968. Natural hydrothermal systems and experimental hot water/rock interaction: reaction with NaCl solutions and trace metal extraction. Geochim. Cosmochim. Acta, 32, 1356-1363.

Ellis, A.J., 1969. Present-day hydrothermal systems and mineral deposition. Proc. 9th Commonwealth mining and metall. congress (mining and petroleum scetion), Instn Min. Metall., London, 1-30.

Ellis, A.J., 1970. Quantitative interpretation of chemical characteristics of hydrothermal systems. Geothermics, Special Issue 2, 1, 516-528.

Ellis, A.J., 1977. Chemical and isotopic techniques in geothermal investigations. Geothermics, 5, 3-12.

Ellis, A.J., 1979. Chemical geothermometry in geothermal systems. Geothermics, 25, 219-226.

Ellis, A.J. and Golding, R.M., 1963. The solubility of carbon dioxide above 100°C in water and in sodium chloride solutions. Am. J. Sci., 261, 47-60.

Ellis, A.J. and Mahon. W.A.J., 1964. Natural hydrothermal systems and experimental hot-water/rock interactions. Geochim. Cosmochim. Acta, 28, 1323-1357.

Ellis, A.J.and Mahon. W.A.J., 1967. Natural hydrothermal systems and experimental hot-water/rock interactions (Part II). Geochim. Cosmochim. Acta, 31, 519-538.

Ellis, A.J.and Mahon. W.A.J., 1977. Chemistry and geothermal systems. Academic Press, New York, 392pp.

Ellis, A.J.and Wilson, S.H., 1960. The geochemistry of alkali metal ions in the Wairakei hydrothermal system. N.Z. J. Geol. Geophys., 3, 593-617.

Ellis, A.J., Mahon, W.A.J. and Ritchie, J.A., 1968. Methods of collection and analysis of geothermal fluids. Second edition. Report CD2103, Chemistry Division, DSIR, New Zealand, 51pp.

EPRI, 1985. A theory on trace arsenic in geothermal fluids. Research Project 1525-6, final report AP-4214. Electric Power Research Institute, California, USA.

EPRI, 1986. A theory on boron in geothermal fluids. Research Project 1525-6, final report AP-4670. Electric Power Research Institute, California, USA.

EPRI, 1987. A theory on mercury in geothermal fluids. Research Project 1525-6, final report AP-AP-5111. Electric Power Research Institute, California, USA.

Finlayson, J.B., 1970. The collection and analysis of volcanic and hydrothermal gases. Geothermics, Special Issue, 2 (2), 1344-1354.

Fletcher, W.F., Hoffman, S.J., Mehrtens, M.B., Sinclair, A.J. and Thomson, I., 1986. Exploration geochemistry: Design and interpretation of soil surveys. Reviews in Economic Geology, 3, Society of Economic Geologists, 180pp..

Fouillac, C. and Michard, G., 1981. Sodium/lithium ratio in water applied to geothermometry of geothermal reservoirs. Geothermics, 10, 55-70.

Fournier, R.O., 1977. Chemical Geothermometers and mixing models for geothermal systems. Geothermics, 5, 41-50.

Fournier, R.O., 1979a. A revised equation for the Na/K geothermometer. Geoth. Res. Council Trans., 3, 221-224.

Fournier, R.O., 1979b. Geochemical and hydrological considerations and the use of enthalpy-chloride diagrams in the prediction of underground conditions in hot-spring systems. J. Volcanol. Geotherm. Res., 5, 1-16.

Fournier, R.O., 1981. Application of water geochemistry to geothermal exploration and reservoir engineering. In: Rybach, L. and Muffler, L.J.P., Geothermal systems: Principals and case histories. Wiley, Chichester, 109-143.

Fournier, R.O., 1983. A method of calculating quartz solubilities in aqueous sodium chloride solutions. Geochim. Cosmochim. Acta, 47, 579-586.

Fournier, R.O., 1985. The behaviour of silica in hydrothermal solutions. In: Berger, B.R. and Bethke, P.M. (eds) Geology and geochemistry of epithermal systems. Reviews in Economic Geology, 2, Society of Economic Geologists, 45-61.

Fournier, R.O., 1989a. Lectures on geochemical interpetation of hydrothermal waters. UNU Geothermal Training Programme, Reykjavik, Iceland, Report 10, 73pp.

Fournier, R.O., 1989b. Geochemistry and dynamics of the Yellowstone National Park hydrothermal system. Ann. Rev. Earth Planet. Sci. 17, 13-53.

Fournier, R.O., 1990. The interpretation of Na-K-Mg relations in geothermal waters. Geoth. Res. Council Trans., 14, 1421-1425.

Fournier, R.O.and Marshall, W.L., 1983. Calculation of amorphous silica solubilities at 25°C to 300°C and apparent cation hydration numbers in aqueous salt solutions using the concept of effective density of water. Geochim. Cosmochim. Acta, 47, 587-596.

Fournier, R.O. and Potter, R.W., 1979. Magnesium correction to the Na-K-Ca chemical geothermometer. Geochim. Cosmochim. Acta, 43, 1543-1550.

Fournier, R.O. and Potter, R.W., 1982a. An equation correlating the solubility of quartz in water from 25°C to 900°C at pressures up to 10,000 bars. Geochim. Cosmochim. Acta, 46, 1969-1974.

Fournier, R.O. and Potter, R.W., 1982b. A revised and expanded silica (quartz) geothermometer. Geoth. Res. Council Bull., November, 3-12.

Fournier, R.O. and Rowe, J.J., 1966. estimation of underground temperatures from the silica content of water from hot springs and wet-steam wells. Amer. J. Sci., 264, 685-697.

Fournier, R.O. and Truesdell, A.H., 1973. An empirical Na-K-Ca geothermometer for natural waters. Geochim. Cosmochim. Acta, 37, 1255-1275.

Fournier, R.O. and Truesdell, A.H., 1974. Geochemical indicators of subsurface temperature - Part 2, estimation of temperature and fraction of hot water mixed with cold water. J. Res. U.S. Geol. Survey, 2, 263-270.

Fournier, R.O., Sorey, M.L., Mariner, R.H. and Truesdell, A.H., 1979. Chemical and isotopic prediction of aquifer temperatures in the geothermal system at Long Valley, California. J. Volcanol. Geotherm. Res., 5, 17-34.

Fournier, R.O., White, D.E. and Truesdell, A.H., 1974. Geochemical indicators of subsurface temperature - Part 1, basic assumptions. J. Res. U.S. Geol. Survey, 2, 259-261.

Friedman, I. and O'Neill, J.R., 1977. Compilation of stable isotope fractionation factors of geochemical interest. In: Fleischer, M. (ed.), Data of geochemistry, U.S. Geol. Survey Prof. Paper, 440-KK, 12pp.

Fritz, J.S. and Schenk, G.H., 1979. Quantitative analytical chemistry. Fourth edition. Allyn and Bacon, Boston, 661pp.

Fritz, P. and Fontes, J.Ch., 1980. Introduction. In: Fritz, P. and Fontes, J.Ch. (eds), Handbook of environmental isotope geochemistry, Volume 1, The terrestrial environment A. Elsevier, Amsterdam, 1-19.

Ghomshel, M.M., Croft, S.A.S. and Stauder, J.J., 1986. Geochemical evidence of chemical equilibria in the south Meager Creek geothermal system, British Columbia, Canada. Geothermics, 15, 49-61.

Giggenbach, W.F., 1971. Isotopic composition of waters of the Broadlands geothermal field. N.Z. J. Sci., 14, 959-970.

Giggenbach, W.F., 1975. A simple method for the collection and analysis of volcanic gas samples. Bull. Volcanol., 39, 132-145.

Giggenbach, W.F., 1978. The isotopic composition of waters from the El Tatio geothermal field, northern Chile. Geochim. Cosmochim. Acta, 42, 979-988.

Giggenbach, W.F., 1980. Geothermal gas equilibria. Geochim. Cosmochim. Acta, 44, 2021-2032.

Giggenbach, W.F., 1981. Geothermal mineral equilibria. Geochim. Cosmochim. Acta, 45, 393-410.

Giggenbach, W.F., 1982. Carbon-13 exchange between CO_2 and CH_4 under geothermal conditions. Geochim. Cosmochim. Acta, 46, 159-165.

Giggenbach, W.F., 1984. Mass transfer in hydrothermal alteration systems - A conceptual approach. Geochim. Cosmochim. Acta, 48, 2693-2711.

Giggenbach, W.F., 1987. Redox process governing the chemistry of fumarolic gas discharges from White Island, New Zealand. Appl. Geochem., 2, 143-161.

Giggenbach, W.F., 1988. Geothermal solute equilibria. Derivation of Na-K-Mg-Ca geoindicators. Geochim. Cosmochim. Acta, 52, 2749-2765.

Giggenbach, W.F. and Goguel, R.L., 1989. Collection and analysis of geothermal and volcanic water and gas discharges. Fourth Edition. Report CD2401, Chemistry Division, DSIR, New Zealand.

Giggenbach, W.F. and Stewart, M.K., 1982. Processes controlling the isotopic composition of steam and water discharges from steam vents and steam-heated pools in geothermal areas. Geothermics, 11, 71-80.

Giggenbach, W.F., Gonfiantini, R., Jangi, B.L. and Truesdell, A.H., 1983. Isotopic and chemical composition of Parbati Valley geothermal discharges, northwest Himalaya, India. Geothermics, 12, 199-222.

Glover, R.B., 1970. Interpretation of gas compositions from the Wairakei Field over 10 years. Geothermics, Special Issue, 2 (2), 1355-1366.

Glover, R.B., 1982. Calculation of the chemistry of some geothermal environments. Report CD 2323, Chemistry Division, DSIR, New Zealand.

Glover, R.B., 1988. Boron distribution between liquid and vapour in geothermal fluids. Proc. 10th New Zealand Geothermal Workshop, Auckland University, 223-227.

Goguel, R.L., 1981. Flame emission for accurate cesium determination in geostandards. Geostandards Newsletter, 5, 95-99.

Goguel, R.L., 1983. The rare alkalies in hydrothermal alteration at Wairakei and Broadlands geothermal fields, N.Z. Geochim. Cosmochim. Acta, 47, 429-437.

Gonfiantini, R., 1978. Standards for stable isotope measurements in natural compounds. Nature, 271, 534-536.

Govett, G.J.S., Rock geochemistry in mineral exploration. Elsevier, Amsterdam, 461pp.

Grant, M.A., Donaldson, I.A. and Bixley, P.F., 1982. Geothermal reservoir engineering. Academic Press, New York, 369pp.

Gunnlaugsson, E. and Arnorsson, S., 1982. The chemistry of iron in geothermal systems in Iceland. J. Volcanol. Geotherm. Res., 14, 281-299.

Gunter, B.D., 1978. $-C_1$ $-C_4$ hydrocarbons in hydrothermal gases. Geochim. Cosmochim. Acta, 42, 137.

Gunter, B.D. and Musgrove, B.C., 1971. New evidence on the origin of methane in hydrothermal gases. Geochim. Cosmochim. Acta, 35, 113-118.

Gupta, M.L., Saxena, V.K. and Sukhija, B.S., 1976. An analysis of the hot spring activity of the Manikaran area, Himachai Pradesh, India, by geochemical studies and tritium concentration of spring waters. Proceedings 2nd UN Symposium on the development and use of geothermal resources, San Francisco, 1975, 1, 741-744.

Gutierrez-Negrin, L.C.A., 1985. Radon emanometry in geothermal exploration of volcanic zones. Geoth. Res. Council Trans., 9 (1), 441-445.

Haas, J.L., 1971. The effect of salinity on the maximum thermal gradient of a hydrothermla system at hydrostatic pressure. Econ. Geol., 66, 940-946.

Harris, W.E. and Kratochvil, B., 1982. An introduction to chemical analysis. Holt-Saunders, Philadelphia, 611.

Hedenquist, J.W and Stewart, M.K., 1985. Natural CO_2-rich steam-heated waters in the Broadlands-Ohakki geothermal system, New Zealand: Their chemistry, distribution and corrosive nature. Geoth. Res. Council Trans., 9, 245-250.

Helgeson, H.C., Delany, J.M., Nesbitt, H.W. and Bird, D.K., 1978. Summary and critique of the thermodynamic properties of the rock forming minerals. Amer. J. Sci., 267, 729-804.

Henley, R.W., 1985. The geothermal framework for epithermal deposits. In: Berger, B.R. and Bethke, P.M. (eds) Geology and geochemistry of epithermal systems. Reviews in Economic Geology, 2, Society of Economic Geologists, 1-24.

Henley, R.W. and Brown, K.L., 1985. A practical guide to the thermodynamics of geothermal fluids and hydrothermal ore deposits. In: Berger, B.R. and Bethke, P.M. (eds) Geology and geochemistry of epithermal systems. Reviews in Economic Geology, 2, Society of Economic Geologists, 25-44.

Henley, R.W. and Stewart, M.K., 1983. Chemical and isotopic changes in the hydrology of the Tauhara geothermal field due to exploitation at Wairakei. J. Volcanol. Geotherm. Res., 15, 285-314.

Henley, R.W., Truesdell, A.H. and Barton, P.B., 1984. Fluid-mineral equilibria in hydrothermal systems. Reviews in Economic Geology 1, Society of Economic Geoogists, 267pp.

Henley, R.W., Hedenquist, J.W. and Roberts, P.J. (eds), 1986. Guide to active epithermal (geothermal) systems and precious metal deposits of New Zealand. Gebruder Borntraeger, Berlin.

Henneberger, R.C., 1986. Ohakuri fossil epithermal system. In: Henley, R.W., Hedenquist, J.W. and Roberts, P.J. (eds). Guide to active epithermal (geothermal) systems and precious metal deposits of New Zealand. Gebruder Borntraeger, Berlin, 121-128.

Henneberger, R.C. and Brown, P.R.L., 1987. Hydrothermal alteration and evolution of the Ohakuri hydrothermal system, Taupo Volcanic Zone, New Zealand. J. Volcanol. Geotherm. Res., 34, 211-231.

Hinkle, M.E. and Harms, T.F., 1978. CS_2 and COS in soil gases of the Roosevelt hot springs known geothermal resource area, Beaver County, Utah. Jour. Research U.S. Geol. Survey, 6, 571-573.

Hinkle, M.E., 1978. Helium, mercury, sulphur compounds, and carbon dioxide in soil gases of the Puhimau thermal area, Hawaii Volcanoes National Park, Hawaii. U.S. Geol. Survey Open File Report 78-246, 15pp.

Hinkle, M.E., Denton, E.H., Biglow, R.C. and Turner, R.L., 1978. Helium in soil gases of the Roosevelt hot springs known geothermal resource area, Beaver County, Utah. Jour. Research U.S. Geol. Survey, 6, 563-570.

Hirabayashi, J., 1986. Sampling of fumarolic gases at vulcano (Italy) and analytical results. Geothermics, 15, 201-203.

Hulson, J.R., 1977. Isotope work applied to geothermal systems at the Institute of Nuclear Sciences, New Zealand. Geothermics, 5, 89-96.

Hulson, J.R., 1978. Interim temperature scales for the methane-water and carbon dioxoide-bicarbonaye isotopic equilibria. N.Z. Inst. Nucl. Sci. Report INS-R-249, 7pp.

Hulson, J.R., 1983. Environmental isotope investigations of New Zealand geothermal systems - A review. Geothermics, 12, 223-232.

Hulson, J.R. and Lyon, G.L., 1991. Isotopic evidence for the origin of methane fron New Zealand geothermal systems. Proc. Deep Gas Workshop, Hannover, May 1990, International Energy Agency, Paris, in press.

Hulson, J.R. and McCabe, W.J., 1962. Mass spectrometer measurements in the thermal areas of New Zealand. 2. Carbon isotopic ratios. Geochim. Cosmochim. Acta, 26, 399-410.

Iwasaki, I., Utzumi, S., Hagino, K., Tarutani, T. and Ozawa, T. (1957). Spectrophotometric method for the determination of small amounts of sulphate ions. Bull. Chem. Soc. Japan, 30, 847-851.

Kahler, D.E., 1981. Helium. A gaseous geochemical guide to faults, fractures and geothermal systems. Geotherm. Res. Council Trans., 5, 87-89.

Keenan, J.H., Keyes, F.G., Hill, P.G. and Moore, J.G., 1969. Steam tables. Wiley, New York, 162pp.

Kharaka, Y.K. and Mariner, R.H., 1989. Chemical geothermometers and their application to formation waters from sedimentary basins. In: Naeser, N.D. and McCulloch, T.H. (eds), Thermal history of sedimentary basins: methods and case histories. Springer-Verlad, New York, 99-117.

Kharaka, Y.K., Lico, M.S. and Law, L.M., 1982. Chemical geothermometers applied to formation waters, Gulf of Mexico and California basins. Am. Assoc. Petrol. Geol. Bull, 66, 588.

Kindle, C.H., 1989. Geothermal fluid sampling techniques. In: Lienau, P.J. and Lunis, B.C. (eds) Geothermal direct use engineering and design guidebook. Geo-Heat center, Oregon Institute of technology, Oregon, USA, 81-94.

Kiyoshu, Y., 1985. Isotopic composition of acid sulphate-chloride waters and volcanic steam from some volcanoes in northeast Japan. J. Volcanol. Geotherm. Res., 26, 25-36.

Klusman, R.W. and Jaacks, J.A., 1987. Environmental influences upon mercury, radon and helium concentrations in soil gases at a site near Denver, Colorado. J. Geochem. Explor., 27, 259-280.

Klusman, R.W. and Landress, R.A., 1978. Secondary controls on mercury in soils of geothermal areas. J. Geochem. Explor., 9, 75-91.

Klusman, R.W. and Landress, R.A., 1979. Mercury in soils of the Long Valley, California, geothermal system. J. Volcanol. Geotherm. Res., 5, 49-65.

Klusman, R.W., Cowling, S. Culvey, B., Roberts, C. and Schwab, A.P., 1977. Preliminary evaluation of secondary controls on mercury in soils of geothermal districts. Geothermics, 6, 1-8.

Klyen, L.E., 1973. A vessel for collecting subsurface water samples from geothermal drillholes. Geothermics, 2, 57-60.

Klyen, L.E., 1981. Recent design improvements to the "Klyen" subsurface sampler. Geothermics, 10, 71-73.

Klyen, L.E., 1982. Sampling techniques for geothermal fluids. Report CD2322, Chemistry Division, DSIR, New Zealand, 88pp.

Koga, A. Geochemistry of the waters discharged from drillholes in Otake and Hatchobaru areas (Japan). Geothermics, Special Issue 2, 2(2), 1422-1425.

Koga, A. and Noda, T., 1976. Geochemical prospecting in vapour-dominated fields for geothermal exploration. Proceedings 2nd UN Symposium on the development and use of geothermal resources, San Francisco, 1975, 1, 761-766.

Koga, A., Taguchi, S. and Mahon, W.A.J., 1982. The use of volatile constituents in geothermal fluids for assessing the type, potential and near surface permeability of a geothermal system: The Broadlands geothermal area, NZ. Proc. 4th NZ Geothermal Workshop, Auckland University, 135-138.

Kristmannsdoittir, H. and Tomasson, J., 1974. Nesjavellir hydrothermal alteration in a high-temperature area. Proc. Int. Symp. Water-rock interation, Prague, 170-177.

Levinson, A.A., 1980. Introduction to exploration geochemistry. Applied Publishing, 924pp.

Liu W. and Nicholson, K. (1990). Boron in soils over Naike and Whitford low-enthalpy geothermal fierlds, New Zealand. In: Harvey C.C., Browne, P.R.L., Freestone, D.H. and Scott, G.L. (eds), Proc. 12th NZ Geothermal Workshop, Auckland University, 177-182.

Lloyd, E.F., 1972. Geology and hot springs of Orakeikorako. N.Z. Geol. Survey Bull., 85, 164pp.

Lloyd, R.M., 1978. Oxygen isotope behaviour in the sulfate-water system. J. Geophys. Res., 73, 6099-6110.

Lyon, G.L., 1974. Geothermal gases. In: Kaplan, I.R. (ed.) Natural gases in marine sediments. Plenum Press, New York, 141-150.

Lyon, G.L. and Hulston, J.R., 1984. Carbon and hydrogen isotopic compositions of New Zraland geothermal gases. Geochim. Cosmochim. Acta, 48, 1161-1171.

Lyon, G.L. and Stewart, M.K., 1985. The Tongariro geothermal system -Stable isotope chemistry. Geoth. Res. Council Trans., 9, 333-337.

MacKenzie, W.F. and Truesdell, A.H., 1977. Geothermal reservoir temperatures estimated from the oxygen isotope compositions of dissolved sulphate and water from hot springs and shallow drillholes. Geothermics, 5, 51-61.

Mahon, W.A.J., 1961. Sampling of geothermal drillhole discharges. Proc. U.N. Conference on New Sources of Energy, Rome, August 1961, 2, 269.

Mahon, W.A.J., 1964. Fluorine in the natural thermal waters of New Zealand. N.Z. J. Sci., 7, 3-28.

Mahon, W.A.J., 1966. Silica in hot water discharged from drillholes at Wairakei, New Zealand. N.Z. J. Sci., 9, 135-144.

Mahon, W.A.J., 1967. Natural hydrothermal systems and the reaction of hot water with sedimentary rocks. N.Z. J. Sci., 10, 206-221.

Mahon, W.A.J., 1970. Chemistry in the exploration and exploitation of hydrothermal systems. Geothermics, Special Issue 2, 2(2), 1310-1322.

Mahon, W.A.J., 1976. Review of hydrogeochemistry of geothermal systems - Prospecting, development and use. Proceedings 2nd UN Symposium on the development and use of geothermal resources, San Francisco, 1975, 1, 775-783.

Mahon, W.A.J., Klyen, L.E. and Rhode, M., 1980a. Neutral sodium/bicarbonate/sulphate hot waters in geothermal systems. Chinetsu (J. Japan Geothermal Energy Association), 17, 11-24.

Mahon, W.A.J., McDowell, G.D. and Finlayson, J.B., 1980b. Carbon dioxide: its role in geothermal systems. N.Z. J. Sci., 23, 133-148.

Malinin, S.D., Kropotova, O.I. and Grineko, V.A., 1967. Experimental determination of carbon isotope exchange constsants in the $CO_{2(gas)}$=$HCO_{3(solution)}$ system under hydrothermal conditions. Geokhimia, 8, 927-935 (in Russian with English abstract).

Marini, L., Chiodini, G. and Cioni, R., 1986. New geothermometers for carbonate-evaporite geothermal reservoirs. Geothermics, 15, 77-86.

Mazor, E. and Manon, M.A., 1979. Geochemical tracing in producing geothermal fields: a case study at Cerro Prieto. Geothermics, 8, 231-240.

Mazor, E. and Truesdell, A.H., 1984. Dynamics of a geothermal field traced by noble gases: Cerro Prieto, Mexico. Geothermics, 13, 91-102.

Mazor, E., 1977. Geothermal tracing with atmospheric and ragiogenic noble gases. Geothermics, 5, 21-36.

McCabe, W.J., Barry, B.J. and Manning, M.R., 1983. Radioactive tracers in geothermal underground water flow studies. Geothermics, 12, 83-110.

McCarthy, K.P., 1983. Helium exploration survey for the Animas Valley, Colorado. Geoth. Res. Council Bull., 12 (7), 9-14.

McCarthy, K.P., Been, J., Reimer, M., Bowles, C.G. and Murrey, D.G., 1982. Helium and ground temperature surveys at Steamboat Springs, Colorado. Geothermal Energy, 10 (9), 13-16.

McNerney, J.J. and Buseck, P.R., 1973. Geochemical exploration using mercury vapour. Econ. Geol., 68, 1313-1320.

McNerney, J.J., Buseck, P.R. and Hanson, R.C., 1972. Mercury detection by means of thin gold films. Science, 178, 611-612.

Mercado, S., 1970. High activity hydrothermal zones detected by Na/K, Cerro Prieto, Mexico. Geothermics, Special Issue, 2(2), 1367-1376.

Minissale, A., 1991. The Larderello geothermal field: A review. Earth Sci. Reviews, 31, 133-151.

Minissale, A.A. and Duchi, V., 1988. Geothermometry on fluids circulating in a carbonate reservoir in north-central Italy. J. Volcanol. Geotherm. Res., 35, 237-252.

Mizutani, Y., 1972. Isotopic composition and underground temperature of the Otake geothermal water, Kyushu, Japan. Geochem. J., 6, 67-73.

Mizutani, Y. and Rafter, T.A., 1969. Oxygen isotopic composition of sulphates, 3. Oxygen isotopic fractionation in the bisulfate ion-water system. N.Z. J. Sci., 12, 54-59.

Mook, W.G., Bommerson, J.C. and Staverman, W.H., 1974. Carbon isotope fractionation betweeen dissolved bicarbonate and gaseous carbon dioxide. Earth Planet. Sci. Lett., 22, 169-176.

Morey, G.W., Fournier, R.O. and Rowe, J.J., 1962. The solubility of quartz in water in the temperature interval from 25°C to 300°C. Geochim. Cosmochim. Acta, 26, 1029-1043.

Mustard, P.S. and Richardson, J.M., 1990. A Lotus 1-2-3 template for triangular plots. Geobyte, 47-53.

Nehring, N.H. and D'Amore, F., 1984. Gas chemistry and thermometry of the Cerro Prieto, Mexico, geothermal field. Geothermics, 13, 75-89.

Nicholson, K., 1983. Fluorine determination in geochemistry: Errors in the electrode method of analysis. Chem. Geol., 38, 1-22.

Nicholson, K., 1988. Geothermal deposits in ancient terrain as a tool in epithermal gold exploration: examples from Scotland. Proc. 10th New Zealand Geothermal Workshop, Auckland University, 151-153.

Nicholson, K., 1989. Early Devonian geothermal systems in northeast Scotland: Exploration targets for epithermal gold. Geology, 17, 568-571.

Nicholson, K., 1990. Stratiform manganese mineralisation near Inverness, Scotland: A Devonian sublacustrine hot-spring deposit? Mineralium Deposita, 25, 126-131.

Nicholson, K. and Aquino, C., 1989. Life in geothermal systems. A key to sinter formation and recognition? In: Browne, P.R.L. and Nicholson, K. (eds), Proc. 11th NZ Geothermal Workshop, Auckland University, 143-148.

Nicholson, K. and Duff, E.J., 1981a. Rapid sample pre-treatment for removal of aluminium from aqueous solutions prior to fluoride determination by fluoride-selective electrode. Analyst, 106, 904-906.

Nicholson, K. and Duff, E.J., 1981b. Errors in the direct potentiometric method of fluoride determination: Adsorption, illumination and temperature effects. Analyst, 106, 985-991.

Nicholson, K. and Duff, E.J., 1981c. Fluoride determination in water: An optimum buffer system for use with the fluoride-selective electrode. Anal. Lett., 14, 493-517.

Nicholson, K. and Parker, R.J., 1990. Geothermal sinter chemistry: Towards a diagnostic signature and a sinter geothermometer. In: Harvey C.C., Browne, P.R.L., Freestone, D.H. and Scott, G.L. (eds), Proc. 12th NZ Geothermal Workshop, Auckland University, 97-102.

Nicholson, K., Franklyn, A.K. and Aredes, S., 1989. Geochemical soil surveys: An exploration technique for low-enthalpy geothermal resources. In: Browne, P.R.L. and Nicholson, K. (eds), Proc. 11th NZ Geothermal Workshop, Auckland University, 189-193.

Nieva, D. and Nieva, R., 1987. Developments in geothermal energy in Mexico, part 12 - A cationic composition geothermometer for prospection of geothermal resources. Heat recovery systems and CHP, 7, 243-258.

Noda, T., 1981. Volatile mercury capture with a gold needle and its application to geothermal prospecting. Proc. NZ Geothermal Workshop, Auckland University, 225-230.

Nuti, S., Noto, P. and Ferrara, G.C., 1980. The system H_2O-CO_2-CH_4-H_2 at Travale, Italy: tentative interpretation. Geothermics, 9, 287-295.

Openshaw, R.E., 1983. Hg and As soil geochemistry of the Meager Creek geothermal area. J. Geochem. Explor., 19, 339-344.

Orion, 1987. Model 95-12 Ammonia electrode instruction manual. Orion Research Inc., Boston, USA, 37pp.

Paces, T., 1975. A systematic deviation from the Na-K-Ca geothermometer below 75°C and above 10^{-4} atm P_{CO_2}. Geochim. Cosmochim. Acta, 39, 541-544.

Panichi, C. and Gonfiantini, R., 1978. Environmental isotopes in geothermal studies. Geothermics, 6, 143-161.

Panichi, C., Ferrara, G.C. and Gonfiantini, R., 1977. Isotope geothermoetry in the Larderello geothermal field. Geothermics, 5, 81-88.

Parker, R.J. and Nicholson, K., 1990. Arsenic in geothemal sinters: Determination and implications for mineral exploration. In: Harvey C.C., Browne, P.R.L., Freestone, D.H. and Scott, G.L. (eds), Proc. 12th NZ Geothermal Workshop, Auckland University, Auckland University, 35-39.

Patterson, J.E., 1980. Algorithms for determinations of sodium, potassium, calcium and lithium over wide concentration ranges by flame emission spectrometry. Anal. Chim. Acta, 107, 201-209.

Phelps, D. and Buseck, P.R., 1980. Distribution of soil mercury and the development of soil mercury anomalies in the Yellowstone geothermal area, Wyoming. Econ. Geol., 75, 730-741.

Pope, L.A., Hajashi, A. and Popp, R.K., 1987. An experimental investigation of the quartz, Na-K, Na-K-Ca geothermometers and the effects of fluid composition. J. Volcanol. Geotherm. Res., 31, 151-161.

Richet, P., Bottinga, Y. and Javoy, M., 1977. A review of hydrogen, carbon, nitrogen, oxygen, sulfur and chlorine stable isotope fractionation among gaseous molecules. Ann. Rev. Earth Planet. Sci., 5, 65-110.

Rimstidt, J.D. and Barnes, H.L., 1980. The kinetics of silica-water reaction. Geochim. Cosmochim. Acta, 44, 1683-1699.

Robinson, B.W., 1973. Sulphur isotope equilibrium during sulphur hydrolysis at high temperatures. Earth Planet. Sci. Lett., 18, 443-450.

Rose, A.W, Hawkes, H.E. and Webb, J.S., 1979. Geochemistry in mineral exploration. Academic Press, London, 657pp.

Rowley, J.C., 1982. Worldwide geothermal resources. In: Edwards, L.M., Chillingar, G.V., Rieke, H.H. and Ferti, W.H., Handbook of geothermal energy. Gulf Publishing Company, Houston, 44-161.

Rybach, L., 1981. Geothermal systems, conductive heat flow, geothermal anomalies. In: Rybach, L. and Muffler, L.J.P. Muffler, Geothermal systems: Principles and case histories. Wiley, Chichester, 3-36.

Sakai, H., 1977. Sulfate-water isotope thermometry applied to geothermal systems. Geothermics, 5, 67-74.

Salvania, N.V. and Nicholson, K. (1990). Chemometrics applied to the fluid chemistry of geothermal fields in the Taupo Volcanic Zone, New Zealand. In: Harvey C.C., Browne, P.R.L., Freestone, D.H. and Scott, G.L. (eds), Proc. 12th NZ Geothermal Workshop, Auckland University, 157-163.

Saracco, L. and D'Amore, F., 1989. CO2B: A computer program for applying a gas geothermometer to geothermal systems. Computers and Geosciences, 15, 1053-1065.

Sheppard, D.S. and Lyon, G.L., 1981. Chemistry of the Ngawha thermal area. In: The Ngawha geothermal area. Geothermal Report 7, DSIR, New Zealand, 95-128.

Sheppard, D.S., Falvre-Pierret, R.X., Orange, C.J. and Le Guern, F., 1990. Soil gas surveys: A cheaper alternative to geophysical surveys: three examples from the taupo Volcanic Zone. In: Harvey C.C., Browne, P.R.L., Freestone, D.H. and Scott, G.L. (eds), Proc. 12th NZ Geothermal Workshop, Auckland University, 125-128.

Sinclair, A.J., 1974. Selection of threshold values in geochemical data using probability graphs. J. Geochem. Explor., 3, 129-149.

Sinclair, A.J., 1981. Applications of probability graphs in mineral exploration. Association of Exploration Geochemists, Special Volume 4, 95pp.

Stafansson, V., Tomasson, J., Gunnlaugsson, E., Sigvaldsson, H., Franzson, H. and Sigurdsson, O., 1983. Nesjavellir, hola Nv-6. Report OS-83023/JHD-04, Orkustofnun, 100pp.

Stewart, M.K. and Taylor, C.B., 1981. Environmental isotopes in New Zealand hydrology. N.Z. J. Sci., 24, 295-311.

Sugisaki, R., 1987. Behaviour and origin of helium, neon, argon and nitrogen from active faults. J. Geophys. Res., 92, 12523-12530.

Sugisaki, R. and Sugiura, T., 1986. Gas anomalies at three mineral springs and a fumarole before an inland earthquake, Central Japan. J. Geophys. Res., 91, 12296-12304.

Sutton, F.M. and McNabb, A., 1977. Boiling curves at Broadlands geothermal field, New Zealand. N.Z. J. Sci., 20, 333-337.

Taran, Y., 1986. Gas geothermometers for hydrothermal systems. Geochem. Int., 111-126.

Thode, H.G., Shima, M., Rees, C.E. and Krishnamurty, K.V., 1965. Carbon-13 isotope effects in systems containing carbon dioxide, bicarbonate, carbonate and metal ions. Can. J. Chem., 43, 582-595.

Tonani, F., 1970. Geochemical methods of exploration for geothermal energy. Geothermics, Special Issue 2, 1, 492-515.

Tonani, F., 1980. Some remarks on the application of geochemical techniques in geothermal exploration. In: Proc. Adv. Eur. Geoth. Res., Second symposium, Strasboug, 428-443.

Truesdell, A.H., 1976. Summary of Section III. Geochemical techniques in exploration. Proceedings 2nd UN Symposium on the development and use of geothermal resources, San Francisco, 1975, 1, liii-lxxix.

Truesdell, A.H. and Fournier, R.O., 1976. Calculations of deep temperatures in geothermal systems from the chemistry of boiling spring waters of mixed origin. Proceedings 2nd UN Symposium on the development and use of geothermal resources, San Francisco, 1975, 1, 837-844.

Truesdell, A.H. and Fournier, R.O., 1977. Procedure for estimating the temperature of a hot-water component in a mixed water by using a plot of silica verses enthalpy. Jour. Research U.S. Geol. Survey, 5, 49-52.

Truesdell, A.H. and Hulston, J.H., 1980. Isotopic evidence on environments of geothermal systems. In: Fritz, P. and Fontes, J.Ch. (eds), Handbook of environmental isotope geochemistry, Volume 1, The terrestrial environment A. Elsevier, Amsterdam, 179-226.

Truesdell, A.H., Nehring, N.L., Thompson, J.M., Janik, C.J. and Coplen, T.B., 1984. A review of progress in understanding the fluid geochemistry of the Cerro Prieto geothermal system. Geothermics, 13, 65-74.

Truesdell, A.H., Haizlip, J.R., Box, W.T. and D'Amore, F., 1987. Fieldwide chemical and isotopic gradients in steam from The Geysers. Proc. 12th Workshop on geothermal engineering, Stanford University, USA, 241-246.

Truesdell, A.H., Nathenson, M. and Rye, R.O., 1977. The effects of subsurface boiling and dilution on the isotopic compositions of Yellowstone thermal waters. J. Geophys. Res., 82, 3694-3703.

van Kooten, G.K., 1987. Geothermal exploration using surface mercury geochemistry. J. Volcanol. Geotherm. Res., 31, 269-280.

Varekamp, J.C. and Buseck, P.R., 1983. Hg anomalies in soils: A geochemical exploration method for geothermal areas. Geothermics, 12, 29-47.

Veldeman, E., Van't dack, L., Gijbels, R. and Pentcheva, E.N., 1990. Thermal waters from south Bulgaria: A multivariate approach for evaluation and interpretation of analytical data. Geoth. Res. Council Trans., 14, 1537-1543.

Vogel, A.I., 1990. Vogel's textbook of quantitative chemical analysis. 5th edition. Longman, Harlow, 877pp.

Walters, F.H., Griffin, K.B. and Keeley, D.F., 1984. Use of ammonia-sensing electrodes in salt-media. Analyst, 109, 663-665.

Watson, J.C., 1979. Sampling and analysis methods for geothermal fluids and gases. PNL-MA-572, Pacific Northwest Laboratory, Richland, Washington, USA.

Webster, J.G., 1989. An analytical scheme for the determination of sulphide, polysulphide, thiosulphate, sulphite and polythionate concentrations in geothermal waters. Report CD 2406, Chemistry Division, DSIR, New Zealand.

Webster, J.G., 1990. The solubility of As_2S_3 and speciation of As in dilute and sulphide-bearing fluids at 25 and 90°C. Geochim. Cosmochim. Acta, 54, 1009-1017.

White, D.E., 1957. Magmatic, connate and metamorphic waters. Bull. Geol. Soc. Amer., 68, 1659-1682.

White, D.E., 1965. Saline waters of sedimentary rocks. In: Fluids in subsurface environments - A symposium. Amer. Assoc. Petrol. Geol. Mem., 4, 342-366.

White, D.E., 1970. Geochemistry applied to the discovery, evaluation and exploitation of geothermal energy resources. Geothermics, Special Issue 2, 1, 58-80.

White, D.E., 1974. Diverse origins of hydrothermal ore fluids. Econ. Geol., 69, 954-973.

White, D.E., 1979. Duration of hydrothermal activity at Steamboat Springs, Nevada, from ages of spatially associated volcanic rocks. U.S. Geol. Survey Prof. Paper 458-D, 13pp.

White, D.E., Muffler, L.P.J. and Truesdell, A.H., 1971. Vapour-dominated hydrothermal systems compared with hot-water systems. Econ. Geol., 66, 75-97.

White, N.C., Wood, D.G., and Lee, M.C., 1989. Epithermal sinters of Paleozoic age in north Queensland, Australia. Geology, 17, 718-722.

Whitehead, N.E., Gingricho, J.E. and Fischer, J.C., 1983. A New Zealand test of the track-etch method of prospecting for geothermal steam. J. Volcanol. Geotherm. Res. 15, 339-354.

Whitehead, N.E., 1981. A test of radon ground measurements as a geothermal prospecting tool in New Zealand. N.Z. J. Sci., 24, 59-64.

Whitehead, N.E., 1984. Geothermal prospecting by ground radon measurements. J. Volcanol. Geotherm. Res., 20, 213-229.

Willard, H.H., Merrit, L.L., Dean, J.A. and Settle, F.A., 1981. Instrumental methods of analysis. Wadsworth Publishing, Belmont, California, 1030pp.

Yoshimura, K., Kariya, R. and Tarutani, T., 1979. Spectrophotometric determination of boron in natural waters and rocks after specific adsorption of Sephadex gel. Anal. Chim. Acta, 109, 115-121.

Zhu, B., Zhang, J. Zhu, L. and Zheng, Y., 1986. Mercury, arsenic, antimony, bismuth and boron as geochemical indicators for geothermal areas. J. Geochem. Explor., 25, 379-388.

Zhu, B., Zhu, L., Shi, C., Yu, H. and Wang, G., 1989. Application of geochemical methods in the search for geothermal fields. J. Geochem. Explor., 33, 171-183.

Zukin, J.G., Hammond, D.E., Ku, T.L. and Elders, W.A., 1987. Uranium thorium series radionuclides in brines and reservoir rocks from two deep geothermal boreholes in the salton Sea geothermal field, southern California. Geochim. Cosmochim. Acta, 51, 2719-2731.

SUBJECT INDEX